University of Sussex

A University of Sussex PhD thesis

This thesis is protected by copyright which belongs to the author

It cannot be reproduced or quoted extensively from without first obtaining permission in writing from the author

The content must not be changed in any way or sold commercially in any format or medium without the formal permission of the author

When referring to this work, full bibliographic details including the author, title, awarding institution and date of the thesis must be given

Please visit Figshare for more information and further details

https://sussex.figshare.com/Theses

Synthesis of Novel Amides and Related Compounds with Applications in Medicinal Chemistry

UNIVERSITY OF SUSSEX

Sirihathai Srikwanjai

Supervisor: Prof. John Spencer

Submitted to the University of Sussex in part fulfilment of the requirements of the degree of Doctor of Philosophy

September 2023

Declaration

I hereby declare that all work described in this thesis was carried out at the University of Sussex under the supervision of Professor John Spencer from September 2019 to September 2023. The work presented in this thesis is my own unless otherwise stated. This thesis comprises a general introduction in Chapter 1. Chapters 2 - 4 contain unpublished content and Chapter 5 contains the conclusions and suggestions for future directions.

Dr. Stephen Hare tragically lost his life during this work and I would like to express my sincere thanks for his enthusiasm and help and send my condolences to his loved ones.

Sirihathai Srikwanjai

Acknowledgements

Abstract

Given the high cost of drug discovery and the high attrition rate of drug candidates, simple and efficient methods for synthesising drug candidates are highly desirable. This thesis focusses on simple routes for synthesising amide libraries and related compounds (sulfonamides, hydrazides) for antimicrobial (*Neisseria gonorrhoeae* bacteria), anticancer (leukaemia) and pain relief applications.

Chapter 1 introduces the importance of amide and sulfonamide compounds in medicinal chemistry, the synthesis of amides using coupling agents, sulfonamide synthesis, acid bioisosteres, key drug properties and SWISS ADME predictions, metabolic stability of amides, protein X-ray crystallography and followed by protein crystallization.

Chapter 2 focuses on treatments and evolution of drug resistance, drug targeting peptidyl-tRNA hydrolase (Pth), the simple synthesis of a furanoyl (amide and hydrazide), and sulfonamide libraries for the potential treatment of bacterial resistance.

Chapter 3 investigates potential leukaemia treatment that inhibit the interaction between LIM only protein 2 (LMO2) and stem cell leukaemia (SCL) by using *tert*-butyl 6-oxo-1,4-oxazepane-4-carboxylate as a building block. Reductive amination and amide coupling chemistries were used for synthesising nM potent compounds with potential use in childhood accute lymphoblastic leukaemia (ALL).

Chapter 4 presents a background of voltage-gated potassium ion channel subtypes 2.1 ($K_v2.1$), and attempts to improve the solubility and permeability of a 'rule of five' lead compound. This collaborative project also looked at other properties of the compound, including efflux and microsomal stability.

List of abbreviations

Å	angstrom
Ac	acetate
AcOH	acetic acid
ADME	Absorption, distribution, metabolism, elimination
AML	acute myeloid leukaemia
ALL	acute lymphoblastic leukaemia
aps	apparent singlet
Ar	aryl
atm	atmosphere
Boc	tert-butyloxycarbonyl
BBB	blood brain barrier
br	broad
brs	broad singlet
CDI	carbonyldiimidazole
CNS	central nervous system
CoA	coenzyme A
d	doublet
DCM	dichloromethane
DMF	dimethylformamide
DMSO	dimethylsulfoxide

DNA	deoxyribonucleic acid
DG	directing group
dd	doublets of doublets
ddd	doublets of doublets of doublets
dt	doublets of triplets
EtOAc	ethyl acetate
ESI	electrospray ionisation
eq	equivalent
FG	functional group
g	gram
GABA	gamma-aminobutyric acid
GIT	gastrointestinal tract
GP	glycoprotein
HRMS	high resolution mass spectrometry
HIA	human intestinal absorption
Hz	hertz
h	hour
LC-MS	liquid chromatography – mass spectrometry
LMO2	LIM only protein 2
m	multiplet
MeOH	methanol
mg	milligram
min	minute

mL	millilitre
mmol	milli-mole
MW	microwave
MHz	megahertz
NMR	nuclear magnetic resonance
nM	nanomolar
PGP	P-glycoprotein
Pth	peptidyl tRNA hydrolase
PNS	peripheral nervous system
K_v	potassium ion channel
PPI	Protein-protein interaction
ppm	parts per million
q	quartet
rt	room temperature
s	singlet
SCL	stem cell leukaemia
SAR	structure activity relationship
t	triplet
TFA	trifluoroacetic acid
THF	tetrahydrofuran
TLC	thin layer chromatography
tR	retention times
W	watt

w/w	weight/weight
µL	microlitre
µg	microgram
µM	micromolar

Table of Contents

Chapter 1

Introduction

1.1 Amide compounds in medicinal chemistry

Amides are an important class of compounds found in a range of agricultural chemicals, pharmaceutical products and biologically active molecules. Protein are form of amide bonds (N-C=O) from amino acids, which play vital role in living cells. Moreover, amides account for about 25% of drugs.[1] Figure 1.1 shows examples of major drugs on the market today that contain an amide bond.[2–6] Amide containing drugs are used in the treatment of a wide range of illness including Atorvastatin (Figure 1.1a) is used to inhibit the production of cholesterol, Lisinopril (Figure 1.1b) is used to treat hypertension and heart failure, Valsartan (Figure 1.1c) is used to reduce blood pressure, aldosterone levels, and increased excretion of sodium, Diltiazem (Figure 1.1d) is used to treat high blood pressure, Lidocaine (sodium ion channel blocker) (Figure 1.1e) is a local anesthetic used millions of times in the world and Prilocaine (Figure 1.1f) has similar properties to lidocaine, often in dentistry, Oseltamivir (Figure 1.1g)is used in the treatment and prophylaxis of infection with influenza viruses A (including pandemic H1N1) and Darunavir (Figure 1.1h) is used in the treatment of human immunodeficiency virus (HIV) infection and, specifically, rather than an amide, contains a carbamate group (N(C=O)OR). Acalabrutinib (Figure 1.1i) is used to treat chronic lymphocytic leukaemia and small lymphocytic lymphoma that was approved as a new tablet formulation by the Food and Drug Administration (FDA) in August 2022.[2–6]
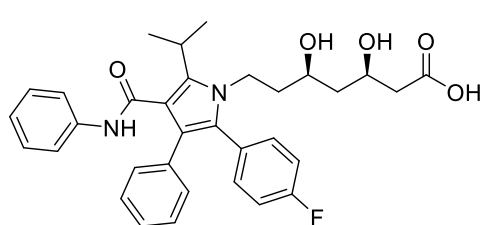
(a) Atovastatin
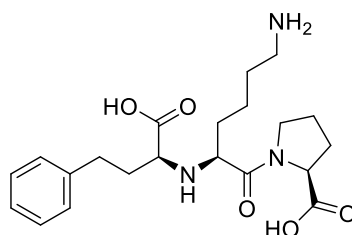
(b) Lisinopril
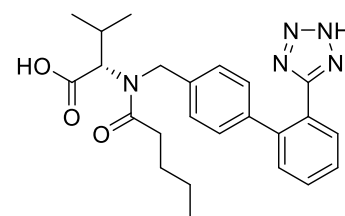
(c) Valsartan
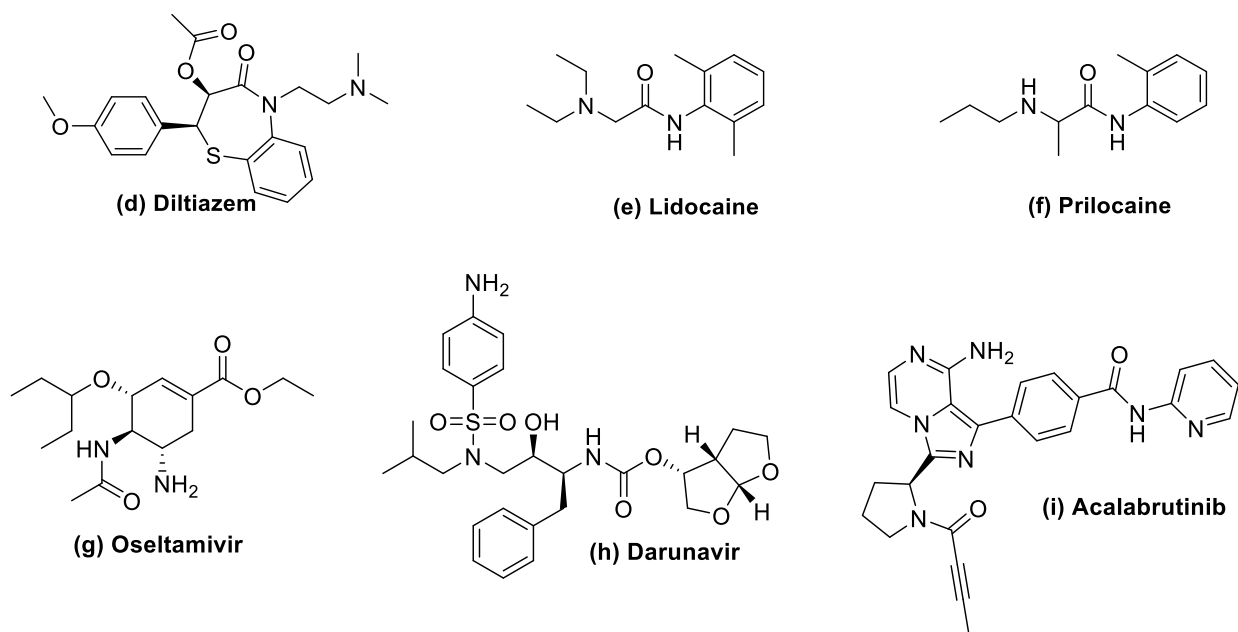
Figure 1.1. *Example of top selling drugs containing an amide or related bond.*[2–6]

1.2 The synthesis of amide compounds

There are many ways to synthesise amide compounds. The most common method to prepare amides is through the reaction between activated carboxylic acids (or their carboxylic derivatives) with an amine.[1,7] However, the direct reaction between amine and carboxylic acids typically requires high temperatures to remove water from the condensation reaction. Thus, it is necessary to convert the -OH group of the acid into a good leaving group before reacting with amine. The reactions using carboxylic acids are treated with activating agents (or so-called coupling agents) in order to transform easily into the desired product as illustrated in Figure 1.2. Therefore, a range of different coupling agents and strategies have been developed for amide bond formation.[1,7-11]

Figure 1.2. *Acid activation and aminolysis step.*[1]

Coupling via activated esters

1.2.1. Carbodiimides

Coupling agents such as dicyclohexyl carbodiimide (DCC), diisopropyl carbodiimide (DIC) and 1-ethyl-3-(3'-dimethylamino)carbodiimide HCl salt (EDC) are commonly used in the synthesis of peptides and amide compounds as shown in Figure 1.3. The concept of carbodiimide mechanisms is the same (Scheme 1.1), examples are displayed for DCC (Scheme 1.2) and EDC (Scheme 1.3).
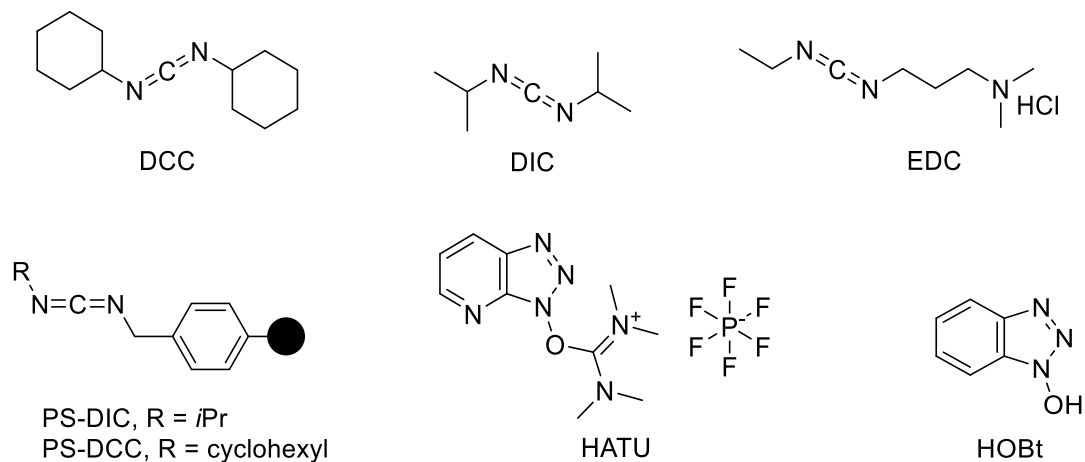
Figure 1.3. *Various coupling agents, polymer-supported reagents and additives.*
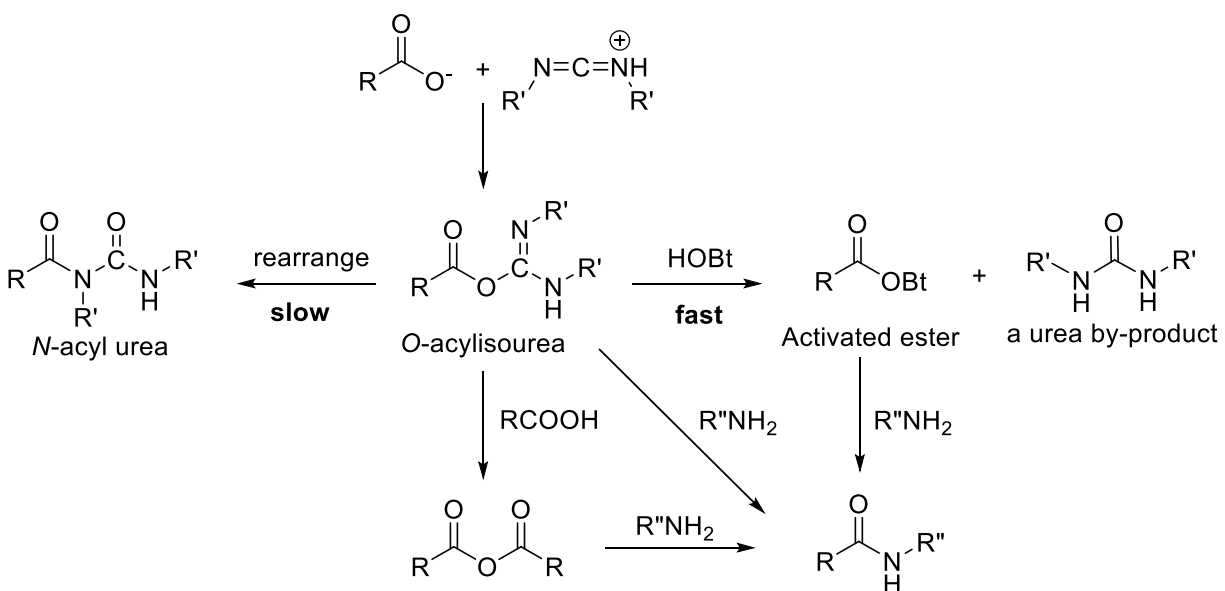
Scheme 1.1. *General pathway for carbodiimides coupling mechanism.*[8]

The use of DCC often generates high yields and also produces urea as a by-product. The activated carbodiimide reacts with the carboxylic acid to form an *O*-acylisourea intermediate then the amine reacts with the *O*-acylisourea intermediate, resulting in the formation of an amide bond then releasing the urea by-product and *O*-acylisourea intermediate also slowly changed to *N*-acyl urea. To prevent this, hydroxybenzotriazole (HOBt) and *N,N*-dimethylaminopyridine (DMAP) are added to the reaction mixture because they react with *O*-acylisourea faster than they generate *N*-acyl urea (Scheme 1.2 and 1.4). The urea by-products produced by 3 coupling agents with different elimination results: 1) DCC, urea by-product is not soluble in water so is removed by filtration, 2) DIC, urea by-product is soluble in dichloromethane (DCM) and thus removed by DCM washes and liquid phase chemistry and 3) EDC, urea by-product is soluble in water thus removed by liquid phase chemistry. Furthermore, using a polymer-supported coupling agent is an applicable method to remove the coupling agent and by-product by filtration, as shown in Scheme 1.5. Interestingly, polymer-supported carbodiimides are well known, such as polymer-supported dicyclohexyl carbodiimide (PS-DCC) and polymer-supported diisopropyl carbodiimide (PS-DIC).[1,9]
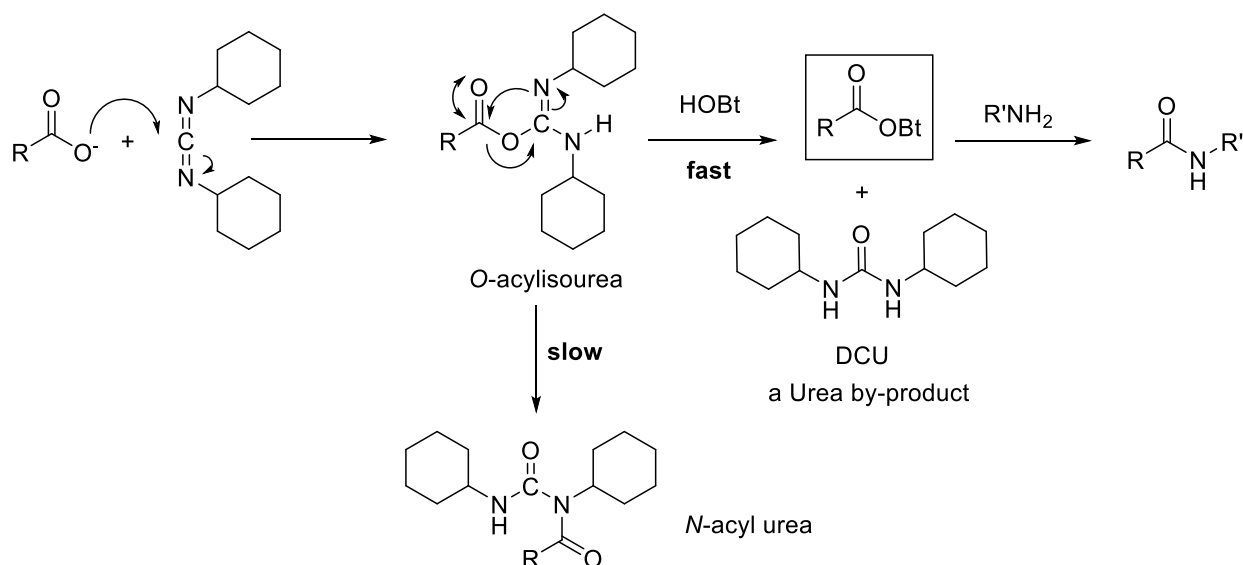
Scheme 1.2. One-pot DCC coupling mechanism and HOBt activation.[1,9]

Scheme 1.3. *One-pot EDC coupling mechanism.*[1,10]

Scheme 1.4. *HOBt activation mechanism when used as additive with DCC.*[1,9]
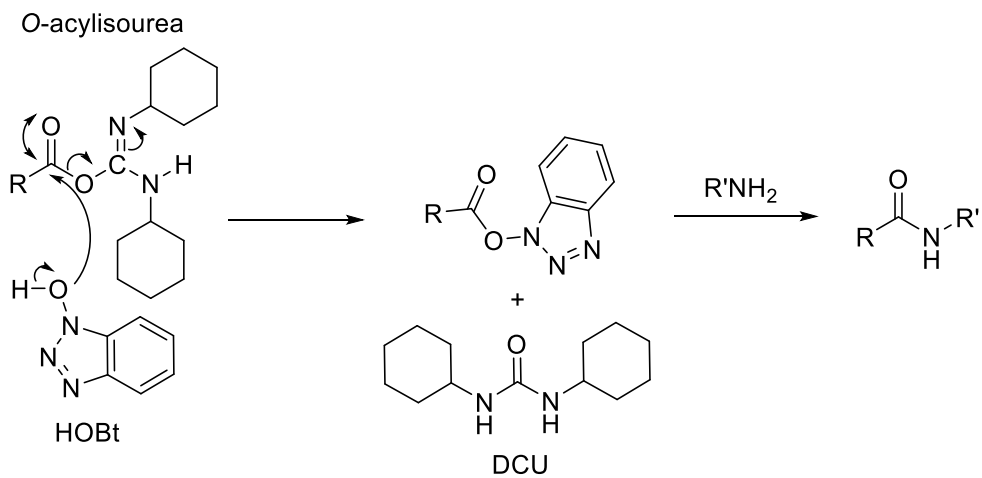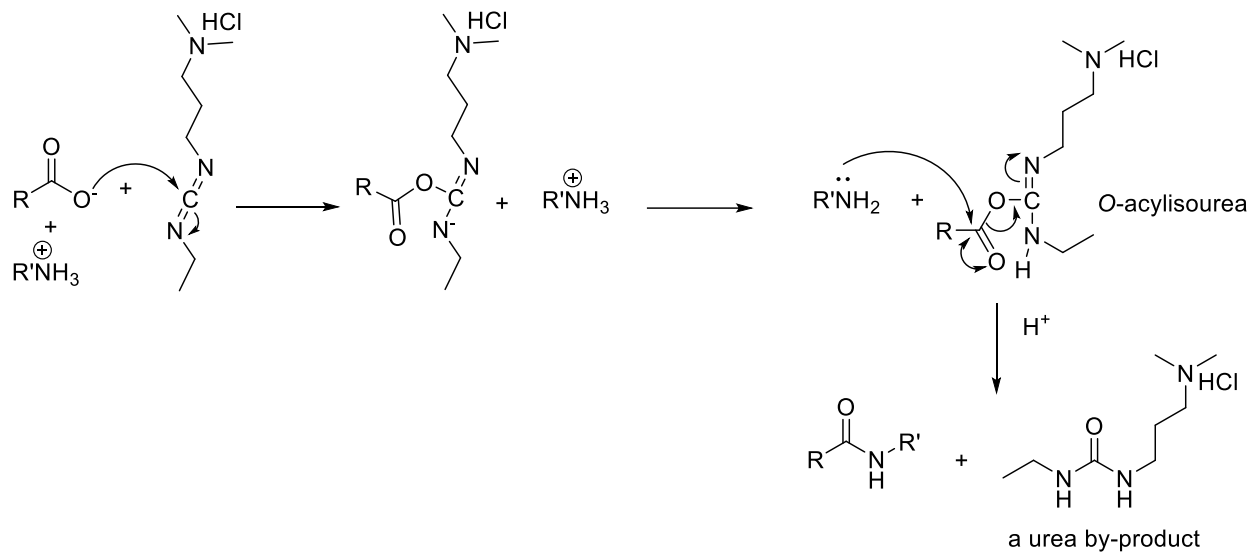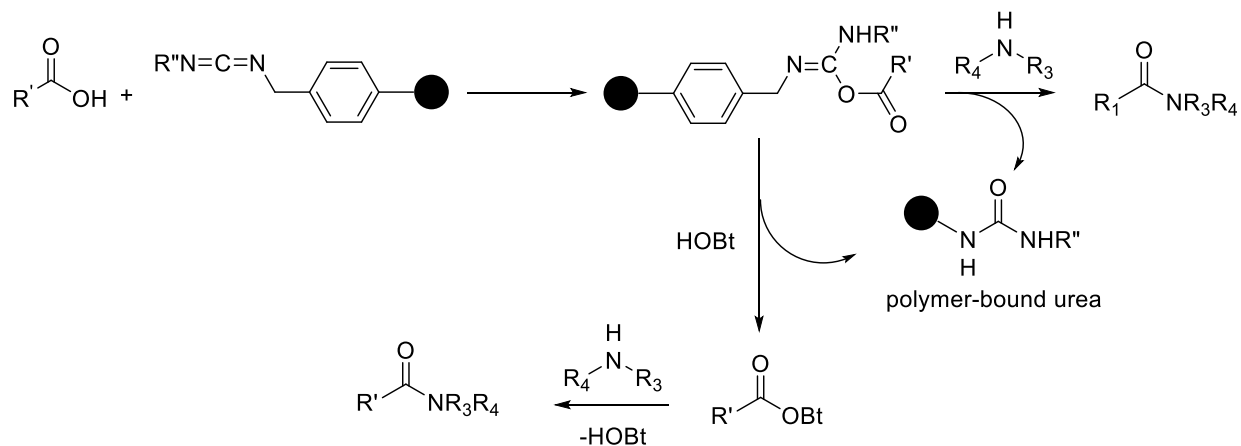
Scheme 1.5. *General mechanism for using polymer-supported carbodiimide as a coupling agent.[11]*

1.2.2 Propyl phosphonic acid cyclic anhydride (T3P)

One of the most attractive coupling agents, beside carbodiimides, is propyl phosphonic acid cyclic anhydride (T3P, Figure 1.4), due to its high yield, low toxicity, environmental friendliness and ease of work-up.[12,13] T3P can be used in a one-pot synthesis of amides typically in combination with amine bases such as *N,N*-diisopropylethylamine (DIEA or DIPEA or i-Pr$_2$NEt) or triethylamine (TEA) (Scheme 1.6). The by-product is highly water-soluble and easily removed by aqueous work-up.[8,12–16] Using T3P is more convenient and is used in a variety of processes, including, peptide synthesis/coupling of amino acids[13] (Scheme 1.7), the conversion of a carboxylic acid to aldehyde[17] and the reduction of a carboxylic acid to an alcohol[14] (Scheme 1.8). Therefore, T3P is an interesting coupling agent in an organic reaction.
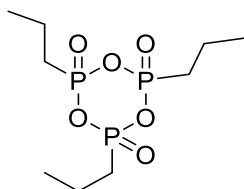
Figure 1.4. *Chemical structure of T3P.[13]*
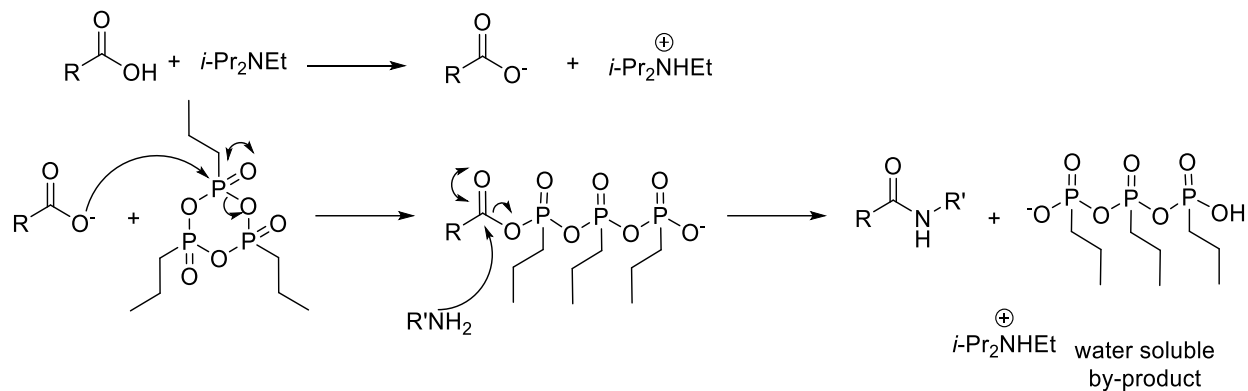
Scheme 1.6. *T3P mechanism of amide formation from carboxylic acid with amimes.*[8]
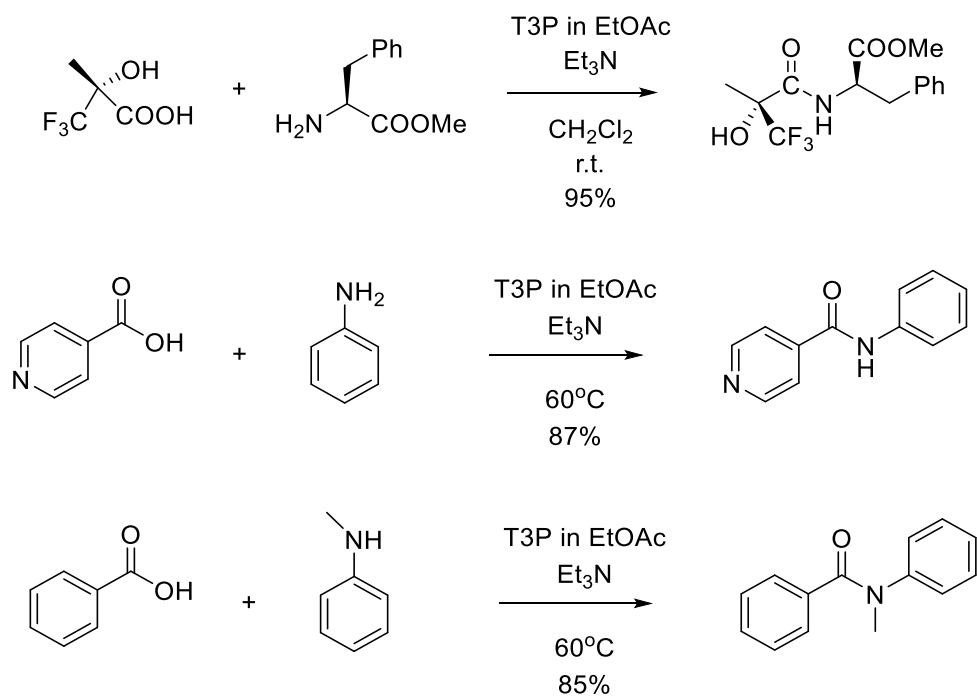
Scheme 1.7. *Coupling of an amino acid, aromatic and heteroaromatic acids with primary and secondary amines.*[13]
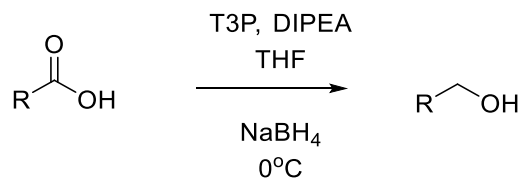
Scheme 1.8. *General reaction for the reduction of carboxylic acid using T3P/NaBH₄.*[14]

1.2.3 *N*-[(dimethylamino)-1*H*-1,2,3-triazolo[4,5-b]pyridin-1-ylmethylene]-*N*-methylmethanaminium hexafluorophosphate *N*-oxide (HATU)

HATU is widely used in pharmaceutical and drug companies because it shows fast reactions with less epimerization.[1,8,13,16] The general mechanism for amide formation using HATU as the coupling agent is exemplified in Scheme 1.9. The carboxylic acid is deprotonated by base such as DIEA or TEA. The resulting the carboxylate anion reacts with HATU to form an activated ester displacing HOAt as the leaving group. HOAt then attacks the activated ester again to obtain the activated HOAt ester and tetramethylurea as by-products. The amine now with activated HOAt ester to form the desired amide product.[1,8]
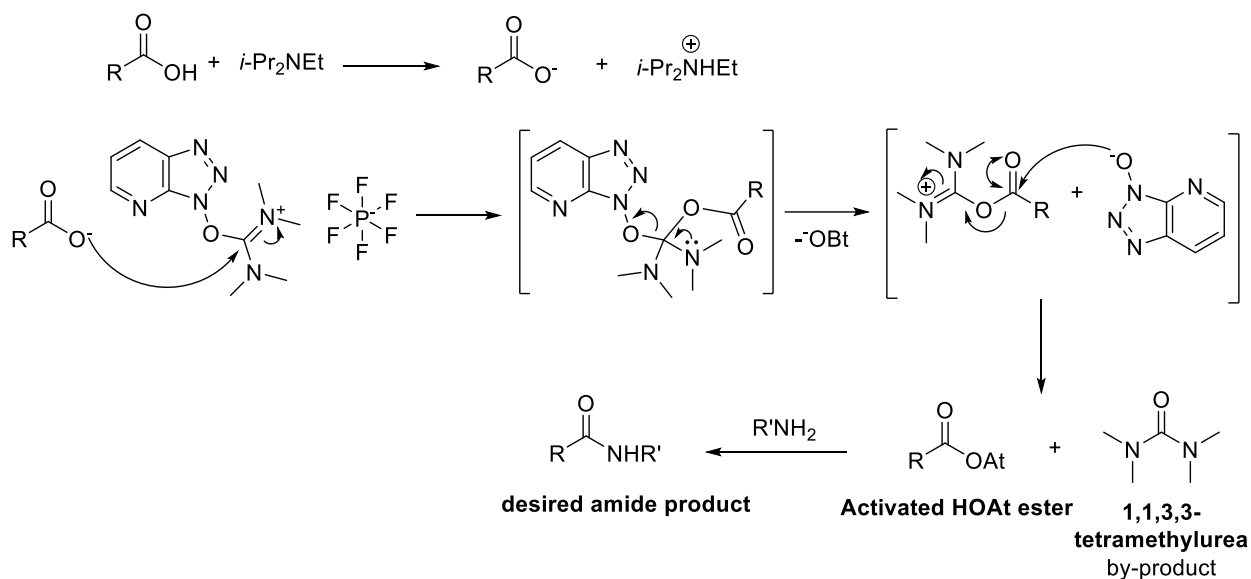
Scheme 1.9. *One-pot HATU coupling mechanism.*[8]

1.3 Sulfonamide compounds in medicinal chemistry

The first reported sulfonamide drug (Prontosil, Figure 1.5) was discovered by Josef Klarer and Fritz Mietzsch as they conducted research into designing new dyes in Bayer factory with shared workroom with Gerhard Domagk.[18] In 1932, Gerhard Domagk tested prontosil and it showed antibacterial activity, he also received the Nobel Prize in Medicine in 1939.[19] The discovery of prontosil led to the production of many types of drugs.

Prontosil
(Antibacteria)
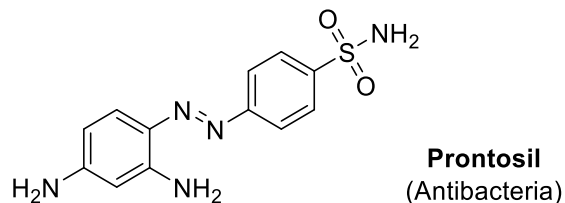
Figure 1.5. The structure of the first sulfonamide drug.[18]

Sulfonamides have many agricultural and drug uses, such as in antibiotics, cardiovascular, infectious, cancer and neurological diseases, examples of which are shown in Figure 1.6 including a few examples of functional groups related to sulfonamides.[19–21] Sildenafil is used for the treatment of erectile dysfunction. Sotalol is used to treat atrial fibrillation and prevent heart rhythms (arrhythmia). Zonisamide is an anticonvulsant. Amprenavir is treatment for HIV infection. Amsacrine is used to treat acute adult leukaemias and malignant lymphomas but has poor activity in solid tumour treatment. It is frequently used in combination with other antineoplastic agents in chemotherapy protocols. Benzthiazide is used to treat high blood pressure and edema.[2–5,19–22]

Sildenafil (Viagra)   **sotalol**   **Zonisamide** (*Zonegran*)

Amprenavir   **Amsacrine**   **Benzthiazide**
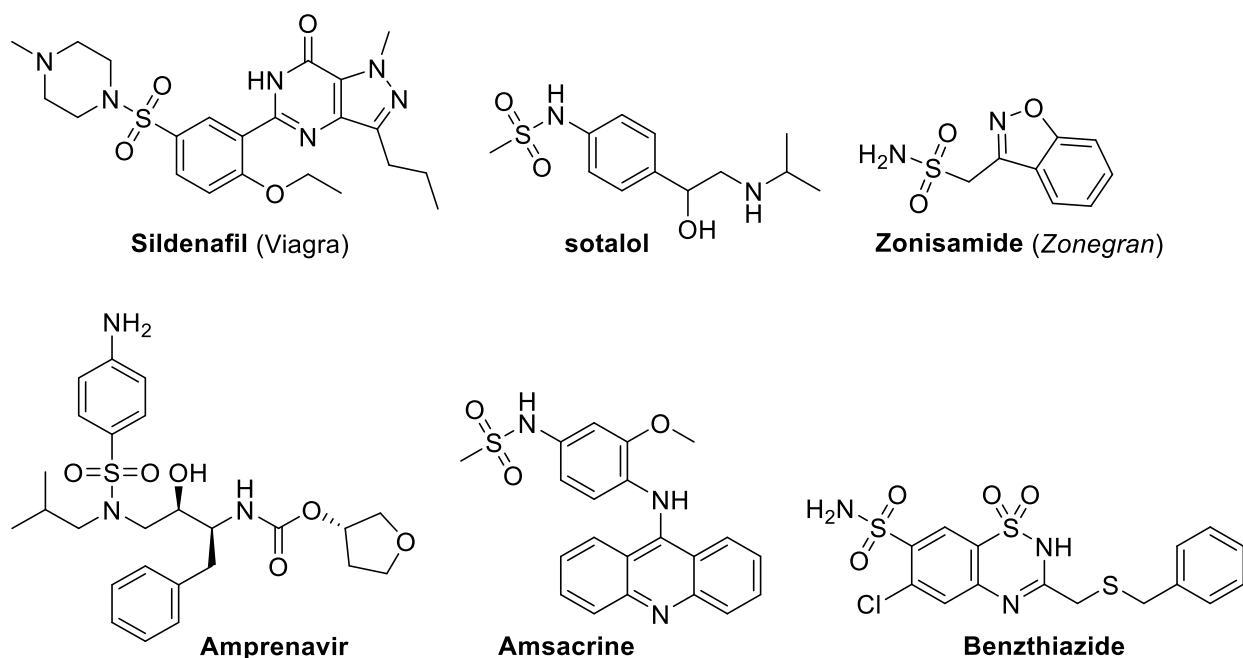
Figure 1.6. Example of top drugs containing sulfonamide.[2–6,19–22]

1.4 Sulfonamide synthesis

Sulfonamides are typically prepared one of several methods. 1) the direct reaction between a sulfonyl chloride and an amine in the presence of a base, the so-called classical method (Scheme 1.10). 2) Using other sources of -SO$_2$ substrates, for example, sulfonic acid, thiol derivatives, etc. Although there are now many ways to produce sulfonamides, the classical method is still in widespread use today. This method shows considerable effectiveness in terms of good reactivity, yield and simplicity. However, there are drawbacks, including the production of acid during the reaction, necessitating, a base to trap this.[19,23,24] However, in some works, there is no need for a base to trap the acid and these displayed good reactivity with both simple and complex amines, which is eco–friendly.[25–28] Therefore, the classical route without using bases was chosen in this research to synthesise sulfonamide libraries.
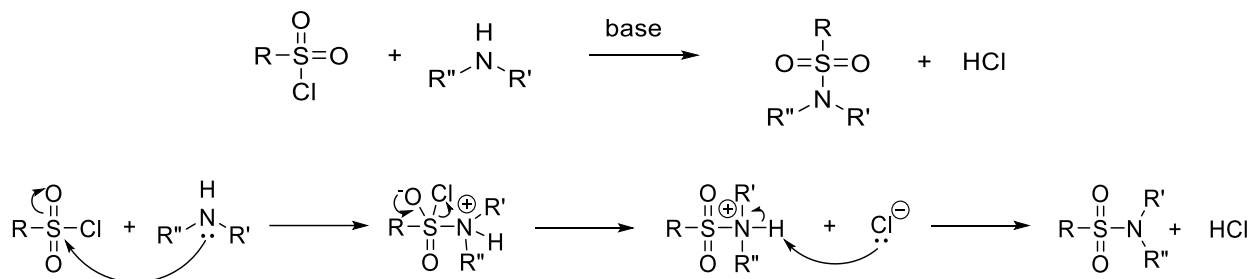
Scheme 1.10. *Classical route to synthesise sulfonamide compounds and mechanism.*

1.5 Acid isosteres

Carboxylic acids are important functional groups in medicinal chemistry, as shown in Figure 1.7. Valproic acid is used to treat epilepsy, bipolar disorder and migraines. Non-steroidal anti-inflammatory drugs (NSAID)s include benoxaprofen (analgesic and anti-inflammatory), diclofenac (pain killer and anti-inflammatory).[29,30] Carboxylic acids have a pK$_a$ value around 3 - 5 depending on the neighbouring groups in their structure and therefore readily ionise to carboxylate ions to improve solubility of drugs in water. However, there are some drawbacks to carboxyl groups in a molecule. For example, the negative charge of the molecule (from the carboxylate group) due to its low pK$_a$ (typically 3 - 5) often means that it cannot permeate through the central nervous system (CNS) or

through a cell membrane, limiting permeability.[30,31] Additionally, drug toxicity, from metabolism of the carboxylic acid moiety in the body, has been found.[29,30] To address this concern, the replacement of carboxylic acids with groups that display similar properties (bioisostere) have been investigated, these replacements often show comparable biological activities and improve safety margins.[29–31]
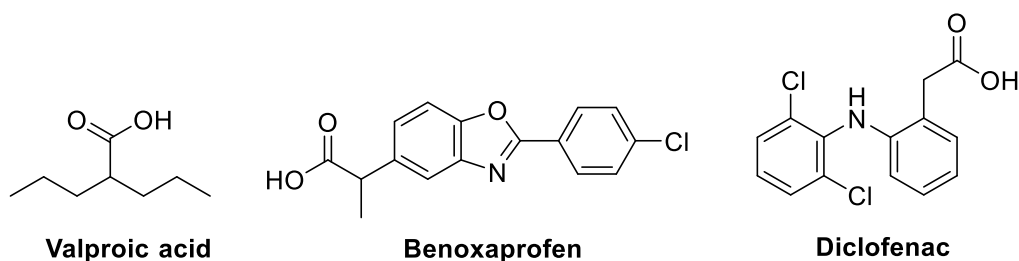
Figure 1.7. *Some drugs containing a carboxylic acid group.*
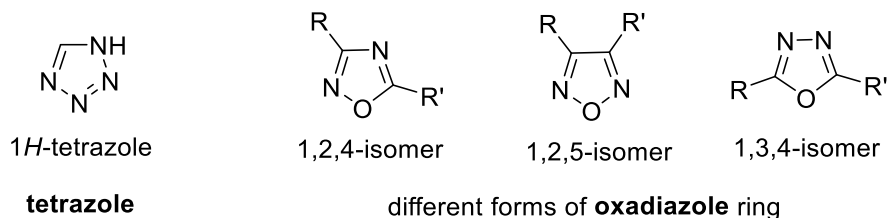
Figure 1.8. *Chemical structure of nonclassical isosteres.*
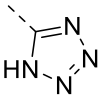
A bioisostere is defined as atoms or molecules that display similar physical and chemical properties, providing broadly similar biological activities. They are classified into two groups: 1) classical isosteres which are functionalities that do not differ much from the original moiety in terms of valence electrons and size, for example, sulfonic acids, phosphonic acids and sulfonamides and 2) nonclassical isosteres which are dramatically different in terms of steric size and the number of atoms from the original group, for instance, tetrazoles and oxadiazoles (Figure 1.8).[30,32] There are numerous carboxylic acid (bio)isosteres, including hydroxamic acids, phosphonic acids, sulfonamides etc. Out of these, tetrazoles are the most commonly used as the representative carboxylic acid (bio)isosteres.

Tetrazoles

Tetrazole is an interesting molecule that is regularly employed as a carboxylic acid bioisosteres.[33] They have been used for many applications, such as anti-bacterial, anti-cancer and anti-hypertensive.[30,34] Interestingly, the exemplar case for tetrazole as a carboxylic acid bioisostere is Losartan. Losartan is a drug which is used to treat hypertension, diabetic nephropathy and to lower the risk of stroke.[2–5,30]

Table 1.1. *In vivo activity of carboxylic acid vs tetrazole bioisostere.*
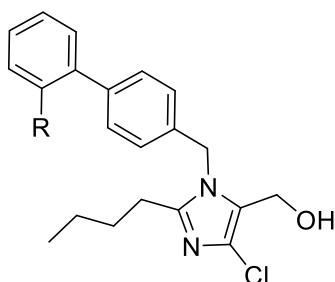
Compound	R	IC_{50}^{a} (µM)	Dose^b (mg/kg)	
			iv	po
1.1	-COOH	0.23	3	11^c
1.2 (**Losartan**)	(tetrazole)	0.019	0.80^c	0.59^c

^{a} Inhibition of specific binding of [^{3}H]angiotensin II (2 nM) to rat adrenal cortical microsomes.

^{b} Intravenous (iv) and oral (po) dose at which statistically significant drops in blood pressure were observed (>15 mmHg) in renal hypertensive rats.

^{c} Value given is ED_{30}, which is the effective dose in mg/kg that lowers the blood pressure by 30 mm Hg.

From Table 1.1, the corresponding carboxylic acid (compound **1.1**) has nearly a twenty-times higher effective dose (oral ED$_{30}$ 11 mg/kg) when compared with Losartan (oral ED$_{30}$ 0.59 mg/kg). The presence of a tetrazole in Losartan led to improved biological activity than the carboxylic acid (compound **1.1**) after oral administration.[31,32,35,36]
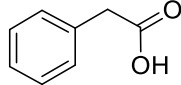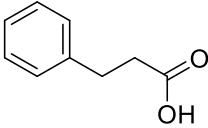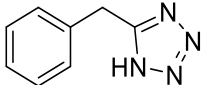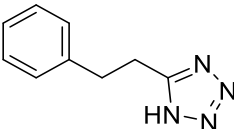
Tetrazole not only has a comparable pK$_a$ (although typically higher cLogP values) to a carboxylic acid, but it also has a higher permeability.[37] Tetrazole typically exists in equilibrium between 1*H* and 2*H*-tetrazole tautomer forms (Scheme 1.11) and some of the evaluation data (Table 1.2) are derived from Kato et al.[30]

1-*H*-tetrazole   2-*H*-tetrazole
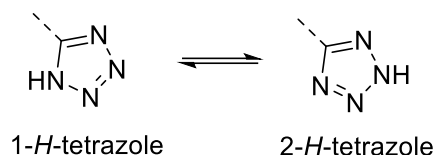
Scheme 1.11. Tautomers between 1H and 2H-tetrazole.[31]

The authors accumulated data including the acidity (pK$_a$) (determined by capillary electrophoresis), lipophilicity (logD$_{7.4}$) which is determined by the distribution coefficient between *n*-octanol and aqueous buffer at pH 7.4 and permeability (logP$_{app}$) (determined by a PAMPA assay (parallel artificial membrane permeability assay)). The PAMPA assay is a method that is used as an *in vitro* model of passive permeation of drug candidates through artificial membranes.[38] From Table 1.2, it was found that tetrazole displayed slightly higher pK$_a$ value and logD$_{7.4}$ but a lower logP$_{app}$ than the corresponding carboxylic acid. This shows that tetrazoles are less acidity and permeability, but higher lipophilicity than a carboxylic acid. The permeability might be related to the ionization of the molecules, as molecules with a neutral charge diffuse easily through membranes. However, the accumulated data is quite close, so tetrazole is an excellent surrogate for use in drug design and drug production.

Table 1.2. *Experimental property comparisons between carboxylic acid and tetrazole compounds.*[30,35]

Class	Compound	Structure	pK_a	$logD_{7.4}$	$logP_{app}$
Carboxylic acid	**1.1**		3.96	-1.5	ND
	1.2		4.64	-0.49 ± 0.19	-5.79 ± 0.10
Tetrazole	**1.3**		4.20	-1.0	ND
	1.4		5.09	-0.25 ± 0.10	-6.33 ± 0.15

Note: pK_a determined by capillary electrophoresis ; $logD_{7.4}$ determined by LC-MS; $logP_{app}$ determined in a parallel artificial membrane permeability assay (PAMPA); ND: not determined.

1.6 Key drug properties and SWISS ADME prediction

Drugs continue to be widely developed as improved treatments to known diseases and due to the emergence of new one, for example, Covid-19. The drug development processes before FDA approval takes many years (12- 16) and can costs more than a few billion dollars.[39] Drug candidates are selected based on various including physicochemical properties, structure-property relationships (SPR), pharmacokinetics and toxicity. For example, in some cases, despite having high potency, the selected substance may have poor solubility or oral bioavailability, which can contribute to its failure in clinical trials.[40] In order to increase the speed and potential for drug candidate screening, computational calculation programs have been developed such as Acceryls

company, CambridgeSoft and SwissADME.[41] The latter is a free online tool used to model/predict some key drug properties.

1.6.1 SwissADME online tool

The SwissADME online tool is used to predict drug candidates' pharmacokinetics, bioavailability drug-likeness and medicinal chemistry "friendliness." The SwissADME tool screens potential drug molecules using computer calculations to estimate individual absorption, distribution, metabolism and excretion (ADME) parameters. The ADME data, Lipinski's 'rule of five' and Veber's rules are considered along with experimental data to select the appropriate molecules to be drug candidates for further studies. The free web tool displays in Google (www.swissadme.com) and was developed by Daina et al.[42–45]

1.6.2 Physicochemical properties

The physicochemical properties are gained from the calculation, which are the molecular formula, molecular weight, number of heavy atoms, number of aromatic heavy atoms, number of rotatable bonds, number of H-bond acceptors, number of H-bond donors, molar refractivity and topological polar surface area (TPSA). These data can then be considered along with other variables to find appropriate drug candidates for further study.

1.6.3 Lipophilicity

Lipophilicity refers to the ability of a compound to partition between a non-polar solvent and a polar solvent. It is represented either as a partition coefficient (logP) or a distribution coefficient (logD). LogP is the partition coefficient of a compound between a non-polar solvent (usually *n*-octanol) and a polar solvent (water), where all the molecules are in the unionised form. LogD is the partition coefficient of the compound between a non-polar solvent (usually *n*-octanol) and a polar solvent (buffer) but at a specific pH where all the molecules are in the ionised form.[46] Lipophilic molecules typically permeate

through a cell membrane more easily than lipophobic molecules. High lipophilicity promotes oral bioavailability via absorption in the gastrointestinal tract. Three experiments are used for lipophilicity measurement: scaled-down shake flask, reversed-phase high-performance liquid chromatography (HPLC) and capillary electrophoresis (CE).[46,47] *In silico* methods include various prediction software sources such as Discovery Studio form Acceryls company, ChemDraw from CambridgeSoft and ADMET Predictor from Simulation Plus etc. The SwissADME software is one of reliable of the programs that analyse the lipophilicity of candidates with five different models i.e. XLOGP3, WLOGP, MLOGP, SILICOS-IT and iLOGP. [42,48–51]

1.6.4 Solubility

Solubility is one of the most important parameters in drug discovery because it is strongly related to biological activity, assay preparation and ADMET properties (absorption, distribution, metabolism, excretion and toxicity). Low solubility can also affect assay preparation because precipitation may occur. Low bioavailability is often caused by poor absorption. This can lead to high toxicity as more drug is required. Therefore, modification of molecules to increase solubility is required in drug development, such as the additional of an ionisable group (Figure 1.9 (a)), add hydrogen bond donors (HBD) (Figure 1.9 (b)) or adding polar groups (Figure 1.9 (c)). In-silico tools for screening drug candidates, as well as Lipinski's 'rule of five'(RO5), can be used to predict solubility during the early drug discovery process.

(a)

solubility 0.04 mg/mL
poor oral bioavailability

solubility 14000 mg/mL
more oral bioavailability

Mebendazole (anthelmintic drug)

(b)

solubility < 1 ug/mL   solubility 656 ug/mL
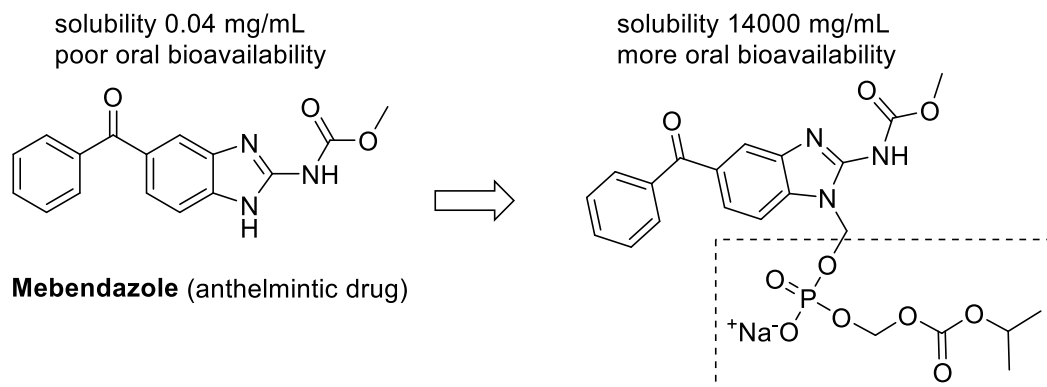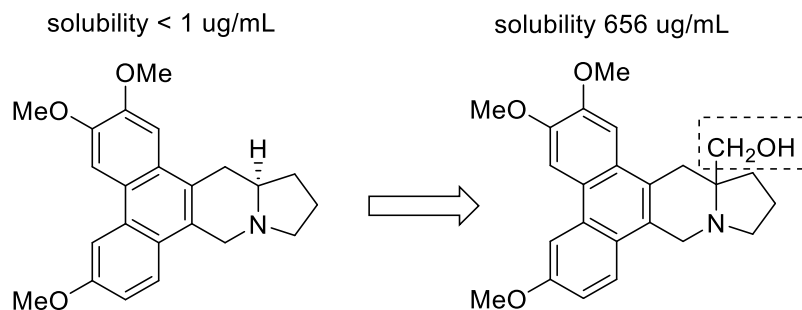
Antofine (against various cancer cell lines)

(c)

solubility 7 ug/mL   solubility 1.76 mg/mL

Third generation human
immunodeficiency virus type 1 (HIV1)
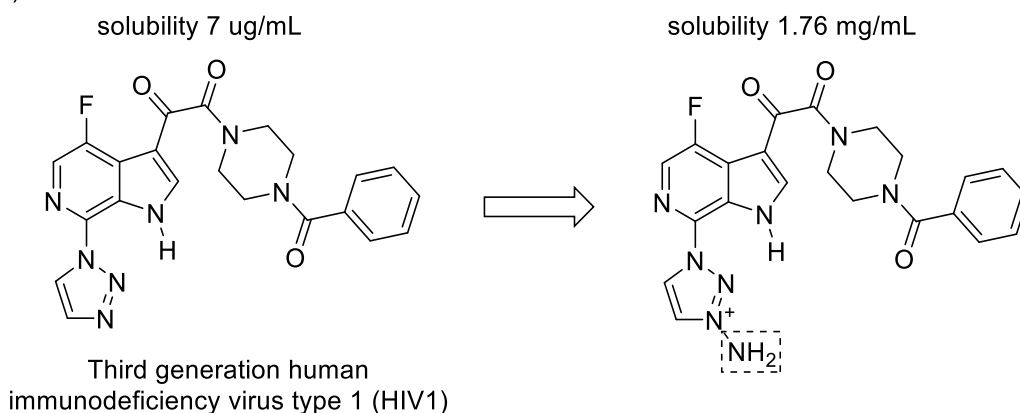
Figure 1.9. *Solubility improvement with adding ionisable group (a) hydrogen bond (b) and polar group (c).*[40,52]

1.6.5 Prediction rules

1.6.5.1 Lipinski's 'rule of five'(RO5)

Lipinski's 'rule of five'(RO5) is used to predict good passive oral availability for a drug and also design the chemistry behavior of the drug in the desired way. To formulate the rule, Lipinski *et al.* screened 2245 compounds from the World Drug Index (WDI).[38,53] These compounds showed superior physicochemical properties and do not contain a polymer, peptide, and O=P-O in the molecule. They found an 11% data set from the United States Adopted Names (USAN) had MW > 500, 10% had cLogP > 5 and 8% had the sum of OHs and NHs in the molecule be larger than 5. Therefore, RO5 defined four

physicochemical parameters that correlate with good absorption or permeation are favorable when:[38,54]

    1) molecular weight (MW) was less than 500 daltons (MW ≤ 500)

    2) partition coefficient log P-value was less than 5 (LogP ≤ 5)

    3) no more than 5 hydrogen bond donors were present (HBD ≤ 5)

    4) no more than 10 hydrogen bond acceptors were present (HBA ≤ 10)

The number of hydrogen bond donor-acceptor can indicate solubility of molecules in the aqueous phase. MW is proportional to molecule size; small molecules tend to absorb well in the intestinal tract and easily permeate through the biological membrane. LogP or clogP (from computational calculation) indicate the lipophillicity of molecule, increasing the LogP reduces absorption.

1.6.5.2 Veber rules

Additionally, Veber rules are also used to predict further parameters. There were 1100 drug candidates analysed which showed a 20% success rate for rat oral bioavailability.[38,55] Based on the authors formulated, Veber rules state that a compound with no more than 10 rotatable bonds, and a polar surface area (PSA) below 140 $Å^2$ (or total hydrogen bond count less than 12) has a high predicted oral bioavailability.[38]

1.6.6 Egan BOILED-Egg

ADME properties are predicted from calculations with the graphical classification model Egan BOILED-Egg. An egg plot is a graph between WLOGP (*y* axis)[51] *versus* TPSA(*x* axis) as shown in Figure 1.10. There are 3 parts of egg plot including an egg yolk (yellow area) which defines a high probability of brain penetration (blood-brain barrier: BBB) while an egg white (white region) defines a high probability of passive absorption by the human gastrointestinal (HIA) tract and grey part is no HIA or BBB access. Additionally, the blue points describe molecules predicted to be actively effluxed from the

central nervous system (CNS) by P-glycoprotein (PGP; PGP+), while red dots indicate molecules predicted as non-substrates of PGP (PGP−). The example of small molecule candidates A, B, C and D are plotted in the BOILED-Egg as shown in Figure 1.10, molecule A is predicted as brain-penetrate in the yolk and not subject to active efflux (red dot) while molecule B is predicted as same as molecule A with a BBB permeability, but actively substrates effluxed from the brain (blue dot). Molecule C was in the white region that is predicted to be well absorbed but has no BBB access. Molecule D is in the grey region, indicating that it has a low absorption and limited brain penetration.
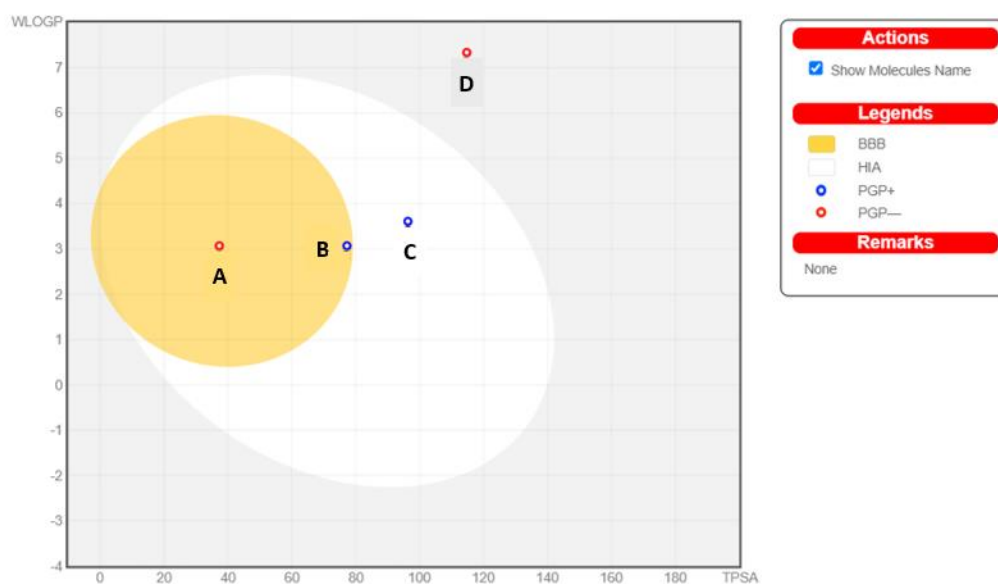
Figure 1.10. *The BOILED-Egg representation for prediction of passive gastrointestinal absorption (HIA) and brain penetration (BBB) of the small molecules (A, B, C and D) in the WLOGP-versus-TPSA graph.*

1.7 Metabolic stability of amides

In drug development, metabolite stability is also an important role in the medicinal chemistry process. High potency, good ADME properties and low toxicity are desirable. However, in some cases, poor bioavailability and toxic metabolites are found with a high clearance rate and high metabolic liability[56] or some drug candidates showed high activity in vitro but high metabolism in the body.[57] Metabolic studies are the half-life, $t_{1/2}$ (min or

hr) that is expressed as the time for 50% disappearance of the parent compound and the clearance, CL (µL/min per mg protein or per million cells). The CL is the volume of drug per unit of time when it passes through a clearance organ such as the liver (the important elimination pathway), kidney, etc.[58] The benefits of improving metabolic stability include increased bioavailability and longer half-life, which allow patients to use a lower dosage. Unfortunately, 462 medicinal products were withdrawn from the post-market because of adverse drug reactions between 1953-2013.[59] Merck & Co. removed rofecoxib (Viox) from market in the year 2004. It was used to treat steoarthritis, rheumatoid arthritis, acute pain, primary dysmenorrhea, and migraine attacks. Long-term usage of rofecoxib led to an increased risk of cardiovascular events and strokes.[60] Valdecoxib was used to treat osteoarthritis and dysmenorrhoea but was also withdrawn due to the risk of heart attact and stroke.[61] Alatrofloxacin was developed by Pfizer and used to treat a variety of bacterial infections but with adverse effects including liver toxicity leading to liver transplant or death; thus, alatrofloxacin was withdrawn in 2006.[61] Some of the withdrawn chemical structures are shown in Figure 1.11.
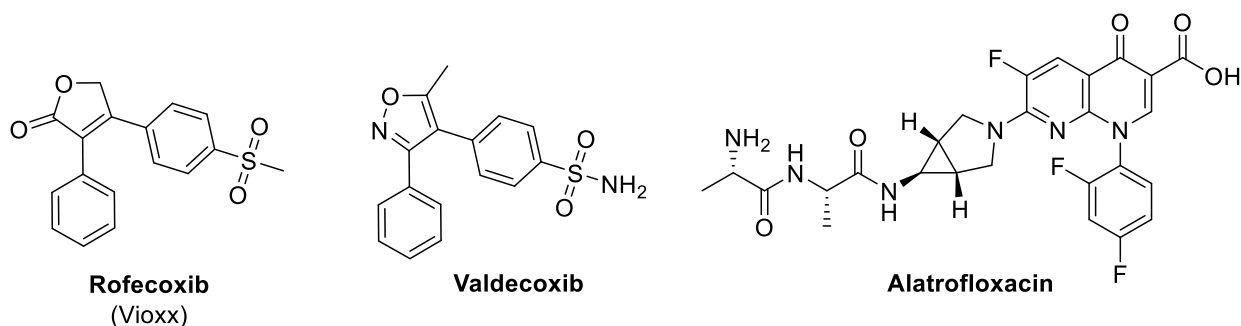
Figure 1.11. *Example of withdrawn drugs.*

Therefore, structural modifications for enhancing metabolite stability and reducing toxicity are often investigated. There are various ways to improve metabolite stability, for instance, replacement of an amide bond with an amide or acid bioisostere, replacement of a labile ester linkage with an amide group, etc. Examples of metabolite stability improvements are displayed in Figure 1.12; the development of an HIV inhibitor was studied by replacement of a 3-isopropyl amino (compound **1.3**) with ethoxy group (compound **1.4**) which increased 4-fold metabolic stability in rat liver microsomes (RLM).[56] In addition, amide bond replacement by a bioisostere can also provide enhanced

metabolic stability, biological properties and prolonging of the desired therapeutic effect. From Figure 1.12, the compound 2-(2-benzamido)ethyl-4-phenylthiazole (**1.5**) inhibited T. brucei rhodesiense growth. It was found that one of the derivatives, (*S*)-*N*-(2-(4-(3,4-difluorophenyl)thiazol-2-yl)ethyl)-3-fluoropyrrolidine-1-carboxamide (**1.6**) also exhibited good potency with low EC_{50} value, metabolic stability of more than 60 min in both mouse and human liver microsomes (MLM $t_{1/2}$ = 1.1 min and HLM $t_{1/2}$ = 28 min respectively) and no toxicity in human cell lines.[62] The effect of stereochemistry on metabolic stability is established for the *N*-hydroxyurea inhibitor of 5-lipoxygenase, compound **1.8** (*R*-configuration), which showed better metabolic stability than compound **1.7** (*S*-configuration).[62] Tetrazole is incorporated as an acid bioisostere (compound **1.10**), which showed good potency as an inhibitor of *S*-nitrosoglutathione reductase (GSNOR) and also found high metabolic stability in human and rat liver microsomes.[63] Therefore, various modifications in chemical structure can help improve metabolic stability, physicochemical properties and potency to produce good effective and safe drugs to the future.

1.3
Metabolic stability in RLM $t_{1/2}$ = 10.8 min

1.4
Metabolic stability in RLM $t_{1/2}$ = 46.8 min

1.5
EC_{50} = 0.191 uM
Metabolic stability in
MLM $t_{1/2}$ = 1.1 min
HLM $t_{1/2}$ = 28 min

1.6
EC_{50} = 0.0348 uM
Metabolic stability in
MLM $t_{1/2}$ = > 60 min
HLM $t_{1/2}$ = > 60 min

1.7

Metabolic stability in monkey liver and plasma
$t_{1/2}$ = 7.70 h

1.8

Metabolic stability in monkey liver and plasma
$t_{1/2}$ = 8.70 h

1.9

IC_{50} = 20 nM
Metabolic stability in
RLM = 64 %*
HLM = 100 %*

1.10

IC_{50} = 14 nM
Metabolic stability in
RLM = 68 %*
HLM = 99 %*

Figure 1.12. *Metabolic stability improvement by bioisostere. *Percentage of compound remaining after 60 min incubation.*[40,52,62]

1.8 Protein X-ray crystallography and protein crystallization

X-ray crystallography is a technique that obtains a three-dimensional molecular structure from a crystal. Interesting samples, such as proteins, nucleic acid, or viruses, are crystallised at a suitable concentration. Crystals are bombarded with an X-ray beam and the resulting diffraction pattern is collected. The diffraction pattern is further analysed to produce an electron density map, into which an atomic model can be built (Figure. 1.13).[64,65]

Protein crystallization was first accidentally discovered in hemoglobin of earthworm blood by Friedrich Ludwig Hünefeld in 1840. After that, many scientists continued to investigate crystals of protein and succeeded to crystallise enzymes causing a significant increase in the need for protein crystals in the 1960s and 1970s.[66,67] At present, protein crystallization technology is advancing and being researched significantly, playing an important role in biochemistry and medicine. One major challenge is the growth of protein crystals. The factors that affect protein crystallisation are

concentration, precipitant, buffer, additive, temperature and the crystallisation technique. The concentration of solution required needs to be enough to enable the crystals to come out of solution and grow under optimum conditions. Figure 1.14 shows a solubility diagram, which correlates protein and salt concentration, divided into 4 regions; 1) undersaturation, the low concentration of solution was not sufficient for precipitation, 2) Metastable (crystal growth), 3) Metastable (nucleation), and 4) precipitation region, very high concentration caused protein to became an amorphous solid.[66] Starting from the black arrow, starting from the soluble state (undersaturation), when we reach the nucleation zone proteins (light blue circle) become bigger then protein crystals occurred. After that, the protein concentration is reduced due to nuclei production then they moved to the crystal growth zone for growing protein crystals.[66,67]
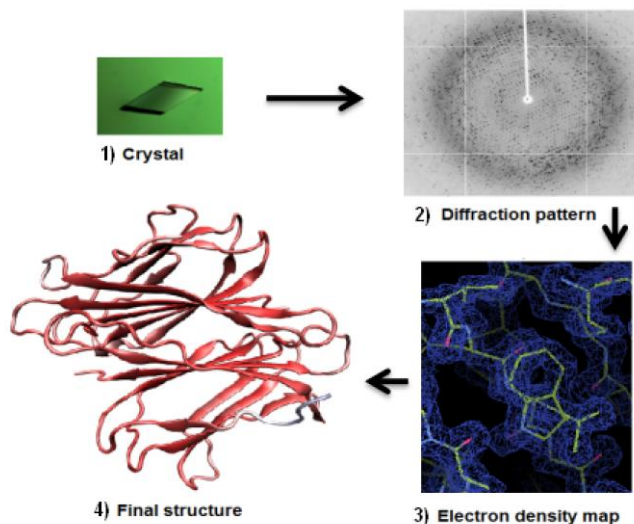
Figure 1.13. The methods to obtain 3D structure from X-ray crystallography.[64,65]

There are several techniques to obtain single crystals[66] but the commonly used one is vapour diffusion. In this experiment used the sitting drop vapour diffusion method to produce single crystals as shown in Figure 1.15. The crystallisation drop (0.5 µL) contained half of the stock protein solution and half of reservoir, which, was composed of salt or polymer precipitant. Water in the crystallisation drop diffuses to the reservoir

causing the concentration of protein and precipitant to increase slowly and reach a chemical equilibrium as a result of supersaturated solution which leads to the crystallisation process.
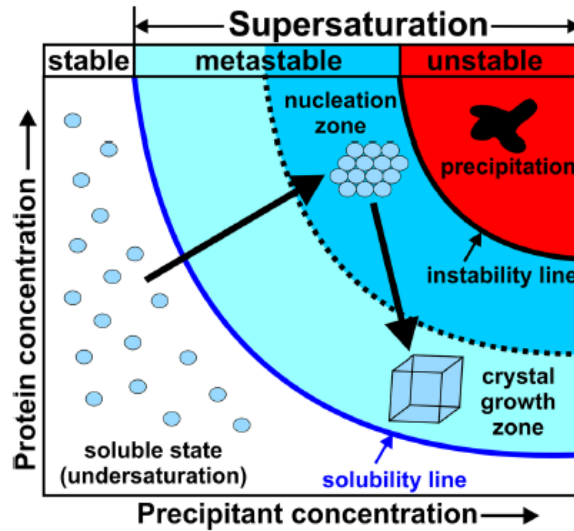
Figure 1.14. Protein crystallisation phase diagram.[66]
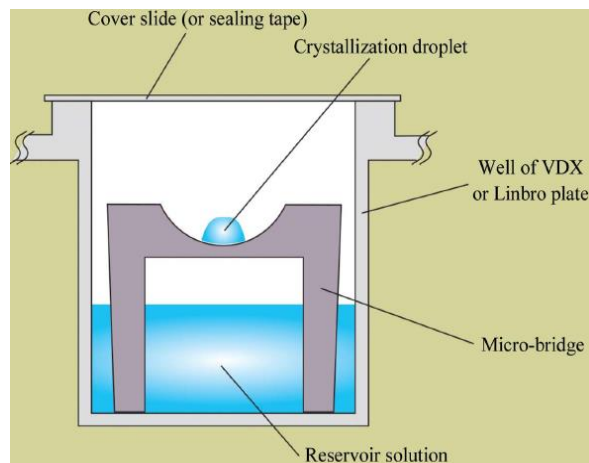
Figure 1.15. The sitting drop vapor diffusion method.[67]

1.9 Objectives

The aims of this thesis are to make libraries (random or focussed) of amides, sulfonamides, ureas in multidisplinary projects working alongside biologists.

Chapter 2 examines mainly sulfonamides and hydrazides with antibacterial properties, based on fragment hits.

Fragment I   Fragment II
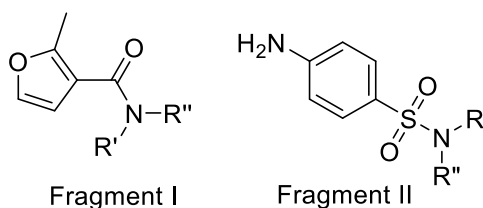
Chapter 3 looks at a leukemia targeting amides based on a 7-membered scaffold.
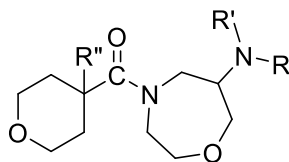
Chapter 4 looks at mainly amide and ureas in scaffolds acting on ion channels involved in pain signalling.
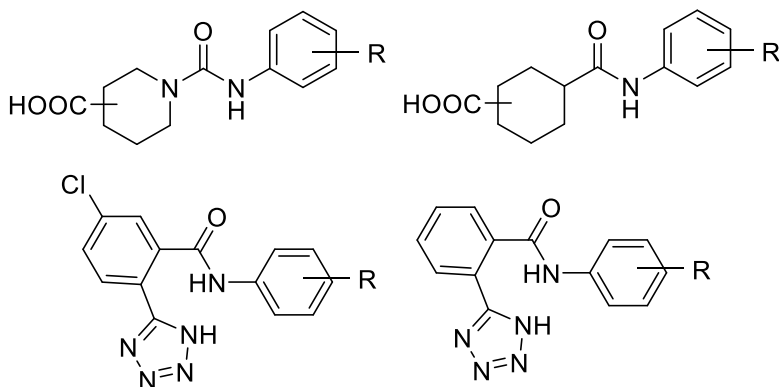
Chapter 5 is a summary and future directions section.

1.10 References

1   C. A. G. N. Montalbetti and V. Falque, *Tetrahedron*, 2005, **61**, 10827–10852.

2   D. S. Wishart, C. Knox, A. C. Guo, S. Shrivastava, M. Hassanali, P. Stothard, Z. Chang and J. Woolsey, *Nucleic Acids Res.*, 2006, **34**, D668–D672.

3   D. S. Wishart, Y. D. Feunang, A. C. Guo, E. J. Lo, A. Marcu, J. R. Grant, T. Sajed, D. Johnson, C. Li, Z. Sayeeda, N. Assempour, I. Iynkkaran, Y. Liu, A. Maclejewski, N. Gale, A. Wilson, L. Chin, R. Cummings, Di. Le, A. Pon, C. Knox and M. Wilson, *Nucleic Acids Res.*, 2018, **46**, D1074–D1082.

4   C. Knox, V. Law, T. Jewison, P. Liu, S. Ly, A. Frolkis, A. Pon, K. Banco, C. Mak, V. Neveu, Y. Djoumbou, R. Eisner, A. C. Guo and D. S. Wishart, *Nucleic Acids Res.*, 2011, **39**, D1035–D1041.

5   V. Law, C. Knox, Y. Djoumbou, T. Jewison, A. C. Guo, Y. Liu, A. Maclejewski, D. Arndt, M. Wilson, V. Neveu, A. Tang, G. Gabriel, C. Ly, S. Adamjee, Z. T. Dame, B. Han, Y. Zhou and D. S. Wishart, *Nucleic Acids Res.*, 2014, **42**, D1091–D1097.

6   D. E. Becker and K. L. Reed, *Anesth. Prog.*, 2012, **59**, 90–102.

7   C. L. Allen and J. M. J. Williams, *Chem. Soc. Rev.*, 2011, **40**, 3405–3415.

8   J. R. Dunetz, J. Magano and G. A. Weisenburger, *Org. Process Res. Dev*, 2016, **20**, 140–177.

9   E. Valeur and M. Bradley, *Chem. Soc. Rev.*, 2009, **38**, 606–631.

10   D. A. East, D. P. Mulvihill, M. Todd and I. J. Bruce, *Langmuir*, 2011, **27**, 13888–13896.

11   P. Cherkupally, S. Ramesh, B. G. De La Torre, T. Govender, H. G. Kruger and F. Albericio, *ACS Comb. Sci.*, 2014, **16**, 579–601.

12   M. Desroses, K. Wieckowski, M. Stevens and L. R. Odell, *Tetrahedron Lett.*, 2011, **52**, 4417–4420.

13   T. M. Vishwanatha, N. R. Panguluri and V. V Sureshbabu, *Synthesis (Stuttg).*,

2013, **45**, 1569–1601.

14   G. Nagendra, C. Madhu, T. M. Vishwanatha and V. V. Sureshbabu, *Tetrahedron Lett.*, 2012, **53**, 5059–5063.

15   A. Llanes García, *Synlett*, 2007, **2007**, 1328–1329.

16   O. Al Musaimi, R. Wisdom, P. Talbiersky and G. D. La Torre, *Chem. Sel.*, 2021, **6**, 2649–2657.

17   F. Burkhart, M. Hoffmann and H. Kessler, *Angew. Chemie (International Ed. English)*, 1997, **36**, 1191–1192.

18   R. P. Rubin, *Intern. Med. Res. Open J.*, 2018, **3**, 1–6.

19   S. Mondal and S. Malakar, *Tetrahedron*, 2020, **76**, 1–38.

20   C. Zhao, K. P. Rakesh, L. Ravidar, W. Fang and H. Qin, *Eur. J. Med. Chem.*, 2019, **162**, 679–734.

21   F. Yousef, O. Mansour and J. Herbali, *IN-VITRO IN-VIVO IN-SILICO*, 2018, **1**, 1–15.

22   D. S. Wishart, C. Knox, A. C. Guo, D. Cheng, S. Shrivastava, D. Tzur, B. Gautam and M. Hassanali, *Nucleic Acids Res.*, 2008, **36**, D901–D906.

23   A. Yasuhara, M. Kameda and T. Sakamoto, *Chem. Pharm. Bull.*, 1999, **47**, 809–812.

24   A. V. Bogolubsky, Y. S. Moroz, P. K. Mykhailiuk, S. E. Pipko, A. I. Konovets, I. V. Sadkova and A. Tolmachev, *ACS Comb. Sci.*, 2014, **16**, 192–197.

25   A. C. Knipe and J. Lound-Keast, *J. Chem. Soc. Perkin Trans. 2*, 1976, **14**, 1741–1748.

26   M. Gollapalli, M. Taha, H. Ullah, M. Nawaz, L. M. R. AlMuqarrabun, F. Rahim, F. Qureshi, A. Mosaddik, N. Ahmat and K. M. Khan, *Bioorg. Chem.*, 2018, **80**, 112–120.

27   C. Bin Park, C. M. Ahn, S. Oh, D. Kwon, W. C. Cho, W. S. Shin, Y. Cui, Y. S. Um,

B. G. Park and S. Lee, *Bioorganic Med. Chem.*, 2015, **23**, 6673–6682.

28 R. Vangala, S. K. Sivan, S. R. Peddi and V. Manga, *J. Comput. Aided. Mol. Des.*, 2020, **34**, 39–54.

29 C. Skonberg, J. Olsen, K. G. Madsen, S. H. Hansen and M. P. Grillo, *Expert Opin. Drug Metab. Toxicol.*, 2008, **4**, 425–438.

30 K. Bredael, S. Geurs, D. Clarisse, K. De Bosscher and M. D'hooghe, *J. Chem.*, 2022, **2022**, 1–21.

31 B. Carlo, M. H. Donna and L. Amos, B. Smith, *ChemMedChem*, 2013, **8**, 385–395.

32 M. A. J. Duncton, R. B. Murray, G. Park and R. Singh, *Org. Biomol. Chem.*, 2016, **14**, 9343–9347.

33 M. A. Malik, M. Y. Wani, S. A. Al-Thabaiti and R. A. Shiekh, *J. Incl. Phenom. Macrocycl. Chem.*, 2014, **78**, 15–37.

34 Y. Zou, L. Liu, J. Liu and G. Liu, *Future Med. Chem.*, 2020, **12**, 91–93.

35 P. Lassalas, B. Gay, C. Lasfargeas, M. J. James, V. Tran, K. G. Vijayendran, K. R. Brunden, M. C. Kozlowski, C. J. Thomas, A. B. Smith, D. M. Huryn and C. Ballatore, *J. Med. Chem.*, 2016, **59**, 3183–3203.

36 D. J. Carini, J. V. Duncia, P. E. Aldrich, A. T. Chiu, A. L. Johnson, M. E. Pierce, W. A. Price, J. B. Santella, G. J. Wells, R. R. Wexler, P. C. Wong, S. E. Yoo and P. B. M. W. M. Timmermans, *J. Med. Chem.*, 1991, **34**, 2525–2547.

37 C. Liljebris, S. D. Larsen, D. Ogg, B. J. Palazuk and J. E. Bleasdale, *J. Med. Chem*, 2002, **45**, 1785–1798.

38 L. Di and E. H. Kerns, in *Drug-Like Properties Concepts, Structure Design and Methods from ADME to Toxicity Optimization*, Elsevier Inc., Second edi., 2016, pp. 29–38.

39 J. P. Hughes, S. S. Rees, S. B. Kalindjian and K. L. Philpott, *Br. J. Pharmacol.*, 2011, **162**, 1239–1249.

40   B. Das, A. T. K. Baidya, A. T. Mathew, A. K. Yadav and R. Kumar, *Bioorganic Med. Chem.*, 2022, **56**, 1–25.

41   L. Di and E. H. Kerns, in *Drug-Like Properties Concepts, Structure Design and Methods from ADME to Toxicity Optimization*, Elsevier Inc., second edi., 2016, pp. 299–306.

42   A. Daina, O. Michielin and V. Zoete, *Sci. Rep.*, 2017, **7**, 1–13.

43   A. Daina and V. Zoete, *ChemMedChem*, 2016, **11**, 1117–1121.

44   A. Daina, M. C. Blatter, V. Baillie Gerritsen, P. M. Palagi, D. Marek, I. Xenarios, T. Schwede, O. Michielin and V. Zoete, *J. Chem. Educ.*, 2017, **94**, 335–344.

45   A. Daina, O. Michielin and V. Zoete, *Chem. Inf. Model.*, 2014, **54**, 3284–3301.

46   L. Di and E. H. Kerns, in *Drug-Like Properties Concepts, Structure Design and Methods from ADME to Toxicity Optimization*, Elsevier Inc., second edi., 2016, pp. 39–50.

47   Ranjith D and Ravikumar C, *J. Pharmacogn. Phytochem.*, 2019, **8**, 2063–2073.

48   T. Cheng, Y. Zhao, X. Li, F. Lin, Y. Xu, X. Zhang, Y. Li, R. Wang and L. Lai, *J. Chem. Inf. Model.*, 2007, **47**, 2140–2148.

49   I. Moriguchi, H. Hirano and I. Nakagome, *Chem. Pharm. Bull.*, 1994, **42**, 976–978.

50   I. Moriguchi, S. Hirono, Q. Liu, I. Nakagome and Y. Matsushita, *Chem. Pharm. Bull.*, 1992, **40**, 127–130.

51   S. A. Wildman and G. M. Crippen, *J. Chem. Inf. Comput. Sci.*, 1999, **39**, 868–873.

52   L. Di and E. H. Kerns, in *Drug-Like Properties Concepts, Structure Design and Methods from ADME to Toxicity Optimization*, Elsevier Inc., Second Edi., 2016, pp. 61–93.

53   C. A. Lipinski, F. Lombardo, B. W. Dominy and P. J. Feeney, *Adv. Drug Deliv. Rev.*, 2001, **46**, 3–26.

54   C. A. Lipinski, *Drug Discov. Today Technol.*, 2004, **1**, 337–341.

55 D. F. Veber, S. R. Johnson, H.-Y. Cheng, B. R. Smith, K. W. Ward and K. D. Kopple, *J. Med. Chem*, 2002, **45**, 2615–2633.

56 A. E. F. Nassar, A. M. Kamel and C. Clarimont, *Drug Discov. Today*, 2004, **9**, 1020–1028.

57 L. Di and E. H. Kerns, in *Drug-Like Properties Concepts, Structure Design and Methods from ADME to Toxicity Optimization*, Elsevier Inc., second edi., 2023, pp. 161–194.

58 K. Słoczyńska, A. Gunia-Krzyzak, P. Koczurkiewicz, K. Wójcik-Pszczoła, D. Zelaszczyk, J. Popiół and E. Pękala, *Acta Pharm.*, 2019, **69**, 345–361.

59 I. J. Onakpoya, C. J. Heneghan and J. K. Aronson, *BMC Med.*, 2016, **14**, 1–11.

60 B. Sibbald, *CMAJ*, 2004, **171**, 1027–1028.

61 Z. P. Qureshi, E. Seoane-Vazquez, R. Rodriguez-Monguio, K. B. Stevenson and S. L. Szeinbach, *Pharmacoepidemiol. Drug Saf.*, 2011, **20**, 772–777.

62 S. Kumari, A. V Carmona, A. K. Tiwari and P. C. Trippier, *J. Med. Chem*, 2020, **63**, 12290–12358.

63 N. Muthukaman, S. Deshmukh, S. Tondlekar, M. Tambe, D. Pisal, N. Sarode, S. Mhatre, S. Chakraborti, D. Shah, V. M. Bhosale, A. Kulkarni, M. Y. A. Mahat, S. B. Jadhav, G. S. Gudi, N. Khairatkar-Joshi and L. A. Gharat, *Bioorganic Med. Chem. Lett.*, 2018, **28**, 3766–3773.

64 S. K. Mishra, G. Demo, J. Koca and M. Wimmerova, *Protein Eng.*, 2012, 307–344.

65 S. M S and M. J H J, *J Clin Pathol Mol Pathol*, 2000, 8–14.

66 A. Bijelic and A. Rompel, *ChemTexts*, 2018, **4**, 1–27.

67 A. McPherson and J. A. Gavira, *Acta Crystallogr. Sect. FStructural Biol. Commun.*, 2014, **70**, 2–20.

Chapter 2

Synthesis of a Library of Amides, Hydrazides, and Sulfonamides for the Potential Treatment of Bacterial Resistance

2.1 Background to the disease

Neisseria gonorrhoeae or gonococcus[1] is a disease caused by a gram-negative bacterium. Gonorrhea was found to be the second most sexually transmitted disease after chlamydia and is a public health problem worldwide.[2] The bacteria generally grow in moist and warm parts in the human body such as the throat, rectum, penis and vagina.[3,4] Gonorrhea is also found in the infected vagina and semen fluid. The spread of gonorrhea occurs primarily through unprotected sexual contact, including vaginal, oral or anal sex with infected partner. The infection does not occur by kissing, swimming in swimming pools, toilet seats or by sharing baths, towels, cups or wounds because the bacteria cannot live long outside of the body.[1] Moreover, gonorrhea can repeat infection in the same human being and easily transmit the pathogen to the others.[5] Gonorrhea is mostly found in young women aged between 15-25 years old.[6] The World Health Organization (WHO) estimated that around 82 million new cases of people were infected by *Neisseria gonorrhoeae* around the world (in 2020).[7]

The evolution and expansion of antimicrobial resistance (AMR) in *Neisseria gonorrhoeae* are serious problems. The European Gonococcal Antimicrobial Surveillance Program (Euro-GASP) reported resistance towards ciprofloxacin (Figure 2.1b), cefixime (Figure 2.1c) and azithromycin (Figure 2.1e) in many countries in Europe. For example, there was an increase in cefixime resistance levels from 0.9% to 12.1% between 2012 – 2014 in Belgium, and high levels of resistance towards azitromycin in Greece (40%) and ciprofloxacin in Italy (78.8%) in 2014.[8] In 2010 a report by the World Health Organization

(WHO) Western Pacific Region (WPR) and South East Asian Region (SEAR) showed widespread resistance to penicillin (Figure 2.1a), quinolone, azithromycin, ceftriaxone in Asia. There has been a high decreasing susceptibility to ceftriaxone and azithromycin was found in China (55.8%) and Mongolia (34%).[9] Therefore, an increasing rate of AMR and decreasing efficacy of drugs make gonorrhea treatment more difficult, requiring stronger drugs or multidrug medication. There is a challenge for scientists develop a new effective treatment, controlling the disease and preventing drug resistance in gonorrhea.

(a) **penicillin** (b) **ciprofloxacin** (c) **cefixime**

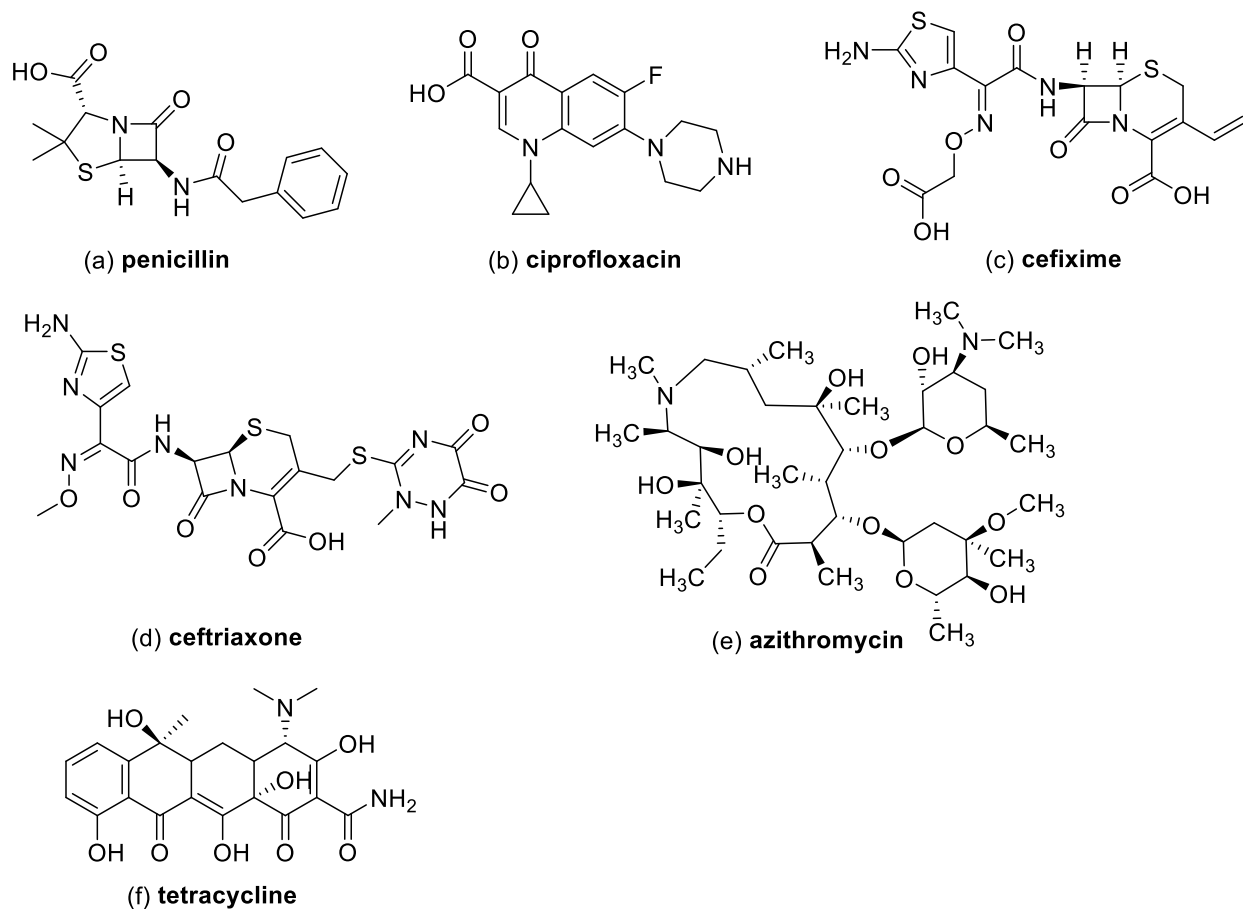(d) **ceftriaxone** (e) **azithromycin**

(f) **tetracycline**

Figure 2.1. *Structure of antibiotic drugs (a) penicillin, (b) ciprofloxacin, (c) cefixime, (d) ceftriaxone and (e) azithromycin (f) tetracycline.*

2.2 Treatments and evolution of drug resistance

In the mid-1930s Gerhard Domagk reported the first use of sulfonamides a treatment for gonorrhea in the mid-1930s.[10] Sulfanilimide (Figure 2.2a) displayed 80 - 90% effectiveness in the treatment of gonorrhea. In the early 1940's sulfapyridine (Figure 2.2b) was introduced as a new treatment. Sulfonamides compete with *p*-aminobenzoic acid (PABA) (which is a natural substance) for binding to the dihydropteroate synthase (DHPS) enzyme, which, leads to a lowered synthesis of folic acid that lowers DNA and protein synthesis in bacteria (Figure 2.3).[11]

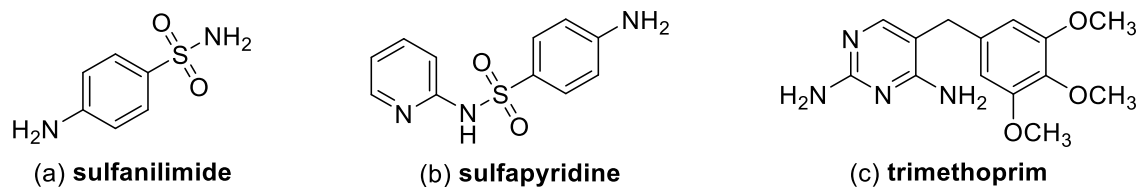(a) **sulfanilimide**   (b) **sulfapyridine**   (c) **trimethoprim**

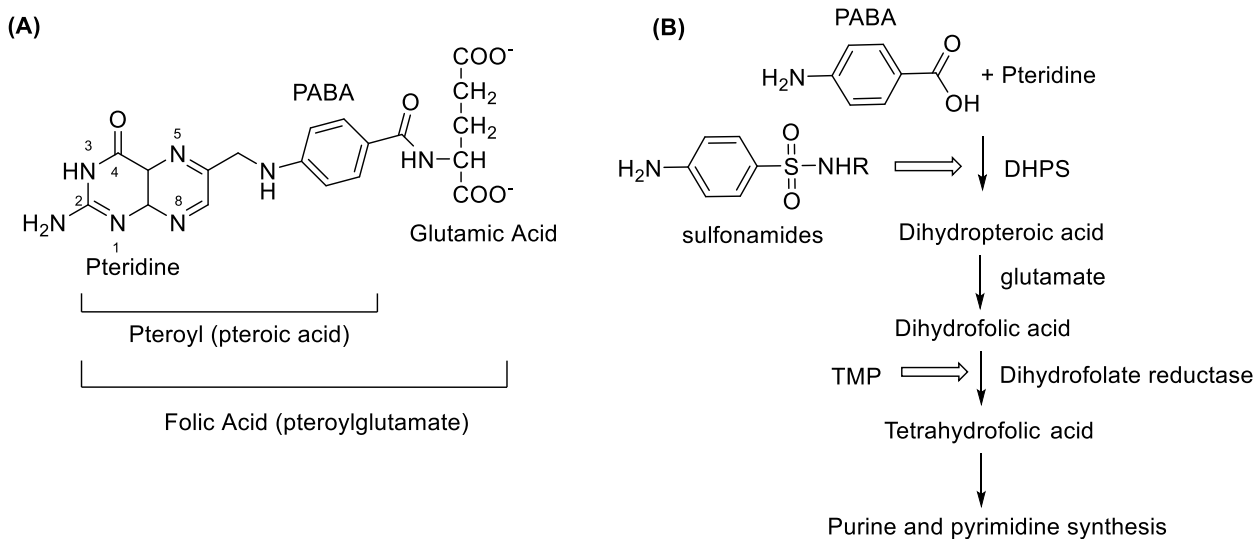**Figure 2.2.** *The structures of sulfanilimide (a) sulfapyridine (b) and trimethoprim (c).*

Figure 2.3. *(A) Structure of folic acid. (B) Biosynthetic pathway of tetrahydrofolic acid and sites of action of sulfonamides.*

By the 1940s, resistance to sulfonamides was observed[5] and an approximate 75% failure of treatment was found during the World War II.[4,5,10] Sulfonamide resistance is caused by the bacteria producing more PABA to outcompete the drugs binding to DHPS which reduces sulfonamide activity on bacteria. In order to increase the efficacy of sulfonamides in treatment of gonorrhea, trimethoprim (TMP, Figure 2.2c) was added as a combination, which was used until the 1970s.

Despite being discovered in 1928, penicillin was not used as antimicrobial treatment for gonorrhea until 1943. Penicillin inhibits the formation of the bacteria cell wall through irreversible covalent binding of the β-lactam ring to the transpeptidase enzyme of bacteria, preventing the enzyme from forming new peptide bonds between amino acids that build up the new cell wall (Figure 2.4 A).[12] Initially, penicillin was highly successful as a first-line treatment of gonorrhea. But during the 1960s, the susceptibility of bacteria to penicillin started to decrease. Despite this, the amounts of penicillin prescribed for gonorrhea treatment increased 24-fold during the 1980s. This increased exposure to penicillin was linked to plasmid–mediated resistance and chromosomal-mediated resistance mutation in different genes. The plasmids of these resistant gonococcal strains contained β-lactamases that hydrolyze and open the β-lactam ring, rendering penicillin inactive (Figure 2.4 B).[10,13] Chromosomal-mediated resistance, caused from mutation in genes, decreases acylation of β-lactams, as a result reduces the effectiveness of penicillin.[4,10] Consequentially there were gonorrhea epidemics in various the resistance strains rapidly spread over the world.
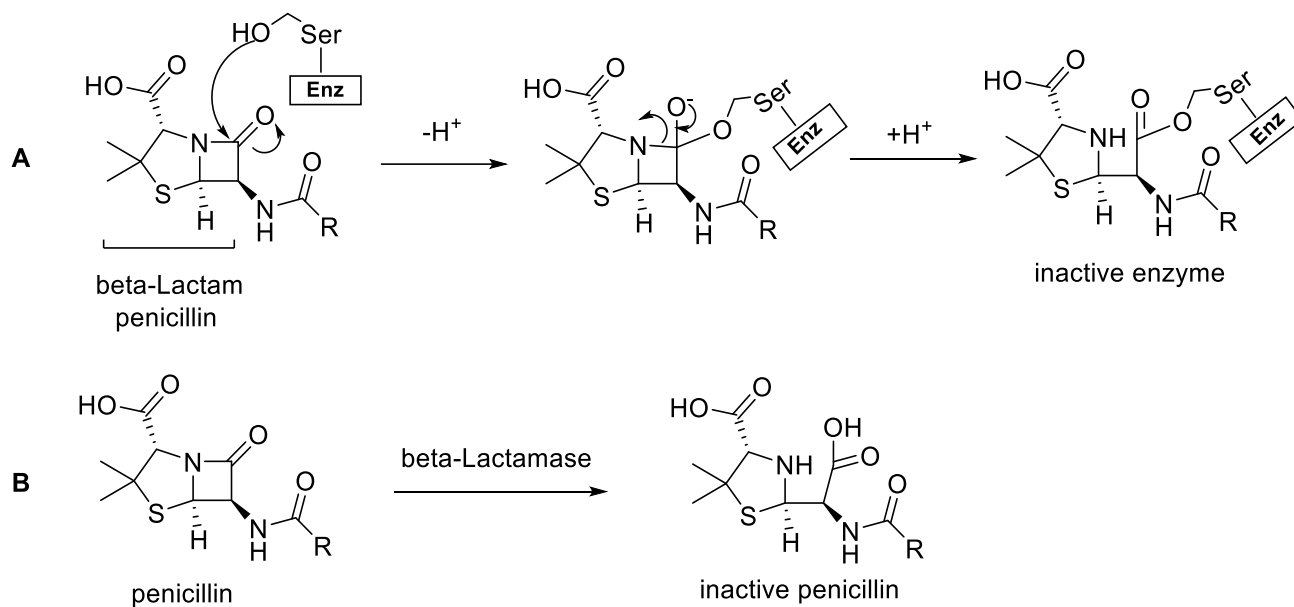
Figure 2.4. A. *The mechanism of penicillin binding with bacterial enzyme.*
B. *The inactivation of penicilin by β-lactamase (resistance).*

To combat the increasing resistance to penicillin, other antimicrobials such as tetracycline began to be used in the treatment of gonorrhea. Tetracycline was discovered by Benjamin Minge Duggar in soil bacteria in 1945. Between the 1950s to 1980s, tetracycline was used as a treatment for patients who had an allergy to penicillin.[4,10]

Tetracycline inhibits protein synthesis by preventing the aminoacyl – tRNA (amino acid) from binding with the mRNA in the 30S ribosomal subunit (Figure 2.5).[14] Tetracycline can bind at one primary and multiple secondary sites within the small subunits. The Tet 1 and primary sites are the key inhibitor positions which are located in the ribosomal A site. Tetracycline suffered a similar fate to penicillin, with bacteria gradually developing a high resistance worldwide.
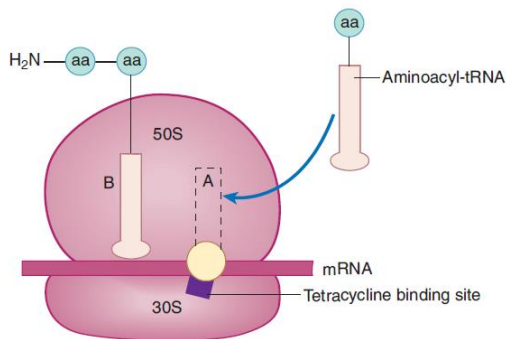
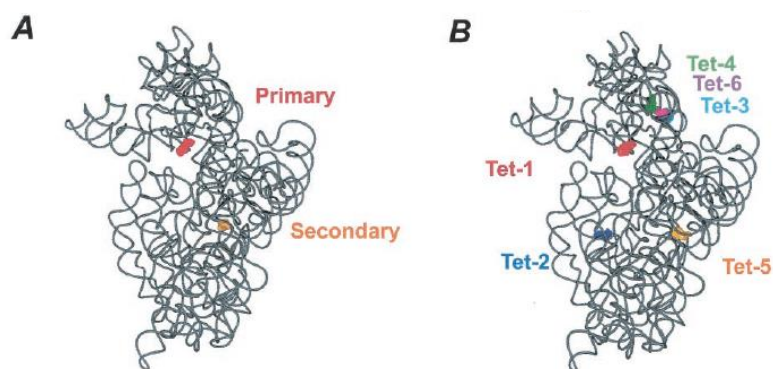***Figure 2.5.*** *Site of action for tetracycline.*

Figure 2.6. *The locations of the tetracycline binding sites on the ribosome. Tetracycline can bind in either two or six sites A and B) on the ribosomal subunit.[15] Tet1 and primary site were found by Pioletti and Broderson, respectively.*

Another interesting drug family is quinolones, which have a broader spectrum of activity against a wider range of bacterial species than tetracyclines, and they work more effective against certain types of infections, such as urinary tract infections or respiratory tract infections.[16] Antimicrobial quinolone drugs were synthesized by Lesher and colleagues in the 1960s. These drugs can kill the bacteria by binding to the DNA gyrase and topoisomerase IV causing DNA double-strand breaks, leading to the inhibition of DNA synthesis and cell death.[10,17] The fluoroquinolone, ciprofloxacin (Figure 2.1b), was widely used to cure gonorrhea from the late 1980s but it was found that the bacteria developed resistance as a worldwide phenomenon, therefore, ciprofloxacin was withdrawn as a first–

line drug in the early to mid-2000s in many Asian and European countries.[10] The resistance of quinolone drugs was caused by a mutation in a gene in bacteria which decreased the binding affinity of the drug.

Erythromycin (Figure 2.7) was the first macrolide discovered and was first used in 1952. Erythromycin was commonly used as a penicillin replacement for people who had an allergic reaction to penicillin.[10] Azithromycin (Figure 2.1e) was developed from an erythromycin derivative in 1980 to treat gonorrhea and showed greater effectiveness. Therefore, azithromycin was selected as a primary treatment and widely used to cure bacterial STIs including gonorrhea, which led to high-levels of resistance emerging towards azithromycin in 2001 in many countries around the world. However, azithromycin is still used to treat gonorrhea in a dual antimicrobial therapy with ciprofloxacin.[4,10]
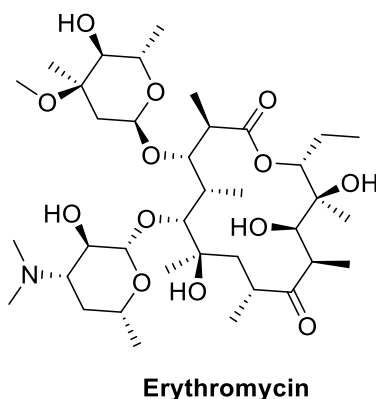

Erythromycin

Figure 2.7. Example of macrolide drugs: Erythromycin.

Fortunately, third generation cephalosporins (cefixime, Figure 2.1c or ceftriaxone, Figure 2.1d) were effective antibiotics and have been used as first–line treatments in many countries from the 1990s until the present. Cephalosporins react via the β-lactam ring leading to the inhibition of cell wall production. However, the susceptibility gonorrhea to cefixime and ceftriaxone has decreased rapidly over the last several years and treatment failure has been reported in Japan.[5,10] Drug combinations will be used as an alternative treatment but will result in high cost treatments and multidrug resistance. The antimicrobial drug development displayed in Figure 2.8. At present, a combination of ceftriaxone and azithromycin is the last option for gonorrhea treatment. If gonorrhea

develops resistance to this it will develop into a superbug in the future. It is imperative to find new drugs as a strategy for the prevention of gonorrhea.
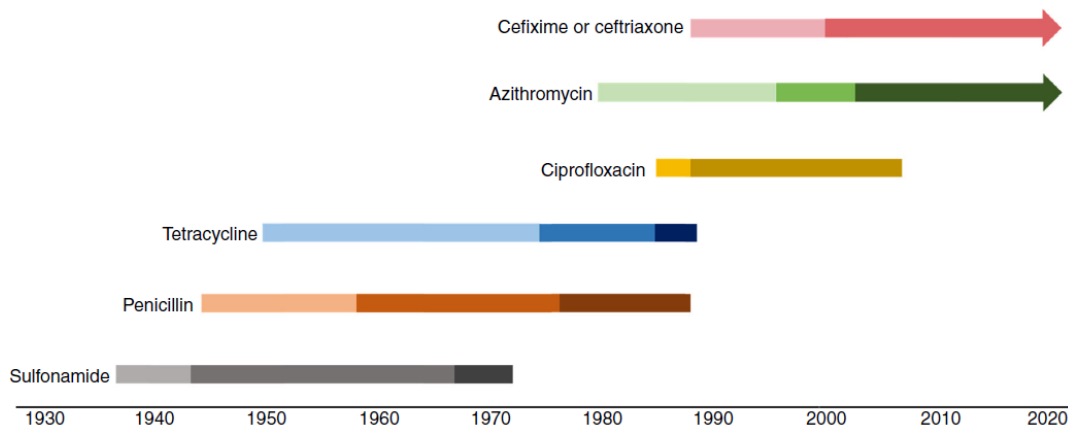

Figure 2.8. *Evolution of gonorrhea resistance. Colour changes explain the resistance level occuring. Sulfonamide: introduction, resistance reported, trimethoprim combination; penicillin and tetracycline: introduction, chromosomally-mediated resistance reported, plasmid-mediated resistance reported; ciprofloxacine: introduction, resistance report; azithromycin: introduction, resistance report, high level resistance report; cefixime or ceftriaxone: introduction, reduce susceptibility report.[4]*
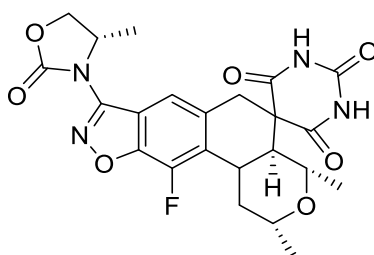
Figure 2.9. *Structure of zoliflodacin.*

Recently, Bradford et al. (2020)[18] synthesized zoliflodacin, a novel drug to treat gonorrhea. Zoliflodacin (Figure 2.9) is based on a benzisoxazole scaffold and contains an aspirocyclic pyrimidinetrione pharmacophore. Zoliflodacin represents the first class of the antibacterial class termed spiropyrimidinetriones with a bacterial topoisomerase inhibitory mode of action. Zoliflodacin inhibits gyrase-catalyzed supercoiling and

topoisomerase IV-catalyzed decatenation in a similar manner to ciprofloxacin. The *in vitro* activity of zoliflodacin against gonorrhea isolates in agar solution showed a higher efficacy than ciprofloxacin, penicillin, azithromycin and tetracycline. Zoliflodacin is capable of treating gonococcal urogenital and rectal infections in phase 2 preclinical trials and is being tested in phase 3 clinical trials. Therefore, zoliflodacin is likely to be a new antibiotic for the treatment of gonorrhea.

2.3 Drug targeting peptidyl-tRNA hydrolase

One potential alternative therapeutic approach for the treatment of gonococcus is stopping the production of proteins in the pathogen through inhibiting peptidyl-tRNA hydrolase (Pth). Without the action of this enzyme, protein production is impeded and the bacterium cannot grow. Pth is a bacterial enzyme which was first identified in *Escherichia coli* and yeast. Pth from *Escherichia coli* has mainly been studied in biochemical processes. Pth is responsible for the cleavage of peptidyl-tRNA to the free peptide and tRNA. Pth acts as an esterase hydrolysing the bond between the carboxy–terminal end of the peptide and the 2' - or 3' – hydroxyl of ribose at the end of tRNA (Figure 2.10).[19,20] The enzyme has a globular structure, comprised of six α – helices and seven β - strands (Figure 2.11).[19–21]

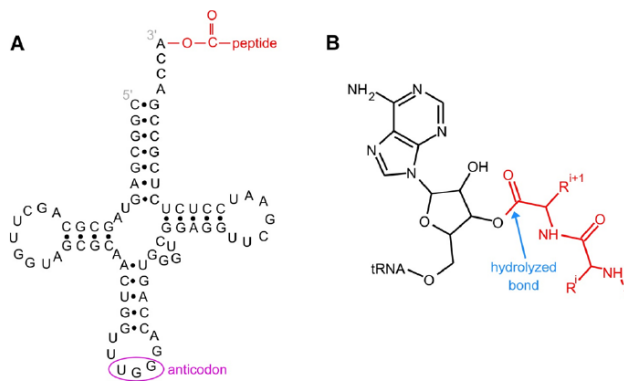
Figure 2.10. **A**. *An example of Pth. The peptide bound 3' end of tRNA, in this case tRNA^Pro.*

B. *Enlarged image of the ester bond between 3'-hydroxyl group of ribose and C-terminus of the peptide chain.*[19,20]
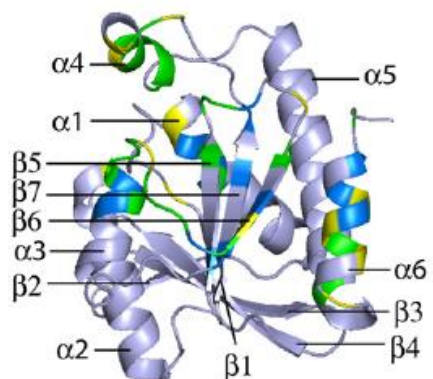
Figure 2.11. *Ribbon representation of peptidyl-tRNA hydrolase from E. coli.*

In order to develop new inhibitors of Pth, a fragment screen was undertaken using X-ray crystallography in collaboration with the Hare group at the University of Sussex (Figure 2.12). A small number of X-ray derived fragment hits were identified that bound in the active site of the enzyme.

Figure 2.12. *Furan containing hit Fragment I in the active site (X-ray structure).*

Fragment I   Fragment II

Figure 2.13. *Initial fragment hits from X-ray crystallography.*

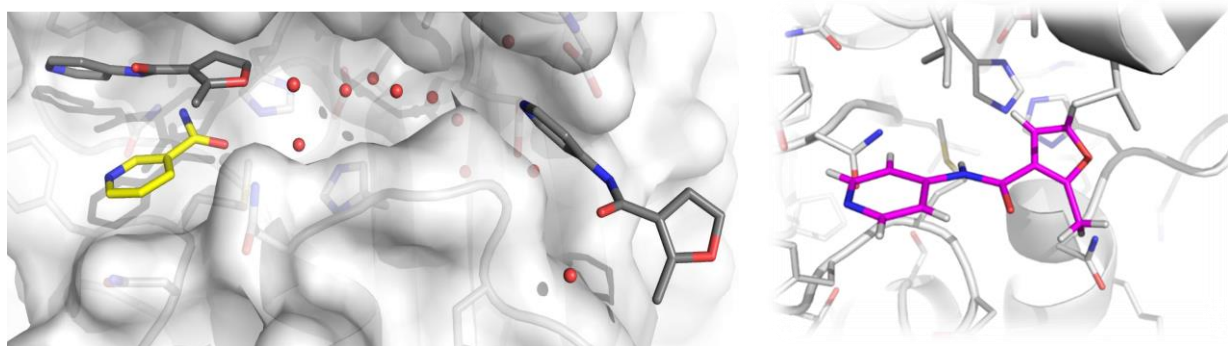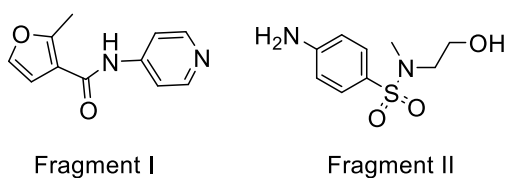The furan ring in fragment I (Figure 2.14) is an interesting group for further modification (Figure 2.13 as it was found to bind to both Pth (Hare group, Sussex) and *Staphylococcus aureus* gyraseB, Figure 2.15).[22] Janupally *et al.* found that the furan ring showed a week binding in the hydrophobic pocket of gyraseB and compounds A and B (methyl-substituted furan, Figure 2.15) showed a good DNA GyrB inhibition, displaying IC_{50} values of 12.88 µM and 5.35 µM respectively.

Figure 2.14. *Compound A in Staphylococcus aureus gyraseB pocket (experimental design).*[22]

compound A

compound B

Figure 2.15. *Structure of compounds that contain a furan ring. DNA Gyrase B inhibition (IC$_{50}$); compound A = 12.88 µM and compound B = 5.35 µM.*

From the analysis of these hits, two molecules (Fragments I and II, Figure 2.16) were identified as synthetically tractable starting points for rapid elaboration. Therefore, the starting goals of this research relate to the synthesis of a library of amide, hydrazides, and sulfonamide analogues of these initial hits which will then be evaluated utilising a combination of antimicrobial activity assays and X-ray screening.
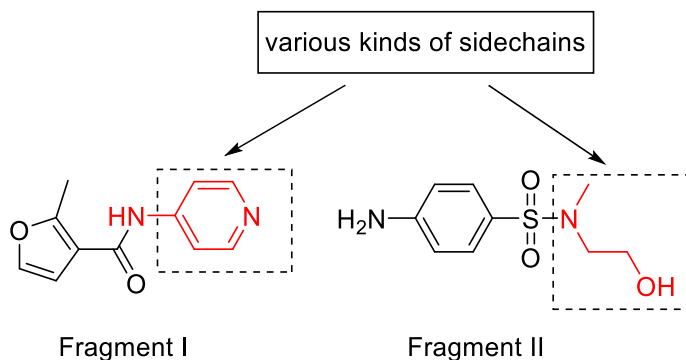

Figure 2.16. *Intended SAR to explore in the fragments.*

2.4 Results and Discussion

The unexplored structure-based drug design approach still needs more investigation for antibiotic production. Therefore, our research designed and synthesised two different series of furans (series I) and sulfonamides (series II) based on fragments I and II with the aim of producing antimicrobial leads. In the drug design process, various amines e.g. primary, secondary, aromatic amines, hydrazines, pyrrolidine and piperazine containing a range of substituents, for example, hydroxyl, halogen and methoxy were also chosen in our synthetic approach because they showed good efficacy in fluoroquinolone-based analogues with antimicrobial activity and DNA gyrase inhibition.[23] A simple one-pot synthesis by using T3P as a coupling agent was selected for making the furan library (series I) and minimal reagents and simpler reaction conditions were chosen for sulfonamide production (series II). The methods are interesting alternatives because of their ease of work up and purification.

Series I

The furanoyl series (Figure 2.17), comprising a 2-methylfuran group, was synthesised. In all cases, a range of amines with different electronic and steric properties, aromatic and non-aromatic amines, of different lipophilicities, chain lengths, were coupled with 2-methylfuran-3-carboxylic acid and yields as shown in Scheme 2.1 and 2.2.
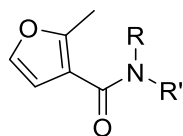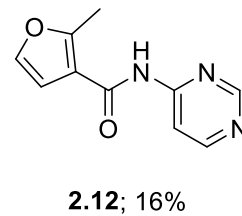

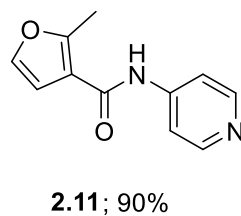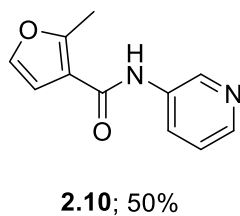**Figure 2.17.** *The structure of furanoyl series (**Series I**).*

2.1; 68%   **2.2**; 90%   **2.3**; 56%   **2.4**; 48%

2.5; 30%   **2.6**; 47%   **2.7**; 48%   **2.8**; 87%

2.9; 39%   **2.10**; 50%   **2.11**; 90%   **2.12**; 16%
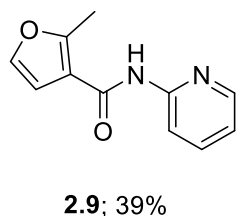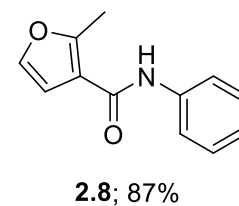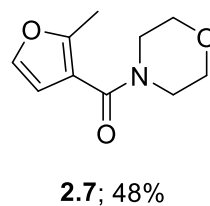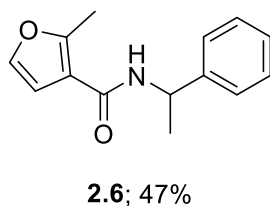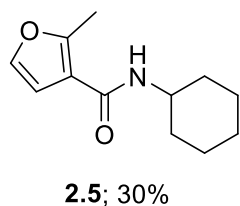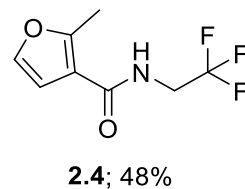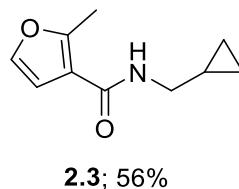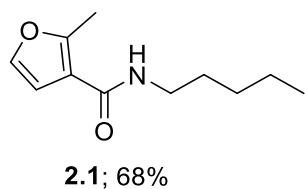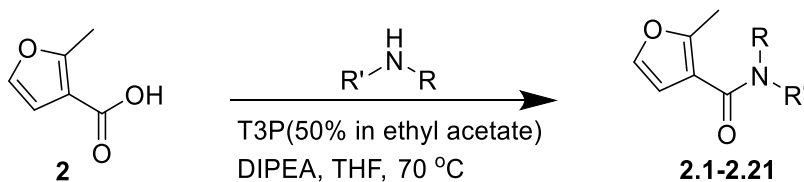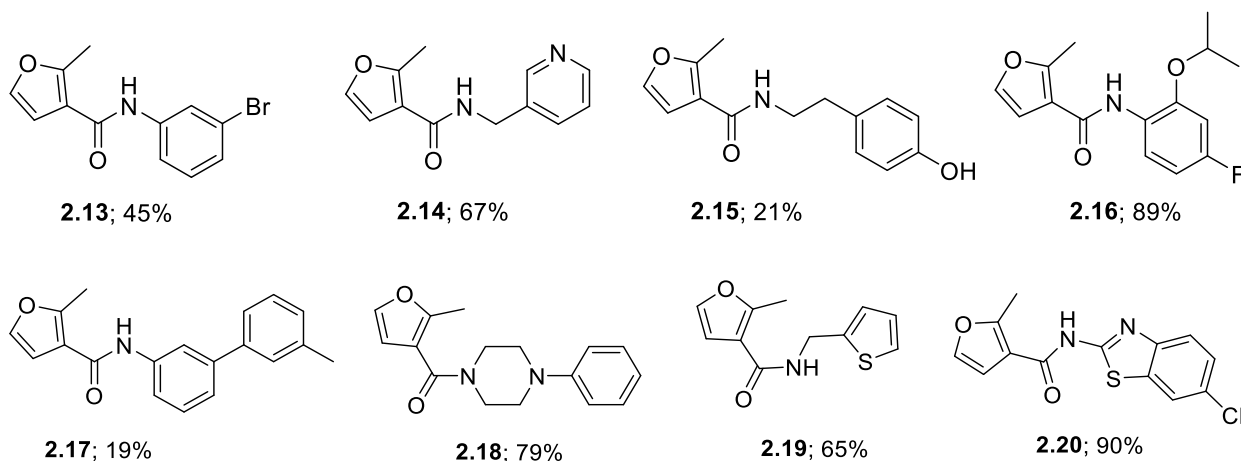
Scheme 2.1. *Synthesised furan compounds.*

Some amides were formed in low yield e.g. compounds **2.15** and **2.17** due to incomplete reaction and/or separation processes, even after twice purifying through an automated chromatography system over silica. Similarly, a few amino-pyridine and – pyrimidine-based analogues were made with excellent purities yet, often poor yields. In many cases, our aim was to provide a diverse series of products with little consideration on yield optimisation; if there was sufficient material to test, once we had an active series, we could address and optimise the yield at a later stage.

Cyclopropyl methanamine (compound **2.3**) and piperazine (compound **2.18**) groups were selected for synthesis because they are part of cyprofloxacin and fluoroquinone drugs. In the same way that some substituents groups on aromatic amines such as fluorine, chlorine, bromine, hydroxy and methoxy shown good performance in inhibiting DNA gyrase these were also selected to synthesise compounds series I.[23] [24]

Additionally, hydrazides and hydrazide derivatives are particularly interesting substances because they are still useful due to their broad range of bio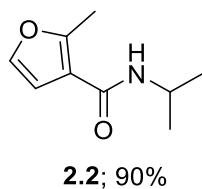logical activity in related antimicrobials[22,25] (e.g. compound B, DNA Gyrase B inhibition, Figure 2.15), anticonvulsant[26] and also as aspartic protease inhibitors.[27] As a results, few hydrazines were coupled as shown in Scheme 2.2.
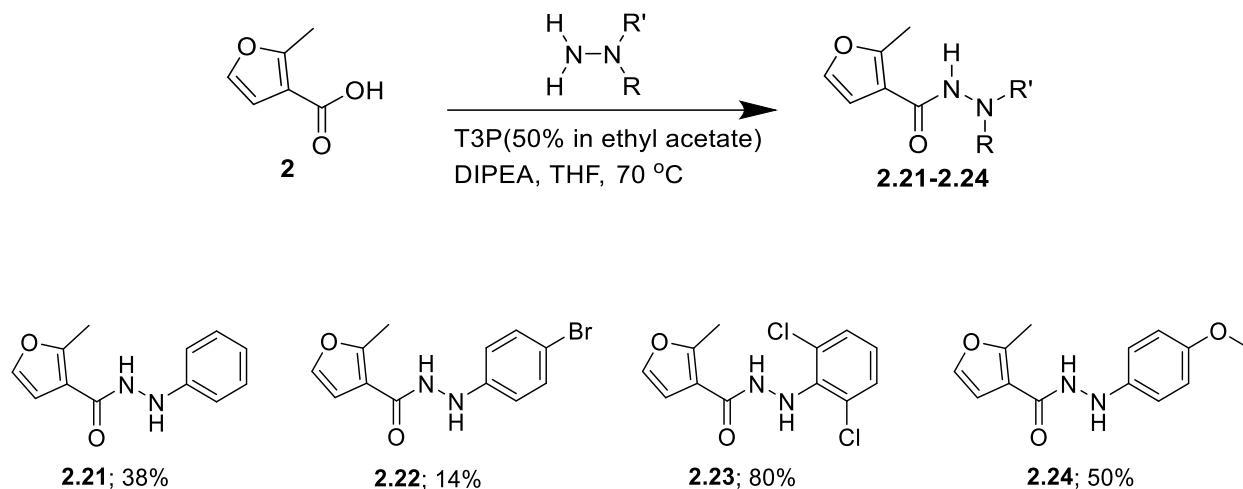
Scheme 2.2. *Synthesised hydrazide compounds.*

Series II

The sulfonamide series (Series II, Figure 2.18) was synthesised as shown in Scheme 2.3, 2.4 and 2.6. Fragment II (Figure 2.17) was deemed to be a suitable starting point on which to base our initial sulfonamide modification efforts. These were conducted on 4-nitrosulfonyl chloride and 2-(methylamino)ethan-1-ol in a one-pot synthesis to afford the corresponding nitro analogue, **2.25** (Table 2.1). The role of solvent, no solvent, stoichiometry of starting materials and temperature as well as thermal vs microwave conditions were investigated.
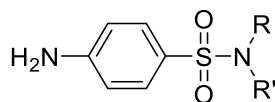
Figure 2.18. *The structure of sulfonamide series (**Series II**).*

A comparison between dichloromethane (DCM), dioxane and no solvent when the reagents were used in a 1:1 ratio (4-nitrosulfonyl chloride:2-(methylamino)ethan-1-ol), temperature (50 °C) and reaction time (30 min) were constant, was carried out. It was found that reaction in 1,4-dioxane gave a good isolated yield, hence, this was chosen as the solvent (entry 2). Then, the temperature was changed to 105 °C and ratios of 4-nitrosulfonyl chloride and 2-(methylamino)ethan-1-ol were also varied i.e. 1:1, 1:1.2 and

1:1.2. The best conversions were achieved by heating to 105 °C overnight, under thermal conditions, and using 1,4-dioxane as a solvent (entry 7). For convenience, entry 5 (microwave) would appear to be very useful since it gives a similar yield but is much faster. Similar microwave-mediated routes showed that one equivalent excess of the amine enabled better conversions than lower ratios (entries 1-5).

Table 2.1. *Brief optimization conditions towards sulfonamide compounds.*

2.25
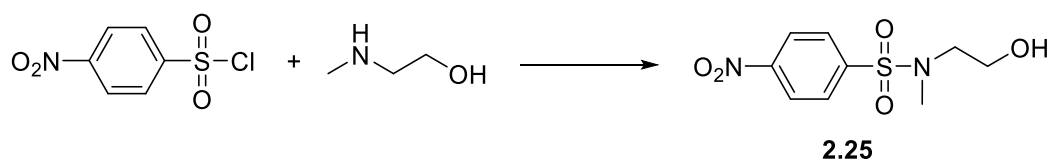
Entry	Method	solvent	Ratio*	2.25 (Yield[a] %)
1	Microwave at 50 °C, 30 min	-	1:1	8
2	Microwave at 50 °C, 30 min	dioxane	1:1	19
3	Microwave at 50 °C, 30 min	DCM	1:1	13
4	Microwave at 105 °C, 60 min	dioxane	1:1.2	50
5	Microwave 105 °C, 60 min	dioxane	1:2	88
6	Reflux at 105 °C, 12 h	dioxane	1:1	22
7	Reflux at 105 °C, 12 h	dioxane	1:2	96

*ratio between 4-nitrosulfonyl chloride and 2-(methylamino)ethan-1-ol

[a] isolated yield and all compounds were characterized by ^{1}H, ^{13}C NMR spectroscopy.

No reaction has occurred on the OH of the amino alcohol.

Next, using the optimised conditions, a library of sulfonamide compounds was synthesised from nitrosulfonyl chloride and various amines. The products **2.26a – 2.26j** were subsequently reduced by hydrogenation over a Pd/C catalyst in COware^{TM} vessel[28] (a commercially available 2-chamber apparatus enabling H_2 generation in one chamber, from Zn/HCl, which diffuses to the neighboring chamber where reduction/hydrogenolysis reaction occurs) to obtain the desired products (Scheme 2.4).
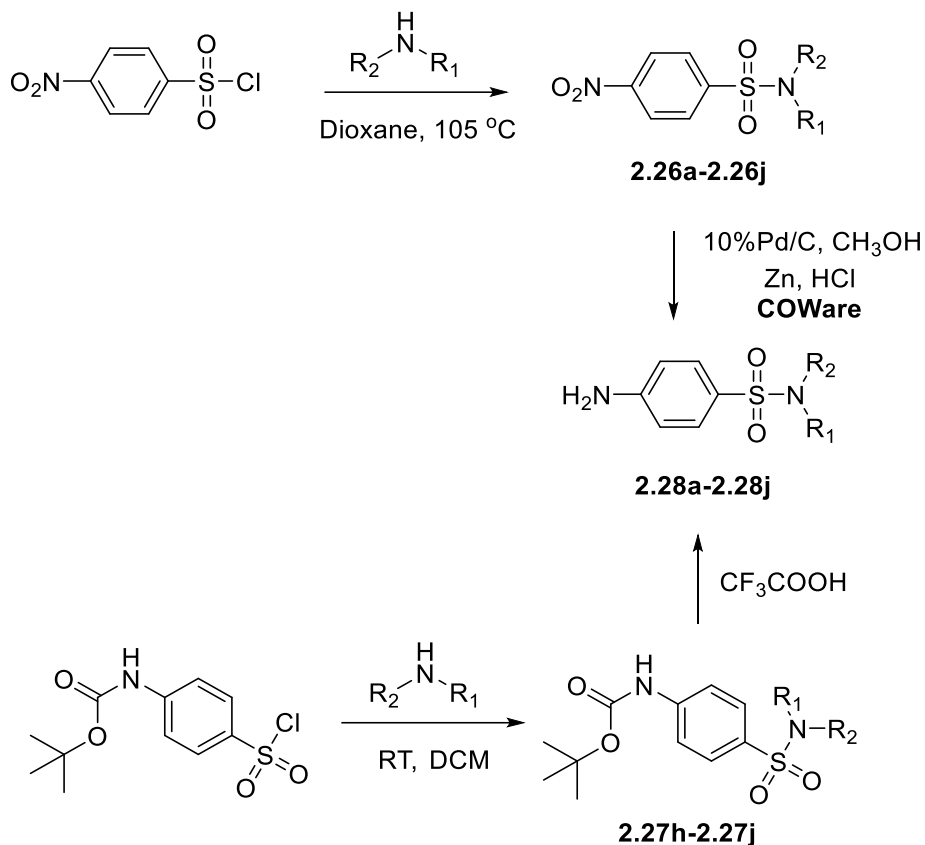
Scheme 2.3. *Sulfonamide compound synthesis.*

Intermediate

2.26a; 96%   **2.26b**; 64%   **2.26c**; 29%   **2.26d**; 57%

2.26e; 59%

2.26f; 73%

2.26g; 76%

2.26h; 53%

2.26i; 57%

2.26j*; 27%

Product

2.28a; 97%

2.28b; 94%

2.28c; 94%

2.28d**

2.28e; 96%

2.28f; 40%

2.28g; 7%

2.28h***

2.28i***

2.26j***
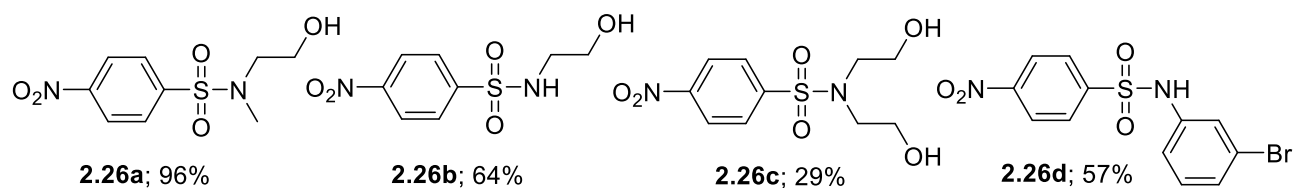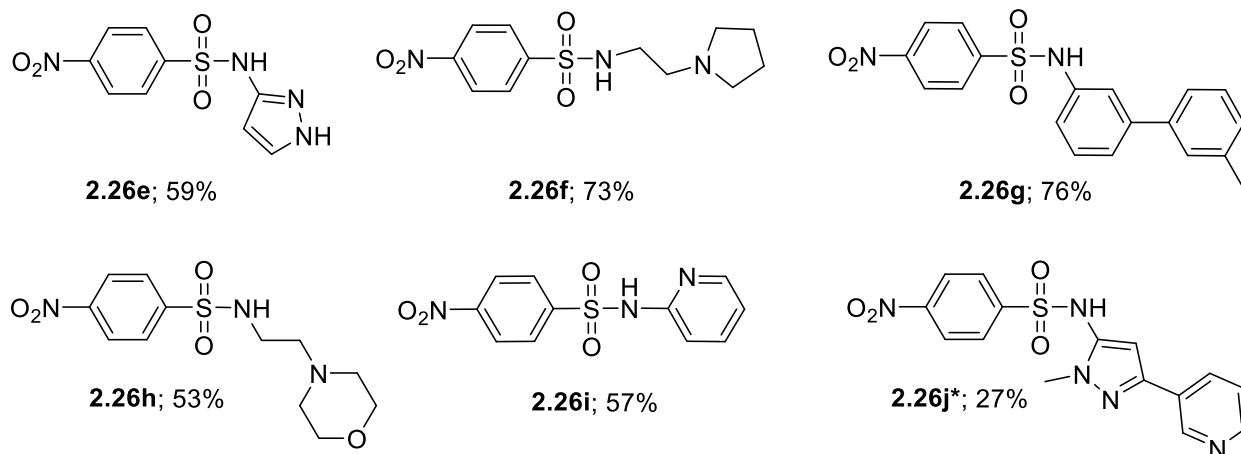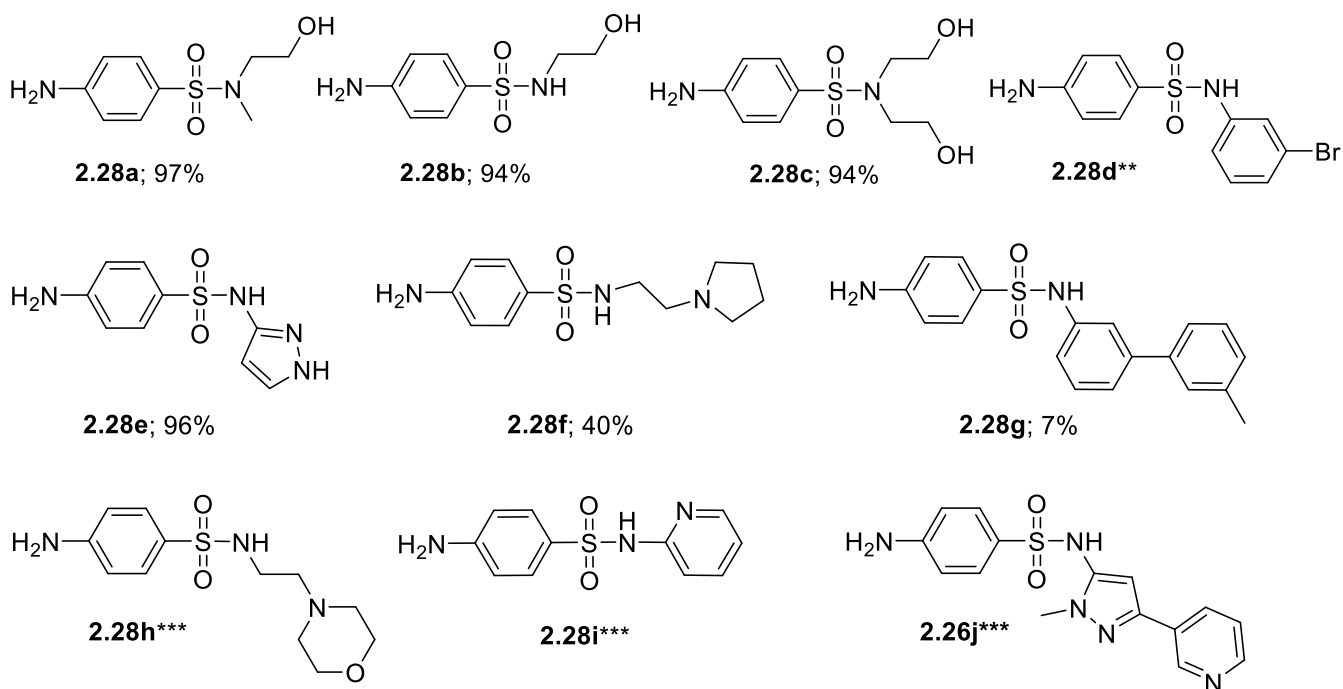
*Scheme 2.4. Synthesis of sulfonamide compounds from 4-nitrosulfonyl chloride and amines and the reduction process. *compound cannot be analysed by LC-MS but gave acceptable NMR spectroscopy. **There was no **2.28d** product obtained from this reaction but it was synthesised by using $Na_2S_2O_4$ and was obtained in 19% yield. ***Limited solubility likely prevents synthesis via hydrogenation reaction.*

The reduction of compound **2.28d** was unsuccessful under the standard palladium hydrogenation conditions because of the loss of a C-Br bond with a C-H bond (hydrodehalogenation) as shown in Scheme 2.5.[29] Therefore, a dithionite-mediated nitro reduction was used to synthesise **2.28d**, as shown in Scheme 2.6.
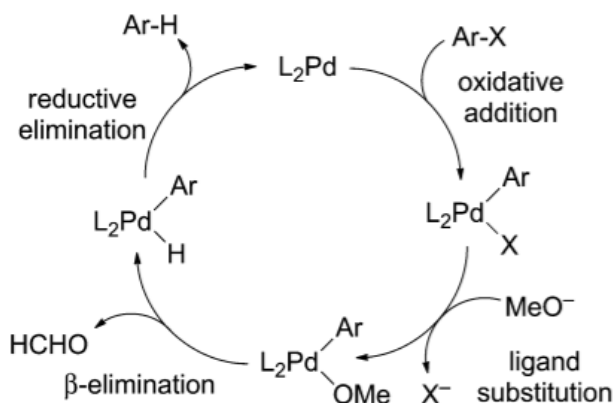
Scheme 2.5. *A proposed mechanism of hydrodehalogenation of aryl halides.*
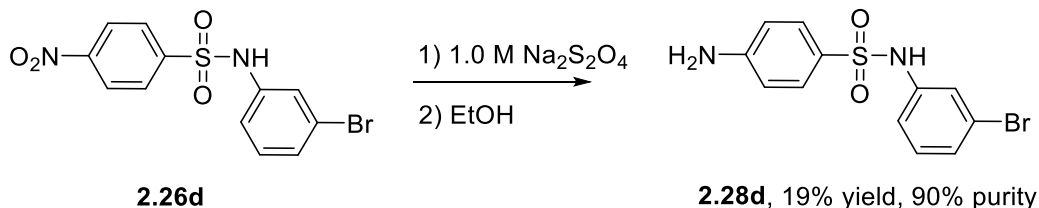
Scheme 2.6. *Nitro group reduction using sodium dithionite.*

In some cases, we found that the limited solubility of the nitro analogues led to poor conversions to the corresponding anilines and compounds **2.26h** – **2.26j** could not be hydrogenated to the anilines **2.28h** – **2.28j.** A more direct route to the anilines, compounds **2.27h** – **2.27j**, was sought. The use of *tert*-butyl (4-(chlorosulfonyl)phenyl)carbamate as the starting material, followed by sulfonamide formation and Boc deprotection was able to synthesise the final compounds (Scheme 2.7).
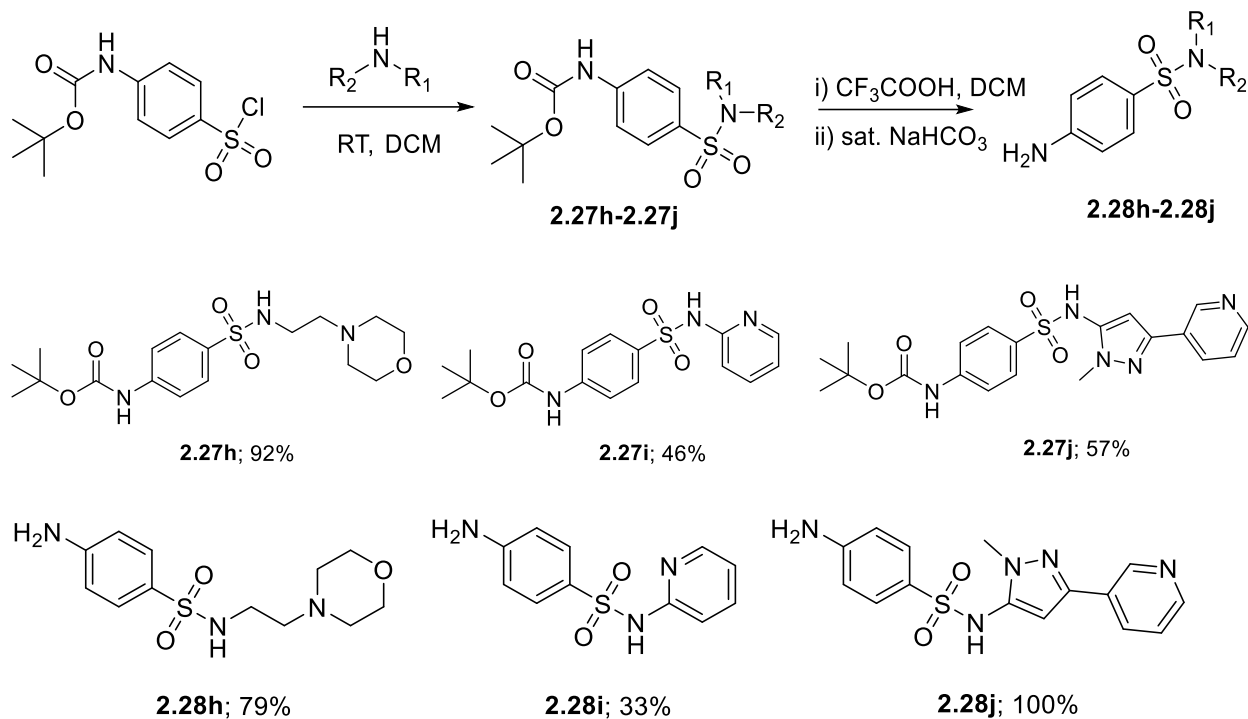
Scheme 2.7. *Synthesis of sulfonamide compounds and the reduction process.*

2.5 Biology results

With our libraries of compounds prepared, the next stage was to investigate and compare the binding modes of the synthesised analogues based on fragments I and II.

Gonococcal Pth crystals were grown in 96-well crystallisation plates. (Figure 2.19) Our results showed rod-shaped protein crystals (a) that were suitable for ligand soaking. Unfortunately, some clear drops (b,c) and precipitate (d) were found, resulting from high and low protein/precipitant, respectively. As a result, both (c) and (d) could not be used for soaking.

(a)　　　　　　　　　　　　　　　　　(b)

(c)　　　　　　　　　　　　　　　　　(d)
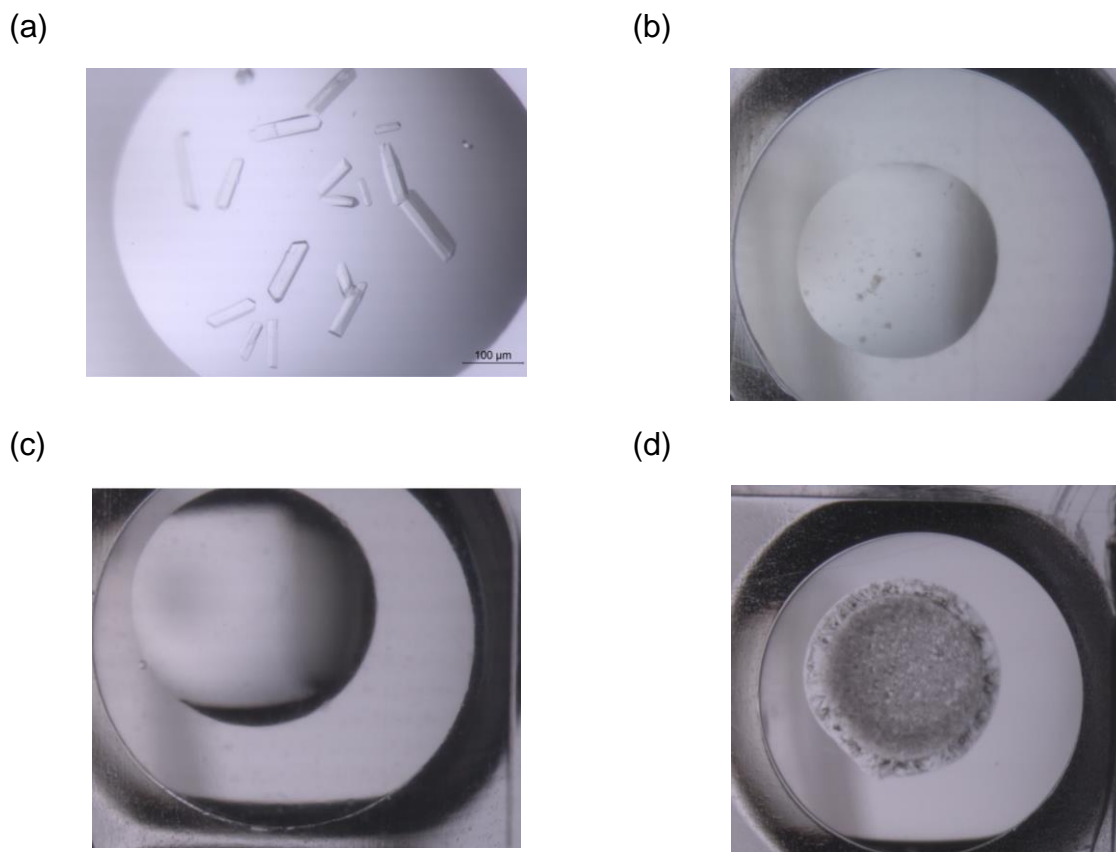
Figure 2.19. *Outcome observations in crystallisation experiments: (a) single crystal,*
(b),(c) clear drop and (d) precipitate drop.

In order to investigate the binding mode between the ligand and Pth, the chosen Pth crystals were soaked with ligands (compounds **2.1-2.25** and **2.28a-2.28j**) for 1 h and 24 h. Unfortunately, the X-ray analysis of the crystals showed no binding between the peptidyl-tRNA hydrolase (Pth) and ligand (furan or sulfonamide compounds). To further probe the potential binding of the series we hoped to develop an assay to deduce the potency of the binding and enable further development of the hit compounds. Regretfully, the assay development was never completed because our beloved collaborator (Dr. Stephen Hare) tragically passed away.

2.6 Pharmacokinetics, bioavailability drug-likeness and medicinal chemistry friendliness prediction of ligands

Since there were no biological results, the synthesised molecules are interesting mainly because they are small molecules, and some of their fragments are present in other active compounds. Consequently, additional investigations in computational chemistry will be carried out to progress the substance towards drug development. Absorption, distribution, metabolism and excretion (ADME) parameters are very important in drug discovery. The prediction of pharmacokinetics, bioavailability, drug-likeness was performed by the SWISS ADME web tool, used to find drug candidates with high activity, low toxicity and therapeutic efficacy.[30] For a passively diffused, orally bioavailable active drug, it tends to have to obey Lipinski's 'rule of five' which relates to: no more than 5 hydrogen bond donors, no more than 10 hydrogen bond acceptors, molecular mass less than 500 daltons, a partition co-efficient log P-value less than 5 and no more than 10 rotatable bonds.[31,32]

Therefore, the 34 molecules in Series I and Series II were investigated by computational predictions. Gratifyingly, physicochemical properties and lipophilicity of all compounds were rule of five-compliant and also showed good potential for drug-likeness (Table 2.2). Moreover, polar surface areas, another useful parameter, in Veber's rules[33], were well within limits. It must also be concluded that many of these drugs are still rule of three fragment-like with molecular weights below 300 Da, a logP < 3, rotational bond < 3, hydrogen bond donor and acceptor each < 3 and much more potential for fragment growth.

Table 2.2. Calculated physicochemical properties and lipophilicity.

compound	MW (g/mol)	nRB*	nHBA*	nHBD*	TPSA* (A^2)	WLogP*
2.1	181.23	5	2	1	42.24	2.12
2.2	167.21	3	2	1	42.24	1.73
2.3	179.22	4	2	1	42.24	1.63
2.4	207.15	4	5	1	42.24	3.14
2.5	207.27	3	2	1	42.24	2.65
2.6	229.27	4	2	1	42.24	2.75
2.7	195.22	2	3	0	42.86	0.68
2.8	201.22	3	2	1	42.24	2.65
2.9	202.21	3	3	1	55.13	2.04
2.10	202.21	3	3	1	55.13	2.04
2.11	202.21	3	3	1	55.13	2.04
2.12	203.2	3	4	1	68.02	1.44
2.13	280.12	3	2	1	42.24	3.41
2.14	216.24	4	3	1	55.13	1.76
2.15	245.27	5	3	2	62.47	2.27
2.16	227.29	5	4	1	51.47	4.00
2.17	291.34	4	2	1	42.24	4.62
2.18	270.33	3	2	0	36.69	1.79
2.19	221.28	4	2	1	70.48	2.43
2.20	292.74	3	3	1	83.37	3.91
2.21	216.24	4	2	2	54.27	2.15
2.22	295.13	4	2	2	54.27	2.92
2.23	285.13	4	2	2	54.27	3.46
2.24	246.26	5	3	2	63.50	2.16

compound	MW (g/mol)	nRB*	nHBA*	nHBD*	TPSA* (A²)	WLogP*
2.28a	230.28	4	4	2	92.01	0.97
2.28b	216.26	4	4	3	100.80	0.63
2.28c	260.31	6	5	3	112.24	0.33
2.28d	327.20	3	2	2	80.57	3.73
2.28e	238.27	3	3	3	109.25	1.69
2.28f	296.36	5	4	2	83.81	1.35
2.28g	338.42	4	2	2	80.57	3.14
2.28h	285.36	5	5	2	93.04	0.59
2.28i	249.29	3	3	2	93.46	2.36
2.28j	329.38	4	4	2	111.28	2.76
Sulfamethoxazole	253.28	3	4	2	106.60	2.26
Azithromycin	748.98	7	14	5	180.08	1.52

*nRB number of rotational bonds, nHBA number of hydrogen bond acceptors, nHBD hydrogen bond donors, TPSA topological polar surface area, WLogP octanol/water partition coefficient.

Moreover, the ADME properties *in vivo* were predicted with the graphical classification model Egan BOILED-Egg. Most of series I (furanoly compounds) were in the egg yolk, which predict as brain-penetrant and not subject to active efflux, while all compounds in series II were in the white egg which shown no predicted BBB permeability as shown in Figure 2.20. Interestingly, only compound 2.28h showed in the blue dot that predicted as well absorbed but not accessing to the brain and PGP+. Compounds in series I and II displayed the prediction of good ADME characteristics including the Lipinsky's rule and GI absorption, as well as very low toxicity. When we compared them with currently available drugs such as Sulfamethoxazole and Azithromycin, it was found that Sulfamethoxazole showed in the red dot in white area as the same as the most our compound but Azithromycin showed in blue dot and was not in the appropriate range in

this model. We hope that all compounds may be useful for further studies on new biologically active antimicrobials.
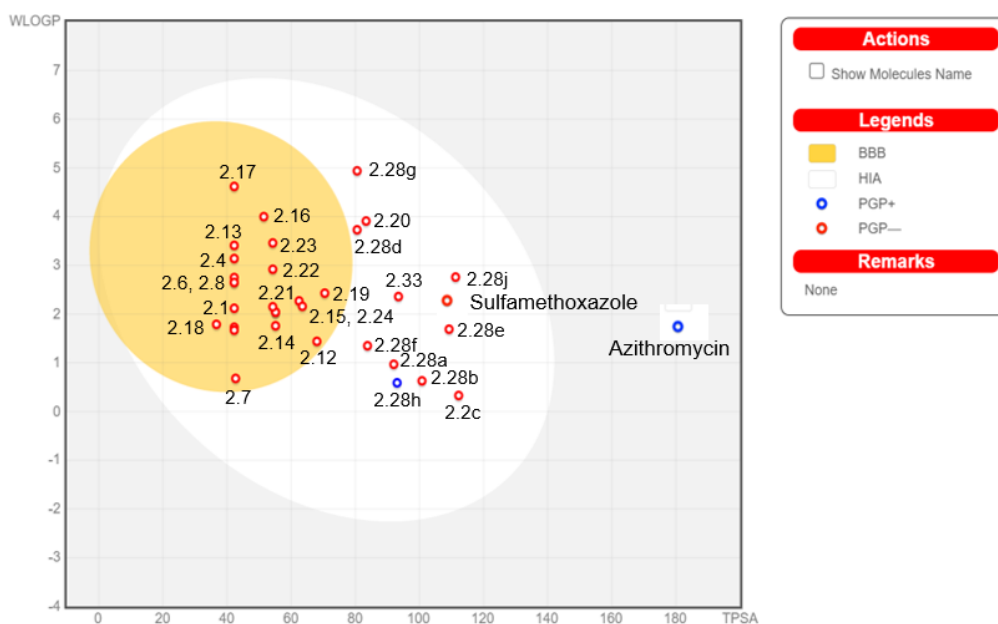

Figure 2.20. *Predicted BOILED-Egg diagram of the series I and II from SwissADME web tool.*

2.7 Conclusions

Our goal to explore structural activity relationships (SAR) in fragments I and II, was partially met as we were able to synthesise a diverse array of heterocyclic, aromatic, alkyl substituted furan and sulfonamide analogues with various subsitutents and changing hydrogen bond acceptor, donor, hydrophobic substituents. We were successful, in many cases in forming libraries on a mmol scale, with purities >90%, employing simple synthesis and work–ups. However, upon further analysis, we found that fragment II was not actually bound to the active site. Nevertheless, this did not prevent us from making a large library of sulphonamide analogues. We hope that a number of these analogues may bind in the Pth pocket and show activity against Pth protein in gonococcal bacteria.

2.8 Experimental

2.8.1 Synthesis of compounds

All commercially purchased materials and solvents were used without further purification unless specified otherwise. ^{1}H, ^{13}C and ^{19}F NMR spectroscopy was performed on a Varian 400 or 600 MHz spectrometer and chemical shifts are reported in ppm, referenced to TMS as an internal standard. ^{1}H and ^{13}C chemical shifts were recorded in parts per million (ppm). LCMS measurements were performed on a Shimadzu LCMS-2020 equipped with a Gemini® 5 μm C18 110 Å column and percentage purity measurements were run over 30 minutes in water/acetonitrile with 0.1% formic acid (5 min at 5%, 5–95% over 20 min, 5 min at 95%) with the UV detector set at 254 nm. High-Resolution Accurate Mass Spectrometry measurements were taken using a Waters Xevo G2 Q-ToF HRMS (Wilmslow, Cheshire, UK), equipped with an ESI source and MassLynx software. Experimental parameters were: (1)—ESI source: capillary voltage 3.0 kV, sampling cone 35 au, extraction cone 4 au, source temperature 120 °C and desolvation gas 450 °C with a desolvation gas flow of 650 L/h and no cone gas; (2)—MS conditions: MS in resolution mode between 100 and 1500 Da. Additionally, a Waters (Wilmslow, Cheshire, UK) Acquity H-Class UHPLC chromatography pumping system with column oven was used, connected to a Waters Synapt G2 HDMS high-resolution mass spectrometer.

2.8.1.1 Synthesis of furanoly series (Series I)

2-Methyl-*N*-pentylfuran-3-carboxamide (2.1)
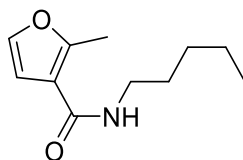
To a mixture of 2-methylfuran-3-carboxylic acid (50.0 mg, 0.39 mmol), pentan-1-amine (41.0 mg, 0.47 mmol), *N,N*-diisopropylethylamine (DIPEA) (101.6 mg, 0.79 mmol) in anhydrous tetrahydrofuran (anh.THF, 5 mL) was added propanephosphonic acid

anhydride (T3P) (625.0 mg, 0.98 mmol) dropwise. The resulting mixture was heated to 70 °C and stirred under an argon atmosphere overnight, The reaction was cooled to ambient temperature and to the reaction mixture was added water (10 mL) and ethyl acetate (EtOAc) (10 mL). The organic layer was separated, the aqueous phase was extracted with EtOAc (20 mL x 3). The combined organic phases were washed with saturated $NaHCO_3$ and brine, dried over Na_2SO_4, filtered and was concentrated in vacuum. The crude material was purified by flash column chromatography (4 g, SiO_2, hexane/EtOAc, 100:0 – 0:100) and the final product was obtained as colourless oil; yield: 48.4 mg (63%).

^{1}H NMR (600 MHz, $CDCl_3$) δ 7.19 (apparent singlet (aps), 1H), 6.45 (aps, 1H), 6.04 (broad singlet (brs), 1H), 3.32 (q, J = 6.9 Hz, 2H), 2.54 (s, 3H), 1.53 (m, 2H), 1.29 (m, 4H), 0.86 (t, J = 6.4 Hz, 3H).

^{13}C NMR (151 MHz, $CDCl_3$) δ 163.9, 156.6, 140.2, 115.6, 108.4, 39.4, 29.4, 29.1, 22.4, 14.0, 13.5.

HR-MS-ESI (m/z) Calculated for $C_{11}H_{18}NO_2$ [M + H]$^+$: 196.1338, found: 196.1337.

LC-MS purity (UV) = 94%, tR 20.73 min; m/z (ESI$^+$) 196.00 [M + H]$^+$.

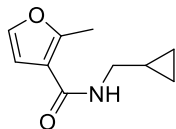***N*-Isopropyl-2-methylfuran-3-carboxamide** (**2.2**)
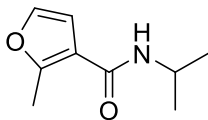
This was synthesised on a 0.39 mmol scale from 2-methylfuran-3-carboxylic acid by the same procedure as **2.1** and isopropylamine (46.5 mg, 0.79 mmol) was used instead of pentan-1-amine. The final product was obtained as a colourless oil; yield: 66.8 mg (90%).

^{1}H NMR (600 MHz, CDCl$_3$) δ 7.22 (d, *J* = 2.1 Hz, 1H), 6.37 (d, *J* = 2.1 Hz, 1H), 5.48 (brs, 1H), 4.21 (h, *J* = 6.6 Hz, 1H), 2.57 (s, 3H), 1.21 (d, *J* = 6.6 Hz, 6H).

^{13}C NMR (151 MHz, CDCl$_3$) δ 163.1, 156.7, 140.2, 115.6, 108.2, 41.2, 22.9, 13.5.

HR-MS-ESI (m/z) Calculated for C$_9$H$_{14}$NO$_2$ [M + H]$^+$: 168.1025, found: 168.1030.

LC-MS purity (UV) = 97%, tR 17.21 min; m/z (ESI$^+$) 167.85 [M + H]$^+$.

***N*-(cyclopropylmethyl)-2-methylfuran-3-carboxamide (2.3)**

This was synthesised on a 0.39 mmol scale from 2-methylfuran-3-carboxylic acid by the same procedure as **2.1** and cyclopropylmethylamine (33.6 mg, 0.47 mmol) was used instead of pentan-1-amine. The final product was obtained as a coloress oil; yield: 39.7 mg (56%).
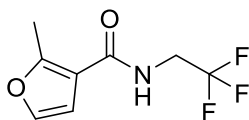
¹H NMR (600 MHz, CDCl₃) δ 7.25 (d, J = 2.0 Hz, 1H), 6.43 (d, J = 2.0 Hz, 1H), 5.79 (brs, 1H), 3.24 (dd, J = 7.2, 5.4 Hz, 2H), 2.54 (s, 3H), 1.02 – 0.94 (m, 1H), 0.51 – 0.45 (m, 2H), 0.20 (m, 2H).

¹³C NMR (151 MHz, CDCl₃) δ 163.9, 156.8, 140.3, 115.5, 108.3, 44.3, 13.5, 10.8, 3.5.

HR-MS-ESI (m/z) Calculated for a dimer, $C_{20}H_{26}N_2O_4$ [M + Na]⁺: 381.1785, found: 381.1780.

LC-MS purity (UV) = 95%, tR 17.65 min; m/z (ESI⁺) 179.85 [M + H]⁺.

2-Methyl-*N*-(2,2,2-trifluoroethyl)furan-3-carboxamide (**2.4**)

This was synthesised on a 0.39 mmol scale from 2-methylfuran-3-carboxylic acid by the same procedure as **2.1** and 1-phenylpiperazine (76.6 mg, 0.47 mmol) was used instead of pentan-1-amine. The final product was obtained as a brown solid; yield: 84.3 mg (79%).

¹H NMR (600 MHz, CDCl₃) δ 7.27 (d, J = 2.1 Hz, 1H), 6.43 (d, J = 2.1 Hz, 1H), 5.88 (brs, 1H), 4.08 – 4.02 (m, 2H), 2.59 (s, 3H).
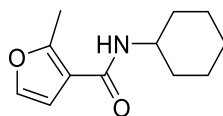
¹³C NMR (151 MHz, CDCl₃) δ 163.6, 158.2, 140.7, 123.2, 114.4, 107.9, 40.5 (q, $^2J_{CF}$ = 34.8 Hz), 13.6.

^{19}F NMR (376 MHz, DMSO-d_6) δ -76.90 – -77.02 (m), -77.05 – -77.29 (m).

HR-MS-ESI (m/z) Calculated for a dimer, $C_{16}H_{16}F_6N_2O_4$ [M + Na]$^+$: 437.0906, found: 437.0899.

LC-MS purity (UV) = 98%, tR 18.41 min; m/z (ESI$^+$) 207.80 [M + H]$^+$.

N-Cyclohexyl-2-methylfuran-3-carboxamide (2.5)

This was synthesised on a 0.39 mmol scale from 2-methylfuran-3-carboxylic acid by the same procedure as **2.1** and cyclohexylamine (46.8 mg, 0.47 mmol) was used instead of pentan-1-amine. The final product was obtained as a brown solid; yield: 24.4 mg (30%).
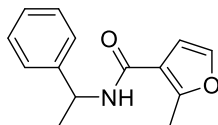
^1H NMR (600 MHz, CDCl$_3$) δ 7.23 (d, J = 2.1 Hz, 1H), 6.38 (d, J = 2.1 Hz, 1H), 5.52 (s, 1H), 3.91 (m, 1H), 2.57 (s, 3H), 1.99 (dd, J = 12.7, 4.2 Hz, 2H), 1.73 (dt, J = 13.8, 4.0 Hz, 2H), 1.61 (s, 2H), 1.44 – 1.37 (m, 2H), 1.21 – 1.17 (m, 2H).

^{13}C NMR (151 MHz, CDCl$_3$) δ 163.0, 156.7, 140.2, 115.7, 108.3, 48.1, 33.4, 25.6, 24.9, 13.5.

HR-MS-ESI (m/z) Calculated for a dimer, $C_{24}H_{34}N_2O_4$ [M + Na]$^+$: 437.2411, found: 437.2416.

LC-MS purity (UV) = 94%, tR 21.31 min; m/z (ESI⁺) 207.85 [M + H]⁺.

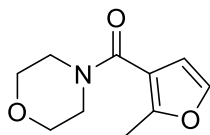**2-methyl-*N*-(1-phenylethyl)furan-3-carboxamide** (**2.6**)

This was synthesised on a 0.39 mmol scale from 2-methylfuran-3-carboxylic acid by the same procedure as **2.1** and 1-phenylethan-1-amine (57.2 mg, 0.47 mmol) was used instead of pentan-1-amine. The final product was obtained as a colourless solid; yield: 93.3 mg (90%).

^{1}H NMR (600 MHz, CDCl$_3$) δ 7.38 – 7.33 (m, 4H), 7.27 (m, 1H), 7.23 (d, *J* = 2.1 Hz, 1H), 6.39 (d, *J* = 2.1 Hz, 1H), 5.89 (d, *J* = 7.4 Hz, 1H), 5.26 (p, *J* = 7.1 Hz, 1H), 2.57 (s, 3H), 1.56 (d, *J* = 6.9 Hz, 3H).

^{13}C NMR (151 MHz, CDCl$_3$) δ 163.0, 157.1, 143.2, 140.3, 128.7, 127.4, 126.2, 115.3, 108.2, 48.6, 21.8, 13.6.

HR-MS-ESI (m/z) Calculated for C$_{14}$H$_{16}$N$_1$O$_2$ [M + H]⁺: 230.1181, found: 230.1171.

LC-MS purity (UV) = 93%, tR 20.96 min; m/z (ESI⁺) 229.85 [M + H]⁺.

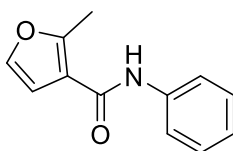**(2-Methylfuran-3-yl)(morpholino)methanone (2.7)**

This was synthesised on a 0.39 mmol scale from 2-methylfuran-3-carboxylic acid by the same procedure as **2.1** and morpholine (41.1 mg, 0.47 mmol) was used instead of pentan-1-amine. The final product was obtained as a colourless solid; yield: 55.1 mg (48%).

^{1}H NMR (600 MHz, CDCl$_3$) δ 7.25 (d, J = 2.0 Hz, 1H), 6.32 (d, J = 2.0 Hz, 1H), 3.76 – 3.56 (m, 8H), 2.38 (s, 3H).

^{13}C NMR (151 MHz, CDCl$_3$) δ 165.4, 153.7, 140.4, 115.2, 110.1, 66.9, 60.4, 12.9.

HR-MS-ESI (m/z) Calculated for C$_{10}$H$_{14}$NO$_3$ [M + H]$^+$: 196.0974, found: 196.0981.

LC-MS purity (UV) = 95%, tR 14.30 min; m/z (ESI$^+$) 195.95 [M + H]$^+$.

2-Methyl-*N*-phenylfuran-3-carboxamide (2.8)

This was synthesised on a 0.39 mmol scale from 2-methylfuran-3-carboxylic acid by the same procedure as **2.1** although aniline (44.0 mg, 0.47 mmol) was used instead of pentan-1-amine. The final product was obtained as a pale yellow solid; yield: 68.8 mg (87%).
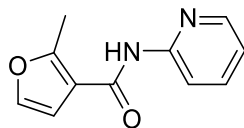
^{1}H NMR (600 MHz, CDCl$_3$) δ 7.57 (d, *J* = 1.2 Hz, 1H), 7.56 (d, *J* = 1.2 Hz, 1H), 7.36 – 7.33 (m, 2H), 7.31 (m, 1H), 7.12 (m, 1H), 6.52 (m, 1H), 2.63 (s, 3H). (NH missing)

^{13}C NMR (151 MHz, CDCl$_3$) δ 160.8, 157.9, 140.5, 137.7, 129.0, 124.3, 120.1, 115.7, 108.0, 13.6.

HR-MS-ESI (m/z) Calculated for C$_{12}$H$_{12}$NO$_2$ [M + H]$^+$: 202.0868, found: 202.0869.

LC-MS purity (UV) = 96%, tR 20.77 min; m/z (ESI$^+$) 201.85 [M + H]$^+$.

2-Methyl-*N*-(pyridin-2-yl)furan-3-carboxamide (2.9)

This was synthesised on a 0.39 mmol scale from 2-methylfuran-3-carboxylic acid by the same procedure as **2.1** and 2-aminopyridine (44.4 mg, 0.47 mmol) was used instead of pentan-1-amine. The final product was obtained as a colourless solid; yield: 39.1 mg (49%).

^{1}H NMR (600 MHz, CDCl$_3$) δ 8.51 (brs, 1H), 8.31 (d, *J* = 8.2 Hz, 1H), 8.22 (d, *J* = 4.8 Hz, 1H), 7.70 (t, *J* = 8.2 Hz, 1H), 7.27 (d, *J* = 2.2 Hz, 1H), 7.04 – 6.99 (m, 1H), 6.59 (d, *J* = 2.1 Hz, 1H), 2.63 (s, 3H).

^{13}C NMR (151 MHz, CDCl$_3$) δ 162.2, 158.6, 151.6, 147.8, 140.6, 138.4, 119.7, 115.6, 114.2, 108.3, 13.7.

HR-MS-ESI (m/z) Calculated for $C_{11}H_{11}N_2O_2$ [M + H]$^+$: 203.0821, found: 203.0814.

LC-MS purity (UV) = 95%, tR 15.45 min; m/z (ESI$^+$) 202.80 [M + H]$^+$.

2-methyl-*N*-(pyridin-3-yl)furan-3-carboxamide (2.10)
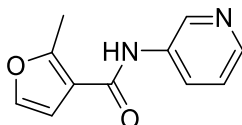
This was synthesised on a 0.39 mmol scale from 2-methylfuran-3-carboxylic acid by the same procedure as **2.1** and aminopyridine (44.4 mg, 0.47 mmol) was used instead of pentan-1-amine. The final product was obtained as a brown solid; yield: 40.2 mg (50%).

1H NMR (600 MHz, CDCl$_3$) δ 8.58 (d, *J* = 2.6 Hz, 1H), 8.32 – 8.29 (m, 1H), 8.21 (ddd, *J* = 8.4, 2.6, 1.4 Hz, 1H), 8.07 (m, 1H), 7.27 (d, *J* = 2.2 Hz, 1H), 7.26 – 7.23 (m, 1H), 6.61 (s, 1H), 2.61 (s, 3H)

^{13}C NMR (151 MHz, CDCl$_3$) δ 162.7, 158.6, 145.1, 141.4, 140.7, 135.0, 127.9, 123.8, 115.3, 108.2, 13.7.

HR-MS-ESI (m/z) Calculated for $C_{11}H_{11}N_2O_2$ [M + H]$^+$: 203.0815, found: 203.0810.

LC-MS purity (UV) = 97%, tR 11.27 min; m/z (ESI$^+$) 202.95 [M + H]$^+$.

2-methyl-*N*-(pyridin-4-yl)furan-3-carboxamide (2.11)

This was synthesised on a 0.39 mmol scale from 2-methylfuran-3-carboxylic acid by the same procedure as **2.1** and 4-aminopyridine (44.4 mg, 0.47 mmol) was used instead of pentan-1-amine. The final product was obtained as a colourless solid; yield: 71.2 mg (90%).
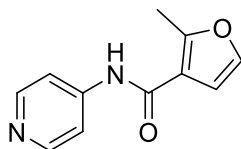
^{1}H NMR (600 MHz, CDCl$_3$) δ 8.52 (s, 2H), 7.75 (brs, 1H), 7.58 – 7.54 (m, 2H), 7.30 (d, *J* = 2.1 Hz, 1H), 6.56 (d, *J* = 2.1 Hz, 1H), 2.63 (s, 3H).

^{13}C NMR (151 MHz, CDCl$_3$) δ 162.4, 159.2, 150.6, 145.1, 140.8, 115.2, 113.9, 107.9, 13.8.

HR-MS-ESI (m/z) Calculated for C$_{11}$H$_{11}$N$_2$O$_2$ [M + H]$^+$: 203.0815, found: 203.0810.

LC-MS purity (UV) = 94%, tR 9.80 min; m/z (ESI$^+$) 202.95 [M + H]$^+$.

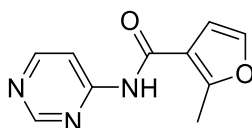**2-Methyl-*N*-(pyrimidin-4-yl)furan-3-carboxamide (2.12)**

This was synthesised on a 0.39 mmol scale from 2-methylfuran-3-carboxylic acid by the same procedure as **2.1** and 4-aminopyrimidine (44.9 mg, 0.47 mmol) was used instead

of pentan-1-amine. The final product was obtained as a colourless solid; yield: 16.9 mg (21%).
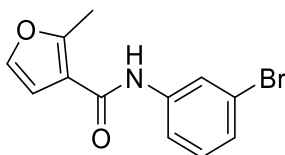
^{1}H NMR (600 MHz, CDCl$_3$) δ 8.86 (s, 1H), 8.64 (d, J = 5.8 Hz, 1H), 8.27 (dd, J = 5.8, 1.4 Hz, 1H), 8.19 (s, 1H), 7.32 (d, J = 2.1 Hz, 1H), 6.59 (d, J = 2.1 Hz, 1H), 2.65 (s, 3H).

^{13}C NMR (151 MHz CDCl$_3$) δ 162.5, 159.8, 158.4, 158.3, 157.2, 141.0, 114.9, 110.3, 107.9, 13.9.

HR-MS-ESI (m/z) Calculated for C$_{10}$H$_9$N$_3$O$_2$ [M + H]$^+$: 226.0587, found: 226.0583.

LC-MS purity (UV) = 97%, tR 16.03 min; m/z (ESI$^+$) 203.85 [M + H]$^+$.

N-(3-bromophenyl)-2-methylfuran-3-carboxamide (2.13)

This was synthesised on a 0.39 mmol scale from 2-methylfuran-3-carboxylic acid by the same procedure as **2.1** and 3-bromoaniline (81.2 mg, 0.47 mmol) was used instead of pentan-1-amine. The final product was obtained as a brown solid; yield: 49.4 mg (45%).
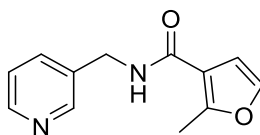
^{1}H NMR (600 MHz, CDCl$_3$) δ 7.85 (t, J = 1.9 Hz, 1H), 7.47 (dt, J = 8.1, 1.5 Hz, 1H), 7.43 (brs, 1H), 7.31 (d, J = 2.0 Hz, 1H), 7.25 (m, 1H), 7.19 (m, 1H), 6.52 (d, J = 2.2 Hz, 1H), 2.63 (s, 3H).

^{13}C NMR (151 MHz, CDCl$_3$) δ 162.0, 158.5, 140.7, 139.0, 130.3, 127.3, 123.0, 122.7, 118.5, 115.4, 107.9, 13.7.

HR-MS-ESI (m/z) Calculated for a dimer, C$_{24}$H$_{20}$N$_2$O$_4$^{81}Br$_2$ [M + Na]$^+$: 580.9682, found: 580.9661.

LC-MS purity (UV) = 97%, tR 23.06 min; m/z (ESI$^+$) 281.65 [M + H]$^+$.

2-Methyl-*N*-(pyridin-3-ylmethyl)furan-3-carboxamide (**2.14**)

This was synthesised on a 0.39 mmol scale from 2-methylfuran-3-carboxylic acid by the same procedure as **2.1** and pyridin-3-ylmethanamine (51.1 mg, 0.47 mmol) was used instead of pentan-1-amine. The final product was obtained as a colourless solid; yield: 57.0 mg (67%).

^{1}H NMR (600 MHz, CDCl$_3$) δ 8.45 (dd, J = 4.7, 2.0 Hz, 2H), 7.65 (dt, J = 7.8, 2.0 Hz, 1H), 7.23 – 7.21 (m, 1H), 7.20 (d, J = 2.0 Hz, 1H), 6.68 (t, J = 6.0 Hz, 1H), 6.47 (d, J = 2.1 Hz, 1H), 4.51 (d, J = 6.0 Hz, 2H), 2.56 (s, 3H).

^{13}C NMR (151 MHz, CDCl$_3$) δ 168.5, 161.7, 149.2, 149.0, 140.5, 135.7, 132.7, 123.6, 114.4, 108.0, 40.8, 13.6.

HR-MS-ESI (m/z) Calculated for dimer, C$_{12}$H$_{13}$N$_2$O$_2$ [M + H]$^+$: 217.0977, found: 217.0984.

LC-MS purity (UV) = 98%, tR 9.12 min; m/z (ESI⁺) 216.95 [M + H]⁺.

N-(4-hydroxyphenethyl)-2-methylfuran-3-carboxamide (**2.15**)

This was synthesised on a 0.39 mmol scale from 2-methylfuran-3-carboxylic acid by the same procedure as 2.1 and 4-(2-aminoethyl)phenol (64.8 mg, 0.47 mmol) was used instead of pentan-1-amine. The final product was obtained as a colorless oil; yield: 20.5 mg (21%).

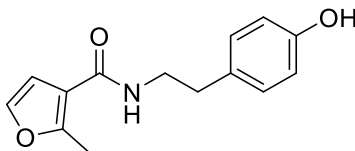^{1}H NMR (600 MHz, CDCl$_3$) δ 7.20 (d, J = 2.0 Hz, 1H), 7.02 (d, J = 8.2 Hz, 2H), 6.80 (d, J = 8.2 Hz, 2H), 6.75 (s, 1H), 6.30 (d, J = 2.1 Hz, 1H), 5.83 (t, J = 5.8 Hz, 1H), 3.58 (q, J = 6.7 Hz, 2H), 2.78 (t, J = 7.0 Hz, 2H), 2.53 (s, 3H).

^{13}C NMR (151 MHz, CDCl$_3$) δ 164.3, 156.8, 155.0, 140.4, 130.1, 129.8, 115.7, 115.4, 108.3, 40.9, 34.8, 13.6.

HR-MS-ESI (m/z) Calculated for C$_{14}$H$_{15}$NO$_3$ [M + Na]⁺: 268.0944, found: 268.0939.

LC-MS purity (UV) = 97%, tR 2.26 min; m/z (ESI⁺) 246.00 [M + H]⁺.

N-(4-Fluoro-2-isopropoxyphenyl)-2-methylfuran-3-carboxamide (2.16)
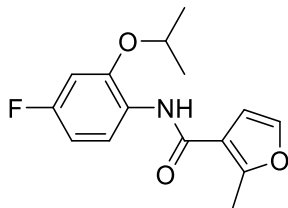
This was synthesised on a 0.39 mmol scale from 2-methylfuran-3-carboxylic acid by the same procedure as **2.1** and 4-fluoro-2-isopropoxyaniline (79.9 mg, 0.47 mmol) was used instead of pentan-1-amine. The final product was obtained as a brown solid; yield: 96.8 mg (89%).

^{1}H NMR (600 MHz, CDCl$_3$) δ 8.42 (t, J = 7.6 Hz, 1H), 8.03 (brs, 1H), 7.30 (d, J = 1.9 Hz, 1H), 6.69 – 6.60 (m, 2H), 6.52 (t, J = 1.9 Hz, 1H), 4.57 (sep, J = 6.1 Hz, 1H), 2.64 (t, J = 1.7 Hz, 3H), 1.40 (d, J = 6.1 Hz, 6H).

^{13}C NMR (151 MHz, CDCl$_3$) δ 161.4, 159.7 (d, $^1J_{CF}$ = 242.1 Hz), 156.9, 146.9 (d, $^3J_{CF}$ = 10.1 Hz), 40.6, 124.8, 120.3, 116.5, 108.5, 106.7 (d, $^2J_{CF}$ = 21.9 Hz), 100.6 (d, $^2J_{CF}$ = 21.9 Hz), 71.8, 22.1, 13.7.

^{19}F NMR (376 MHz, CDCl$_3$) δ -116.96 – -117.12 (m).

HR-MS-ESI (m/z) Calculated for C$_{15}$H$_{16}$FNO$_3$ [M + Na]$^+$: 300.1006, found: 300.1004.

LC-MS purity (UV) = 97%, tR 23.09 min; m/z (ESI$^+$) 277.85 [M + H]$^+$.

2-Methyl-*N*-(3'-methyl-[1,1'-biphenyl]-3-yl)furan-3-carboxamide (**2.17**)
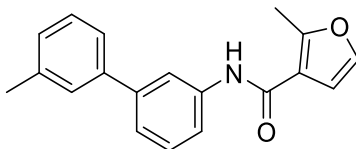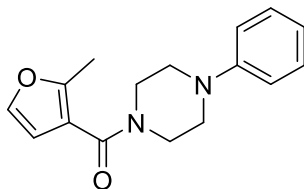

This was synthesised on a 0.39 mmol scale from 2-methylfuran-3-carboxylic acid by the same procedure as **2.1** and 3'-methyl-[1,1'-biphenyl]-3-amine (103.7 mg, 0.47 mmol) was used instead of pentan-1-amine. The final product was obtained as a colorless liquid; yield: 22.2 mg (19%).

^{1}H NMR (600 MHz, CDCl$_3$) δ 7.80 (t, J = 1.9 Hz, 1H), 7.57 – 7.52 (m, 2H), 7.42 – 7.36 (m, 3H), 7.36 – 7.30 (m, 2H), 7.29 (d, J = 2.1 Hz, 1H), 7.16 (m, 1H), 6.56 (d, J = 2.1 Hz, 1H), 2.64 (s, 3H), 2.40 (s, 3H).

^{13}C NMR (151 MHz, CDCl$_3$) δ 162.2, 158.0, 142.3, 140.6, 140.5, 138.3, 138.1, 129.3, 128.6, 128.3, 128.0, 124.3, 123.2, 119.0, 115.8, 111.0, 108.2, 21.5, 13.7.

HR-MS-ESI Calculated for C$_{38}$H$_{34}$N$_2$O$_4$ [M + Na]$^+$: 605.2411, found: 605.2419.

LC-MS purity (UV) = 96%, tR 25.14 min; m/z (ESI$^+$) 291.90 [M + H]$^+$.

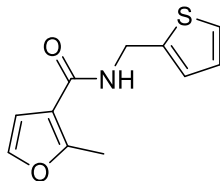**(2-methylfuran-3-yl)(4-phenylpiperazin-1-yl)methanone** (**2.18**)

This was synthesised on a 0.39 mmol scale from 2-methylfuran-3-carboxylic acid by the same procedure as **2.1** and 1-phenylpiperazine (76.6 mg, 0.47 mmol) was used instead of pentan-1-amine. The final product was obtained as a brown solid; yield: 84.3 mg (79%).

^{1}H NMR (600 MHz, CDCl$_3$) δ 7.31 – 7.28 (m, 2H), 7.28 (d, J = 1.9 Hz, 1H), 6.94 (d, J = 8.1 Hz, 2H), 6.91 (t, J = 7.3 Hz, 1H), 6.37 (d, J = 1.9 Hz, 1H), 3.85 (s, 2H), 3.73 (s, 2H), 3.19 (s, 4H), 2.41 (s, 3H).

^{13}C NMR (151 MHz, CDCl$_3$) δ 165.3, 153.7, 151.0, 140.4, 129.3, 120.6, 116.7, 115.4, 110.2, 61.3, 56.5, 13.0.

HR-MS-ESI (m/z) Calculated for a dimer, C$_{32}$H$_{36}$N$_4$O$_4$ [M + Na]$^+$: 563.2629, found: 563.2626.

LC-MS purity (UV) = 100%, tR 2.66 min; m/z (ESI$^+$) 271.05 [M + H]$^+$.

2-methyl-*N*-(thiophen-2-ylmethyl)furan-3-carboxamide (**2.19**)

This was synthesised on a 0.39 mmol scale from 2-methylfuran-3-carboxylic acid by the same procedure as **2.1** and thiophen-2-ylmethanamine (53.4 mg, 0.47 mmol) was used instead of pentan-1-amine. The final product was obtained as a colourless solid; yield: 56.3 mg (65%).

^{1}H NMR (600 MHz, CDCl$_3$) δ 7.24 – 7.22 (m, 2H), 7.01 (d, *J* = 2.0 Hz, 1H), 6.95 (dd, *J* = 5.1, 3.5 Hz, 1H), 6.39 (d, *J* = 2.0 Hz, 1H), 6.04 (brs, 1H), 4.73 (d, *J* = 5.7 Hz, 2H), 2.59 (s, 3H).

^{13}C NMR (151 MHz, CDCl$_3$) δ 163.5, 157.3, 141.0, 140.4, 126.9, 126.1, 125.3, 115.1, 108.2, 38.1, 13.6.

HR-MS-ESI (m/z) Calculated for C$_{11}$H$_{11}$N$_1$O$_2$S [M + Na]$^+$: 244.0403, found: 244.0401.

LC-MS purity (UV) = 95%, tR 19.84 min; m/z (ESI$^+$) 221.75 [M + H]$^+$.
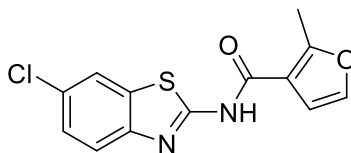
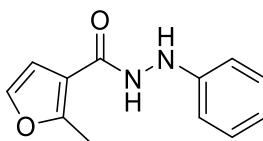**N-(6-Chlorobenzo[d]thiazol-2-yl)-2-methylfuran-3-carboxamide** (**2.20**)

This was synthesised on a 0.39 mmol scale from 2-methylfuran-3-carboxylic acid by the same procedure as **2.1** and 2-amino-6-chlorobenzothiazole (87.2 mg, 0.47 mmol) was used instead of pentan-1-amine. The final product was obtained as a colourless solid; yield: 136.5 mg (90%).

^{1}H NMR (600 MHz, CDCl$_3$) δ 9.90 (brs, 1H), 7.81 (d, J = 2.1 Hz, 1H), 7.58 (d, J = 8.6 Hz, 1H), 7.37 (dd, J = 8.6, 2.1 Hz, 1H), 7.31 (d, J = 2.1 Hz, 1H), 6.60 (d, J = 2.1 Hz, 1H), 2.71 (s, 3H).

^{13}C NMR (151 MHz, CDCl$_3$) δ 160.6, 155.6, 146.7, 141.3, 133.7, 129.5, 126.9, 121.6, 121.0, 113.6, 110.2, 107.8, 14.0.

HR-MS-ESI (m/z) Calculated for C$_{13}$H$_9$N$_2$O$_2$SCl [M + Na]$^+$: 314.9965, found: 314.9958.

LC-MS purity (UV) = 97%, tR 24.82 min; m/z (ESI$^+$) 292.75 [M + H]$^+$.

2-Methyl-N'-phenylfuran-3-carbohydrazide (**2.21**)

This was synthesised on a 0.39 mmol scale from 2-methylfuran-3-carboxylic acid by the same procedure as **2.1** and phenylhydrazine (51.0 mg, 0.47 mmol) was used instead of

pentan-1-amine. The final product was obtained as a off-colourless solid; yield: 32.2 mg (38%).
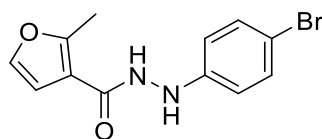
^{1}H NMR (600 MHz, CDCl$_3$) δ 7.48 (brs, 1H), 7.30 (d, J = 2.1 Hz, 1H), 7.25 – 7.21 (m, 2H), 6.92 – 6.88 (m, 3H), 6.52 (d, J = 2.1 Hz, 1H), 6.23 (d, J = 3.8 Hz, 1H), 2.59 (s, 3H).

^{13}C NMR (151 MHz, CDCl$_3$) δ 164.1, 158.3, 148.1, 140.8, 129.2, 126.3, 121.4, 113.7, 107.8, 13.6.

HR-MS-ESI (m/z) Calculated for C$_{12}$H$_{13}$N$_2$O$_2$ [M + H]$^+$: 217.0972, found: 217.0967.

LC-MS purity (UV) = 94%, tR 5.36 min; m/z (ESI$^+$) 216.85 [M + H]$^+$.

N'-(4-Bromophenyl)-2-methylfuran-3-carbohydrazide (2.22)

This was synthesised on a 0.79 mmol scale from 2-methylfuran-3-carboxylic acid by the same procedure as **2.1** and 4-bromophenylhydrazine (211 mg, 0.47 mmol) was used instead of pentan-1-amine. The final product was obtained as a brown liquid; yield: 15.9 mg (7%).
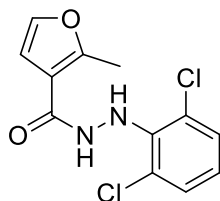
^{1}H NMR (600 MHz, CDCl$_3$) δ 7.60 (d, J = 4.1 Hz, 1H), 7.30 (d, J = 8.8 Hz, 2 H), 7.29 (d, J = 2.1 Hz, 1H), 6.76 (d, J = 8.8 Hz, 2H), 6.52 (d, J = 2.1 Hz, 1H), 6.26 (d, J = 4.1 Hz, 1H), 2.57 (s, 3H).

^{13}C NMR (151 MHz, CDCl$_3$) δ 164.2, 158.5, 147.3, 140.9, 132.0, 115.3, 113.4, 112.8, 107.7, 13.7.

HR-MS-ESI (m/z) Calculated for C$_{12}$H$_{11}$BrN$_2$O$_2$ [M + Na]$^+$: 316.9896, found: 316.9895.

LC-MS purity (UV) = 93%, tR 20.97 min; m/z (ESI$^+$) 294.75 [M + H]$^+$.

N'-(2,6-dichlorophenyl)-2-methylfuran-3-carbohydrazide (**2.23**)

This was synthesised on a 0.39 mmol scale from 2-methylfuran-3-carboxylic acid by the same procedure as **2.1** and 2,6-dichlorophenylhydrazine (100.8 mg, 0.47 mmol) was used instead of pentan-1-amine. The final product was obtained as a colourless solid; yield: 89.2 mg (80%).

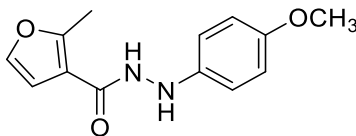^{1}H NMR (600 MHz, CDCl$_3$) δ 7.94 (d, J = 4.9 Hz, 1H), 7.24 (d, J = 2.2 Hz, 2H), 7.23 (s, 1H), 6.98 (d, J = 4.9 Hz, 1H), 6.89 (t, J = 8.0 Hz, 1H), 6.48 (d, J = 2.2 Hz, 1H), 2.55 (s, 3H).

^{13}C NMR (151 MHz, CDCl$_3$) δ 163.1, 157.9, 141.3, 140.7, 129.0, 125.9, 124.0, 112.9, 108.0, 13.6.

HR-MS-ESI (m/z) Calculated for C$_{12}$H$_{11}$Cl$_2$N$_2$O$_2$ [M + H]$^+$: 285.0198, found: 285.0206.

76

LC-MS purity (UV) = 96%, tR 21.73 min; m/z (ESI$^+$) 284.75 [M + H]$^+$.

N'-(4-Methoxyphenyl)-2-methylfuran-3-carbohydrazide (2.24)

This was synthesised on a 0.39 mmol scale from 2-methylfuran-3-carboxylic acid by the same procedure as **2.1** and (4-methoxyphenyl)hydrazine (44.4 mg, 0.47 mmol) was used instead of pentan-1-amine. The final product was obtained as a brown solid; yield: 48.1 mg (50%).

^{1}H NMR (600 MHz, CDCl$_3$) δ 9.84 (s, 1H), 7.46 (d, J = 8.0 Hz, 2H), 7.33 (aps, 1H), 7.17 (s, 1H), 7.01 (d, J = 8.4 Hz, 2H), 6.90 (app. s, 1H), 3.98 (s, 3H), 2.72 (s, 3H).

^{13}C NMR (151 MHz, CDCl$_3$) δ 159.0, 158.7, 140.1, 139.5, 128.3, 114.2, 113.0, 110.6, 108.5, 55.5, 13.6.

HR-MS-ESI (m/z) Calculated for C$_{13}$H$_{14}$N$_2$O$_3$ [M + Na]$^+$: 269.0902, found: 269.0913.

LC-MS purity (UV) = 93%, tR 17.38 min; m/z (ESI$^+$) 246.80 [M + H]$^+$.

2.8.1.2 Synthesis of sulfonamide series (Series II)
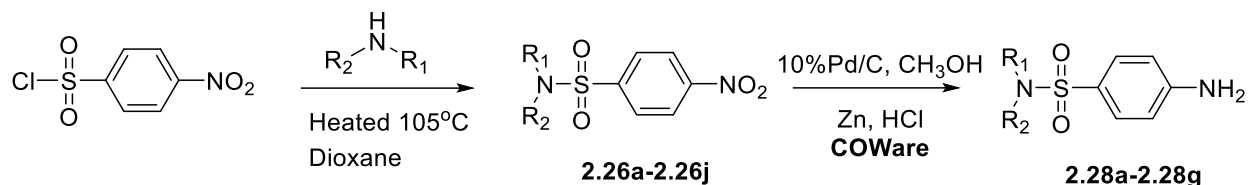
N-(2-hydroxyethyl)-N-methyl-4-nitrobenzenesulfonamide (2.26a)
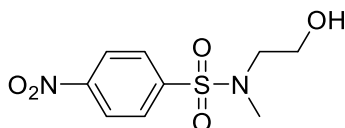
Dissolved 4-nitrosulfonyl chloride (100.0 mg, 0.45 mmol) and (2-(methylamino)ethan-1-ol, (67.8 mg, 0.90 mmol) in 1,4-dioxane (0.5 mL) were heated under reflux at 105°C overnight. When the reaction was complete, the cooled reaction mixture was concentrated in vacuum. The crude material was purified by flash column chromatography and the final product was obtained as yellow solid; yield: 112.7 mg (96%).

^{1}H NMR (600 MHz, CDCl$_3$): δ 8.37 (d, J = 8.7 Hz, 2H), 7.98 (d, J = 8.7 Hz, 2H), 3.77 (t, J = 5.3 Hz, 2H), 3.23 (t, J = 5.3 Hz, 2H), 2.88 (s, 3H), 2.28 (s, 1H).

^{13}C NMR (151 MHz, CDCl$_3$) δ 150.1, 143.5, 128.6, 124.5, 60.2, 52.4, 35.9.

HRMS m/z (ESI+) Calculated for C$_9$H$_{13}$N$_2$O$_5$S [M + H]$^+$: 261.0545, found: 261.0559.

LC-MS purity (UV) = 95%, tR 17.44 min; m/z (ESI$^+$) 260.95 [M + H]$^+$.

N-(2-Hydroxyethyl)-4-nitrobenzenesulfonamide (**2.26b**)
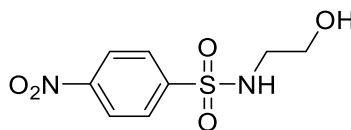
This was synthesised on a 2.58 mmol scale from 4-nitrosulfonyl chloride by the same procedure of **2.26a** and 2-aminoethan-1-ol (150.0 mg, 2.46 mmol) was used instead of 2-(methylamino)ethan-1-ol. The final product was obtained as a colourless solid; yield: 406.9 mg (64%).

^{1}H NMR (600 MHz, DMSO-d_6) δ 8.39 (d, J = 8.5 Hz, 2H), 8.03 (d, J = 8.5 Hz, 3H), 4.72 (brs, 1H), 3.35 (t, J = 6.2 Hz, 2H), 2.84 (t, J = 6.1 Hz, 2H).

^{13}C NMR (151 MHz, DMSO-d_6) δ 149.9, 146.7, 128.5, 125.0, 60.3, 45.5.

HRMS m/z (ESI+) Calculated for $C_8H_{10}N_2O_5S$ [M + Na]$^+$: 269.0208, found: 269.0219.

LC-MS purity (UV) = 97%, tR 15.02 min; m/z (ESI$^+$) 244.90 [M + H]$^+$.

N,N-bis(2-Hydroxyethyl)-4-nitrobenzenesulfonamide (**2.26c**)
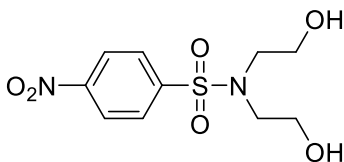
This was synthesised on a 0.90 mmol scale from 4-nitrosulfonyl chloride by the same procedure as **2.26a** and 2,2'-azanediylbis(ethan-1-ol) (191.5 mg, 1.80 mmol) was used

instead of 2-(methylamino)ethan-1-ol. The final product was obtained as a colourless solid; yield: 75.5 mg (29%).

^{1}H NMR (600 MHz, DMSO-d_6) δ 8.37 (d, J = 8.8 Hz, 2H), 8.06 (d, J = 8.8 Hz, 2H), 4.83 (t, J = 5.4 Hz, 2H), 3.49 (t, J = 6.0 Hz, 4H), 3.22 (t, J = 6.0 Hz, 4H).

^{13}C NMR (151 MHz, DMSO-d_6) δ 150.1, 145.4, 129.0, 125.0, 60.0, 51.2.

HRMS m/z (ESI+) Calculated for $C_{10}H_{15}N_2O_6S$ [M + H]$^+$: 291.0651, found: 291.0658.

LC-MS purity (UV) = 93%, tR 18.18 min; m/z (ESI$^+$) 312.90 [M + Na]$^+$.

N-(3-Bromophenyl)-4-nitrobenzenesulfonamide (2.26d)
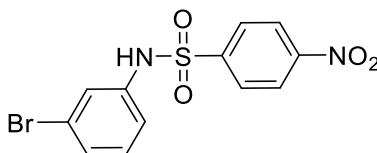
This was synthesised on a 0.45 mmol scale from 4-nitrosulfonyl chloride by the same procedure as **2.26a** and 3-bromoaniline (155.2 mg, 0.90 mmol) was used instead of 2-(methylamino)ethan-1-ol. The final product was obtained as a pale yellow powder; yield: 92.4 mg (57%).

^{1}H NMR (600 MHz, CDCl$_3$) δ 8.31 (d, J = 8.8 Hz, 2H), 7.97 (d, J = 8.8 Hz, 2H), 7.31 – 7.27 (m, 2H), 7.14 (t, J = 8.0 Hz, 1H), 7.03 (dd, J = 8.3, 2.2 Hz, 1H). (NH not visible)

^{13}C NMR (151 MHz, CDCl$_3$) δ 150.4, 144.3, 136.6, 131.0, 129.4, 128.5, 124.8, 124.5, 123.2, 120.2.

HRMS m/z (ESI+) Calculated for C$_{12}$H$_8$N$_2$O$_4$SBr [M + H]$^+$: 354.9388, found: 354.9381.

LC-MS purity (UV) = 90%, tR 22.69 min; m/z (ESI$^+$) 354.75 [M + H]$^+$.

4-Nitro-*N*-(1*H*-pyrazol-3-yl)benzenesulfonamide (2.26e)
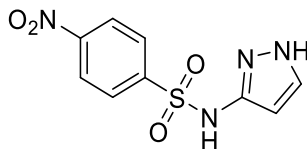
This was synthesised on a 1.44 mmol scale from 4-nitrosulfonyl chloride by the same procedure of **2.26a** and 1*H*-pyrazol-3-amine (100.0 mg, 1.20 mmol) was used instead of 2-(methylamino)ethan-1-ol. The final product was obtained as a yellow solid; yield: 90.3 mg (28%).

^{1}H NMR (600 MHz, DMSO-d_6) δ 12.42 (s, 1H), 10.75 (s, 1H), 8.36 (d, *J* = 8.8 Hz, 2H), 7.99 (d, *J* = 8.8 Hz, 2H), 7.56 (s, 1H), 5.98 (s, 1H).

^{13}C NMR (151 MHz, DMSO-d_6) δ 150.1, 146.1, 145.3, 130.2, 128.8, 124.9, 97.9.

HRMS m/z (ESI+) Calculated for C$_9$H$_9$N$_4$O$_4$S [M + H]$^+$: 269.0345, found: 269.0332.

LC-MS purity (UV) = 97%, tR 26.98 min; m/z (ESI$^+$) 268.75 [M + H]$^+$.

4-Nitro-*N*-(2-(pyrrolidin-1-yl)ethyl)benzenesulfonamide (2.26f)
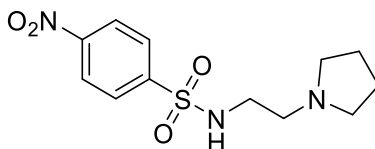
This was synthesised on a 0.45 mmol scale from 4-nitrosulfonyl chloride by the same procedure as **2.26a** and 2-(pyrrolidin-1-yl)ethan-1-amine (77.3 mg, 0.68 mmol) was used instead of 2-(methylamino)ethan-1-ol. The final product was obtained as a yellow solid; yield: 98.6 mg (73%).

^{1}H NMR (600 MHz, DMSO-*d*6) δ 8.42 (d, *J* = 8.7 Hz, 2H), 8.09 (d, *J* = 8.7 Hz, 2H), 3.16 – 2.89 (m, 8H), 1.84 (s, 4H). (NH not visible)

^{13}C NMR (151 MHz, DMSO-*d*6) δ 150.2, 145.8, 128.7, 125.1, 53.7, 53.6, 40.3, 23.0.

HRMS m/z (ESI+) Calculated for $C_{12}H_{18}N_3O_4S$ [M + H]$^+$: 300.1018, found: 300.1017.

LC-MS purity (UV) = 91%, tR 10.67 min; m/z (ESI$^+$) 300.20 [M + H]$^+$.

N-(3'-Methyl-[1,1'-biphenyl]-3-yl)-4-nitrobenzenesulfonamide (2.26g)

This was synthesised on a 0.45 mmol scale from 4-nitrosulfonyl chloride by the same procedure as **2.26a** and 3'-methyl-[1,1'-biphenyl]-3-amine (148.7 mg, 0.68 mmol) was

used instead of 2-(methylamino)ethan-1-ol. The final product was obtained as a yellow oil; yield: 127.0 mg (76%).

^{1}H NMR (600 MHz, CDCl$_3$) δ 8.28 (d, J = 8.8 Hz, 2H), 7.96 (d, J = 8.8 Hz, 2H), 7.41 (d, J = 7.9 Hz, 1H), 7.32 (q, J = 7.9 Hz, 2H), 7.30 – 7.26 (m, 3H), 7.18 (d, J = 7.3 Hz, 1H), 7.04 (m, 1H), 6.80 (brs, 1H), 2.40 (s, 3H).

^{13}C NMR (151 MHz, CDCl$_3$) δ 150.2, 144.6, 143.1, 139.7, 138.6, 135.7, 130.0, 128.8, 128.7, 128.6, 127.8, 125.3, 124.3, 124.1, 121.1, 120.8, 21.5.

HRMS m/z (ESI+) Calculated for C$_{19}$H$_{15}$N$_2$O$_4$S [M + H]$^+$: 367.0753, found: 367.0752.

LC-MS purity (UV) = 96%, tR 24.48 min; m/z (ESI$^+$) 367.85 [M - H]$^-$.
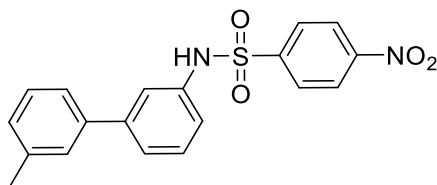
N-(2-Morpholinoethyl)-4-nitrobenzenesulfonamide (**2.26h**)
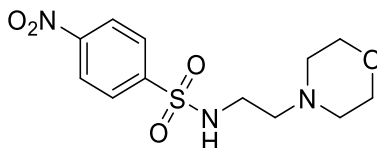
This was synthesised on a 0.45 mmol scale from 4-nitrosulfonyl chloride by the same procedure as **2.26a** and 2-morpholinoethan-1-amine (58.8 mg, 0.45 mmol) was used instead of 2-(methylamino)ethan-1-ol. The final product was obtained as a pale pink solid; yield: 75.8 mg (53%).

^{1}H NMR (600 MHz, DMSO-d_6) δ 11.31 (brs, 1H), 8.61 (t, J = 5.9 Hz, 1H), 8.42 (d, J = 8.9 Hz, 2H), 8.08 (d, J = 8.9 Hz, 2H), 3.90 (d, J = 12.8 Hz, 2H), 3.76 (t, J = 12.2 Hz, 2H), 3.38 (s, 1H), 3.25 (q, J = 6.5 Hz, 2H), 3.16 (q, J = 5.8 Hz, 2H), 3.06 (m, 2H).

^{13}C NMR (151 MHz, DMSO-d_6) δ 150.2, 145.7, 128.8, 125.2, 63.4, 55.5, 51.6, 37.1.

HRMS m/z (ESI$^+$) Calculated for $C_{12}H_{18}N_3O_5S$ [M + H]$^+$: 316.0967, found: 316.0966.

LC-MS purity (UV) = 99%, tR 1.15 min; m/z (ESI$^+$) 316.05 [M + H]$^+$.

4-Nitro-*N*-(pyridin-2-yl)benzenesulfonamide (2.26i)
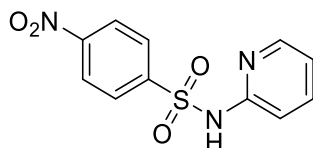
This was synthesised on a 0.45 mmol scale from 4-nitrosulfonyl chloride by the same procedure to **2.26a** and pyridin-2-amine (63.7 mg, 0.68 mmol) was used instead of 2-(methylamino)ethan-1-ol. The final product was obtained as a pale yellow solid; yield: 72.2 mg (57%).

^{1}H NMR (600 MHz, DMSO-d_6) δ 13.35 (brs, 1H), 8.32 (d, J = 8.9 Hz, 2H), 8.06 (d, J = 8.9 Hz, 2H), 7.92 (d, J = 6.5 Hz, 1H), 7.79 (t, J = 7.0 Hz, 1H), 7.24 (d, J = 6.5 Hz, 1H), 6.84 (t, J = 6.4 Hz, 1H).

^{13}C NMR (151 MHz, DMSO-d_6) δ 154.7, 149.5, 149.1, 143.0, 141.1 – 139.2 (m), 128.2, 124.8, 115.6, 114.4.

HRMS m/z (ESI$^+$) Calculated for $C_{11}H_{10}N_3O_4S$ [M + H]$^+$: 280.0392, found: 280.0403.

LC-MS purity (UV) = 98%, tR 3.74 min; m/z (ESI$^+$) 280.00 [M + H]$^+$.

N-(1-methyl-3-(pyridin-3-yl)-1H-pyrazol-5-yl)-4-nitrobenzenesulfonamide (**2.26j**)

This was synthesised on a 0.45 mmol scale from 4-nitrosulfonyl chloride by the same procedure of **2.26a** and 1-methyl-3-(pyridin-3-yl)-1H-pyrazol-5-amine (117.9 mg, 0.68 mmol) was used instead of 2-(methylamino)ethan-1-ol. The final product was obtained as a pale yellow solid; yield: 43.9 mg (27%).
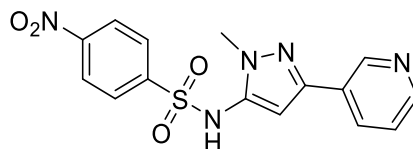
^{1}H NMR (600 MHz, DMSO-d_6) δ 9.13 (s, 1H), 8.74 (d, J = 5.5 Hz, 1H), 8.69 (d, J = 8.1 Hz, 1H), 8.43 (d, J = 8.9 Hz, 2H), 8.04 (d, J = 8.9 Hz, 2H), 7.93 (dd, J = 8.2, 5.5 Hz, 1H), 6.60 (s, 1H), 3.70 (s, 3H). (NH not visible).

^{13}C NMR (151 MHz, DMSO-d_6) δ 150.5, 145.0, 143.9, 142.2, 139.7, 136.4, 131.9, 128.9, 127.3, 125.3, 100.8, 66.8, 36.4.

HRMS m/z (ESI$^+$) Calculated for $C_{15}H_{14}N_5O_4S$ [M + H]$^+$: 360.0766, found: 360.0775.

LC-MS purity (UV) = 97%, tR 3.64 min; m/z (ESI$^+$) 360.00 [M + H]$^+$.

Reduction process
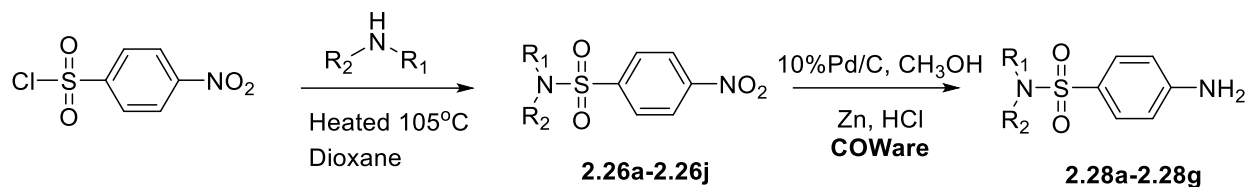
COware two chamber system

Chamber A: compound **b**, 10%Pd/C, MeOH

Chamber B: Zn, HCl

4-amino-*N*-(2-hydroxyethyl)-*N*-methylbenzenesulfonamide (2.28a)
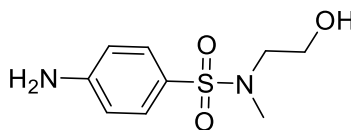
The dissolved compound **2.26a** (100.0 mg, 0.38 mmol) in methanol (MeOH, 5.6 mL) and 5.6 mg of 10% Pd/C was added to form a suspension that placed in a chamber A. In chamber B, hydrogen gas was produced by using 7M HCl 3.43 mL and Zn 928.5 mg. The reaction was stirred under a hydrogen gas atmosphere at 1 atmospheric pressure at room temperature for 12 hrs. After that, the palladium catalyst was removed by filtration through celite from the mixture then the filtrate was concentrated in vacuum. The crude material was purified by flash column chromatography and the final product **2.28a** was obtained as orange solid: 86.2 mg (98%).

^{1}H NMR (600 MHz, DMSO-d_6) δ 7.34 (d, J = 8.6 Hz, 2H), 6.60 (d, J = 8.6 Hz, 2H), 6.00 (s, 2H), 4.73 (t, J = 5.1 Hz, 1H), 3.45 (q, J = 5.7 Hz, 2H), 2.85 (t, J = 6.2 Hz, 2H), 2.58 (s, 3H).

^{13}C NMR (151 MHz, DMSO-d_6) δ 153.4, 129.6, 121.9, 113.2, 59.6, 52.4, 36.2.

HR-MS-ESI (m/z) calculated for $C_9H_{15}N_2O_3S$ [M + H]$^+$: 231.0803; found: 231.0794.

LC-MS purity (UV) = 94%, tR 13.23 min; m/z (ESI$^+$) 230.80 [M + H]$^+$.

4-amino-*N*-(2-hydroxyethyl)benzenesulfonamide (2.28b)
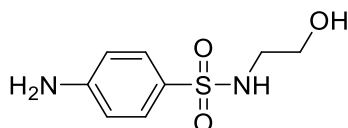
This was synthesised on a 0.61 mmol scale from **2.26e** by the same procedure of **2.28a.** The MeOH 9.0 mL, 10% Pd/C 8.9 mg , 7M HCl 3.14 mL and Zn 1200.0 mg were used. The final product was obtained as a brown powder; yield: 123.2 mg (94%).

^{1}H NMR (600 MHz, DMSO-d_6) δ 7.38 (d, J = 8.6 Hz, 2H), 7.03 (t, J = 6.1 Hz, 1H), 6.58 (d, J = 8.6 Hz, 2H), 5.90 (s, 2H), 4.62 (t, J = 5.7 Hz, 1H), 3.31 (q, J = 6.2 Hz, 2H), 2.67 (q, J = 6.2 Hz, 2H).

^{13}C NMR (151 MHz, DMSO-d_6) δ 152.9, 128.9, 125.9, 113.1, 60.3, 45.4.

HR-MS-ESI (m/z) calculated for $C_8H_{13}N_2O_3S$ [M + H]$^+$: 217.0647; found: 217.0647.

LC-MS purity (UV) = 95%, tR 11.13 min; m/z (ESI$^+$) 238.90 [M + Na]$^+$.

4-amino-*N,N*-bis(2-hydroxyethyl)benzenesulfonamide (**2.28c**)
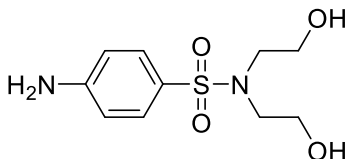
This was synthesised on a 0.61 mmol scale from **2.26f** by the same procedure of **2.28a.** The MeOH 9.0 mL, 10% Pd/C 8.9 mg, 7M HCl 3.14 mL and Zn 1.20 g were used. The final product was obtained as a brown powder; yield: 123.2 mg (94%).

^{1}H NMR (600 MHz, DMSO-d_6) δ 7.38 (d, J = 8.4 Hz, 2H), 6.60 (d, J = 8.4 Hz, 2H), 5.98 (s, 2H), 4.77 (t, J = 5.5 Hz, 2H), 3.46 (q, J = 6.5 Hz, 4H), 3.02 (t, J = 6.5 Hz, 4H).

^{13}C NMR (151 MHz, DMSO-d_6) δ 153.3, 129.3, 124.1, 113.2, 60.6, 51.7.

HR-MS-ESI (m/z) calculated for C$_{10}$H$_{17}$N$_2$O$_4$S [M + H]$^+$: 261.0909; found: 261.0920.

LC-MS purity (UV) = 95%, tR 11.65 min; m/z (ESI$^+$) 260.90 [M + H]$^+$.

4-amino-*N*-(1*H*-pyrazol-3-yl)benzenesulfonamide (**2.28e**)

This was synthesised on a 0.22 mmol scale from **2.26d** by the same procedure of **2.28a.** The MeOH 3.3 mL, 10% Pd/C 10.0 mg , 7M HCl 3.40 mL and Zn 1,260.0 mg were used. The final product was obtained as a brown powder; yield: 57.3 mg (96%).

^{1}H NMR (600 MHz, DMSO-d_6) δ 12.22 (brs, 1H), 9.93 (brs, 1H), 7.48 (s, 1H), 7.36 (d, *J* = 8.3 Hz, 2H), 6.50 (d, *J* = 8.3 Hz, 2H), 5.90 (s, 2H), 5.89 (s, 1H).

^{13}C NMR (151 MHz, DMSO-d_6) δ 152.9, 146.9, 129.0, 122.7, 112.9, 112.8, 96.6.

HR-MS-ESI (m/z) calculated for $C_9H_{11}N_4O_2S$ [M + H]$^+$: 239.0603; found: 239.0605.

LC-MS purity (UV) = 94%, tR 14.50 min; m/z (ESI$^+$) 238.95 [M + H]$^+$.

4-amino-*N*-(2-(pyrrolidin-1-yl)ethyl)benzenesulfonamide (**2.28f**)

This was synthesised on a 0.21 mmol scale from **2.26b** by the same procedure of **2.28a.** The MeOH 3.0 mL, 10% Pd/C 5.6 mg , 7M HCl 3.43 mL and Zn 1,075.2 mg were used. The final product was obtained as a yellow solid; yield: 23.3 mg (41%).

^{1}H NMR (600 MHz, DMSO-d_6) δ 7.40 (d, J = 8.6 Hz, 2H), 6.59 (d, J = 8.6 Hz, 2H), 5.96 (s, 2H), 3.06 – 2.60 (m, 8H), 1.83 – 1.68 (m, 4H). (NH not visible)

^{13}C NMR (151 MHz, DMSO-d_6) δ 153.1, 129.0, 125.2, 113.1, 54.4, 53.8, 40.5, 23.2.

HR-MS-ESI (m/z) calculated for $C_{12}H_{20}N_3O_2S$ [M + H]$^+$: 270.1276; found: 270.1273.

LC-MS purity (UV) = 94%, tR 8.09 min; m/z (ESI$^+$) 269.80 [M + H]$^+$.

4-amino-*N*-(3'-methyl-[1,1'-biphenyl]-3-yl)benzenesulfonamide (**2.28g**)
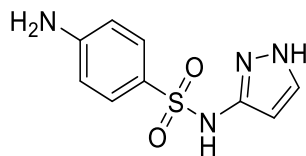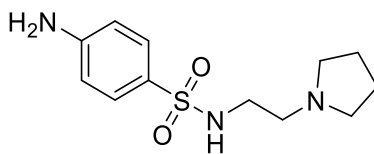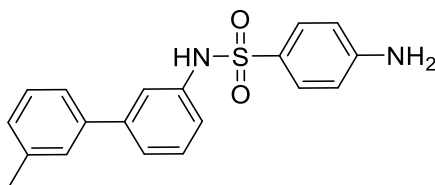

This was synthesised on a 0.13 mmol scale from **2.26c** by the same procedure of **2.28a.** The MeOH 2.0 mL, 10% Pd/C 1.83 mg , 7M HCl 3.43 mL and Zn 1,092.5 mg were used. The final product was obtained as a yellow oil; yield: 3.0 mg (2%).

^{1}H NMR (600 MHz, CDCl$_3$) δ 7.54 (d, J = 8.7 Hz, 2H), 7.29 – 7.26 (m, 2H), 7.26 (s, 1H), 7.25 (d, J = 3.7 Hz, 1H), 7.24 – 7.21 (m, 2H), 7.12 (d, J = 6.6 Hz, 1H), 7.00 (m, 1H), 6.62 (s, 1H), 6.55 (d, J = 8.7 Hz, 2H), 4.06 (s, 2H), 2.37 (s, 3H).

^{13}C NMR (151 MHz, CDCl$_3$) δ 150.7, 142.5, 140.2, 138.4, 137.2, 129.5, 129.5, 128.7, 128.4, 127.9, 127.1, 124.2, 123.9, 120.2, 120.1, 114.0, 21.5.

HR-MS-ESI (m/z) calculated for $C_{19}H_{19}N_2O_2S$ [M + H]$^+$: 339.1167; found: 339.1160.

LC-MS purity (UV) = 93%, tR 22.33 min; m/z (ESI$^+$) 338.95 [M + H]$^+$.

Sulfonamide synthesis from *tert*-Butyl (4-(chlorosulfonyl)phenyl)

2.27h-2.27j   **2.28h-2.28j**
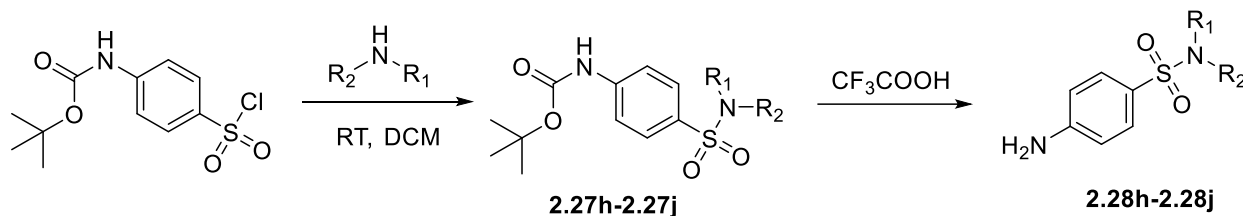
tert-butyl (4-(*N*-(2-morpholinoethyl)sulfamoyl)phenyl)carbamate (**2.27h**)
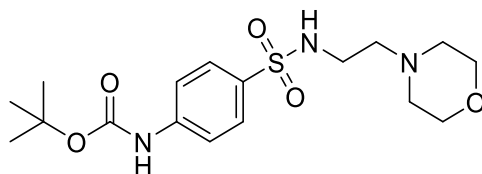
tert-Butyl (4-(chlorosulfonyl)phenyl) (74.3 mg, 0.26 mmol) and 2-morpholinoethan-1-amine (41.0 mg, 0.31 mmol) were combined in DCM (1 mL). The solution was stirred at room temperature for 30 min or until starting material disappeared by TLC then the solution was concentrated in vacuum. The crude material was purified by flash column chromatography and the final product **2.27h** was obtained as a colourless solid, yield: 91.1 mg (92%).

^{1}H NMR (600 MHz, CDCl$_3$) δ 7.76 (d, *J* = 8.3 Hz, 2H), 7.50 (d, *J* = 8.3 Hz, 2H), 6.91 (brs, 1H), 5.17 (brs, 1H), 3.59 (t, *J* = 4.5 Hz, 4H), 2.95 (*m*, 2H), 2.37 (t, *J* = 5.7 Hz, 2H), 2.24 (t, *J* = 4.5 Hz, 4H), 1.50 (s, 9H).

^{13}C NMR (151 MHz, CDCl$_3$) δ 152.2, 142.6, 132.8, 128.4, 117.8, 81.5, 66.8, 56.1, 52.9, 38.9, 28.2.

HRMS *m/z* (ESI$^+$) Calculated for C$_{17}$H$_{28}$N$_3$O$_5$S [M + H]$^+$: 386.1750, found: 386.1768.

LC-MS purity (UV) = 93%, tR 13.22 min; m/z (ESI$^+$) 386.4 [M + H]$^+$.

tert-butyl (4-(*N*-(pyridin-2-yl)sulfamoyl)phenyl)carbamate (2.27i)
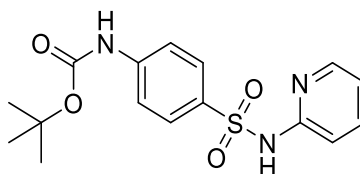
This was synthesised on a 0.24 mmol scale from *tert*-Butyl (4-(chlorosulfonyl)phenyl) by the same procedure of **2.27h** and pyridin-2-amine (27.1 mg, 0.29 mmol) was used instead of 2-(methylamino)ethan-1-ol. The final product was obtained as a colourless solid; yield: 38.4 mg (46%).

^{1}H NMR (600 MHz, DMSO-d_6) δ 11.62 (brs, 1H), 9.74 (brs, 1H), 7.99 (d, *J* = 5.3 Hz, 1H), 7.73 (d, *J* = 8.9 Hz, 2H), 7.63 (m, 1H), 7.53 (d, *J* = 8.9 Hz, 2H), 7.05 (d, *J* = 8.6 Hz, 1H), 6.81 (t, *J* = 6.3 Hz, 1H), 1.44 (s, 9H).

^{13}C NMR (151 MHz, DMSO-d_6) δ 153.9, 153.0, 143.4, 134.2, 128.3, 117.8, 113.7, 110.6, 109.6, 100.2, 80.2, 28.4.

HRMS *m/z* (ESI$^+$) Calculated for C$_{16}$H$_{20}$N$_3$O$_4$S [M + H]$^+$: 350.1175, found: 350.1184.

LC-MS purity (UV) = 93%, tR 13.22 min; m/z (ESI$^+$) 349.95 [M + H]$^+$.

tert-butyl (4-(_N_-(1-methyl-3-(pyridin-3-yl)-1_H_-pyrazol-5-yl)sulfamoyl)phenyl)carbamate (**2.27j**)
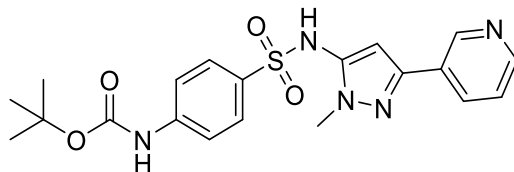
This was synthesised on a 0.26 mmol scale from _tert_-Butyl (4-(chlorosulfonyl)phenyl) by the same procedure of **2.27h** and 1-methyl-3-(pyridin-3-yl)-1H-pyrazol-5-amine (89.5 mg, 0.51 mmol) was used instead of 2-(methylamino)ethan-1-ol. The final product was obtained as a pale orange solid; yield: 62.4 mg (57%).

^{1}H NMR (600 MHz, CDCl$_3$) δ 8.72 (brs, 1H), 8.48 (d, J = 4.8 Hz, 1H), 8.04 (d, J = 7.9 Hz, 1H), 7.65 (d, J = 8.8 Hz, 2H), 7.50 (d, J = 8.8 Hz, 2H), 7.47 (s, 1H), 7.31 (dd, J = 8.0, 4.8 Hz, 1H), 5.97 (s, 1H), 3.83 (s, 3H), 1.49 (s, 9H). (NH not visible)

^{13}C NMR (151 MHz, CDCl$_3$) δ 152.1, 148.6, 146.6, 143.5, 135.0, 132.7, 131.5, 129.1, 129.0, 123.7, 117.7, 100.2, 81.8, 36.0, 28.2.

HRMS _m/z_ (ESI$^+$) Calculated for C$_{20}$H$_{24}$N$_5$O$_4$S [M + H]$^+$: 430.1549, found: 430.1566.

LC-MS purity (UV) = 96%, tR 16.26 min; m/z (ESI$^+$) 430.35 [M + H]$^+$.

Removal of an NH-Boc group

2.27h-2.27j   **2.28h-2.28j**
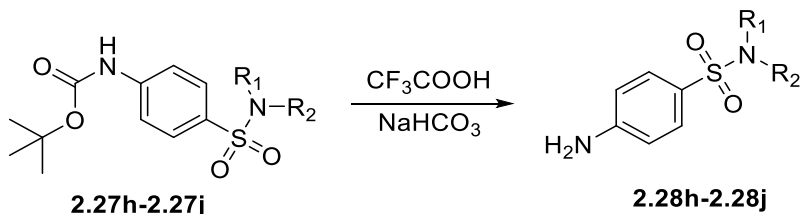
4-amino-*N*-(2-morpholinoethyl)benzenesulfonamide (**2.28h**)
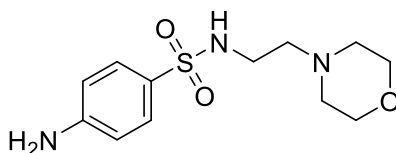
2.27h (32.4 mg, 0.084 mmol) and trifluoroacetic acid (TFA, 77.8 uL) were combined in DCM (1 mL). The mixture was stirred at room temperature for 12 hrs and saturated sodium bicarbonate solution (20 mL) was added. The mixture was extracted with DCM (20 mL×3). The organic phases were combined, washed with saturated NaCl aqueous solution, dried with anhydrous sodium sulfate, and concentrated under reduced pressure to remove the solvent, to afford the title compound **2.28h**. The final product was obtained as a colorless oil; yield: 18.9 mg (79%).

^{1}H NMR (600 MHz, DMSO-d_6) δ 7.39 (d, J = 8.7 Hz, 2H), 6.96 (t, J = 5.9 Hz, 1H), 6.58 (d, J = 8.7 Hz, 2H), 5.91 (brs, 2H), 3.48 (t, J = 4.7 Hz, 4H), 2.73 (q, J = 6.6 Hz, 2H), 2.25 (m, 6H).

^{13}C NMR (151 MHz, DMSO-d_6) δ 152.9, 128.9, 125.7, 113.1, 66.5, 57.5, 53.6, 40.4.

HR-MS-ESI (m/z) calculated for $C_{11}H_{12}N_3O_3S$ [M + H]$^+$: 286.1225; found: 286.1208.

LC-MS purity (UV) = 92%, tR 8.61 min; m/z (ESI$^+$) 286.20 [M + H]$^+$.

4-amino-*N*-(pyridin-2-yl)benzenesulfonamide (2.28i)
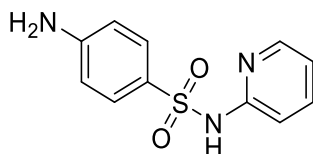
This was synthesised on a 0.10 mmol scale from **2.27i** and TFA 92.5 µL by the same procedure of **2.28h.** The final product was obtained as a yellow solid; yield: 25.1 mg (100%).

^{1}H NMR (600 MHz, DMSO-d_6) δ 10.96 (brs, 1H), 8.07 (d, *J* = 3.2 Hz, 1H), 7.62 (m, 1H), 7.49 (d, *J* = 8.8 Hz, 2H), 7.04 (d, *J* = 8.5 Hz, 1H), 6.90 – 6.85 (m, 1H), 6.52 (d, *J* = 8.8 Hz, 2H), 5.94 (brs, 2H).

^{13}C NMR (151 MHz, DMSO-d_6) δ 153.2, 152.7, 146.9, 139.2, 129.4, 126.0, 117.5, 112.8, 112.5.

HR-MS-ESI (m/z): calculated for $C_{11}H_{12}N_3O_2S$ [M + H]$^+$: 250.0650; found: 250.0641.

LC-MS purity (UV) = 94%, tR 13.47 min; m/z (ESI$^+$) 250.05 [M + H]$^+$.

4-amino-*N*-(1-methyl-3-(pyridin-3-yl)-1*H*-pyrazol-5-yl)benzenesulfonamide (2.28j)
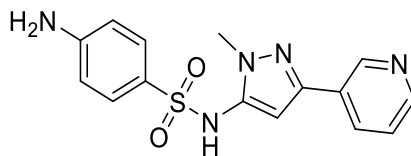
This was synthesised on a 0.04 mmol scale from **2.27j** and TFA 37.1 uL by the same procedure of **2.28h.** The final product was obtained as a pale orange solid; yield: 36.9 mg (100%).

^{1}H NMR (600 MHz, DMSO-d_6) δ 10.01 (s, 1H), 8.87 (s, 1H), 8.46 (s, 1H), 8.02 (d, J = 8.0 Hz, 1H), 7.35 (d, J = 8.5 Hz, 3H), 6.57 (d, J = 8.5 Hz, 2H), 6.30 (s, 1H), 6.09 (brs, 2H), 3.55 (s, 3H).

^{13}C NMR (151 MHz, DMSO-d_6) δ 158.2, 153.7, 148.9, 146.0, 137.3, 132.4, 129.3, 124.3, 122.5, 113.1, 103.2, 99.1, 35.8.

HR-MS-ESI (m/z) calculated for $C_{15}H_{16}N_5O_2S$ [M + H]$^+$: 330.1009; found: 330.1025.

LC-MS purity (UV) = 91%, tR 11.63 min; m/z (ESI$^+$) 330.25 [M + H]$^+$.

2.8.1.3 Reduction by using sodium dithionite

2.26d → **2.28d**, 19% yield, 90% purity

Reagents: 1) 1.0 M $Na_2S_2O_4$ 2) EtOH
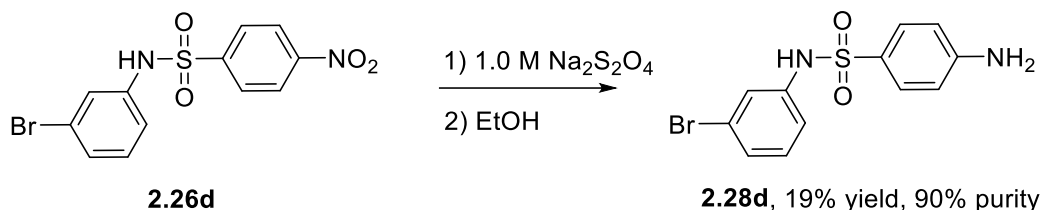
4-amino-*N*-(3-bromophenyl)benzenesulfonamide (**2.28d**)
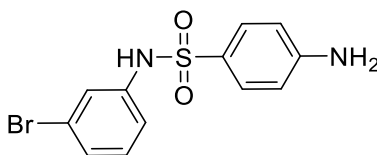
This was synthesised on a 0.14 mmol scale from **2.25.** Dissolved **2.26d** (171.7 mg, 0.48 mmol) in ethanol (7.4 mL) was added 1.0 M aq. $Na_2S_2O_4$ (7.4 mL). The reaction was heated under reflux at 85 °C for 1 hr. The cooled reaction was partitioned between 10% NH_3 (20 mL) and EtOAc (20 mL). The organic phase was extracted using EtOAc and washed with brine then dried over $MgSO_4$. The solvent was concentrated in vacuum. The crude material was purified by flash column chromatography (4 g, SiO_2, hexane/EtOAc, 100:0 – 0:100) and the final product was obtained as pale orange solid; yield: 29.4 mg (19%).

^{1}H NMR (600 MHz, DMSO-d_6) δ 10.14 (brs, 1H), 7.38 (d, *J* = 8.8 Hz, 2H), 7.19 (t, *J* = 1.9 Hz, 1H), 7.16 – 7.11 (m, 2H), 7.05 (dt, *J* = 7.6, 1.8 Hz, 1H), 6.53 (d, *J* = 8.8 Hz, 2H), 6.03 (s, 2H).

^{13}C NMR (151 MHz, DMSO-d_6) δ 153.3, 138.9, 129.4, 129.1, 129.0, 124.8, 123.7, 119.8, 119.7, 113.0.

HR-MS-ESI (m/z) calculated for $C_{12}H_{10}N_2O_2SBr$ [M + H]$^+$: 324.9646; found: 324.9643.

LC-MS purity (UV) = 90%, tR 20.02 min; m/z (ESI$^+$) 328.80 [M + H]$^+$.

2.8.2 Crystallization and structure determination

All crystals were grown in sitting drops by vapour diffusion in 90-well crystallisation plates. Pipette 60 µL of reservoir solution which contained 100 mM Bis-Tris Propane pH 5.95, 200 mM Li_2SO_4 and 30% PEG 3350 into the wells of 90-well crystallisation plates. The drop volume is 0.5 µL that composed of 200 nL of 13.7 mg/mL gonoccocal Pth, 200 nL reservoir solution and 100 nL seed crystals. Sealed the plate quickly and kept in a fridge at 18°C and the single crystals occurred in 2-7 days. Soaking protein crystal by pipette 1 µL of furan, hydrazide or sulphonamide compounds (ligands) into the drop for 1 hr and 24 hr. Cut and open the sealing tape then immediately fished the crystal and placed it in liquid nitrogen. Data from all crystals were collected at Diamond light source (Oxfordshire, UK).

2.9 References

1   NHS, Gonorrhoea, https://www.nhs.uk/conditions/gonorrhoea/, (accessed 18 April 2020).

2   C. Cheng, L. Li, C. Su and S. Li, *J. Microbiol. Immunol. Infect.*, 2016, **49**, 708–716.

3   T. H. Trust, ○Gonorrhoea, https://www.tht.org.uk/hiv-and-sexual-health/sexual-health/stis/gonorrhoea?gclid=CjwKCAjw0vTtBRBREiwA3URt7hkTEnnrYT0o-BIwwrdhE5zVzb3f11JC9imcZpRrFRz_teqJepOBQBoC3PsQAvD_BwE, (accessed 19 April 2020).

4   A. Paula, K. Thaís, B. M. Moreira, S. Eduardo, L. Fracalanzza and R. R. Bonelli, *Brazilian J. Microbiol.*, 2017, **8**, 617–628.

5   M. Unemo and W. M. Shafer, *Ann. N. Y. Acad. Sci.*, 2011, **1230**, 19–28.

6   L. W. Dicker, D. J. Mosure, S. M. Berman and W. C. Levine, *Sex. Transm. Dis.*, 2003, **30**, 472–476.

7   World Health Organization, Multi-drug resistant gonorrhoea fact sheet, https://www.who.int/news-room/fact-sheets/detail/multi-drug-resistant-gonorrhoea, (accessed 24 September 2022).

8   M. Unemo, S. Jacobsson, M. Cole and F. Tripodo, *Gonococcal antimicrobial susceptibility surveillance in Europe 2014*, 2014.

9   M. M. Lahra, *Commun. Dis. Intell.*, 2012, **36**, 95–100.

10   M. Unemo and M. Shafer, *Clin. Microbiol. Rev.*, 2014, **27**, 587–613.

11   L. R. Engelking and L. R. Engelking, *Textb. Vet. Physiol. Chem.*, 2015, 93–97.

12   W. C., *Nature*, 2000, **406**, 775–781.

13   C. L. Tooke, P. Hinchliffe, E. C. Bragginton, C. K. Colenso, V. H. A. Hirvonen, Y. Takebayashi and J. Spencer, *J. Mol. Biol.*, 2019, 431, 3472–3500.

14   M. Kester, K. K. D and K. E. Vrana, in *Elsevier's Integrated Review Pharmacology (Second Edition)*, Elsevier Inc., second edi., 2012, pp. 41–78.

15   S. R. Connell, D. M. Tracz, K. H. Nierhaus and D. E. Taylor, *Antimicrob. Agents Chemother.*, 2003, **47**, 3675–3681.

16   A. Artero, I. López-Cruz, L. Piles, J. Alberola, J. M. Eiros, S. Salavert and M. Madrazo, *Antibiotics*, 2023, **12**, 1–9.

17   M. A. Kohanski, D. J. Dwyer and J. J. Collins, *Nat. Rev. Microbiol.*, 2010, **8**, 423–435.

18   P. A. Bradford, A. A. Miller, J. O'Donnell and J. P. Mueller, *ACS Infect. Dis.*, 2020, **6**, 1332–1345.

19   S. Sharma, S. Kaushik, M. Sinha, G. S. Kushwaha, A. Singh, J. Sikarwar, A. Chaudhary, A. Gupta, P. Kaur and T. P. Singh, *BBA - Proteins Proteomics*, 2014,

1844, 1279–1288.

20   H. McFeeters, *J. Anal. Bioanal. Tech.*, 2014, **5**, 1–4.

21   L. Giorgi, F. Bontems, M. Fromant, C. Aubard, S. Blanquet and P. Plateau, *J. Biol. Chem.*, 2011, **286**, 39585–39594.

22   R. Janupally, B. Medepi, P. Brindha Devi, P. Suryadevara, V. U. Jeankumar, P. Kulkarni, P. Yogeeswari and D. Sriram, *Chem. Biol. Drug Des.*, 2015, **86**, 918–925.

23   S. N. Dighe and T. A. Collet, *Eur. J. Med. Chem.*, 2020, **199**, 1–34.

24   J. R. Menninger and D. P. Otto, *Antimicrob. Agents Chemother.*, 1982, **21**, 811–818.

25   Ł. Popiołek, *Int. J. Mol. Sci.*, 2021, **22**, 1–20.

26   V. Angelova, V. Karabeliov, P. A. Andreeva-Gateva and J. Tchekalarova, *Drug Dev. Res.*, 2016, **77**, 379–392.

27   W. Ahmed, M. Rani, I. A. Khan, A. Iqbal, K. M. Khan, M. A. Haleem and M. K. Azim, *J. Enzyme Inhib. Med. Chem.*, 2010, **25**, 673–678.

28   A. K. Edmonds, C. S. Oakes, S. Hassell-Hart, D. Bruyère, G. J. Tizzard, S. J. Coles, R. Felix, H. J. Maple, G. P. Marsh and J. Spencer, *Org. Biomol. Chem.*, 2022, **20**, 4021–4029.

29   Z. Ahmadi and J. S. McIndoe, *Chem. Commun.*, 2013, **49**, 11488–11490.

30   A. Daina, O. Michielin and V. Zoete, *Sci. Rep.*, 2017, **7**, 1–13.

31   P. Tripathi, S. Ghosh and S. Nath Talapatra, *World Sci. News*, 2019, **131**, 147–163.

32   C. A. Lipinski, *Drug Discov. Today Technol.*, 2004, **1**, 337–341.

33   D. F. Veber, S. R. Johnson, H.-Y. Cheng, B. R. Smith, K. W. Ward and K. D. Kopple, *J. Med. Chem*, 2002, **45**, 2615–2633. .

Chapter 3

Synthesis of LMO2-SCL inhibitors in leukaemia by using the 7-membered ring of *tert*-butyl 6-oxo-1,4-oxazepane-4-carboxylate as a building block

3.1 Background

Leukaemia is a cancer which starts from the bone marrow that leads to overproduction of abnormal white blood cells. Leukaemia is divided into 2 groups, which depend on disease progress: acute and chronic. Acute leukaemia worsens rapidly while chronic leukaemia may take a while to worsen. Acute leukaemia can be classified by the type of white blood cells involved and includes acute myeloid leukaemia (AML) and acute lymphoblastic leukaemia (ALL), which is mostly found in children under 15 with peak incidence aged between 2-5 years old.[1–4] Figure 3.1 shows the production of blood cell in bone marrow in a normal cell that generates red blood cells, platelets and various white blood cells (**3.1A**), blood forming process resulting in the blast (**3.1B**) and (**3.1D**) ALL patients have many white blood cells (purple colour) in blood compared with normal blood (**3.1C**). From ALL-Image Database (IDB), the data set showed that cancerous white blood cells (lymphoblasts) showed small or medium sizes, insufficient cytoplasm and do not contain vacuoles when compared with lymphocytes (Figure3.2). At present, there are 3 main ways to treat ALL: chemotherapy, radiation therapy and stem cell transplant. Unfortunately, as a result of treatment of adult white blood cells of ALL, the number of recovered patients is lower than 40%.[2] Moreover, limitation of traditional therapies, such as toxicity of curative chemotherapeutic agents, which lead to off target effects on theheart and brain, in children and long – term damage of the physical and intellectual development of survivors.
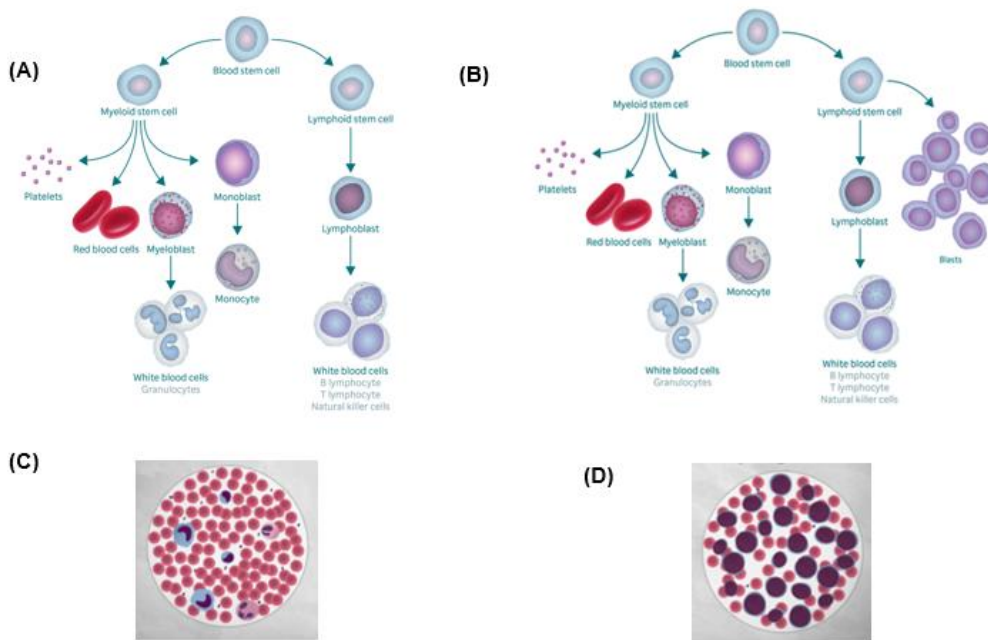
Figure 3.1. *Blood cell development. (A) blood stem cells generate red blood cells, platelets and various white blood cells. (B) the formation of blood resulting in blast. (C) normal blood and (D) blood during leukaemia.*[5]
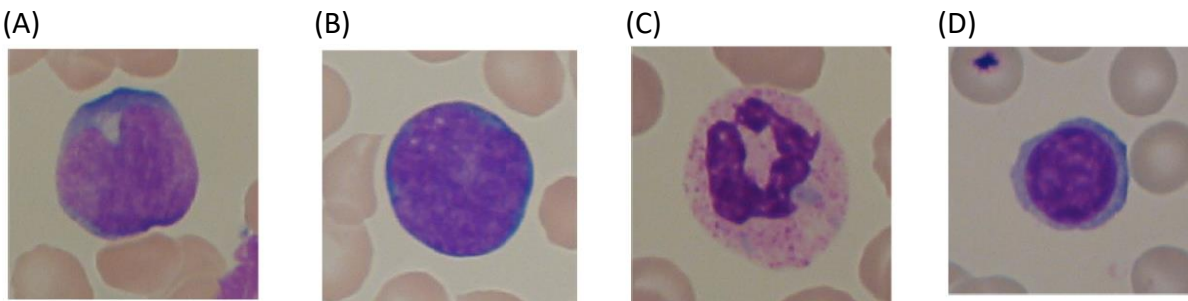

Figure 3.2. *Acute lymphoblastic leukaemia-Image DataBase (IDB) of 2 sample images. (A), (B) are leukaemia cell, (C), (D) are normal cells.*[6]

3.2 Drugs in ALL

Conventional treatments mainly focus in drug combinations, for instant, 1) asparaginase (derived from *Escherichia coli)* plus methotrexate (Figure 3.3)[7] 2) cytarabine (high dose) (Figure 3.3)[7] 3) methotrexate (high dose) (Figure 3.3) and teniposide (Figure 3.3) plus cytarabine followed with mercaptopurine (Figure 3.3)[8,9] and 4) combination of vincristine (Figure 3.5), corticosteroid and with or with out anthracycline.[7,9] Moreover, some of the conventional drugs mechanisms of action, e.g. methotrexate inhibits dihydrofolate reductase, stopping cancer cells from growing and block DNA synthesis or anthracyclines incorporate with DNA and topoisomerase II, and cause doublestranded DNA breaks.[7,10] However, the adverse effects of conventional drugs are their cytotoxicity towards normal tissues.

Cytarabine

Methotrexate

Teniposide

Mercaptopurine
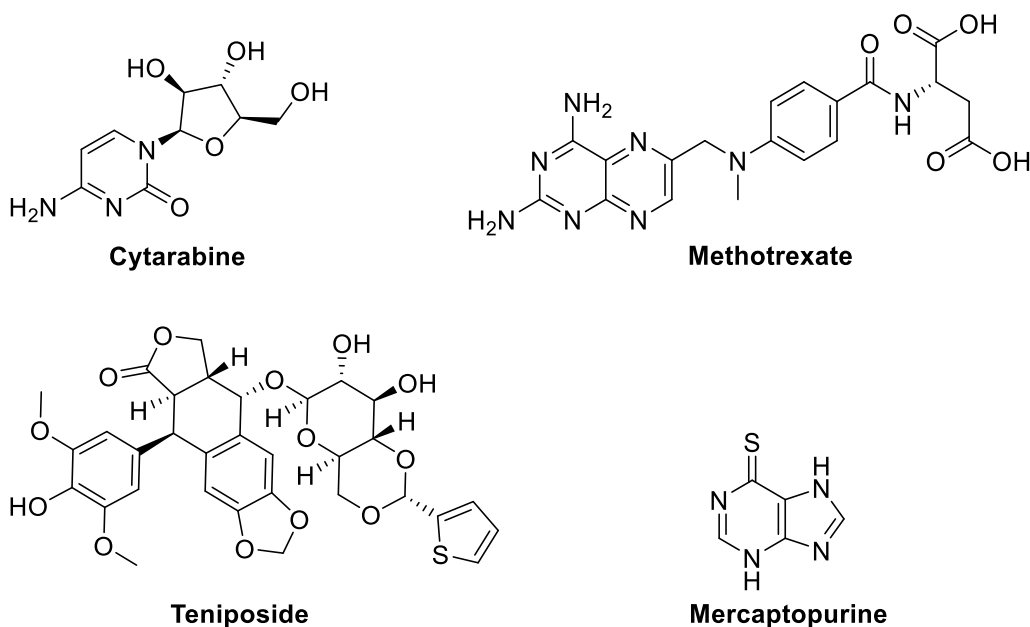
Figure 3.3. *Current ALL drugs.*[7–15]

Due to the lack of uncontrollable disease, poor results are reported in recurrent ALL. Some new drugs are being studied in clinical trials that include new formulations and nucleoside analogues. Encapsulating old drugs with liposomes increases their efficacy (Figure 3.5). For example, liposomal vincristine can reduce neurotoxicity and also benefit from prolonged exposure. Liposomal doxorubicin and PEGylated formulation can reduce

cardiotoxicity of the parent drug. Nelarabine showed good activity in recurrent T-lineage lymphoid malignancies in children and adults.[7,16] Therefore, there is a real need for ALL drugs to be developed in order to enhance their efficacy and improve their safety margins.

Clofarabine   **Nelarabine**   **Forodesine**

Figure 3.4. Drugs in ALL: Nucleoside analogues.[7,10,16,17]

Vincristine   **Doxorubicin**

Daunorubicin   **Idarubicin**

Figure 3.5. Drugs in ALL: drugs were encapsulated with Liposomes and PEGylated.[7,10,16,17]

3.3 Genetic abnormalities of leukaemic blasts
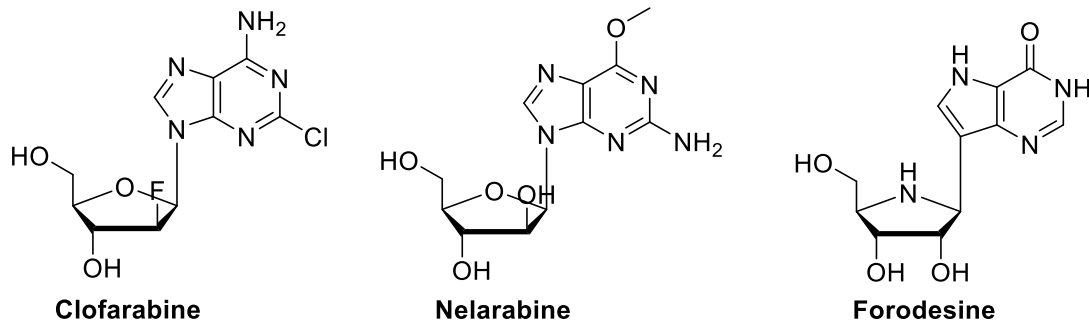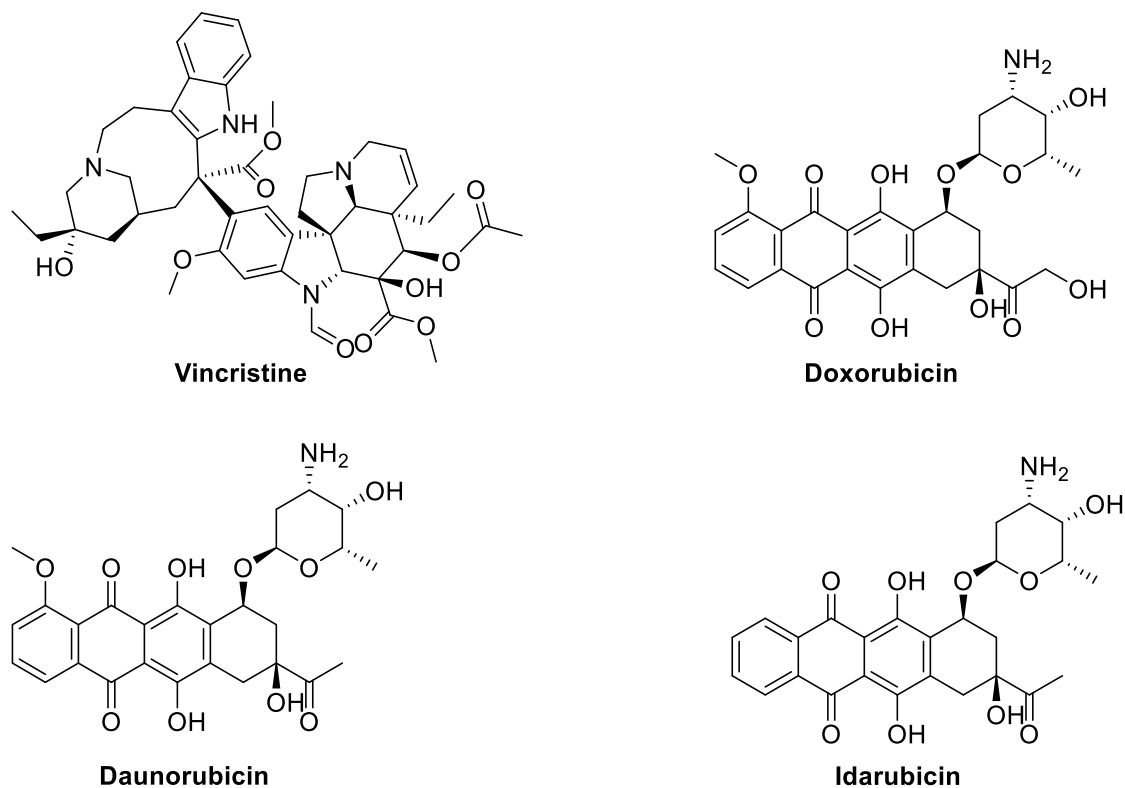
Haematopoietic transcription co-factor LIM only protein 2 (LMO2) is an essential transcriptional regulator in early haematopoiesis. Interestingly, it was found that around 50% of patients with T-ALL had a high level of LMO2 expression, leading to an interaction between LMO2 and stem cell leukaemia (SCL, also known as T-cell acute lymphocytic leukaemia 1; TAL1).[3,18–23] The protein-protein interaction (PPI) of SCL-LMO2 in oncogenic formation was studied (Figure 3.6).
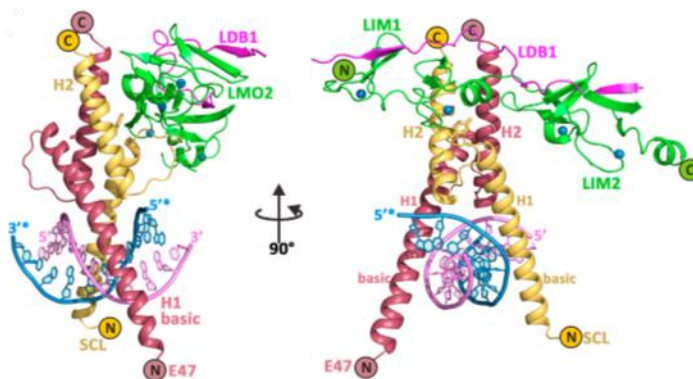
Figure 3.6. *Crystal structure of DNA-Bound SCL:E47bHLH:LMO2:LDB1LID.*[21]

Therefore, we investigated chemicals that can interrupt the interaction of LMO2 and SCL. Milton-Harris L. *et. al.*[3] screened 1534 compounds for inhibiting the SCL-LMO2 PPI, and it was found that two compounds, named in their paper as **3K7** and **5C7** (Figure 3.7), no K_d was reported for the latter), can induce a conformational change in LMO2 preventing SCL from binding with LMO2. **3K7** was a better inhibitor than **5C7** but both suffered from poor solubility to be more amenable for crystallography and more druglike. Therefore, the aim of our research was to synthesise analogues of **3K7** with lower logP and increased ligand efficacy (better potency, lower molecular weight).
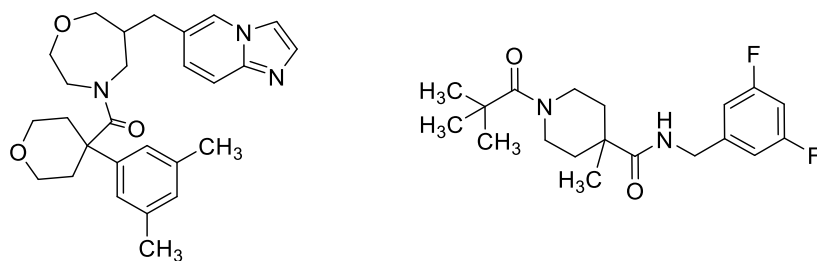
3K7 (K_d = 1.2 µM, IC$_{50}$ = 14.7 µM)   **5C7** (IC$_{50}$ = 18.7 µM)

Figure 3.7. *Structures of compound **3K7** and **5C7** (no report of K_d for 5C7).*

3.4 Results and Discussions

The aim of our study was the synthesis of LMO2-SCL inhibitors by using the 7-membered ring precursor *tert*-butyl 6-oxo-1,4-oxazepane-4-carboxylate (**3.0**) as a building block via reductive amination and amide couplings (Scheme 3.1). There are two obvious routes for synthesising compounds. Route 1, a reductive amination, was studied at room temperature in a one-pot synthesis using sodium cyanoborohydride (NaBH$_3$CN) to afford products **A**. After deprotection, either neutral **B** (after treatment with supported base) or protonated **B**' were coupled with activated acid to afford **C**. Route 2, starts with a Boc protecting group removal then amide formation from tetrahydro-2*H*-pyran-4-carbonyl chloride and compound **D**, after which, NaBH$_3$CN was used for reductive amination as in route1.

Interestingly, route 1 is the preferred method for synthesising compounds that have the same amine but where a carboxylic acid can be changed. On the other hand, route 2 is a suitable method for synthesising compounds that have the same carboxylic acid but where the amine can be changed. Despite their differences, both methods wereused to synthesise the target compounds. Product **C** was investigated for the binding interaction between SCL-LMO2 PPI by using Microscale Thermophoresis (MST). MST is a good technique for determining biomolecular interactions. The dissociation constant (K_d) shows affinity interactions between biomolecules, and the K_d values for binding were obtained from the MST curves.[3]

Route 1
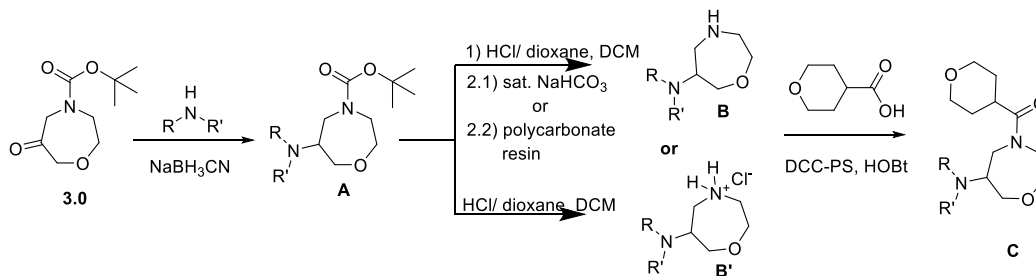
Route 2
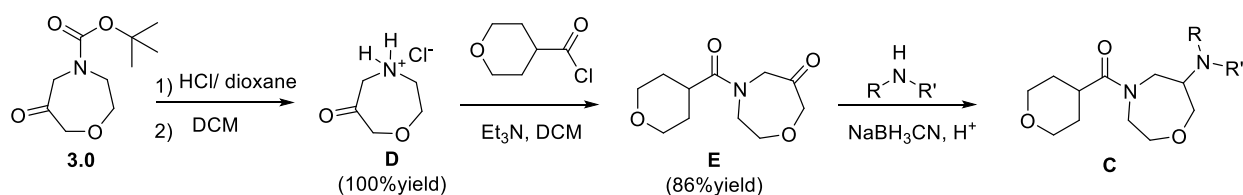
Scheme 3 1. *Synthesis of inhibitor by two routes; route 1 : reductive amination then an amide coupling reaction using N,N'-dicyclohexylcarbodiimide-polystyrene (DCC-PS). Route 2 is Boc group removal followed by amide synthesis and reductive amination.*

From route 1, Compound **3.1** was synthesised by a reductive amination using *N*-methyl benzylamine then the Boc group was removed to obtain compound **3.2** in 54% yield. Next, compound **3.2** was coupled with different carboxylic acids by using PS-DCC as a coupling agent to afford the corresponding amide compounds **3.3** – **3.5** (Table 3.1). It was found that compound **3.3** had the lowest K_d, which signifies excellent binding with LMO2 at low concentration. Hence, **3.3** is a good potential inhibitor lead compound. On the other hand, compounds **3.4** and **3.5** showed a higher K_d value than compound **3.3**, which might be explained by steric hindrance disfavouring binding to the protein. Thus, we further synthesised compounds (**3.16** – **3.21**), that were based on the structure of **3.3** in order to potentially improve solubility (Table 3.2 and Table 3.3). The products from route 1 were mesured K_d from MST. The results showed that **3.18**, containing a nitrogen atom in the *ortho* position in the benzene ring, had the lowest K_d (0.006 µM) with

the LMO2 protein (Table 3.3). Thus, compound **3.18** is an interesting molecule to be further studied.

Table 3.1. *K$_d$ values and (% yields) of compounds **3.3** - **3.5**.*
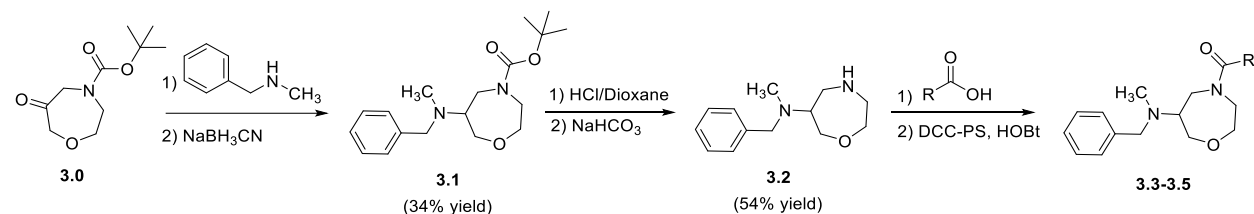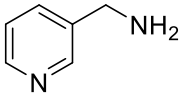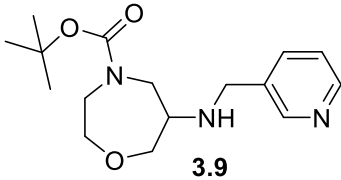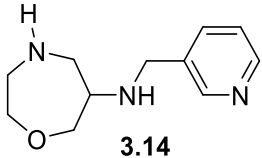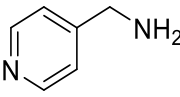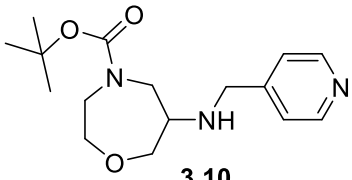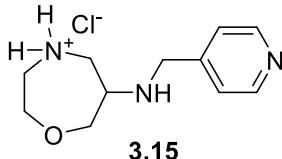
Carboxylic acid	Product (3.3-3.5)	% yield[a]	K$_d$ (µM)
	3.3	46	0.017
	3.4	61	0.379
	3.5	37	1.6

[a]isolated yield and all compounds were characterized by ^{1}H, ^{13}C NMR spectroscopy, compound cannot be analysed by LC-MS because of low ionisable but had a satisfactory NMR spectra.

Table 3.2. *The % yields of compounds* **3.1**, **3.2** *and* **3.6** – **3.21**.
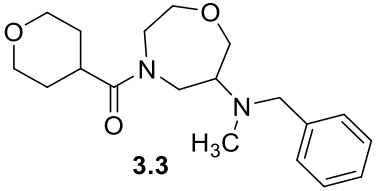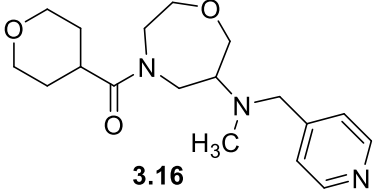
amine	compound	% yield[a]	compound	% yield[b]
	3.1	54	**3.2**	-
	3.6	32	**3.11**	-
	3.7	37	**3.12**	-
	3.8	46	**3.13**	-
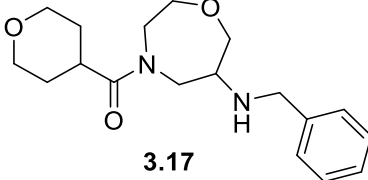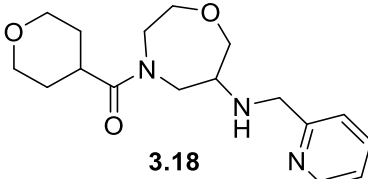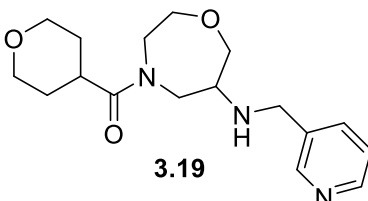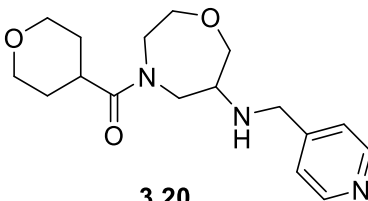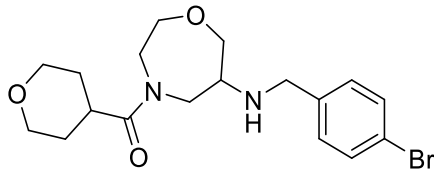
amine	compound	% yield[a]	compound	% yield[b]
	3.9	46	**3.14**	-
	3.10	25	**3.15**	-

[a]Isolated yield and all compounds were characterized by ^{1}H, ^{13}C NMR spectroscopy, compound cannot be analysed by LC-MS because of low ionisable but had a satisfactory NMR spectra.
[b]*All yields deemed to be quantitative. Compounds were used crude for the next step.*

Table 3.3. *K$_d$ and (% yield) of compounds* **3.3** *and* **3.16 – 3.21**.

compound	% yield[a]		K$_d$ (µM)[b]
	Route 1	Route 2	
3.3	46	-	0.017
3.16	48	-	0.019

compound	% yield[a]		K_d (μM)[b]
	Route 1	Route 2	
3.17	33	51	0.016
3.18	41	6	0.006
3.19	24	12	0.055
3.20	70	8	n/a
3.21	-	43	n/a

[a]isolated yield and all compounds were characterized by ^{1}H, ^{13}C NMR spectroscopy, compound cannot be analysed by LC-MS because of low ionisable but had a satisfactory NMR spectra.
[b]MST testing for product from route 1.

3.5 Pharmacokinetics, bioavailability drug-likeness and drug likeness prediction of ligands

Pharmacokinetics, bioavailability drug-likeness were predicted using the SwissADME program[24] as shown in Table 3.4. All compounds were under Lipinski's 'rule of five' that predicts good passive oral availability for a drug that has: no more than 5 hydrogen bond donors, no more than 10 hydrogen bond acceptors, molecular mass less than 500 Daltons, a partition coefficient, log P,value less than 5, [25,26] and also under Verber's rule that are a compound with no more than 10 rotatable bonds, polar surface area (PSA) no more than 140 $Å^2$ (or total hydrogen bond count no more than 12).[27,28] All synthesised compounds showed lower WLogP than **3K7** that the compounds are predicted to be more soluble than **3K7**.

Human intestinal absorption (HIA), blood-brain barrier (BBB) access and substrates of P-glycoprotein (PGP) were predicted to be with the graphical classification model Egan BOILED-Egg (Figure. 3.8).[29] The graph showed a grey region (no HIA or BBB acess), a white area (HIA) and a yellow (yolk) (BBB access).[30] All of the compounds were represented by the blue dots indicating actively effluxed substrates of PGP from the CNS. Compounds **3.1**-**3.17** and **3.21** were in the yolk area, which were predicted as and BBB permeability while compounds **3.18**-**3.20** were located in the white area, indicating no BBB access. Comparison of mercaptopurine (known drug) was in the red dot (represented as PGP−) indicating molecule is predicted as non-substrates of PGP in the central nervous system (CNS) efflux transporter which was in the egg white that means well-absorbed and no BBB access. As a result, some of these compounds had promising predictions for future drug development.

Table 3.4. *Physicochemical Properties and lipophilicity.*

compound	MW (g/mol)	nRB*	nHBA*	nHBD*	TPSA* (A^2)	WLogP*
3.3	332.44	5	4	0	42.01	1.24
3.4	408.53	6	4	0	42.01	2.56
3.5	436.59	6	4	0	42.01	3.18
3.16	333.43	5	5	0	54.90	0.63
3.17	318.41	5	4	1	50.80	0.90
3.18	319.4	5	5	1	63.69	0.29
3.19	319.4	5	5	1	63.69	0.29
3.20	319.4	5	5	1	63.69	0.29
3.21	397.31	5	4	1	50.8	1.66
3K7	447.57	5	4	0	56.07	3.34
mercaptopurine	152.18	0	3	1	93.26	0.64

*nRB number of rotational bond, nHBA number of hydrogen bond acceptors, nHBD hydrogen bond donors, TPSA topological polar surface area, WLogP octanol/water partition coefficient.
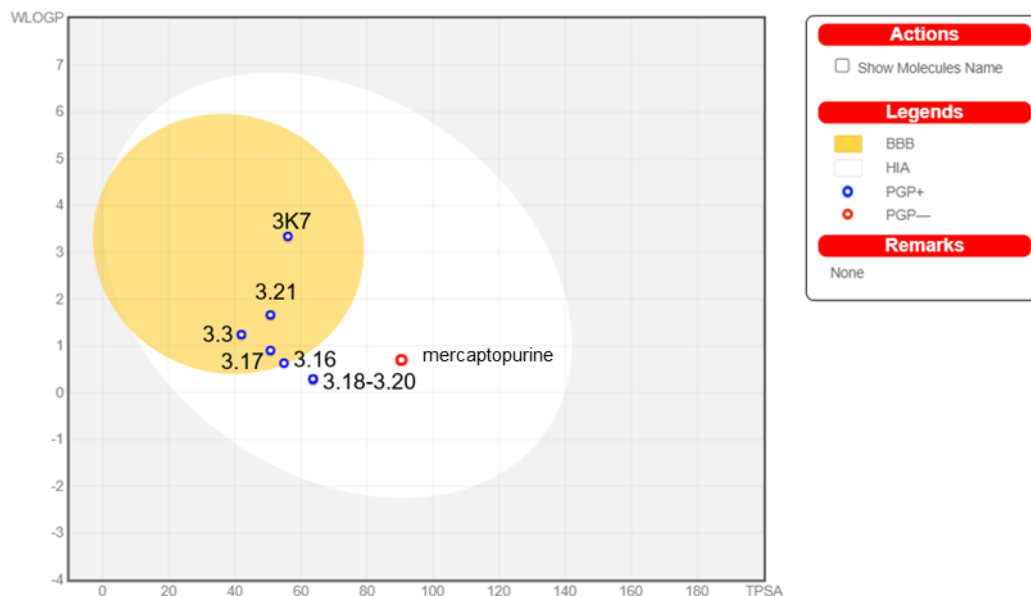
Figure 3.8. *Predicted BOILED-Egg diagram of the active compounds from SwissADME web tool.*[24,31–33]

3.6 Conclusions

A library of seven-membered ringcontaining LMO2-SCL inhibitors was synthesised using amide coupling and reductive amination reactions. The synthesis of substances can be done in two ways: starting with reductive amination reaction then doing amide coupling (route 1) or starting with amide synthesis followed by reductive amination reaction (route 2). It was found that making smaller molecule than the original lead **3K7** (K_d = 1.2 μM) led also to lower K_d values and higher solubility. Compound **3.18** showed good inhibition of SCL-LMO2 binding (lowest K_d, 0.006 μM), good properties in SwissAdme prediction and may be a useful lead for developing inhibitors in the future.

3.7 Experimental

General Experimental

Solvents, reagents, and consumables were purchased from commercial suppliers and solvents and reagents were used without purification. ^{1}H, ^{13}C NMR spectroscopy was performed on a Varian 600 MHz spectrometer, Varian 400 MHz spectrometer for measuring a variable temperature NMR and chemical shifts are reported in ppm, referenced to TMS as an internal standard. LCMS measurements were performed on a Shimadzu LCMS-2020 equipped with a Gemini® 5 μm C18 110 Å column and percentage purity measurements were run over 30 minutes in water/acetonitrile with 0.1% formic acid (5 min at 5%, 5–95% over 20 min, 5 min at 95%) with the UV detector set at 254 nm. High-Resolution Accurate Mass Spectrometry measurements were taken using a Waters Xevo G2 Q-ToF HRMS (Wilmslow, Cheshire, UK), equipped with an ESI source and MassLynx software. Experimental parameters were: (1)—ESI source: capillary voltage 3.0 kV, sampling cone 35 au, extraction cone 4 au, source temperature 120 °C and desolvation gas 450 °C with a desolvation gas flow of 650 L/h and no cone gas; (2)—MS conditions: MS in resolution mode between 100 and 1500 Da. Additionally, a Waters (Wilmslow, Cheshire, UK) Acquity H-Class UHPLC chromatography pumping system with column oven was used, connected to a Waters Synapt G2 HDMS high-resolution mass spectrometer.

3.7.1 Microscale Thermo Phoresis (MST)

This and the other bioassays, were carried out at the Sussex Drug Discovery Centre (SDDC), University of Sussex in the Biology Division by Dr. Sarah Connery and Dr. Jessica Booth.

Purified LMO2 proteins were labelled with fluorescent dye NT647 using a Monolith NTTM Protein Labeling Kit (NanoTemper Technologies). Serial dilutions of compounds (100 μM–6 nM) in MST buffer (50 mM Tris-HCl pH 7.8, 150 mM NaCl, 10 mM $MgCl_2$, 0.05% Tween 20, 2% DMSO) were mixed with 100 nM NT647-labeled protein, incubated for 15 minutes at room temperature and loaded into standard glass capillaries (Monolith NT.115 Capillaries, NanoTemper Technologies). Thermophoresis analysis was performed over

30 seconds on a Monolith NT.115 instrument (20% LED, 20/40% MST power) at 22 °C. The MST curves were fitted using NT Analysis software (NanoTemper Technologies) to obtain K_d values for binding.[3]

3.7.2 Synthesis of compounds

Compounds were synthesised and characterised on the basis of ^{1}H NMR, ^{13}C NMR and mass spectrometry. The dissociation constants (K_d) were performed by SDDC, University of Sussex. In many cases, we were unable to observe a M^+ or M^- so we have no LC-MS data/ purity for a number of products. ^{13}C-NMR spectra often showed a wrong number of peaks due to rotamers, unresolved with variable temperature NMR, so are not reported. Moreover, variable temperature NMR was used for the final compounds.

3.7.2.1 Route 1 synthesis
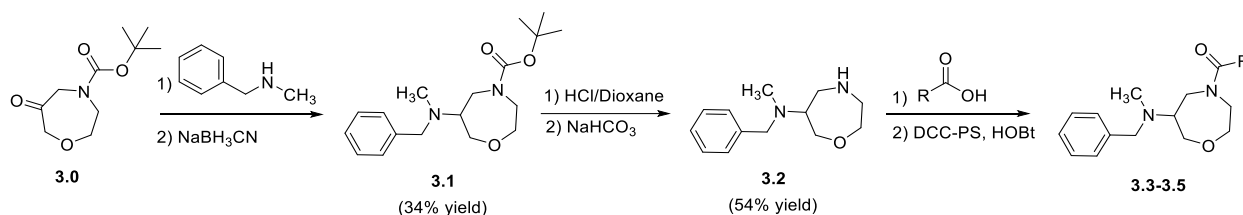
tert-butyl 6-(benzyl(methyl)amino)-1,4-oxazepane-4-carboxylate (3.1)
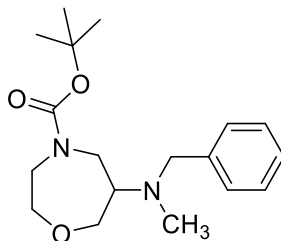
A solution of *tert*-butyl 6–oxo-1,4-oxazepane-4-carboxylate (600 mg, 2.79 mmol) in THF (6 mL) then methyl benzylamine (676.2 mg, 5.58 mmol) sodium cyanoborohydride (350.6 mg, 5.58 mmol) and acetic acid (0.31 mL) was added. The reaction mixture was stirred

at room temperature overnight, when the reaction completed, the reaction mixture was concentrated in vacuum. The residual was dissolved in ethyl acetate and washed with saturated $NaHCO_3$. The aqueous phase was extracted with ethyl acetate (EtOAc) (3x). The combined organic phases was added brine then dried with $MgSO_4$, filtered and concentrated in vacuum The crude material was purified by flash column chromatography and the final product was obtained as colorless oil; yield: 300.7 mg (33%).

^{1}H NMR (600 MHz, CDCl$_3$) δ 7.28 (m, 4H), 7.22 – 7.19 (m, 1H), 4.13 (dd, J = 13.6, 2.5 Hz, 1H), 4.05 – 3.99 (m, 1H), 3.95 (m, 1H), 3.86 – 3.84 (m, 1H), 3.76 – 3.70 (m, 2H), 3.55 (m, 1H), 3.49 – 3.45 (m, 1H), 3.18 – 3.14 (m, 2H), 3.06 – 2.98 (m, 1H), 2.30 (s, 3H), 1.37 (s, 9H).
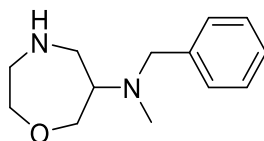
HR-MS-ESI (m/z) Calculated for $C_{18}H_{29}N_2O_3$ [M + H$^+$], 321.2178, found; 321.2147.

N-benzyl-N-methyl-1,4-oxazepan-6-amine (**3.2**)

A solution of **3.1** (288.4 mg, 0.90 mmol) in dichloromethane (DCM) (3 mL) was treated with 4.0 M HCl in 1,4-Dioxane (3 mL) and stirred for 24 hr. The mixture was concentrated in vacuo to give a residual was dissolve in DCM (12 mL) and neutralized by saturated $NaHCO_3$ (12 mL). the solution was stirred at room temperature for 2 hr. The mixture was extracted with DCM (3x). The combined organic phases was added with brine then dried with $MgSO_4$, filtered and concentrated in vacuum. The final product was obtained as white solid; yield: 167.2 mg (90%). The product was used without further purification.

^{1}H NMR (600 MHz, CDCl$_3$): δ 7.30 (m, 4H), 7.25 – 7.20 (m, 1H), 4.03 (dd, J = 13.0, 5.0 Hz, 1H), 3.88 – 3.79 (m, 2H), 3.69 – 3.58 (m, 2H), 3.53 (m, 1H), 3.15 (m, 1H), 3.08 – 3.02 (m, 1H), 2.97 (m, 1H), 2.94 – 2.87 (m, 2H), 2.26 (s, 3H). (NH not visible)

HR-MS-ESI (m/z) Calculated for C$_{13}$H$_{21}$N$_2$O [M + H$^+$], 221.1654, found; 221.1667.

(6-(benzyl(methyl)amino)-1,4-oxazepan-4-yl)(tetrahydro-2H-pyran-4-yl)methanone (3.3)
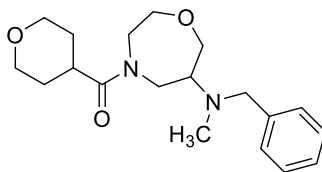
To a solution **3.2** (103.7 mg, 0.47 mmol), tetrahydro-2H-pyran-4-carboxylic acid (146.5 mg, 1.13 mmol), Hydroxybenzotriazole monohydrate (HOBt) (0.094 mmol) in DMF (5 mL) then N-cyclohexylcarboiimide,-N-methylpolystyrene (DCC-PS) (0.61 g) and N,N-diisopropylethylamine (0.94 mmol) were added to solution. The reaction mixture was stirred at room temperature overnight, when the reaction completed, the reaction mixture was filtered and concentrated in vacuum. The residual was dissolved in EtOAc and washed with H$_2$O. The aqueous phase was extracted with EtOAc (3x). The combined organic phases was washed with saturated NaHCO$_3$. the solution was added with brine then dried with MgSO$_4$, filtered and concentrated in vacuum. The crude material was purified by flash column chromatography and the final product was obtained as pink oil; yield: 72.5 mg (47%).

^{1}H NMR (399 MHz, toluene-d_8, 105 °C) δ 7.28 (d, J = 7.5 Hz, 2H), 7.23 – 7.19 (m, 3H), 7.15 – 7.11 (m, 1H), 3.95 – 3.88 (m, 4H), 3.66 – 3.60 (m, 2H), 3.55 – 3.49 (m, 2H), 3.37 – 3.22 (m, 4H), 3.21 – 3.12 (m, 2H), 3.03 (s, 1H), 2.88 (s, 1H), 2.50 – 2.43 (m, 1H), 2.27 (s, 3H), 2.01 – 1.92 (m, 1H), 1.43 (d, J = 13.6 Hz, 1H), 1.33 (d, J = 13.8 Hz, 1H).

HR-MS-ESI (m/z): Calculated for $C_{19}H_{29}N_2O_3$ [M + H$^+$], 333.2178, found; 333.2168.

(6-(benzyl(methyl)amino)-1,4-oxazepan-4-yl)(4-phenyltetrahydro-2*H*-pyran-4-yl)methanone (3.4)
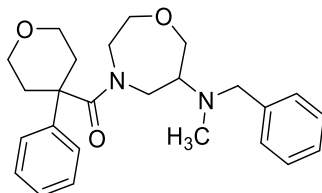
This was synthesised on a 0.59 mmol scale of **3.2** by the same procedure of **3.3** and 4-phenyltetrahydro-2*H*-pyran-4-carboxylic acid (0.29 g, 1.42 mmol) was use instead of tetrahydro-2*H*-pyran-4-carboxylic acid. The final product was obtained as brown oil; yield: 148.7 mg (61.5%).

^{1}H NMR (399 MHz, toluene-*d*$_8$, 105 ^{o}C) δ 7.20 (d, *J* = 7.6 Hz, 2H), 7.15 – 7.11 (m, 2H), 7.08 – 7.07 (m, 1H), 7.05 – 7.01 (m, 3H), 6.96 – 6.89 (m, 2H), 4.01 (d, *J* = 11.7 Hz, 1H), 3.90 (td, *J* = 11.1, 2.6 Hz, 1H), 3.77 – 3.71 (m, 4H), 3.63 (dd, *J* = 12.7, 4.3 Hz, 1H), 3.46 (t, *J* = 13.4 Hz, 2H), 3.40 – 3.29 (m, 3H), 3.24 – 3.19 (m, 1H), 2.87 – 2.77 (m, 2H), 2.75 – 2.66 (m, 2H), 2.27 – 2.21 (m, 1H), 2.04 (s, 3H), 1.95 – 1.87 (m, 1H), 1.79 – 1.71 (m, 1H).

HR-MS-ESI (m/z) Calculated for $C_{25}H_{33}N_2O_3$ [M + H$^+$], 409.2491, found; 409.2468.

(6-(benzyl(methyl)amino)-1,4-oxazepan-4-yl)(4-(3,5-dimethylphenyl)tetrahydro-2*H*-pyran-4-yl)methanone (3.5)
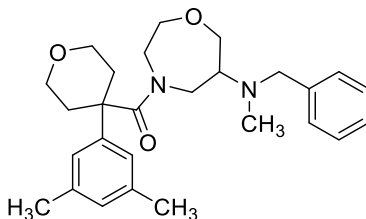

This was synthesised on a 0.25 mmol scale of **3.2** by the same procedure of **3.3** and 4-(3,5-dimethylphenyl)tetrahydro-2*H*-pyran-4-carboxylic acid (0.059 g, 0.25 mmol) was use instead of tetrahydro-2*H*-pyran-4-carboxylic acid. The final product was obtained as yellow oil; yield: 40.5 mg (36.7%).

^{1}H NMR (399 MHz, toluene-d_8, 105 °C) δ 7.19 (d, J = 7.6 Hz, 2H), 7.13 (t, J = 7.6 Hz, 2H), 7.03 (d, J = 7.2 Hz, 1H), 6.82 (d, J = 7.6 Hz, 2H), 6.62 (d, J = 8.0 Hz, 1H), 4.02 – 3.95 (m, 1H), 3.94 – 3.89 (m, 1H), 3.80 – 3.74 (m, 3H), 3.67 – 3.60 (m, 1H), 3.49 – 3.40 (m, 3H), 3.39 – 3.31 (m, 2H), 3.30 – 3.23 (m, 1H), 2.90 – 2.82 (m, 2H), 2.80 – 2.71 (m, 2H), 2.29 – 2.22 (m, 1H), 2.07 (s, 6H), 2.03 (s, 4H), 1.85 – 1.77 (m, 1H), 1.27 (s, 1H).

HR-MS-ESI (m/z) Calculated for $C_{27}H_{37}N_2O_3$ [M + H$^+$], 437.2804; found; 437.2787.
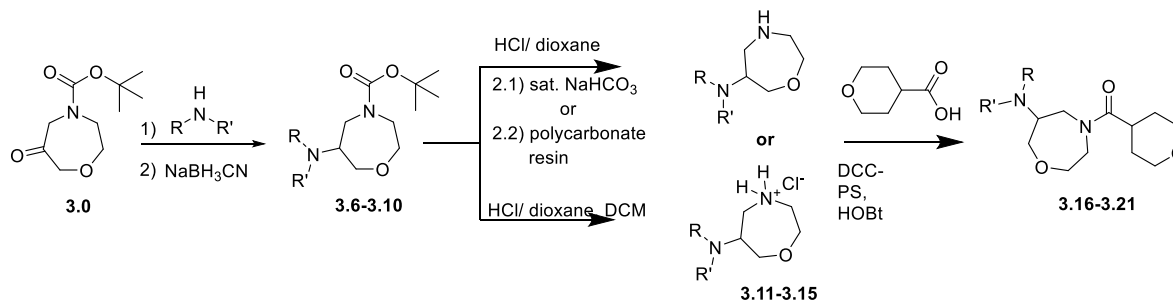
Compounds 3.6 - 3.15 were used crude in the reaction sequence, hence, only a ^{1}H NMR spectrum was recorded .

tert-butyl 6-(methyl(pyridin-4-ylmethyl)amino)-1,4-oxazepane-4-carboxylate (**3.6**)
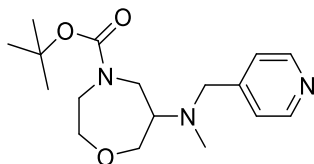
This was synthesised on a 348 mg, 1.62 mmol scale of the *tert*-butyl 6–oxo-1,4-oxazepane-4-carboxylate by the same procedure of **3.1** and *N*-methyl-1-(pyridin-4-yl)methanamine (396 mg, 3.24 mmol) was used instead of methyl benzylamine. The final product was obtained as colorless oil; yield: 167 mg (32%).

^{1}H NMR (600 MHz, CDCl$_3$): δ 8.46 (t, J = 6.9 Hz, 2H), 7.20 (d, J = 4.9 Hz, 2H), 3.99 (dd, J = 13.7, 4.3 Hz, 1H), 3.94 (m, 1H), 3.86 – 3.81 (m, 1H), 3.82 – 3.68 (m, 2H), 3.60 – 3.49 (m, 2H), 3.42 (m, 1H), 3.23 – 2.94 (m, 3H), 2.23 (d, J = 30.3 Hz, 3H), 1.37 (s, 9H).

tert-butyl 6-(benzylamino)-1,4-oxazepane-4-carboxylate (**3.7**)
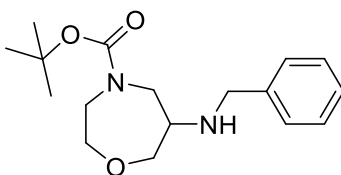
This was synthesised on a 360 mg, 3.36 mmol scale of the *tert*-butyl 6–oxo-1,4-oxazepane-4-carboxylate by the same procedure of **3.1** and benzylamine (360.1 mg, 3.36 mmol) was used instead of methyl benzylamine. The final product was obtained as yellow oil; yield: 188 mg (37%).

^{1}H NMR (600 MHz, CDCl$_3$) δ 7.36 (m, 4H), 7.31 – 7.27 (m, 1H), 3.94 (d, J = 13.1 Hz, 1H), 3.88 (s, 1H), 3.86 – 3.82 (m, 1H), 3.81 – 3.69 (m, 5H), 3.58 – 3.47 (m, 2H), 3.45 – 3.31 (m, 1H), 3.08 (dt, J = 24.6, 5.3 Hz, 1H), 1.50 (s, 9H).

tert-butyl 6-((pyridin-2-ylmethyl)amino)-1,4-oxazepane-4-carboxylate (**3.8**)

This was synthesised on a 270 mg, 1.25 mmol scale of the *tert*-butyl 6–oxo-1,4-oxazepane-4-carboxylate by the same procedure of **3.1** and pyridin-2-ylmethanamine (270 mg, 2.5 mmol) was used instead of methyl benzylamine. The final product was obtained as colorless oil; yield: 213 mg (55%).

^{1}H NMR (600 MHz, CDCl$_3$) δ 8.46 (t, J = 6.4 Hz, 1H), 7.59 – 7.54 (m, 1H), 7.27 (s, 1H), 7.11 – 7.05 (m, 1H), 3.95 – 3.87 (m, 2H), 3.72 – 3.54 (m, 6H), 3.33 – 3.22 (m, 2H), 3.04 – 2.97 (m, 1H), 2.24 (s, 1H), 1.38 (s, 9H).

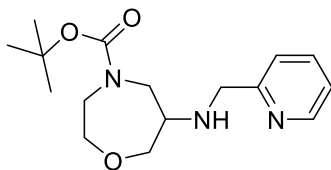**tert-butyl 6-((pyridin-3-ylmethyl)amino)-1,4-oxazepane-4-carboxylate** (**3.9**)

This was synthesised on a 348 mg, 1.62 mmol scale of the *tert*-butyl 6–oxo-1,4-oxazepane-4-carboxylate by the same procedure of **3.1** and pyridin-3-ylmethanmine (351 mg, 3.24 mmol) was used instead of benzylamine. The final product was obtained as yellow oil; yield: 229 mg (46%).

^{1}H NMR (600 MHz, CDCl$_3$) δ 8.51 (s, 1H), 8.43 (dd, J = 11.4, 3.8 Hz, 1H), 7.65 (s, 1H), 7.23 – 7.16 (m, 1H), 3.89 (d, J = 13.2 Hz, 1H), 3.80 (s, 1H), 3.74 (d, J = 13.3 Hz, 1H), 3.70 – 3.65 (m, 2H), 3.63 – 3.54 (m, 4H), 3.46 – 3.29 (m, 2H), 2.98 – 2.92 (m, 1H), 1.40 (s, 9H).

HR-MS-ESI (m/z) Calculated for $C_{16}H_{26}N_3O_3$ [M + H$^+$], 308.1974, found; 308.1969.

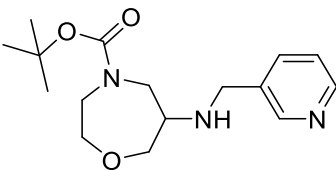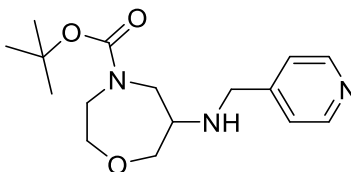**tert-butyl 6-((pyridin-4-ylmethyl)amino)-1,4-oxazepane-4-carboxylate** (**3.10**)

This was synthesised on a 398 mg, 1.85 mmol scale of the *tert*-butyl 6–oxo-1,4-oxazepane-4-carboxylate by the same procedure of **3.1** and pyridin-4-ylmethanmine (400 mg, 3.7 mmol) was used instead of methyl benzylamine. The final product was obtained as colorless oil; yield: 143.0 mg (25%).

^{1}H NMR (600 MHz, CDCl$_3$) δ 8.47 (dd, J = 12.8, 5.0 Hz, 2H), 7.25 (s, 2H), 3.89 (d, J = 14.5 Hz, 1H), 3.82 (s, 1H), 3.76 (d, J = 14.3 Hz, 1H), 3.71 – 3.67 (m, 1H), 3.65 – 3.55 (m, 4H), 3.42 – 3.29 (m, 2H), 2.96 – 2.90 (m, 1H), 2.23 (s, 1H), 1.40 (s, 9H).

N-methyl-N-(pyridin-4-ylmethyl)-1,4-oxazepan-6-amine (**3.11**)
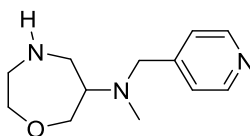
This was synthesised on a 71.6 mg, 0.28 mmol scale of **3.6i** by the same procedure of **3.2.** The final product was obtained as white solid; yield: 85.0 mg (90%). The product was used without further purification.

^{1}H NMR (600 MHz, DMSO, d_6) δ 8.45 (d, J = 5.6 Hz, 2H), 7.27 (d, J = 5.0 Hz, 2H), 3.85 (dd, J = 12.8, 5.1 Hz, 1H), 3.72 (dd, J = 12.8, 5.7 Hz, 1H), 3.67 – 3.57 (m, 4H), 2.97 (dd,

J = 13.3, 6.3 Hz, 1H), 2.90 (p, *J* = 6.1 Hz, 1H), 2.79 – 2.75 (m, 1H), 2.73 (t, *J* = 4.0 Hz, 1H), 2.70 – 2.66 (m, 1H), 2.14 (s, 3H).

N-benzyl-4-chloro-1,4λ5-oxazepan-6-amine (3.12)
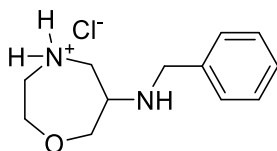
A solution of **3.7l** (178.4 mg, 0.58 mmol) in dichloromethane (DCM) (2 mL) was treated with 4.0 M HCl in 1,4-Dioxane (2 mL) and stirred for 24 hr. The mixture was concentrated in vacuo. DCM was added into the mixture and was concentrated in vacuo 3-4 times. The final product was obtained as white solid; yield: 148.9 mg (90%). The product was used without further purification.

^{1}H NMR (600 MHz, DMSO, *d*6) δ 9.94 (s, 2H), 9.68 (s, 1H), 7.60 (d, *J* = 7.0 Hz, 2H), 7.44 – 7.39 (m, 3H), 4.27 (d, *J* = 13.1 Hz, 1H), 4.20 (d, *J* = 13.1 Hz, 1H), 4.12 (d, *J* = 4.3 Hz, 2H), 3.96 – 3.91 (m, 1H), 3.84 – 3.80 (m, 2H), 3.63 – 3.54 (m, 2H), 3.34 (d, *J* = 5.4 Hz, 2H).

### 4-chloro-*N*-(pyridin-2-ylmethyl)-1,4λ5-oxazepan-6-amine (3.13)

This was synthesised on a 197.4 mg, 0.64 mmol scale of **3.8i** by the same procedure of **3.7ii.** The final product was obtained as white solid; yield: 178.2 mg (90%). The product was used without further purification.

¹H NMR (600 MHz, DMSO, *d*₆) δ 10.25 (s, 1H), 10.04 (s, 2H), 8.66 (d, *J* = 5.0 Hz, 1H), 7.99 (t, *J* = 7.8 Hz, 1H), 7.71 (d, *J* = 7.8 Hz, 1H), 7.52 (t, *J* = 6.5 Hz, 1H), 4.68 – 4.60 (m, 4H), 4.16 (d, *J* = 4.3 Hz, 2H), 3.93 (p, *J* = 6.1 Hz, 2H), 3.84 – 3.80 (m, 1H), 3.65 – 3.56 (m, 2H).

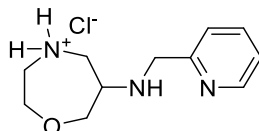**N-(pyridin-3-ylmethyl)-1,4-oxazepan-6-amine** (**3.14**)
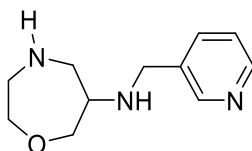
A solution of **3.9i** (148.2 mg, 0.48 mmol) in dichloromethane (DCM) (3 mL) was treated with 4.0 M HCl in 1,4-Dioxane (3 mL) and stirred for 24 hr. The mixture was concentrated in vacuo to give a residual was dissolve in DCM (10 mL) and methanol (5 mL). Polymer-supported carbonate resin (350 mg) was added to the mixture and stirred at room temperature for 2 hr. The resin was removed by filtered through celite. The final product was obtained as white solid; yield: 180.6 mg (90%). The product was used without further purification.

¹H NMR (600 MHz, DMSO, *d*₆) δ 9.42 (s, 1H), 8.70 (s, 1H), 8.54 (d, *J* = 6.5 Hz, 1H), 8.00 (d, *J* = 7.8 Hz, 1H), 7.42 (dd, *J* = 7.9, 4.8 Hz, 1H), 4.16 (d, *J* = 13.4 Hz, 1H), 4.09 – 4.02 (m, 2H), 4.00 – 3.94 (m, 1H), 3.92 – 3.88 (m, 1H), 3.82 – 3.78 (m, 1H), 3.64 – 3.60 (m, 1H), 3.51 – 3.44 (m, 3H), 3.31 – 3.26 (m, 2H).

4-chloro-*N*-(pyridin-4-ylmethyl)-1,4l5-oxazepan-6-amine (**3.15**)

This was synthesised on a 50 mg, 0.16 mmol scale of **3.10i** by the same procedure of **3.7ii.** The final product was obtained as white solid; yield: 48.1 mg (90%). The product was used without further purification.
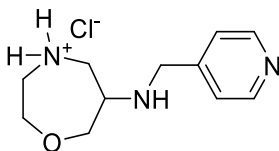
^{1}H NMR (600 MHz, DMSO, d_6) δ 9.99 (s, 2H), 8.85 (d, *J* = 5.4 Hz, 2H), 8.02 (s, 2H), 4.51 (d, *J* = 14.3 Hz, 1H), 4.42 (d, *J* = 13.9 Hz, 1H), 4.17 – 4.11 (m, 2H), 3.98 – 3.91 (m, 2H), 3.87 – 3.81 (m, 3H), 3.36 (d, *J* = 4.5 Hz, 2H), 3.14 (s, 1H).

(6-(methyl(pyridin-4-ylmethyl)amino)-1,4-oxazepan-4-yl)(tetrahydro-2H-pyran-4-yl)methanone (**3.16**)
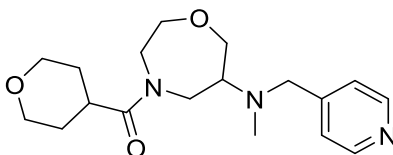
This was synthesised on a 0.26 mmol scale of **3.6ii** by the same procedure of **3.3.** The tetrahydro-2*H*-pyran-4-carboxylic acid (0.082 g, 0.63 mmol), (HOBt) (0.079 mmol) in DMF (3 mL) then DCC-PS (0.61 g) and *N,N*-diisopropylethylamine (0.94 mmol) were used. The final product was obtained as yellow oil; yield: 41.6 mg (48%).

^{1}H NMR (399 MHz, toluene-d_8, 105 °C) δ 8.44 (d, *J* = 4.6 Hz, 2H), 6.92 (d, *J* = 8.3 Hz, 2H), 3.85 – 3.80 (m, 2H), 3.72 (d, *J* = 13.6 Hz, 1H), 3.51 – 3.42 (m, 2H), 3.37 (d, *J* = 18.3 Hz, 2H), 3.29 (d, *J* = 13.8 Hz, 1H), 3.15 (d, *J* = 11.4 Hz, 4H), 2.96 (dd, *J* = 14.5, 9.8 Hz, 1H), 2.81 (d, *J* = 44.1 Hz, 2H), 2.32 (s, 1H), 2.06 – 2.00 (m, 3H), 1.88 (s, 2H), 1.33 – 1.23 (m, 2H).

HR-MS-ESI (m/z) Calculated for $C_{18}H_{28}N_3O_3$ [M + H$^+$], 334.2140; found; 334.2131.

(6-(benzylamino)-1,4-oxazepan-4-yl)(tetrahydro-2H-pyran-4-yl)methanone (3.17)
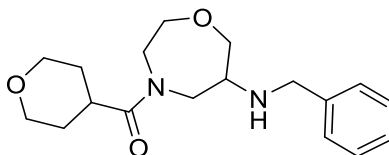
This was synthesised on a 0.61 mmol scale of **3.7ii** by the same procedure of **3.3.** The tetrahydro-2*H*-pyran-4-carboxylic acid (0.191 g, 1.47 mmol), (HOBt) (0.31 mmol) in DMF (5 mL) then DCC-PS (0.800 g) and *N,N*-diisopropylethylamine (2.45 mmol) were used. The final product was obtained as yellow oil; yield: 64.1 mg (33%).

^{1}H NMR (399 MHz, toluene-*d*$_8$, 105 °C) δ 7.17 (d, *J* = 6.8 Hz, 2H), 7.11 (t, *J* = 7.0 Hz, 2H), 7.02 (t, *J* = 7.0 Hz, 1H), 3.85 – 3.80 (m, 2H), 3.59 (d, *J* = 6.1 Hz, 2H), 3.47 – 3.33 (m, 6H), 3.23 – 3.12 (m, 4H), 2.72 (s, 1H), 2.47 (s, 1H), 1.93 – 1.84 (m, 2H), 1.37 – 1.26 (m, 2H), 1.07 (s, 1H).

HR-MS-ESI (m/z) Calculated for $C_{18}H_{27}N_2O_3$ [M + H$^+$], 319.2034; found; 319.2022.

(6-((pyridin-2-ylmethyl)amino)-1,4-oxazepan-4-yl)(tetrahydro-2H-pyran-4-yl)methanone (3.18)
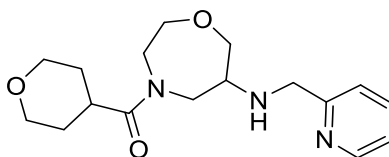
This was synthesised on a 0.73 mmol scale of **3.8ii** by the same procedure of **3.3.** The tetrahydro-2*H*-pyran-4-carboxylic acid (0.228 g, 1.75 mmol), (HOBt) (2.19 mmol) in DMF

(5 mL) then DCC-PS (0.952 g) and *N,N*-diisopropylethylamine (2.92 mmol) were used. The final product was obtained as brown oil; yield: 94.8 mg (41%).

^{1}H NMR (600 MHz, DMSO, d_6) δ 8.46 (m, 1H), 7.73 (dt, *J* = m, 1H), 7.41 (m, 1H), 7.22 (m, 1H), 3.86 (dd, *J* = 14.2, 9.6 Hz, 2H), 3.82 – 3.77 (m, 3H), 3.72 (d, *J* = 10.8 Hz, 1H), 3.68 – 3.53 (m, 4H), 3.51 – 3.48 (m, 1H), 3.28 – 3.19 (m, 2H), 2.86 – 2.80 (m, 2H), 2.39 (s, 1H), 1.61 – 1.46 (m, 4H), 1.36 (d, *J* = 13.3 Hz, 1H).

HR-MS-ESI (m/z) Calculated for $C_{17}H_{26}N_3O_3$ [M + H$^+$], 320.1975; found; 320.1974.

**(6-((pyridin-3-ylmethyl)amino)-1,4-oxazepan-4-yl)(tetrahydro-2H-pyran-4-yl)methanone** (**3.19**)

This was synthesised on a 0.36 mmol scale of **3g** by the same procedure of **3.3.** The tetrahydro-2*H*-pyran-4-carboxylic acid (0.111 g, 0.86 mmol), (HOBt) (0.072 mmol) in DMF (5 mL) then DCC-PS (0.467 g) and *N,N*-diisopropylethylamine (0.72 mmol) were used. The final product was obtained as yellow oil; yield: 27.0 mg (24%).

^{1}H NMR (399 MHz, toluene-d_8, 105 °C) δ 8.65 (m, 1H), 8.55 – 8.43 (m, 1H), 7.48 – 7.37 (m, 1H), 6.91 – 6.85 (m, 1H), 4.01 – 3.89 (m, 2H), 3.62 – 3.40 (m, 8H), 3.36 – 3.20 (m, 4H), 2.76 (s, 1H), 2.53 (s, 1H), 2.25 – 2.15 (m, 1H), 1.40 (t, *J* = 17.3 Hz, 3H), 1.09 (s, 1H).

HR-MS-ESI (m/z) Calculated for $C_{17}H_{26}N_3O_3$ [M + H$^+$], 320.1993; found; 320.1974.

(6-((pyridin-4-ylmethyl)amino)-1,4-oxazepan-4-yl)(tetrahydro-2H-pyran-4-yl)methanone (3.20)
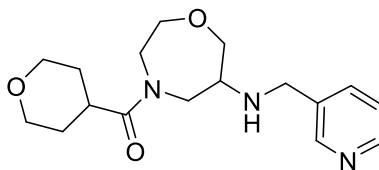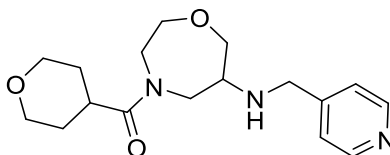

This was synthesised on a 0.19 mmol scale of **3.10ii** by the same procedure of **3.3.** The tetrahydro-2*H*-pyran-4-carboxylic acid (0.059g, 0.46 mmol), (HOBt) (0.10 mmol) in DMF (5 mL) then DCC-PS (0.248 g) and *N,N*-diisopropylethylamine (0.76 mmol) were used. The final product was obtained as yellow oil; yield: 42.6 mg (70%).

^{1}H NMR (600 MHz, DMSO, d_6) δ 8.48 (d, J = 5.0 Hz, 1H), 8.45 (d, J = 5.0 Hz, 1H), 7.35 (d, J = 5.0 Hz, 1H), 7.31 (d, J = 5.0 Hz, 1H), 3.84 – 3.74 (m, 5H), 3.73 – 3.67 (m, 2H), 3.67 – 3.63 (m, 1H), 3.63 – 3.55 (m, 2H), 3.55 – 3.43 (m, 2H), 3.29 – 3.19 (m, 2H), 2.83 – 2.74 (m, 2H), 1.62 – 1.45 (m, 4H), 1.33 (m, 1H).

HR-MS-ESI (m/z) Calculated for $C_{17}H_{26}N_3O_3$ [M + H$^+$], 320.1975; found; 320.1974.

3.7.2.2 Route 2 synthesis
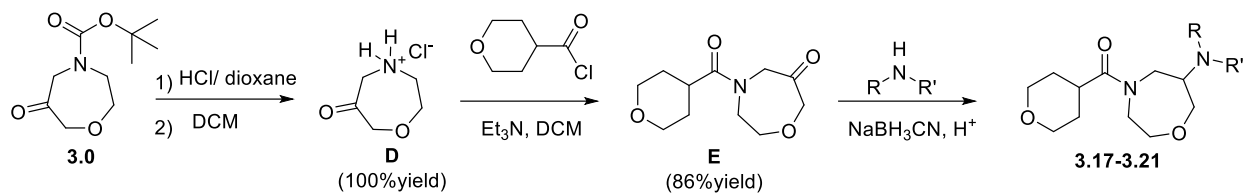
6-oxo-1,4-oxazepan-4-ium chloride (D)
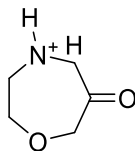
Dissolved *tert*-butyl 6–oxo-1,4-oxazepane-4-carboxylate (0.25 g, 1.16 mmol) in dichloromethane (DCM, 3.5 mL) then 4.0 M HCl in 1,4-dioxane (3.5 mL) was added. The reaction mixture was stirred at room temperature overnight and concentrate with vacuo. The final product was obtained as white solid; yield: 187.3 mg (100%).

^{1}H NMR (600 MHz, DMSO-d_6) δ 10.31 (s, 2H), 4.27 (s, 2H), 4.06 – 4.03 (m, 2H), 3.87 (s, 2H), 3.37 – 3.34 (m, 2H).

^{13}C NMR (151 MHz, DMSO-d_6) δ 206.1, 78.2, 69.8, 55.2, 49.7.

4-(tetrahydro-2*H*-pyran-4-carbonyl)-1,4-oxazepan-6-one (E)
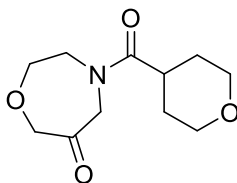
To a solution of **D** (533.4 mg, 3.54 mmol), triethylamine (1.23 mL) and DCM (3.0 mL) was cooled around 3 °C then a solution of tetrahydro-2*H*-pyran-4-carbonyl chloride (526 mg, 3.54 mmol in DCM (2.0 mL) was slowly added. The reaction mixture was strried under inert atmosphere overnight. Then the reaction mixture was added with water and extracted with ethyl acetate (3x). The organic layer was washed with brine, dried over MgSO$_4$ and concentrated with vacuo. The resulting residue was purified by flash column chromatography. The final product was obtained as colorless oil; yield: 712.1 mg (86%).

^{1}H NMR (600 MHz, CDCl$_3$): δ 4.23 (s, 1H), 4.13 (m, 1H), 4.05 – 3.85 (m, 3H), 3.86 – 3.51 (m, 3H), 3.42 (t, *J* = 11.8 Hz, 2H), 3.26 (s, 1H), 2.76 – 2.50 (m, 1H), 1.89 – 1.83 (m, 1H), 1.55 (m, 2H), 1.09 (m, 1H), 0.85 (m, 1H).

HR-MS-ESI (m/z) Calculated for C$_{11}$H$_{18}$NO$_4$ [M + H$^+$], 228.1236, found; 228.1233.

(6-(benzylamino)-1,4-oxazepan-4-yl)(tetrahydro-2*H*-pyran-4-yl)methanone (3.17)
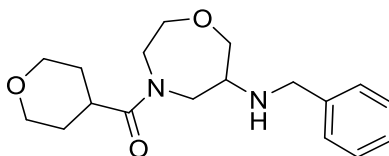
A solution of 4-(tetrahydro-2H-pyran-4-carbonyl)-1,4-oxazepan-6-one (84.5 mg, 0.37 mmol) in THF (3.0 mL) then methyl benzylamine (79.3 mg, 0.74 mmol) sodium cyanoborohydride (46.5 mg, 0.74 mmol) and acetic acid (35.6µL) were added. The reaction mixture was stirred at room temperature overnight, when the reaction completed,

the reaction mixture was concentrated in vacuum. The residual was dissolved in ethyl acetate and saturated $NaHCO_3$. The aqueous phase was extracted with ethyl acetate (EtOAc) (3x). The combined organic phases was added brine then dried with $MgSO_4$, filtered and concentrated in vacuum The crude material was purified by flash column chromatography and the final product was obtained as colorless oil; yield: 60.0 mg (51%).

^{1}H NMR (399 MHz, toluene-d_8, 105 °C) δ 7.23 – 7.18 (m, 1H), 7.10 (t, J = 7.5 Hz, 2H), 7.06 – 6.99 (m, 2H), 3.87 – 3.77 (m, 2H), 3.61 (s, 2H), 3.40 (s, 6H), 3.18 (s, 4H), 2.73 (s, 1H), 2.46 (s, 1H), 1.88 (s, 3H), 1.32 (t, J = 15.9 Hz, 2H).

HR-MS-ESI (m/z) Calculated for $C_{18}H_{27}N_2O_3$ [M + H$^+$], 319.2022; found; 319.2039.

(6-((pyridin-2-ylmethyl)amino)-1,4-oxazepan-4-yl)(tetrahydro-2*H*-pyran-4-yl)methanone (3.18)
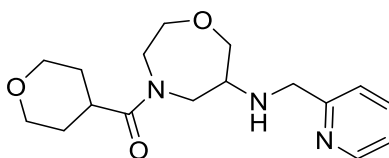
This was synthesised on a 94.5 mg, 0.42 mmol scale of the 4-(tetrahydro-2*H*-pyran-4-carbonyl)-1,4-oxazepan-6-one by the same procedure of **3.7** and pyridin-2-ylmethanamine (90.84 mg, 0.84 mmol) was used instead of benzylamine. The final product was obtained as colorless oil; yield: 8.5 mg (6%).

^{1}H NMR (399 MHz, toluene-d_8, 105 °C) δ 8.25 (s, 1H), 7.54 (s, 1H), 7.12 (s, 1H), 6.46 (s, 1H), 4.20 – 4.16 (m, 2H), 3.97 – 3.90 (m, 3H), 3.52 – 3.44 (m, 5H), 3.43 – 3.38 (m, 2H), 3.34 – 3.29 (m, 2H), 3.24 – 3.17 (m, 1H), 2.73 (s, 1H), 2.54 (s, 1H), 2.01 – 1.93 (m, 2H), 1.43 (d, J = 13.8 Hz, 2H).

HR-MS-ESI (m/z) Calculated for $C_{17}H_{26}N_3O_3$ [M + H$^+$], 320.1974; found; 320.1973.

(6-((pyridin-3-ylmethyl)amino)-1,4-oxazepan-4-yl)(tetrahydro-2*H*-pyran-4-yl)methanone (3.19)

This was synthesised on a 88.0 mg, 0.39 mmol scale of the 4-(tetrahydro-2*H*-pyran-4-carbonyl)-1,4-oxazepan-6-one by the same procedure of **3.7** and pyridin-3-ylmethanamine (84.35 mg, 0.78 mmol) was used instead of benzylamine. The final product was obtained as colorless oil; yield: 15 mg (12%).

^{1}H NMR (399 MHz, toluene-d_8, 105 ^{o}C) δ 8.43 (s, 1H), 7.98 (s, 1H), 7.28 (s, 1H), 6.56 (s, 1H), 3.97 – 3.90 (m, 2H), 3.58 – 3.37 (m, 6H), 3.34 – 3.19 (m, 7H), 2.62 – 2.45 (m, 2H), 1.96 (d, *J* = 11.6 Hz, 2H), 1.44 – 1.38 (m, 2H).

HR-MS-ESI (m/z) Calculated for $C_{17}H_{26}N_3O_3$ [M + H$^+$], 320.1974; found; 320.1984.

(6-((pyridin-4-ylmethyl)amino)-1,4-oxazepan-4-yl)(tetrahydro-2*H*-pyran-4-yl)methanone (3.20)

This was synthesised on a 77.6 mg, 0.34 mmol scale of the 4-(tetrahydro-2*H*-pyran-4-carbonyl)-1,4-oxazepan-6-one by the same procedure of **3.7** and pyridin-4-

ylmethanamine (73.54 mg, 0.68 mmol) was used instead of benzylamine. The final product was obtained as colorless oil; yield: 8.5 mg (8%).

^{1}H NMR (399 MHz, toluene-d_8, 105 ^{o}C) δ 7.99 (d, J = 6.0 Hz, 2H), 6.80 (d, J = 6.0 Hz, 2H), 3.94 (d, J = 11.9 Hz, 3H), 3.41 (s, 3H), 3.33 – 3.15 (m, 8H), 2.58 (s, 1H), 2.40 (s, 1H), 1.97 (d, J = 13.4 Hz, 2H), 1.41 – 1.32 (m, 3H).

HR-MS-ESI (m/z) Calculated for $C_{17}H_{26}N_3O_3$ [M + H$^+$], 320.1974; found; 320.1973.

(6-((4-bromobenzyl)amino)-1,4-oxazepan-4-yl)(tetrahydro-2H-pyran-4-yl)methanone (3.21)
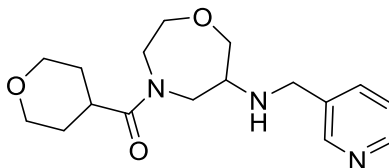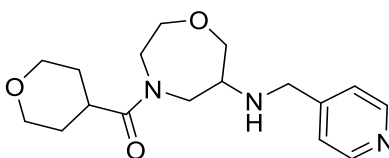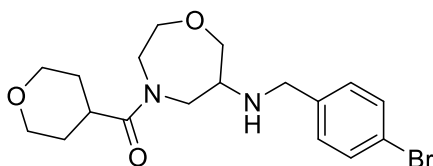

This was synthesised on a 77.9 mg, 0.35 mmol scale of the 4-(tetrahydro-2H-pyran-4-carbonyl)-1,4-oxazepan-6-one by the same procedure of **3.7** and (4-bromophenyl)methanamine (130.2 mg, 0.70 mmol) was used instead of benzylamine. The final product was obtained as colorless oil; yield: 60 mg (43%).

^{1}H NMR (399 MHz, toluene-d_8, 105 ^{o}C) δ 7.24 – 7.19 (m, 2H), 6.95 – 6.92 (m, 2H), 3.86 – 3.80 (m, 2H), 3.47 – 3.39 (m, 3H), 3.39 – 3.28 (m, 5H), 3.21 – 3.11 (m, 4H), 2.65 (s, 1H), 2.41 (s, 1H), 1.93 – 1.82 (m, 2H), 1.37 – 1.23 (m, 3H).

HR-MS-ESI (m/z) Calculated for $C_{18}H_{26}N_2O_3Br$ [M + H$^+$], 397.1127; found; 397.1129.

3.8 References

1   S. P. Hunger and C. G. Mullighan, *N. Engl. J. Med.*, 2015, **373**, 1541–1552.

2   C.-H. Pui and W. E. Evans, *N. Engl. J. Med.*, 2006, **354**, 166–178.

3   L. Milton-Harris, M. Jeeves, S. A. Walker, S. E. Ward and E. J. Mancini, *Oncotarget*, 2020, **11**, 1737–1748.

4   E. Roman, J. Simpson, P. Ansell, S. Kinsey, C. D. Mitchell, P. A. McKinney, J. M. Birch, M. Greaves and T. Eden, *Am. J. Epidemiol.*, 2007, **165**, 496–504.

5   Together Powered by St. Jude Children's Research Hospital, Leukemia in Children and Teens, https://together.stjude.org/en-us/about-pediatric-cancer/types/leukemia.html, (accessed 25 May 2021).

6   S. Shafique and S. Tehsin, *Technol. Cancer Res. Treat.*, 2018, **17**, 1–7.

7   S. Faderl, S. O'Brien, C. H. Pui, W. Stock, M. Wetzler, D. Hoelzer and H. M. Kantarjian, *Cancer*, 2010, **116**, 1165–1176.

8   W. E. EVANS and C.-H. P. MARY V. RELLING , JOHN H. RODMAN, WILLIAM R. CROM , JAMES M. BOYETT, *N. Engl. J. Med.*, 1998, **338**, 499–505.

9   M. Kato and A. Manabe, *Pediatr. Int.*, 2018, **60**, 4–12.

10   C. H. Pui and S. Jeha, *Nat. Rev. Drug Discov.*, 2007, **6**, 149–165.

11   D. S. Wishart, C. Knox, A. C. Guo, S. Shrivastava, M. Hassanali, P. Stothard, Z. Chang and J. Woolsey, *Nucleic Acids Res.*, 2006, **34**, D668–D672.

12   D. S. Wishart, C. Knox, A. C. Guo, D. Cheng, S. Shrivastava, D. Tzur, B. Gautam and M. Hassanali, *Nucleic Acids Res.*, 2008, **36**, D901–D906.

13   D. S. Wishart, Y. D. Feunang, A. C. Guo, E. J. Lo, A. Marcu, J. R. Grant, T. Sajed, D. Johnson, C. Li, Z. Sayeeda, N. Assempour, I. Iynkkaran, Y. Liu, A. Maclejewski, N. Gale, A. Wilson, L. Chin, R. Cummings, Di. Le, A. Pon, C. Knox and M. Wilson, *Nucleic Acids Res.*, 2018, **46**, D1074–D1082.

14   V. Law, C. Knox, Y. Djoumbou, T. Jewison, A. C. Guo, Y. Liu, A. Maclejewski, D.

Arndt, M. Wilson, V. Neveu, A. Tang, G. Gabriel, C. Ly, S. Adamjee, Z. T. Dame, B. Han, Y. Zhou and D. S. Wishart, *Nucleic Acids Res.*, 2014, **42**, D1091–D1097.

15   C. Knox, V. Law, T. Jewison, P. Liu, S. Ly, A. Frolkis, A. Pon, K. Banco, C. Mak, V. Neveu, Y. Djoumbou, R. Eisner, A. C. Guo and D. S. Wishart, *Nucleic Acids Res.*, 2011, **39**, D1035–D1041.

16   S. L. Berg, S. M. Blaney, M. Devidas, T. A. Lampkin, A. Murgo, M. Bernstein, A. Billett, J. Kurtzberg, G. Reaman, P. Gaynon, J. Whitlock, M. Krailo and M. B. Harris, *J. Clin. Oncol.*, 2005, **23**, 3376–3382.

17   J. M. Rowe, G. Buck, A. K. Burnett, R. Chopra, P. H. Wiernik, S. M. Richards, H. M. Lazarus, I. M. Franklin, M. R. Litzow, N. Ciobanu, H. G. Prentice, J. Durrant, M. S. Tallman and A. H. Goldstone, *Blood*, 2005, **106**, 3760–3767.

18   T. Morishima, A. C. Krahl, M. Nasri, Y. Xu, N. Aghaallaei, B. Findik, M. Klimiankou, M. Ritter, M. D. Hartmann, C. J. Gloeckner, S. Stefanczyk, C. Lindner, B. Oswald, R. Bernhard, K. Hähnel, U. Hermanutz-Klein, M. Ebinger, R. Handgretinger, N. Casadei, K. Welte, M. Andre, P. Müller, B. Bajoghli and J. Skokowa, *Blood*, 2019, **134**, 1159–1175.

19   J. Raboso-Gallego, A. Casado-García, M. Isidro-Hernández and C. Vicente-Dueñas, *Front. Cell Dev. Biol.*, , DOI:10.3389/fcell.2019.00137.

20   K. El Omari, S. J. Hoosdally, K. Tuladhar, D. Karia, P. Vyas, R. Patient, C. Porcher and E. J. Mancini, *Blood*, 2011, **117**, 2146–2156.

21   K. El Omari, S. J. Hoosdally, K. Tuladhar, D. Karia, E. Hall-Ponselé, O. Platonova, P. Vyas, R. Patient, C. Porcher and E. J. Mancini, *Cell Rep.*, 2013, **4**, 135–147.

22   P. Van Vlierberghe, M. Van Grotel, H. B. Beverloo, C. Lee, T. Helgason, J. Buijs-Gladdines, M. Passier, E. R. Van Wering, A. J. P. Veerman, W. A. Kamps, J. P. P. Meijerink and R. Pieters, *Blood*, 2006, **108**, 3520–3529.

23   C. Porcher, W. Swat, K. Rockwell, Y. Fujiwara, F. W. Alt and S. H. Orkin, *Cell*, 1996, **86**, 47–57.

24   A. Daina, O. Michielin and V. Zoete, *Sci. Rep.*, 2017, **7**, 1–13.

25   C. A. Lipinski, F. Lombardo, B. W. Dominy and P. J. Feeney, *Adv. Drug Deliv. Rev.*, 2001, **46**, 3–26.

26   C. A. Lipinski, *Drug Discov. Today Technol.*, 2004, **1**, 337–341.

27   L. Di and E. H. Kerns, in *Drug-Like Properties Concepts, Structure Design and Methods from ADME to Toxicity Optimization*, Elsevier Inc., Second edi., 2016, pp. 29–38.

28   D. F. Veber, S. R. Johnson, H.-Y. Cheng, B. R. Smith, K. W. Ward and K. D. Kopple, *J. Med. Chem*, 2002, **45**, 2615–2633.

29   S. A. Wildman and G. M. Crippen, *J. Chem. Inf. Comput. Sci.*, 1999, **39**, 868–873.

30   P. Panyatip, N. Nunthaboot and P. Puthongking, *Int. J. Tryptophan Res.*, 2020, **13**, 1–7.

31   A. Daina and V. Zoete, *ChemMedChem*, 2016, **11**, 1117–1121.

32   A. Daina, M. C. Blatter, V. Baillie Gerritsen, P. M. Palagi, D. Marek, I. Xenarios, T. Schwede, O. Michielin and V. Zoete, *J. Chem. Educ.*, 2017, **94**, 335–344.

33   A. Daina, O. Michielin and V. Zoete, *Chem. Inf. Model.*, 2014, **54**, 3284–3301

Chapter 4

Synthesis of Potential Compounds for
Potassium Ion Channel Targets in Pain Relief

4.1 Background

A hundred million people worldwide are affected by chronic pain,[1] which is a widespread issue that leads to a decreased ability of sufferers to perform daily activities. There is a long time for treatment results due to the higher workloads of medical staff and financial pressures on healthcare systems. Chronic pain may be brought on by repeated activation of nociceptors in regions of tissue destruction and also from neuropathic pain, which is difficult to cure. At present, drug treatment is very effective for chronic pain, for instance, NSAIDs (e.g., naproxen, Figure 4.1) and opioids (e.g., morphine, oxycodone and fentanyl, Figure 4.1) however, there are some side effects, including dizziness, nausea, pruritus, dry mouth and the risk of addiction in the case of opioiods. Therefore, the need to control adverse effects and effective treatment for neurotherapeutic targets should be considered.[2,3]
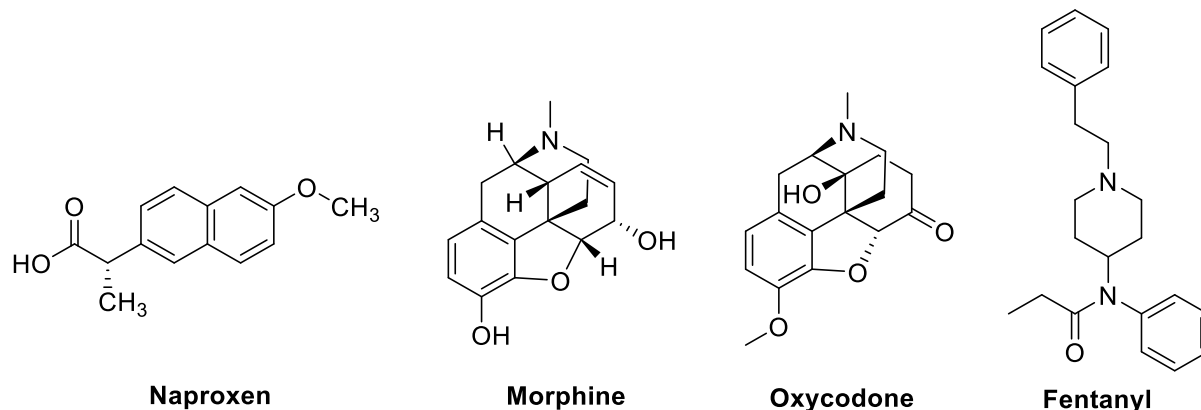
Figure 4.1. *Example of drugs for chronic pain treatment.*[4–8]

Ion channels are large membrane-spanning proteins that selectively transport ions into and out of cells. These channels transmit pain signals into the nervous system and relate to neuronal excitablity[9]. There are many current diseases based on ion channel targets, for instance, hypertension (related to calcium and potassium channels), cardiac arrhythmias (related to sodium, potassium and calcium channels) and diabetes (related to potassium channels). It has also been found that ion channels are the second most common gene family target (13.4%).[10]

When nerve impulse transmission is stimulated by a variety of factors such as heat, cold and inflammation, electrical signals are sent through the neuron to the spinal cord or brain, resulting in a sensation of pain. Voltage-gated sodium and potassium ion channel (Na_v and K_v respectively) display an important role in the transmission of electrical signals (or an action potential, AP) along an axon. At the resting membrane state, the membrane voltage is around -60 mV (Na_v close) when the action potential is triggered, Na^+ passes through the cell membrane (Na_v open) that causes the voltage reach to the threshold (value around -45 mV), then the voltage raised rapidly (depolarization) until reached the top then repolarization occurred where Na_v closed and K_v opened that allows K^+ moved out from the cell. Finally, the potentials drop below the resting state (hyperpolarization), Na_v and K_v are inactivated, then the voltage returns to the resting stage again, and is ready for the next action potential as shown in Figure 4.2.[11–13] There are many studies in the field of Na_v, whereas there are fewer investigations into K_v's function in pain. However, researchers found that nerve damage and inflammation affect K_v activity in the neuronal pain pathway and the inhibition of K_v (inhibitor) changes the membrane potential in the depolarization state, meanwhile a K_v opener (activator) changes the hyperpolarization potential. Therefore, the possibility of using K_v activity is an alternative way as a novel therapeutic in a chronic pain target.[2,12,14]
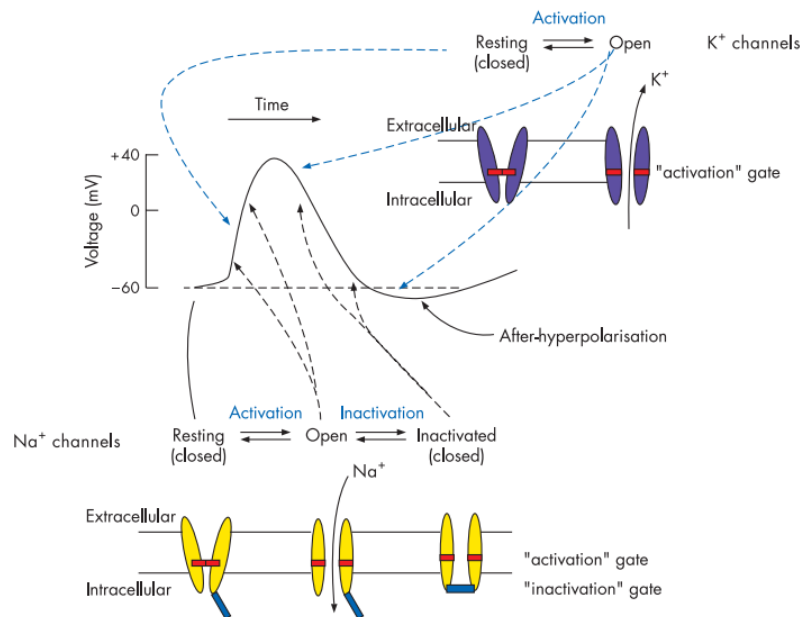
Figure 4.2. *The action potential and related model depicting activated and inactivated voltage gate sodium and potassium ion channels.*[11]

Potassium ion channels (K^+ channels) are the most common type of ion channel and can be found in almost all living creatures. The structure of K^+ channels is composed of lipid bilayer membranes that control the movement of potassium ions inside and outside of the cell. The ion penetration between cell membranes is highly specific and regulated by their subunits. The general structure of K^+ channels was studied from *Streptomyces lividans* [KcsA (K^+ channel of streptomyces A. Figure 4.3 displays the structure, which comprises 4 subuints forming the channels, the conducted K^+ are represented by a blue sphere that can be bound by the backbone carbonyl or hydroxyl group in binding positions (S0 – S4, TVGYG) and sodium ions (orange) also coordinated with carbonyl oxygen in S3 and S4.[15,16]
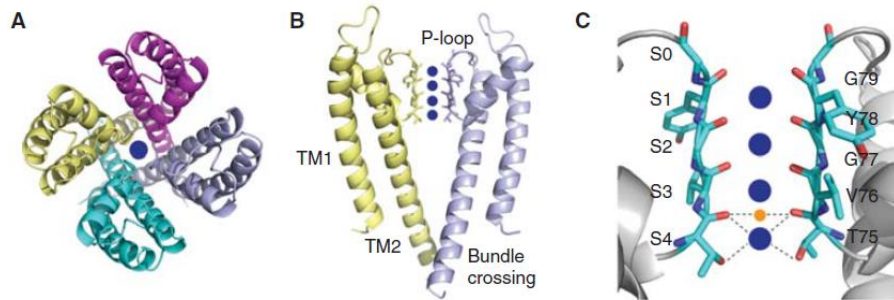
Figure 4.3. *KcsA structure.* **A, B** *are KcsA tetramer as viewed from the top and side along the membrane, respectively.* **C** *potassium ions pass through the selectivity filter (binding site, S0 – S4).*[15,16]

There are 4 main types of K^+ channels; 1) Calcium - activated potassium channel (K_{Ca}^{2+}), the gate response with calcium ions or other signaling molecules, 2) Inwardly rectifying potassium channels (K_{IR}), which pass positive charge currents into the cell, 3) Tandem pore domain potassium channels (K_{2p}), which produce a leaky K^+ current that balances depolarization by stabilising the negative membrane potential, 4) Voltage-gated potassium channel (K_v), which rely on the changing of transmembrane voltage to cause opening or closing of the channels.
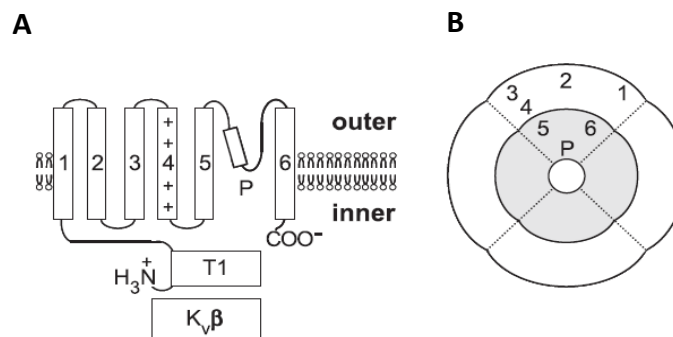

Figure 4.4. *Representation of K_v channel of α subunit structure (***A***) and tetramer quaternary structure (***B***).*[17]

K_v channels are the largest family of K^+ channels that are found in all animal cells such as K_v1.1/1.2 and involved in epilepsy. Neuro drug pain, K_v7.1 involves cardiac muscle and K_v4.2 is target for inflammatory pain.[18] The structure of the K_v channel comprises tetramers of α subunits (Figure 4.4A) that contain six transmembrane domains (1 - 6) in α subunits, a pore - forming loop, N – termini intramolecular domain (T1) that interact with β subunit (K_vβ). A pore-forming motif (grey) is constructed from the P-loop and transmembrane domains 5 and 6 (Figure 4.4B).

Moreover, the positive charged in the fourth transmembrane domain allows the channel to open when the cell is depolarized.[17] The majority of drug action in K^+ channels is blocking ion flux or a few are found that lead to bending the gate when it binds to the ion–conducting pores.[18] Regulating the opening and closing of potassium channels plays an important role in medicine and treatment design, especially in neurology for pain relief.

4.2 Drug targeting in K_v channels for chronic pain treatment

Opioid drugs are widely known to be highly effective in treating chronic pain. However, they have also found several drawbacks such as addiction, side effects and death. Moreover, an increasing in opioid-related deaths in the United States was found during 1990-2010.[19,20] Therefore, new, safe nonopioid compounds are developed. In this research the investigations on K_v channels were focused on. There are many more clinical tests and some interesting compounds as follows: some of the venoms from natural predators can block K_v channels e.g. toxins from scorpions or spiders, snakes, etc or some compounds are able to open the K_v channels e.g. retigabine, flupirtine, etc.
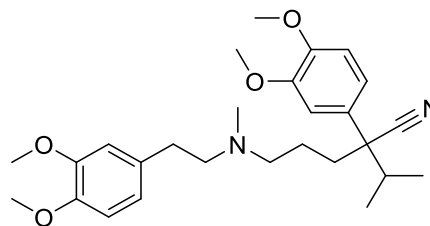
Unselective K_v channel inhibitors
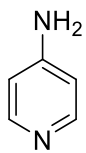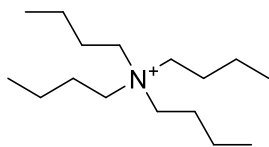
4-AP   **tetrabutyl ammonium, TBA**   **Verapamil**

2

2

2

2

2

2

2

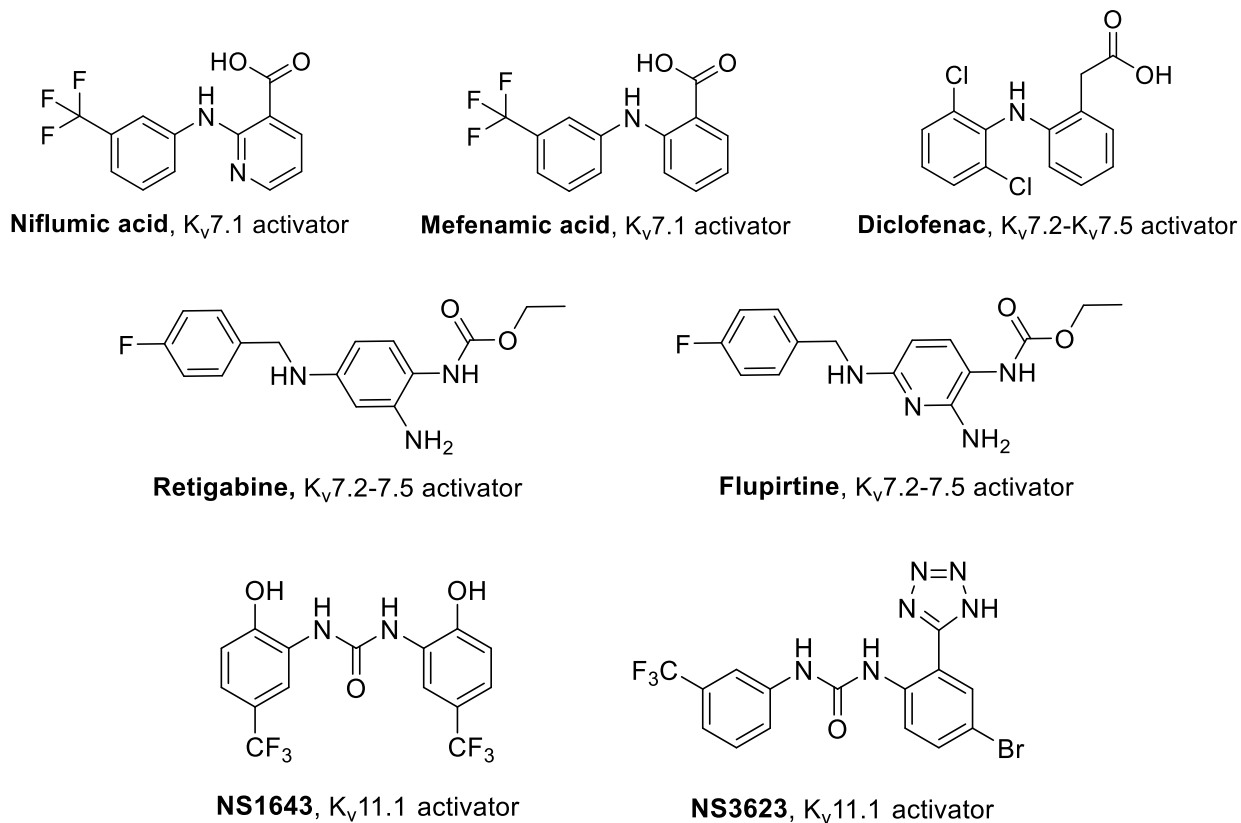2

2

2

2

2

2

2

2

2

2

2

Activators

Figure 4.5. Structures of Unselective K_v channel inhibitors and activators K_v channel modulators.[18]

Furthermore, some blocker of K_v channels as shown in Figure 4.5 e.g., 4-aminopyridine (4-AP), tetrabutylammonium (TBA) and Verapamil are unselective blockers, which are commonly used in cardiac arrhythmia treatment. The activator compounds of K_v channels (Figure 4.5) e.g., Niflumic acid and Mefenamic acid are K_v7.1 activators that stimulate channel activity caused by prolonged hyperpolarization. Diclofenac is well known for anti-inflammatory treatment. Retigabine and flupirtine directly bind to K_v7 channels leading to a conformational change causing K_v 7 channels to open. It was found that side effects of using retigabine include dizziness, somnolence, headache, and fatigue in clinical tests and it has been discontinued since 2017. Flupirtine (similar structure to retigabine) also displayed a similar mechanism in K_v7 so has been

used to treat acute and chronic pain in Europe since the 1980s and also for neuropathic pain.[18,21] Diphenyl urea compounds, NS1643 and NS3623 have shown potential in the $K_v11.1$ channel for cardiac arrhythmia treatment. It can be seen that these molecules were recently advanced into preclinical and clinical studies and also shown great potential for drug development.

Interestingly, our research focuses on K_v2 and K_v9, especially subtypes $K_v2.1/K_v9.1$. The K_v2 channel consists of $K_v2.1$ and $K_v2.2$. $K_v2.1$ is mostly found in some tissues and organs such as the brain, retina, heart, skeleton muscle and pancrease.[22,23] $K_v2.2$ is mainly found in brain tissue. The $K_v2.1$ channel shows many functions of neurons, for example, cell discharge and neuronal action potential repolarization. Diabetic peripheral neuropathy (DPN) is also related to $K_v2.1$. Pain, sensory loss and foot ulceration impact diabetic patients' life and medical treatment for this disease is needed. Dfe, drofenine hydrochloride (chemical structure shown in Figure 4.6) was determined to a potentially inhibited $K_v2.1$ channel in diabetic mice. The 50% inhibitory concentration (IC_{50}) of Dfe of 9.53 µM was detected by the whole-cell patch-clamp technique, and Dfe is also currently investigated in clinical trials.[22] In the same way, Tsantoulas *et. al.* discovered that knocking down $K_v9.1$ resulted in lowered firing thresholds and increased firing rates of potassium accumulating outside the cell during prolonged activity.[24] It was also found that co-expression between $K_v9.1$ and $K_v2.1$ resulted in a slower rate of activation of $K_v2.1$ when compared with $K_v2.1$ alone. Therefore, the synthesis of highly effective drugs is still needed to improve the potential in the $K_v2.1$ targent for chronic pain treatment.
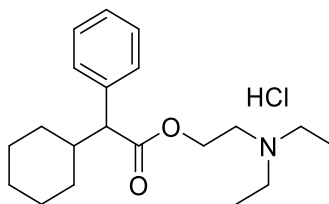

Figure 4.6. *Chemical structure of Dfe with an IC_{50} = 9.53 µM vs $K_v2.1$.*

4.3 Results and Discussion

Compounds for the $K_v2.1$ channel were studied by a medium throughput screen (HTS) at Sussex Drug Discovery (SDDC). More than 1,400 compounds were screened. The effective concentration (EC_{50}) is the concentration of a chemical that leads to 50% efficiency and % maximum efficacy (E_{max}) which is the ability of a drug to generate a maximum response obtained from the Thallium Flux FluxOR™ assay. The Principle of the Thallium Flux FluxOR™ assay are basal fluorescence from cells loaded with the FluxOR™ dye as shown in Figure 4.7. When the potassium channel is stimulated, thallium flows into the cell and binds the FluxOR™ dye, generating a fluorescent signal. The fluorescence signals are changed to %activation (or %efficacy) then EC_{50} and E_{max} are obtained as represented in Figure 4.8.
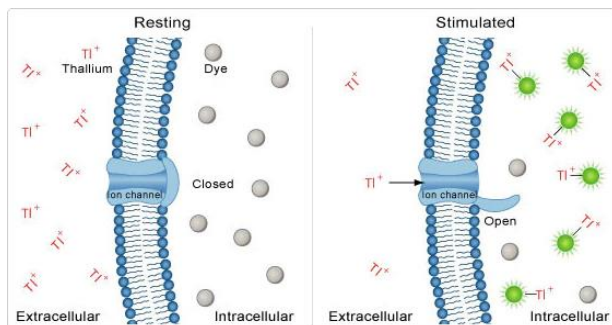

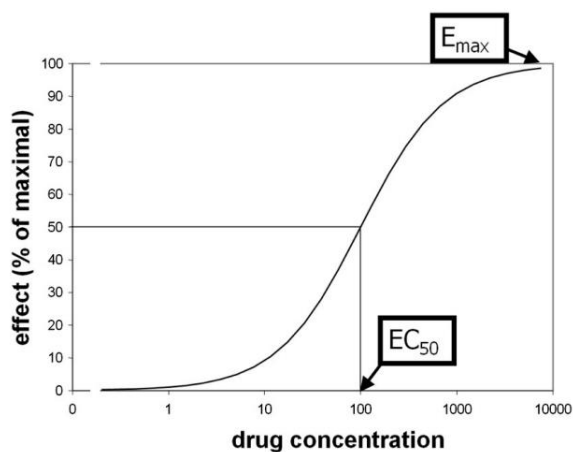*Figure 4.7.* Thallium redistribution in FluxOR™ Green assay.[25]

Figure 4.8. Illustration of EC_{50} and E_{max}.[26]

We found that one of the lead compounds **UOS–58757** and **UOS–58789** (Figure 4.9) displayed good performance which E_{max} values over the control by around 9% and 96%, respectively. Nevertheless, **UOS–58757** had poor permeability and low solubility at pH 7.4. Both **UOS–58757** and **UOS–58789** showed a good performance but still needed improvements in efficacy and solubility. From early structure-activity relationship (SAR) observation, the carboxyl group (-COOH) and NH on the amide are required. Substituents such as F, Cl, Br, or tetrazole are interesting groups to modify. Therefore, the synthesis of potential compounds in this research is divided into 2 themes that are developed from the lead compounds.
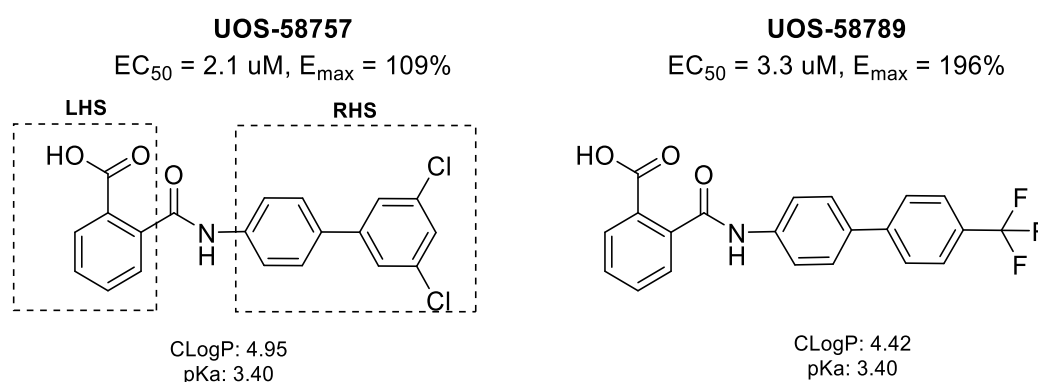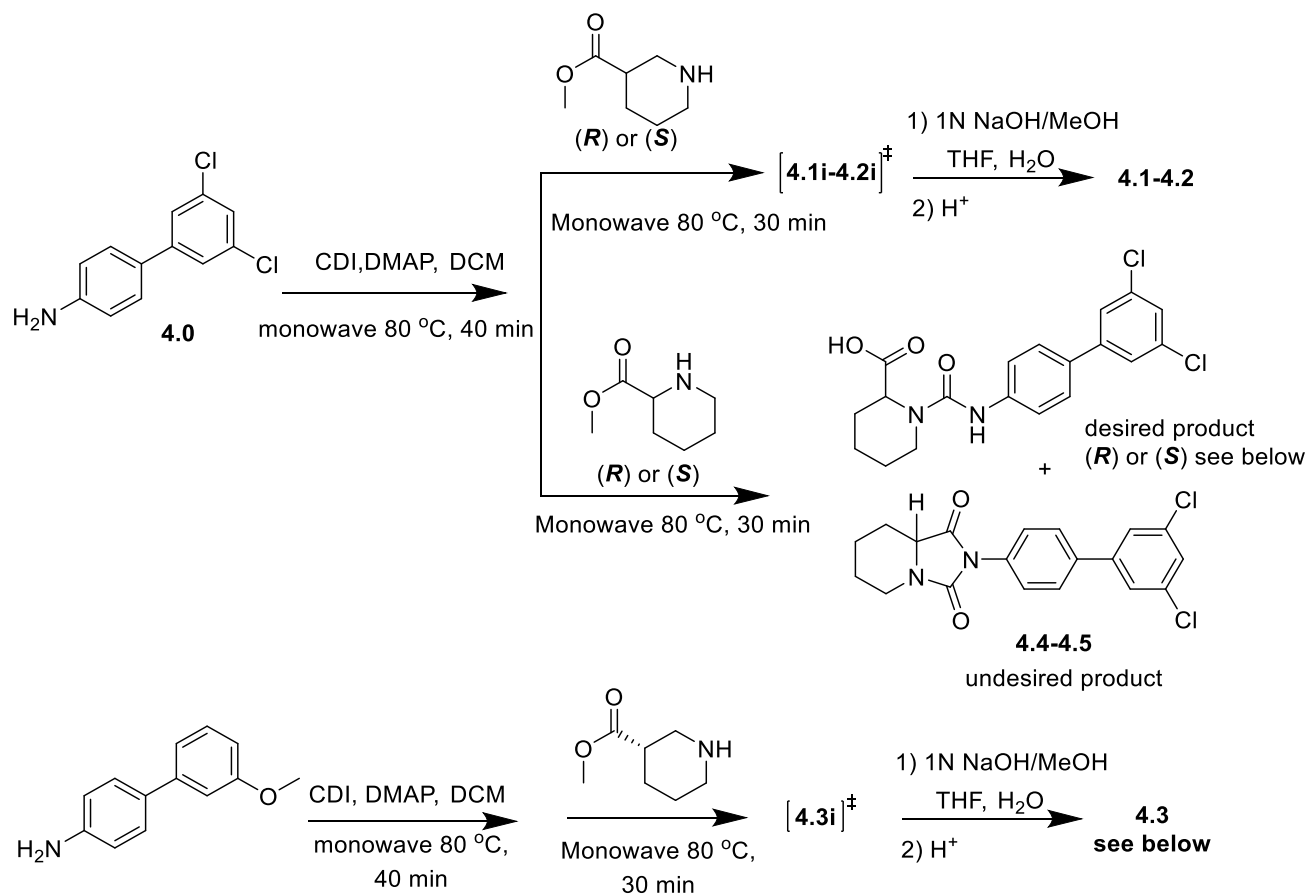

UOS-58757
EC_{50} = 2.1 uM, E_{max} = 109%

UOS-58789
EC_{50} = 3.3 uM, E_{max} = 196%

CLogP: 4.95
pKa: 3.40

CLogP: 4.42
pKa: 3.40

Figure 4.9. *Lead compounds,* ***UOS–58757*** *and* ***UOS-58789.*** *The left-hand side (LHS) and the right-hand side (RHS) are separated by a dashed line.*

4.3.1 Modification of LHS by using cyclohexane instead of phenyl ring

Firstly, development of the LHS, aimed to install a saturated cyclohexane and piperidine carboxylate with *R,S* configuration instead of a benzene ring, with 1,2- and 1,3-carboxyl groups , while keeping the RHS unchanged. This was to probe the effect of "escape from flatland" groups to improve solubility, possibly receptor binding.[27] Hence, for synthetic accessibility, methyl piperidine-3-carboxylate and methyl piperidine-2-carboxylate were selected and we made in a first instance, urea analogues (**Scheme 4.1**).

Intermediates (**4.1i-4.3i**)

4.1i
(*S*-configuration)
(22% yield)

4.2i
(*R*-configuration)
(20% yield)

4.3i
(*S*-configuration)
(24% yield)

Product (**4.1**-**4.5**)

4.1
(**S**-configuration)
EC_{50} = 8.5 uM, E_{max} = 161.7%
(26% yield)

4.2
(**R**-configuration)
EC_{50} = 6.9 uM, E_{max} = 163.9%
(49% yield)

4.3
(**S**-configuration)
inactive
(26% yield)

4.4
(**R**-configuration)
inactive
(39% yield)

4.5
(**S**-configuration)
inactive
(23% yield)
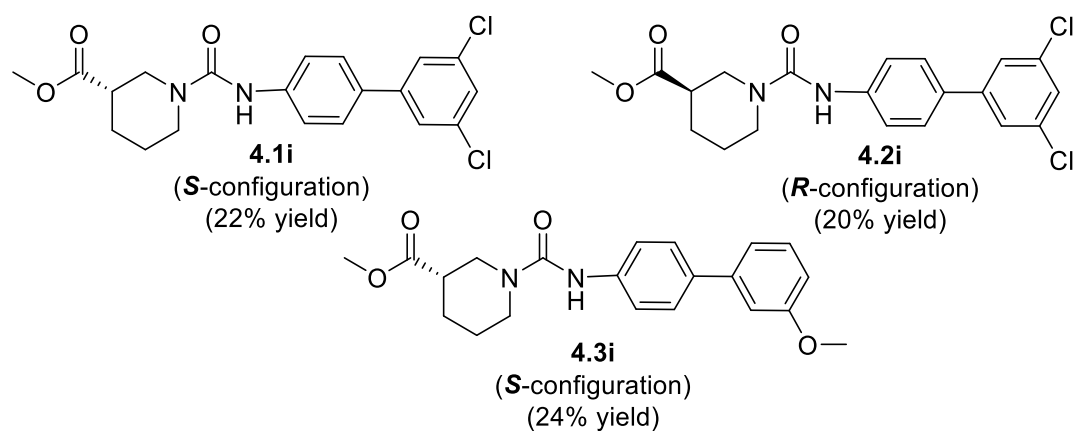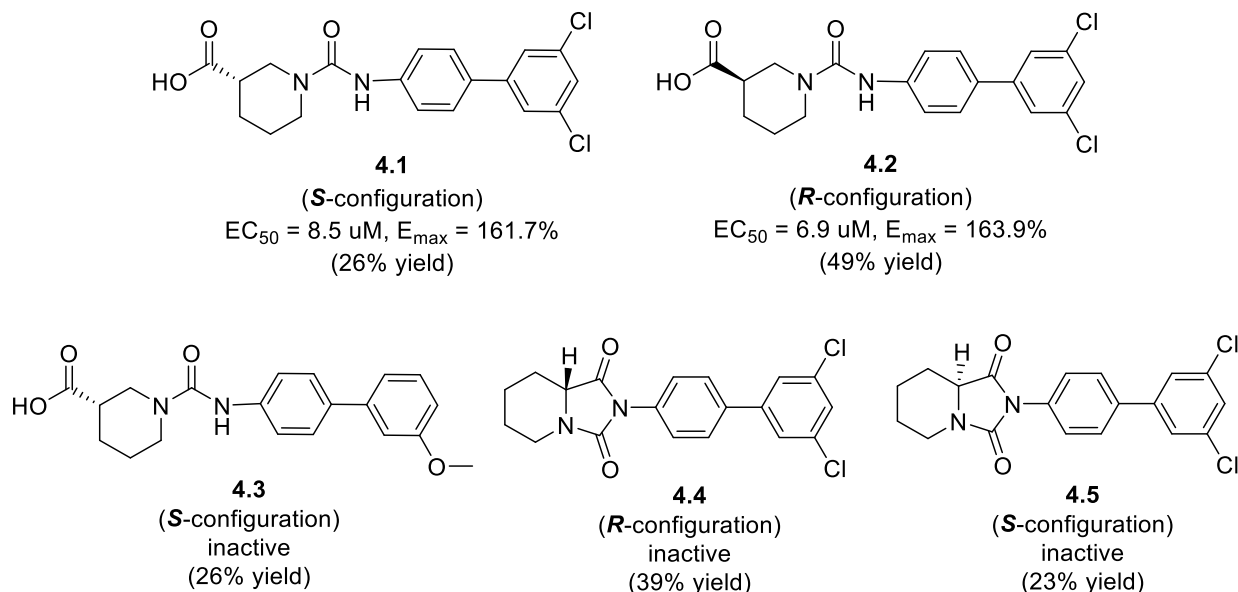
Scheme 4.1. *Synthesis of urea compounds by using CDI.*

Intermediate compounds (**4.1i-4.3i**) were synthesised by using a Monowave in around 20-25% yield. After that the product was obtained via hydrolysis in 26% yields (**4.1** and **4.3**) and 49% yield (**4.2**). Both compounds **4.1** and **4.2** are active so 3'-methoxy-[1,1'-biphenyl]-4-amine was used instead of **4.0** to generate the biaryl compound **4.3** but this was found to be inactive. There are unexpected products (**4.4** and **4.5)** via cyclization reaction from using 1,2-carboxyl groups (methylpiperidine-2-carboxylate hydrochloride) and were also inactive.

(A)

Chromatogram

4.1
(*S*-configuration)
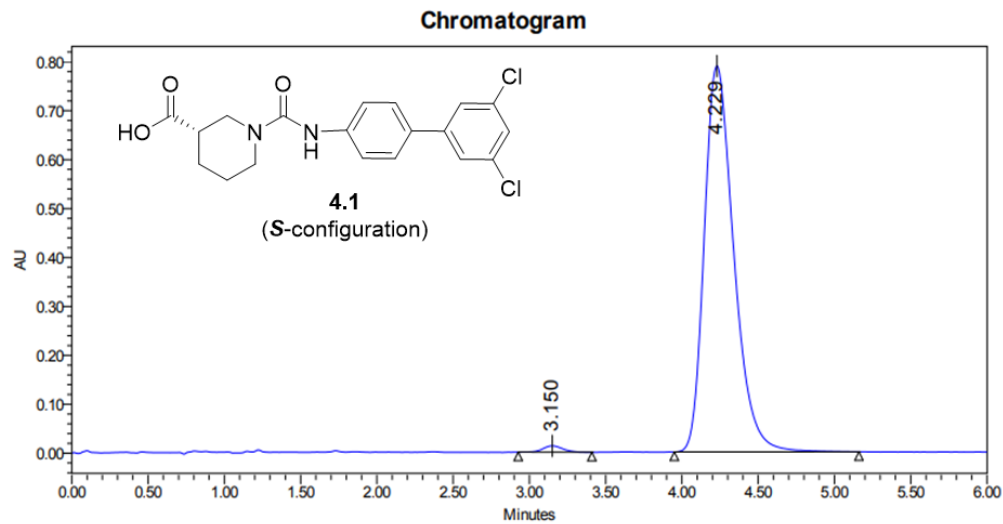
Peak Results

	Retention Time (min)	Area (µV*sec)	% Area	Width @ 50%
1	3.15	118161	1.1	
2	4.23	10596428	98.9	

(B)

Chromatogram

4.2
(*R*-configuration)
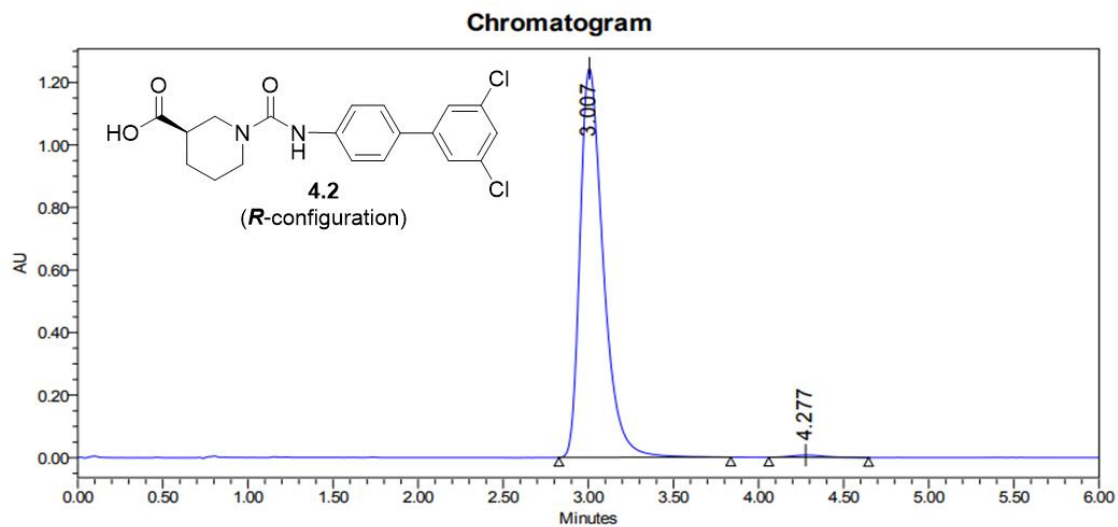
Peak Results

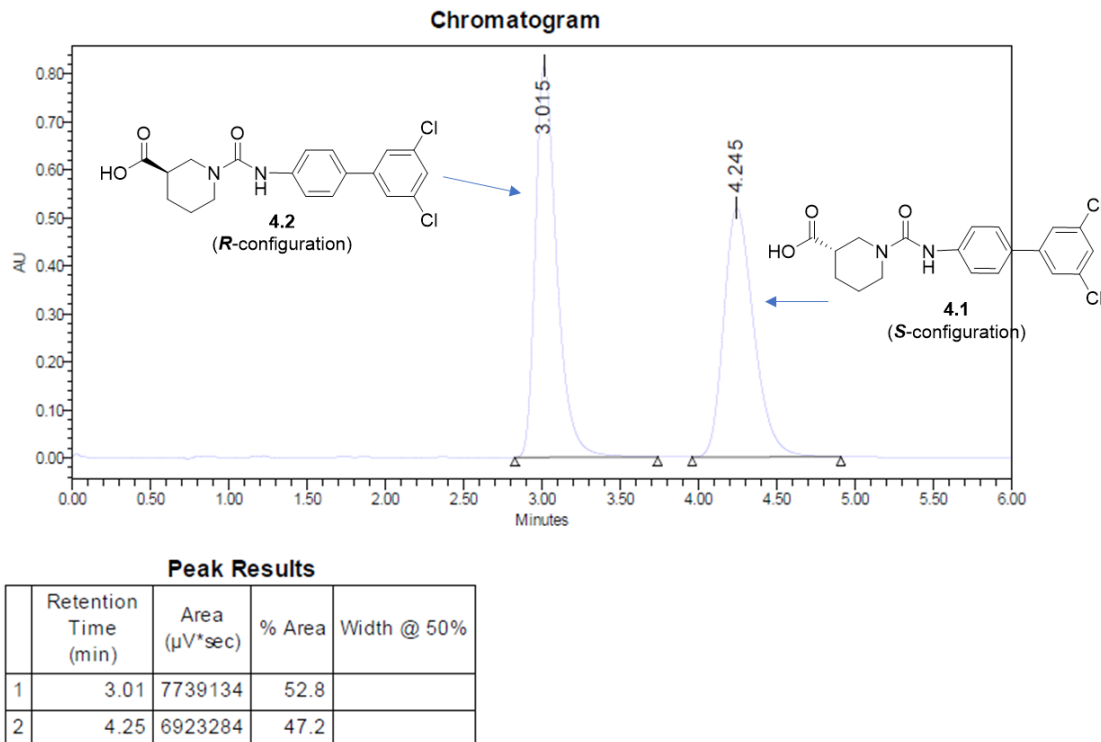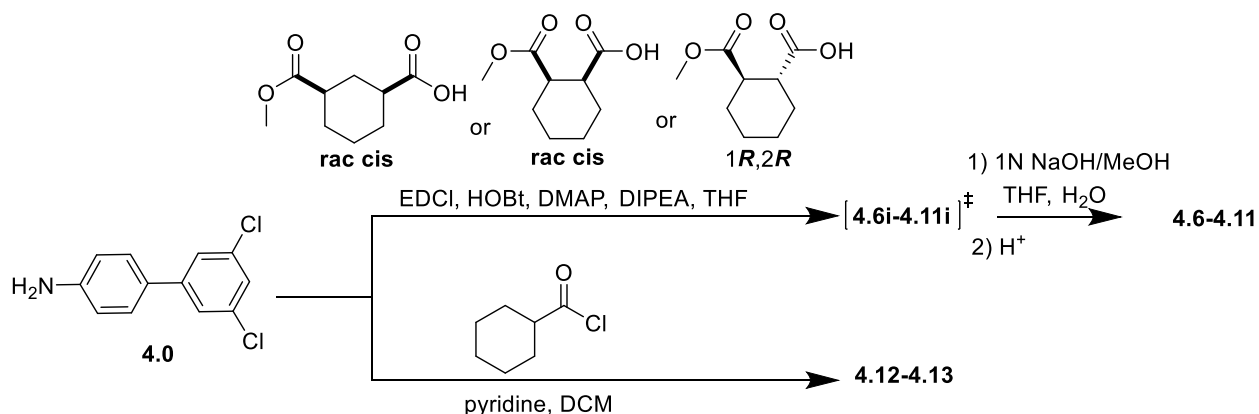|	Retention Time (min)	Area (µV*sec)	% Area	Width @ 50%
1	3.01	11785280	99.2	
2	4.28	98409	0.8	

(C)

Figure 4.10. *Chiral HPLC chromatogram, chiral purity of compounds 4.1 (A) and 4.2 (B) and the mixture of both compounds (C) (Analysed by Reach Separations,UK)*
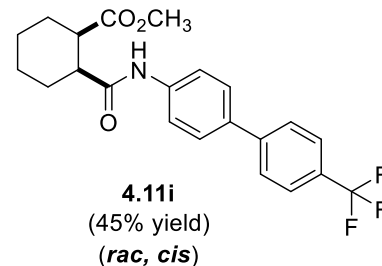
The stereochemical integrity of the products was confirmed by chiral HPLC as shown in Figure 4.10. Compounds **4.1** and **4.2** showed 97.8% and 98.4% enantiomeric excess, respectively, indicating, as expected, no loss of stereochemistry upon coupling.

In the same way, 3-(methoxycarbonyl)cyclohexane-1-carboxylic and 2-(methoxycarbonyl)cyclohexane-1-carboxylic were making the amide analogues (**Scheme 4.2**). Derivatives with 1,3- substituted carboxyl groups have better potency than those in the 1,2- position and inactive cyclization products from the 1,2-position presumably due to a loss of a carboxyl group. In order to prove that the -COOH is a necessary group for binding, the cyclohexane analogues devoid of a carboxyl group were synthesised by using cyclohexanecarbonyl chloride as a starting material that was coupled with amine

4.0 (3',5'-dichloro-4-biphenylamine) or (4'-(trifluoromethyl)-[1,1'-biphenyl]-4-amine). The 1,3-dicarboxy analogue, **4.6**, is active and the other analogues seem to be inactive except for the related **4.9**, which differs from **4.9** in having a para CF₃-substituted aromatic instead of a dichloro-substituted aromatic, and displays approximately double its activity. The related 1,2-substituted dicarboxy compounds as well as the "deletion" compounds **4.12** and **4.13** are inactive.

Intermediates (**4.6i-4.11i**)

4.6i
(38% yield)
(*rac, cis*)

4.7i
(29% yield)
(*1R, 2R*)

4.8i
(28% yield)

4.9i
(10% yield)
(*rac, cis*)

4.10i
(26% yield)
(*1R, 2R*)

4.11i
(45% yield)
(*rac, cis*)

Products (**4.6**-**4.13**)

4.6
EC$_{50}$ = 6.7 uM, E$_{max}$ = 167%
(37% yield)
(***rac, cis***)

4.7
inactive
(59% yield)
(**1R, 2R**)

4.8
inactive
(64% yield)
(***rac, cis***)

4.9
EC$_{50}$ = 3.5 uM, E$_{max}$ = 89.6%
(79% yield)
(***rac, cis***)

4.10
EC$_{50}$ > 30 uM, E$_{max}$ = 100%
(30% yield)
(**1R, 2R**)

4.11
EC$_{50}$ > 30 uM, E$_{max}$ = 105% @ 30 uM
(48% yield)
(***rac, cis***)

4.12
inactive
(27% yield)

4.13
inactive
(36% yield)
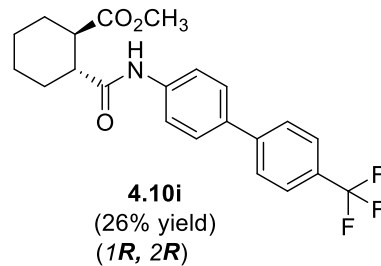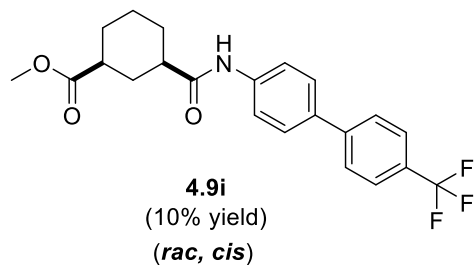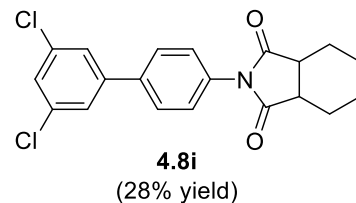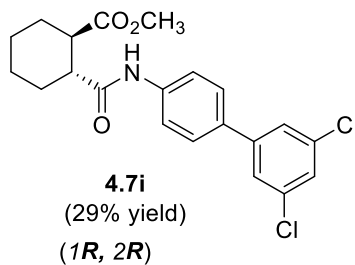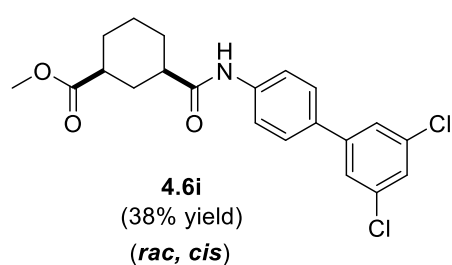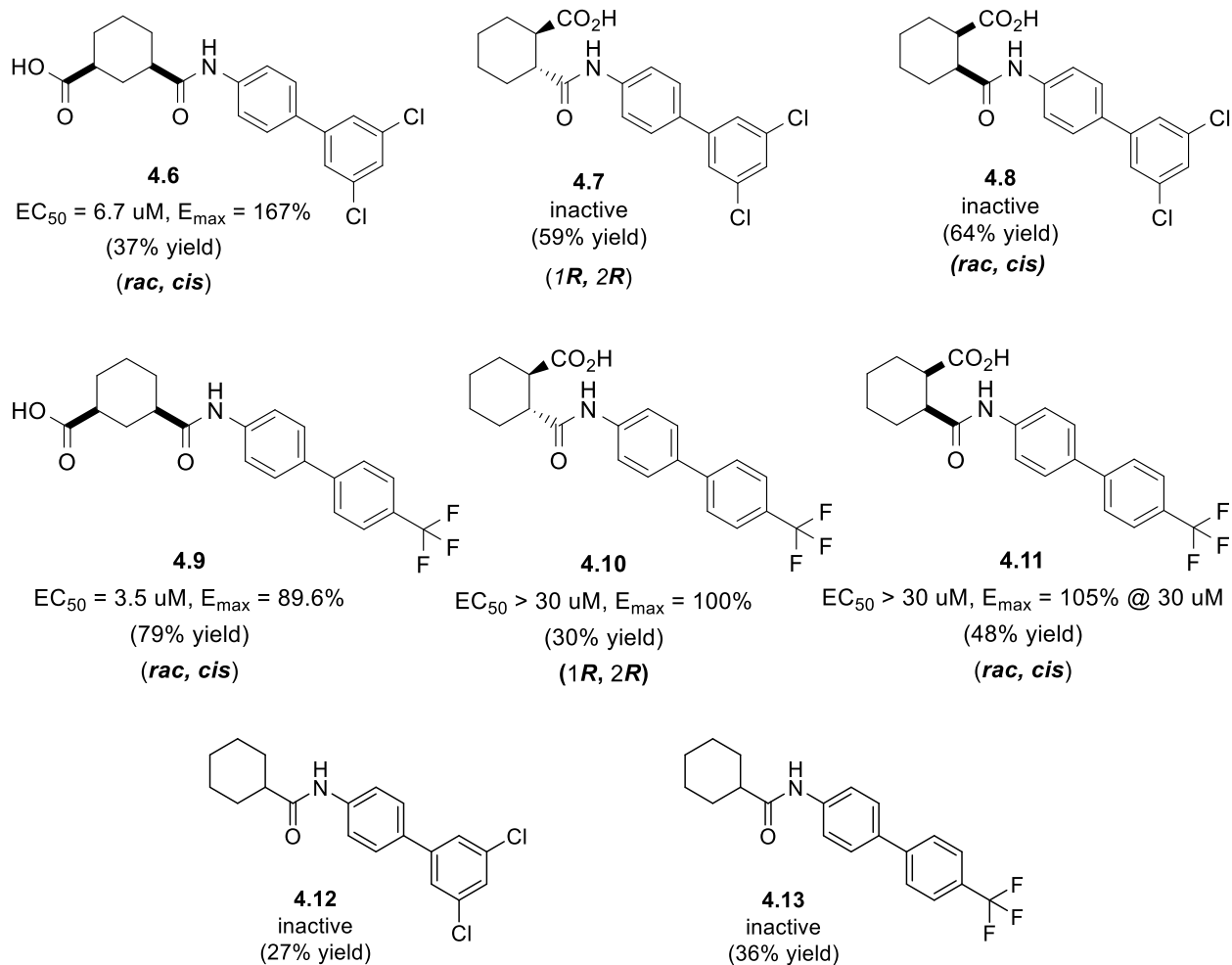
Scheme 4.2. *Synthesis of amide compounds by changing LHS.*

4.3.2 Modification of LHS by using tetrazole instead of carboxyl group in phenyl ring: Hybrid Series

Next, the hybrid series were investigated because of compounds **4.1**, **4.2** and **4.6** showed good performance and they were synthesized by coupling biphenyl amine (3',5'-dichloro-4-biphenylamine or 4'-(trifluoromethyl)-[1,1'-biphenyl]-4-amine) with 1,3-dicarboxy analogue. Hence, optimisation of the LHS started by using tetrazole instead of –COOH that are shown in Scheme 4.3. Tetrazole was selected because it is often used as a carboxylic acid bioisostere[28] that not only has a similar properties in terms of pK$_a$

(often higher CLogP) compared with a carboxylic acid but also often display a higher permeability than carboxylic acids.[29] From the scheme 4.3, compound **4.14** (EC$_{50}$ 3.3 µM, 177%) and compound **4.15** (EC$_{50}$ 3.3 µM, 193%) displayed both good efficacy and EC$_{50}$, respectively but **4.16** was inactive.
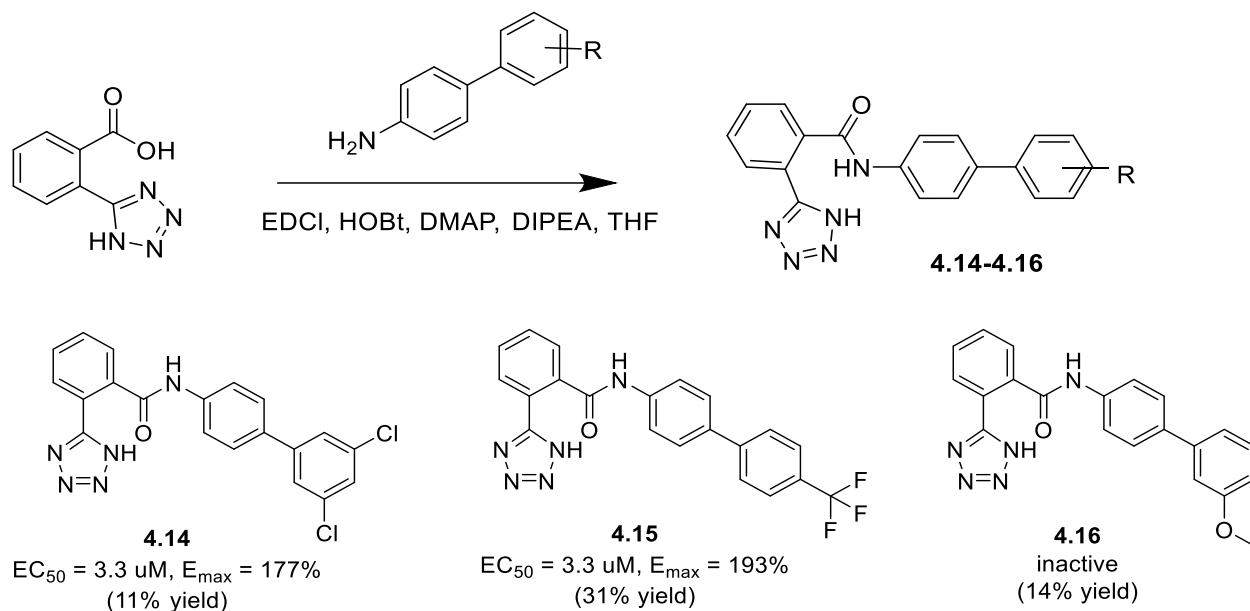
Scheme 4.3. Synthesis of tetrazole hybrid series.

Comparison of EC$_{50}$ and E$_{max}$ in the similar structure between **UOS-58757**, **4.1**, **4.2, 4.6** and hybrid series, it is found that **4.6** and **4.14** had ClogP-value higher than **UOS-58757** but **4.1**, **4.2** and **4.15** had lower values, as shown in Figure 4.11. Interestingly, **4.1**, **4.2, 4.6, 4.14** and **4.15** show better E$_{max}$ than **UOS-58757** but poor in EC$_{50}$, especially **4.15** that showed the 193% E$_{max}$ and lower ClogP than lead compound. Therefore, changing LHS from benzene ring to saturated cyclohexane, to a piperidine carboxylate with *R,S* configuration and tetrazole replacement might improve E$_{max}$ and solubility (ClogP).

UOS-58757
EC$_{50}$ = 2.1 uM, E$_{max}$ = 109%

CLogP: 4.95
pK$_a$: 3.40

4.1
(*S*-configuration)
EC$_{50}$ = 8.5 uM, E$_{max}$ = 161.7%
CLogP: 4.61
pK$_a$: 4.42

4.2
(*R*-configuration)
EC$_{50}$ = 6.9 uM, E$_{max}$ = 163.9%
CLogP: 4.61
pK$_a$: 4.42

4.6
(*rac, cis*)
EC$_{50}$ = 6.7 uM, E$_{max}$ = 167%
CLogP: 5.57
pK$_a$: 4.52

4.14
EC$_{50}$ = 3.3 uM, E$_{max}$ = 177%
(11% yield)
CLogP: 5.07
pKa: N/A

4.15
EC$_{50}$ = 3.3 uM, E$_{max}$ = 193%
(31% yield)
CLogP: 4.54
pKa: N/A
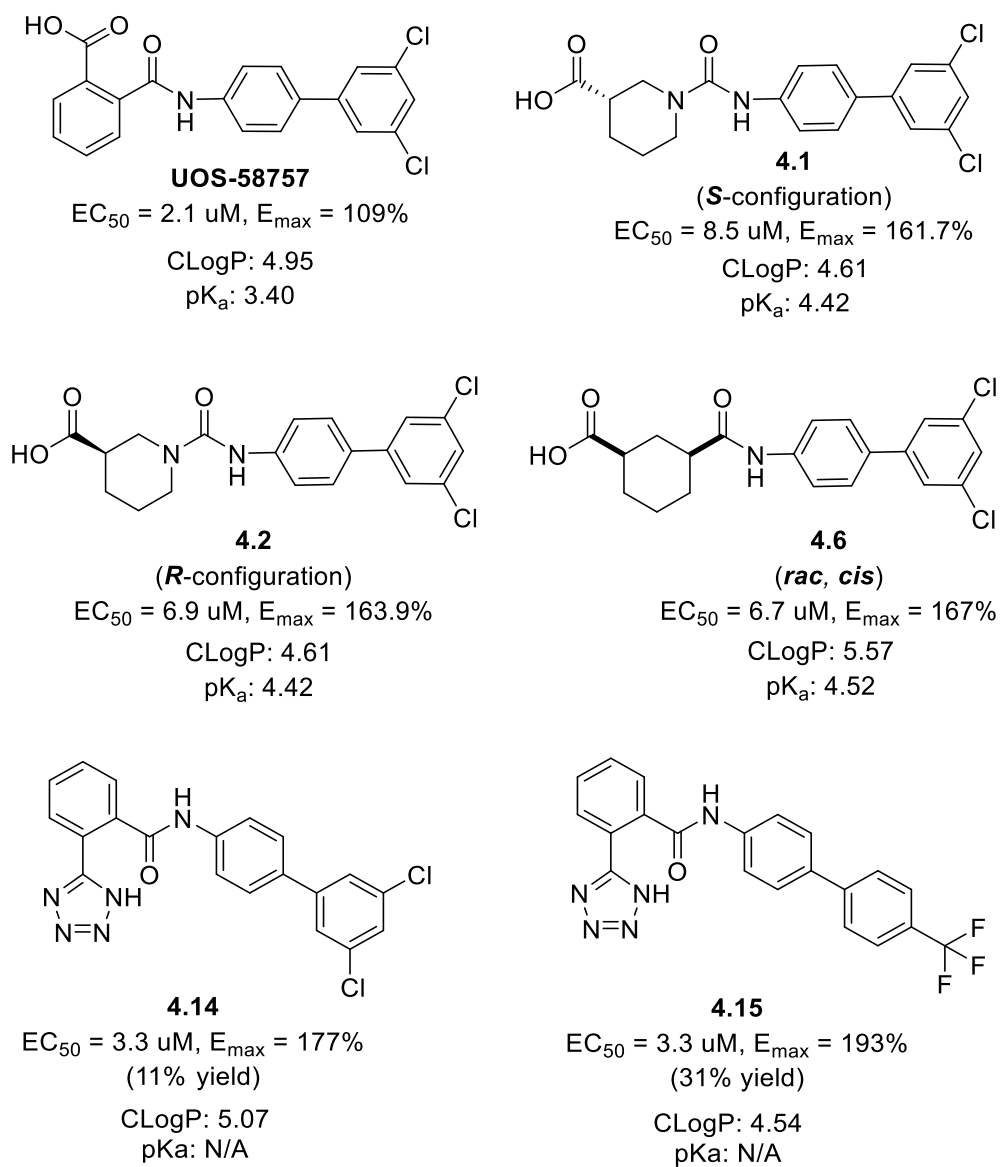
Figure 4.11. *ClogP and pK$_a$ of **UOS-58757**, **4.1**, **4.2**, **4.6** and hybrid series (ClogP and pK$_a$ are derived from ChemDraw).*

4.3.3 Modification of RHS with containing tetrazole on LHS: Trans amide Series

As previously stated, the presence of tetrazole in the left-hand side (LHS) led to high E_{max} values so changing the righthand side (RHS) from a biphenyl ring to various types of a phenyl analogues containing tetrazole in the LHS were investigated.

From the results, all compounds showed lower ClogP and E_{max} than **UOS-58757**. However, compound **4.26** had good potency (EC$_{50}$ 2.9 µM, E_{max}149%), that of a lead-like compound. The *para-* iodo substituent in compound **4.26** was advantageous, thus we scoped halogen substituents and regiochemistry in analogues.

i) HATU, Et$_3$N, DMF
or
ii) EDCl, HOBt, DMAP, DIPEA, THF

i) **4.17-4.21, 4.23-4.25**
ii) **4.22, 4.26**

4.17
inactive
(42% yield)

CLogP: 1.46
pKa: N/A

4.18
EC$_{50}$ = 4.4 uM, E_{max} = 94.5%
(10% yield)

CLogP: 2.03
pKa: N/A

4.19
EC$_{50}$ = 4.5 uM, E_{max} = 90.1%
(48% yield)

CLogP: 2.35
pKa: N/A

4.20
EC$_{50}$ = 2.3 uM, E_{max} = 86%
(31% yield)

CLogP: 3.08
pKa: N/A
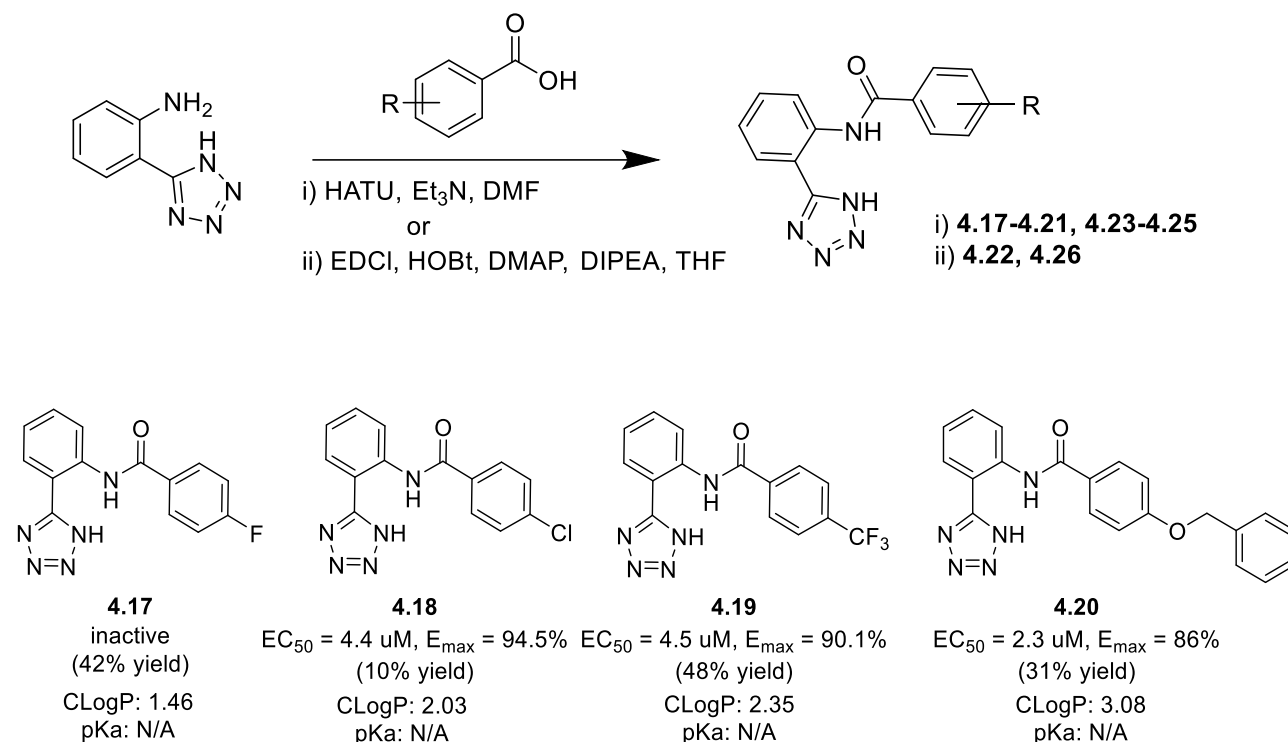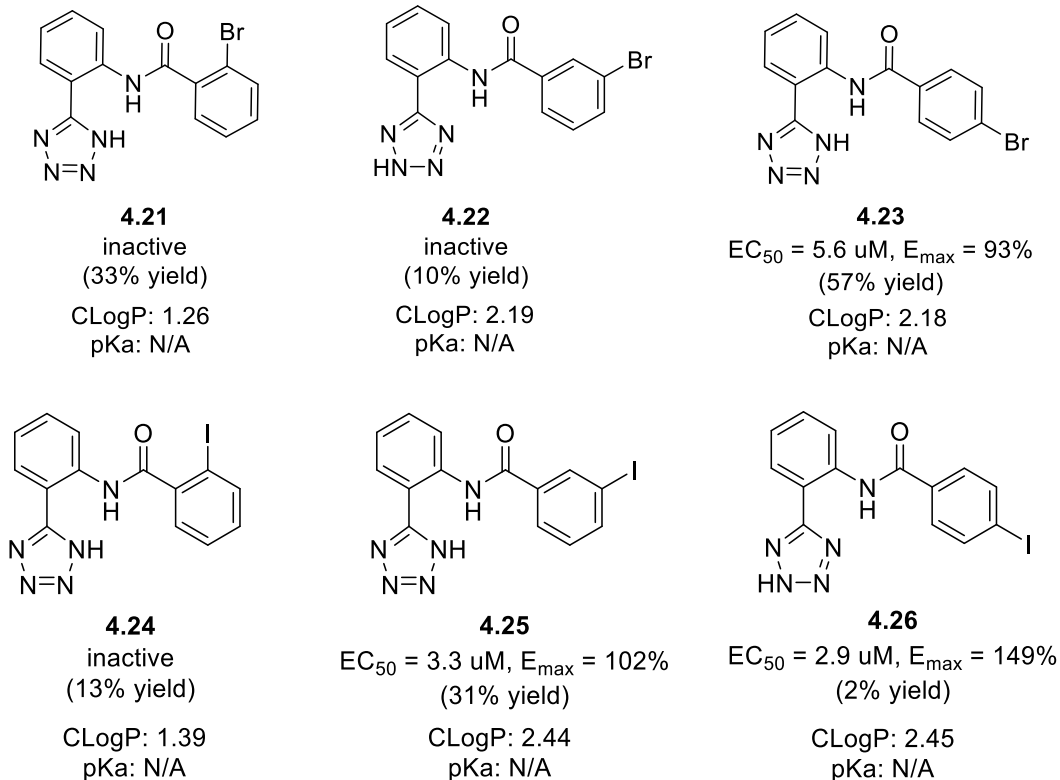
Scheme 4.4. *Synthesis of tetrazole analogues. ClogP and pKa derived from ChemDraw.*
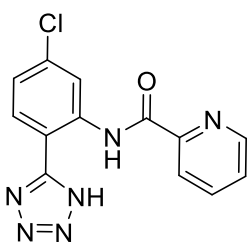
Additionally, we explored the synthesis of tetrazole derivatives by changing the RHS of the molecule together with Cl group containing in the LHS. Cl substituent is found in well-known drugs and also showed good properties in medicinal chemistry. Here, 5-chloro-2-(1*H*-tetrazol-5-yl)aniline was used instead of 2-(1*H*-tetrazol-5-yl)-phenylamine and the RHS consisted of pyridine analogues (**Scheme 4.4**). We observed a low % yield of product, and most RHS heterocyclic compounds displayed lower activity towards $K_v2.1$. For example, compounds **4.28**-**4.30** displayed lower % efficacy and higher EC_{50} values when compared with compound **4.27** (EC_{50} = 3.4 µM, E_{max} 93%). Moreover, **4.35**, with a CF_3 group in the *para-* position, was a promising lead molecule (EC_{50} = 0.89 µM, E_{max} 142%) and better compared with its *meta-* **4.34** (EC_{50} = 1.2 µM, E_{max} 125.6%) and *otho-* regioisomers **4.33** (EC_{50} = 7.9 µM, E_{max} 109.0%) respectively. Related CF_3-substituted pyridines were slightly less active and had poorer efficacy (**4.31,** EC_{50} = 4.2 µM, E_{max} 102.4%) and **4.32,** EC_{50} = 4.5 µM, E_{max} 99.3%). The *p*-methoxy analogues appeared to

show good activity in both the RHS phenyl (**4.36**) or pyridyl (**4.37**) series. Although slightly less potent, these might be useful analogues to balance pharmacodynamics (PD, e.g. selectivity, potency) and pharmacokinetic (PK, e.g. ClogP, metabolism) properties in future lead programmes.
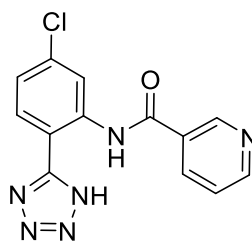

i) HATU, Et$_3$N, DMF
or
ii) EDCI, HOBt, DMAP, DIPEA, THF

i) **4.27, 4.29, 4.31-4.38**
ii) **4.28, 4.30**
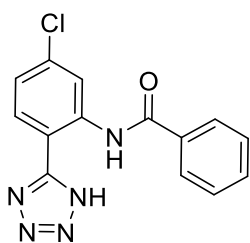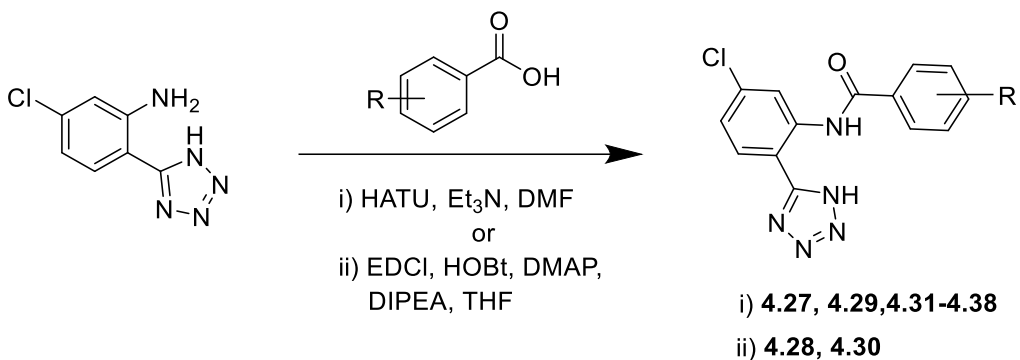
4.27*
EC$_{50}$ = 3.4 uM,
E$_{max}$ = 193%
(16% yield)

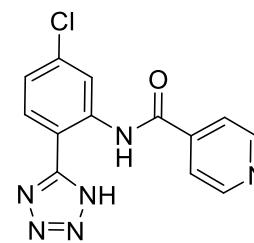CLogP: 2.08
pKa: N/A

4.28
EC$_{50}$ = 30 uM
E$_{max}$ = 30%, not active
(8% yield)
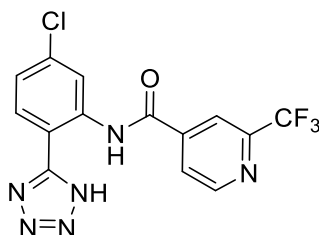
CLogP: 1.51
pKa: N/A

4.29
EC$_{50}$ = 30 uM
E$_{max}$ = 48%, not active
(7% yield)

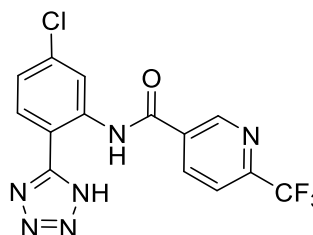CLogP: 1.16
pKa: N/A

4.30
EC$_{50}$ = 27.2 uM
E$_{max}$ = 48.1%, not active
(5% yield)
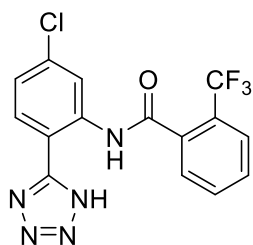
CLogP: 1.16
pKa: N/A

4.31
EC$_{50}$ = 4.2 uM, E$_{max}$ = 102.4%
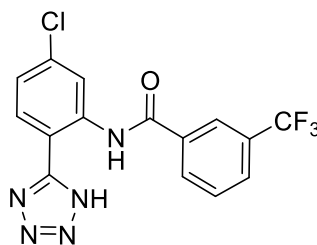(8% yield)

CLogP: 2.09
pKa: N/A

4.32
EC$_{50}$ = 4.5 uM, E$_{max}$ = 99.3%
(29% yield)

CLogP: 2.09
pKa: N/A

4.33
EC$_{50}$ = 7.9 uM, E$_{max}$ = 109.0%
(14% yield)

CLogP: 1.94
pKa: N/A

4.34
EC$_{50}$ = 1.2 uM, E$_{max}$ = 125.6%
(21% yield)

CLogP: 3.15
pKa: N/A
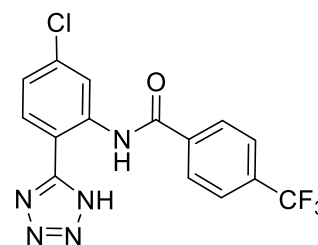
4.35*
EC$_{50}$ = 0.89 uM, E$_{max}$ = 142.0%
(19% yield)

CLogP: 3.15
pKa: N/A
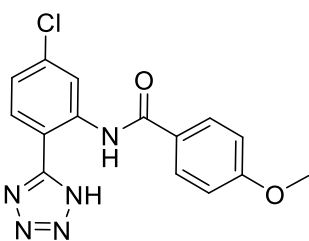
4.36
EC$_{50}$ = 1.8 uM, E$_{max}$ = 119.2%
(18% yield)

CLogP: 2.21
pKa: N/A
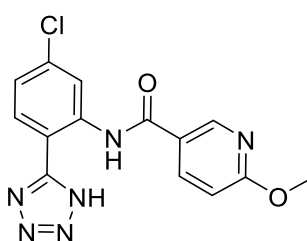
4.37
EC$_{50}$ = 3.1 uM, E$_{max}$ = 98.4%
(16% yield)

CLogP: 1.94
pKa: N/A
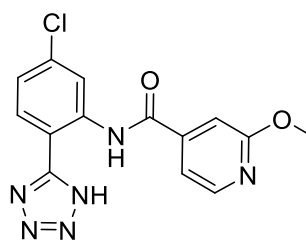
4.38
EC$_{50}$ = 6.5 uM, E$_{max}$ = 94.4%
(4% yield)

CLogP: 1.94
pKa: N/A
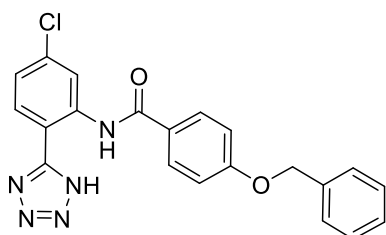
4.39
EC$_{50}$ = 2.1 uM, E$_{max}$ = 89.3%
(5% yield)

CLogP: 3.97
pKa: N/A
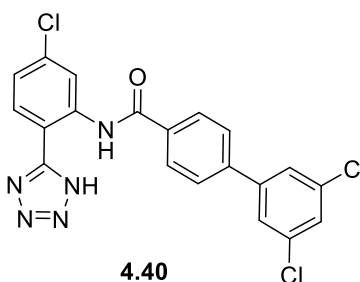
4.40
Inactive
(40% yield)

CLogP: 5.42
pKa: N/A
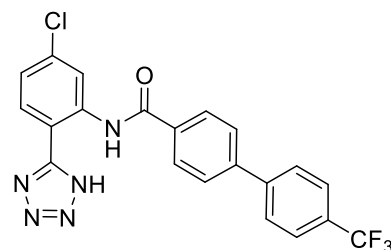
4.41
EC$_{50}$ = 2.9 uM, E$_{max}$ = 94.0%
(28% yield)

CLogP: 4.88
pKa: N/A

Scheme 4.5. Synthesis of a library of tetrazole analogues. *Synthesised by Dr.Andrew McGown, Research Fellow, University of Sussex. ClogP and pKa derived from ChemDraw.
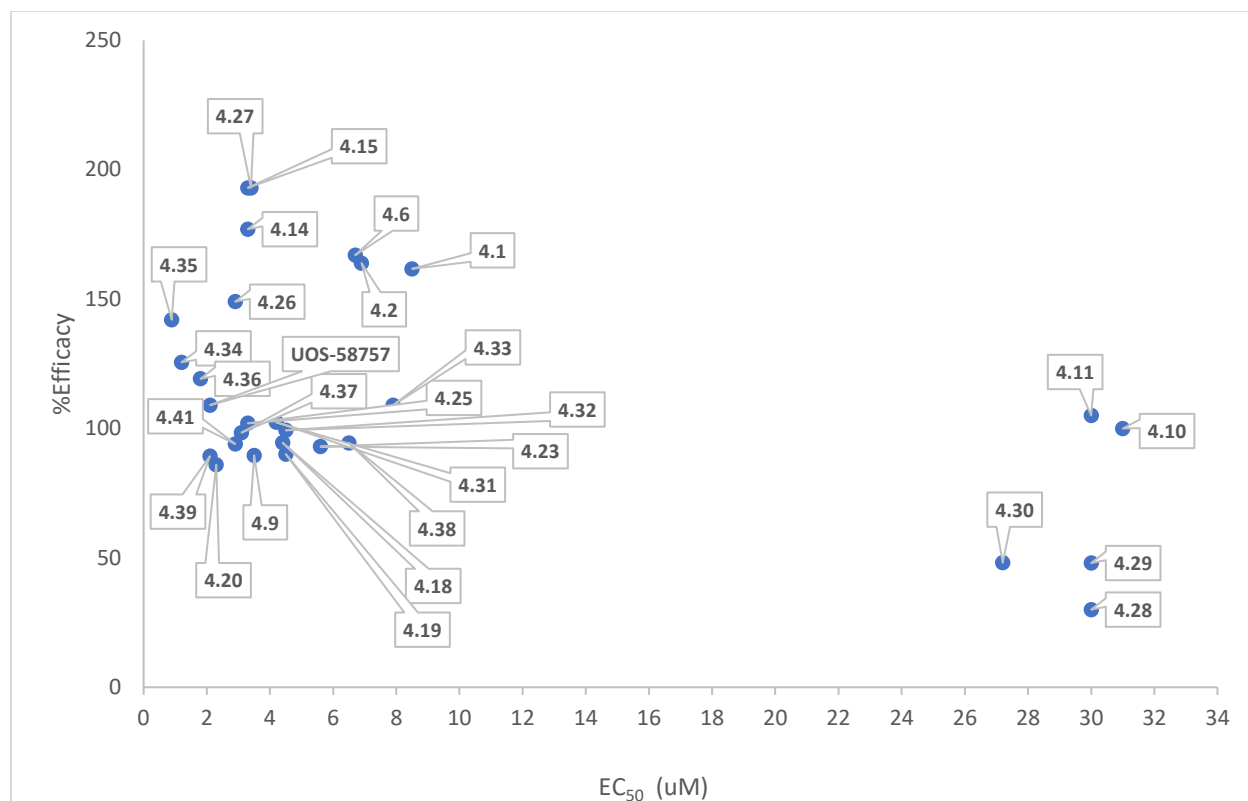
Figure 4.12. *The %efficacy and EC$_{50}$ of active compounds.*

The %efficacy and EC$_{50}$ of all active compounds and **UOS-58757** are plotted as shown in Figure 4.12, the position in upper left-hand side show a good performance because high % efficacy and low EC$_{50}$. Our goals are EC$_{50}$ < 1 µM, high % efficacy and high solubility hence, compounds **4.34**, **4.35**, **4.36** are good in both EC$_{50}$ and high % efficacy. However, the interesting compounds **4.1**, **4.2**, **4.6**, **4.14**, **4.15**, **4.26** and **4.27** show high % efficacy (>140%) but poor EC$_{50}$. Therefore, compounds **4.1**, **4.2** and **4.35** were selected for further study in terms of permeability and solubility.

4.4 Permeability, Solubility and Microsomal stability of selected compounds

Permeability and solubility studies of selected compounds (lead compounds **UOS-58757**, **4.1**, **4.35**) were performed by Pharmidex (which is a contract research organisation, CRO), UK. Apparent permeability (P_{app}) was determined by monolayer efflux as presented in Table 4.1. The P_{app} data is defined in the range:

low permeability $P_{app} < 2 \times 10^{-6}$ cm/s

medium permeability 2×10^{-6} cm/s $< P_{app} < 20 \times 10^{-6}$ cm/s

high permeability $P_{app} > 20 \times 10^{-6}$ cm/s

It was found that **UOS-58757**, **4.1**, **4.35** showed poorer P_{app} than labetolol, which is the internal standard. However, **4.1**, **4.35** had higher P_{app} than lead compound **UOS-58757**.

Table 4.2 showed the solubility investigation of compound **4.1** (0.036 mg/ mL), **4.2** (0.042 mg/ mL) and **4.35** (0.143 mg/ mL), with pimozide (0.002 mg/ mL) and propranolol (0.891 mg/ mL) as a low and a high aqueous solubility control, respectively. Moderate solubility was found for compound **4.35** followed by low solubility for **4.2** and **4.1**. Interestingly, the solubility of compounds **4.1** and **4.2**, which are enantiomers, was different, as shown in Table 4.2.

Although the ideal purpose of research is to improve the efficacy, permeability and solubility of lead compounds but in the experiment, it was found that all selected compounds presented low permeability and solubility in addition to high efflux. All selected compounds were deemed to be substrates of P-glycoprotein (PGP).

Table 4.1. *Permeability of selected compounds.*
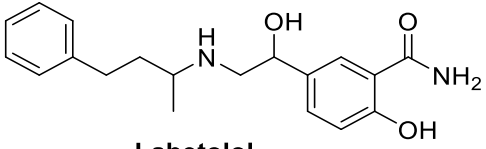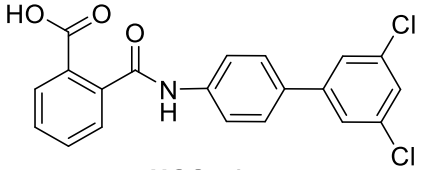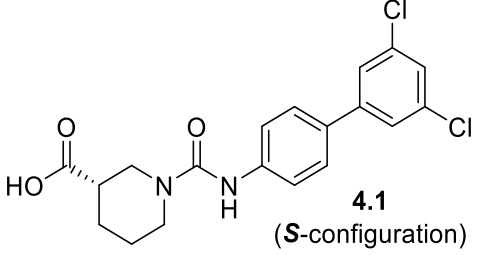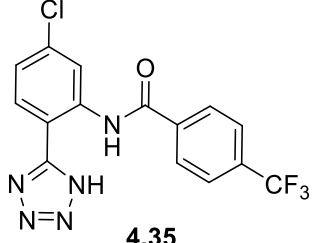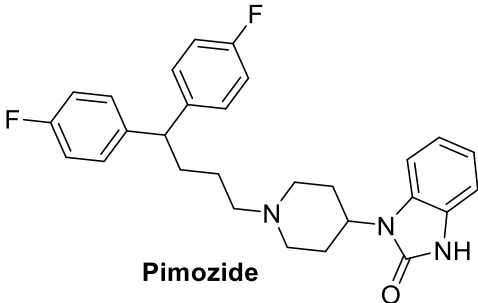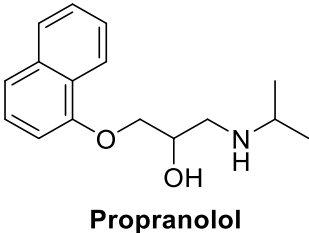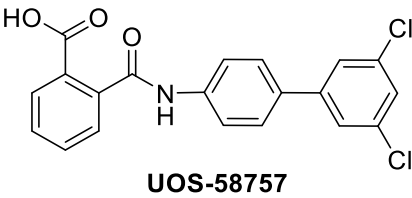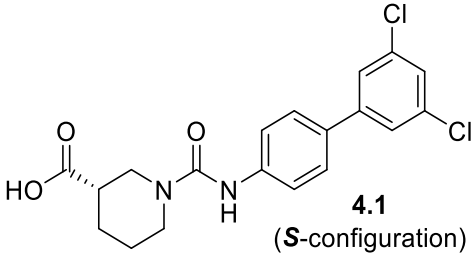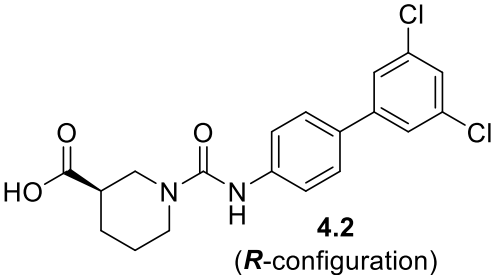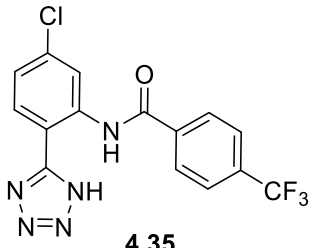
Compound	P_{app} (cm/sec, x10^{-6})	Permeability	Efflux Ratio B-A/A-B	PGP Substrate
Labetolol	2.1	Medium	7.2	Substrate
UOS-58757	0.36	Low	10.7	Substrate
4.1 (*S*-configuration)	1.5	Low	8.4	Substrate
4.35	0.8	Low	29.8	Substrate
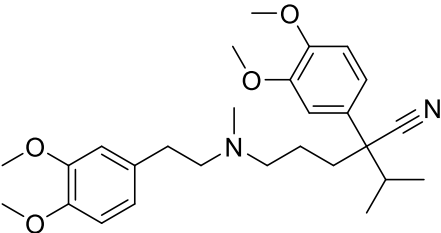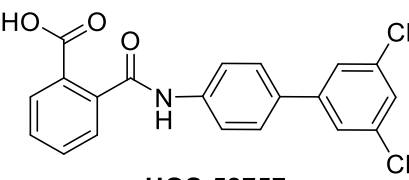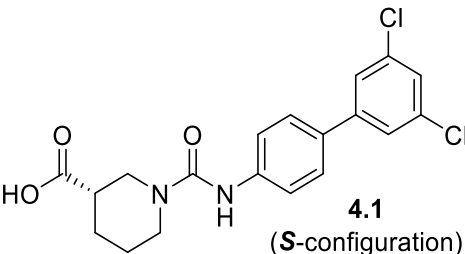
Table 4.2. *Solubility of selected compounds.*
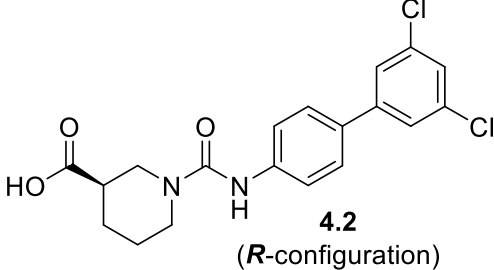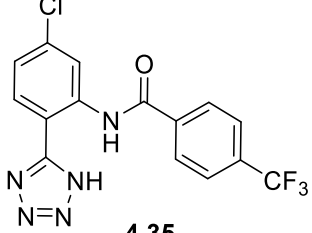
Compound	Solubility (mg/ mL)*
Pimozide	0.002 (Low)
Propranolol	0.891 (High)
UOS-58757	0.022 (Low)
4.1 (*S*-configuration)	0.036 (Low)
4.2 (*R*-configuration)	0.042 (Low)

Compound	Solubility (mg/ mL)*
4.35 | 0.143
(Medium) |

* Results are reported as Low (less than 0.1 mg/ml), Medium (0.1 – 0.5 mg/ml) and High (>0.5 mg/ml).

Table 4.3. *Microsomal stability of selected compounds.*

Compound	Metabolic stability in liver microsomes			
	Human		Rat	
	$t_{1/2}$ (min)	CL_{int} (μL/min/mg)	$t_{1/2}$ (min)	CL_{int} (μL/min/mg
Verapamil	11.37	121.92	8.01	172.97
UOS-58757	1037.93	1.34	509.69	2.72
4.1
(*S*-configuration) | 372.24 | 3.72 | 677.82 | 2.04 |

Compound	Metabolic stability in liver microsomes			
	Human		Rat	
	$t_{1/2}$ (min)	CL_{int} (µL/min/mg)	$t_{1/2}$ (min)	CL_{int} (µL/min/mg
4.2 (**R**-configuration)	ND	ND	ND	ND
4.35	317.69	4.36	476.21	2.91

- ND is not determined

Additionally, some potent selected compounds were further evaluated for microsomal stability in human and rat liver (Table 4.3). Compounds **4.1** and **4.35** showed high microsomal stability in both human and rat when compared with verapamil (reference standard). Notably, compound **4.1** showed the highest microsomal stability in rat. In contrast, the intrinsic clearance (CL_{int}) is the volume of drug per unit of time when it passes through, in this research, liver. It was found that, compound **4.1** and **4.35** had low CL_{int} while compared with verapamil.

4.5 Pharmacokinetics, bioavailability drug-likeness and drug likeness prediction of ligands

The SwissADME program[30] was used to predict pharmacokinetics, bioavailability drug-likeness of active compounds, from below, (Table 4.4). *In vivo* absorption, distribution, metabolism and excretion (ADME) properties were predicted with the graphical classification model Egan BOILED-Egg (Figure. 4.12).

Table 4.4. *Physicochemical Properties and lipophilicity.*

compound	MW (g/mol)	nRB*	nHBA*	nHBD*	TPSA* (A^2)	WLogP*
4.1	393.26	5	3	2	69.6	4.4
4.6	392.28	5	3	2	66.4	5.3
4.9	391.38	6	6	2	66.4	6.2
4.14	410.26	5	4	2	83.6	4.9
4.15	409.36	6	7	2	83.6	5.8
4.18	299.72	4	4	2	83.6	2.6
4.19	333.27	5	7	2	83.6	4.1
4.20	371.39	7	5	2	92.8	3.4
4.23	344.17	4	4	2	83.6	2.7
4.25	391.17	4	4	2	83.6	2.5
4.26	391.17	4	4	2	83.6	2.5
4.31	368.7	5	8	2	96.4	4.1
4.32	368.7	5	8	2	96.4	4.1
4.33	367.71	5	7	2	83.6	4.7
4.34	367.71	5	7	2	83.6	4.7
4.35	367.71	5	7	2	83.6	4.7
4.36	329.74	5	5	2	92.8	2.6
4.37	330.73	5	6	2	105.7	2.0

compound	MW (g/mol)	nRB*	nHBA*	nHBD*	TPSA* (A^2)	WLogP*
4.38	330.73	5	6	2	105.7	2.0
4.39	405.84	7	5	2	92.8	4.0
4.40	444.70	5	4	2	83.6	5.6
4.41	443.81	6	7	2	83.6	6.4
morphine	285.34	0	4	2	52.93	0.82

*nRB number of rotational bond, nHBA number of hydrogen bond acceptors, nHBD hydrogen bond donors, TPSA topological polar surface area, WLogP octanol/water partition coefficient.

Lipinski's 'rule of five' predicts good passive oral availability for a drug that has: no more than 5 hydrogen bond donors, no more than 10 hydrogen bond acceptors, molecular mass less than 500 daltons, a partition coefficient log P-value less than 5.[31,32] The partition coefficient indicates the partition of a solute (or drug) between two liquids (most commoly, octanol and water). Hydrophobic drugs show a high octanol-water partition coefficient, which means drugs distribute to a hydrophobic area such as a lipid bilayer of cells. On the contrary, hydrophillc drugs have a low octanol-water partition co-efficient which means they distribute to a hydrophilic area such as blood. Generally, drugs, have a logP up to around 2.5, and can be both reasonable water soluble and cell permeable. Veber rules add further parameters with no more than 10 rotatable bonds required for good oral bioavailability.[32] All of our compounds fell in the range of Lipinski's 'rule of five' except **4.6**, **4.9**, **4.40** and **4.41**, with Clog P-values more than 5.
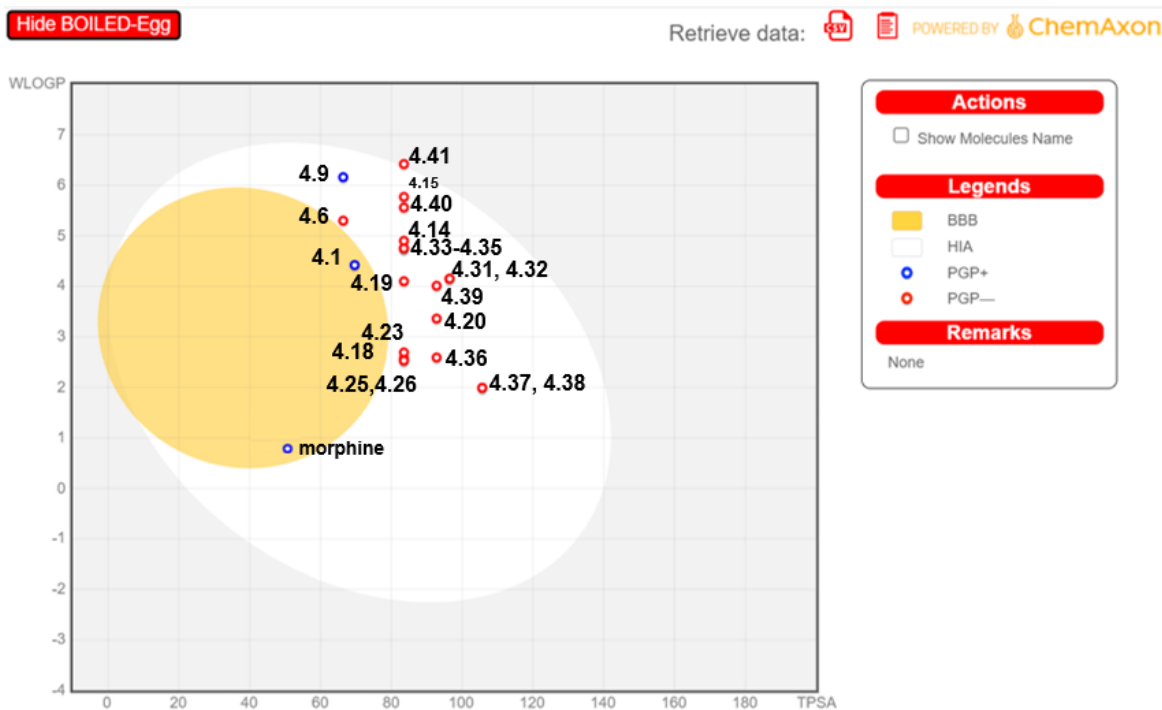
Figure 4.13. *Predicted BOILED-Egg diagram of the active compounds from SwissADME web tool.*[30,33–35]

We studied compounds in Egan BOILED-Egg, which was plotted to predict human intestinal absorption (HIA), blood-brain barrier (BBB) access and compounds were predicted to be substrates of P-glycoprotein (PGP) (Figure 4.13). The egg plot composes of 3 parts: a grey region (no HIA or BBB acess), a white area (HIA) and a yellow (yolk) (BBB access)[36]. It was found that most of them fall in the red dot (represented as PGP−) indicating molecules are predicted as non-substrates of PGP in the central nervous system (CNS) efflux transporter which were in the egg white that means well-absorbed and no BBB access. Interestingly, there were 2 compounds (**4.1** and **4.9**) in the blue points (represented as PGP+) that describe molecules predicted as actively substrates effluxed of PGP from the CNS. Additionally, compound **4.1** and morphine (well-known drug) were in the egg york that predicted BBB permeability while the another compound **4.9** was in the egg white region that was no BBB access. Therefore, most of our synthetic substances showed good prediction for drug in the future.

4.6 Conclusions

We have synthesised a series of cyclohexane carboxylic acid, piperidine carboxylate and tetrazoles as potential $K_v2.1$ acting ligands. The results demonstrate that tetrazole analogues exhibit good activity in biological assays. However, compounds with an EC_{50} lower than 1 µM, high %efficacy and good solubility are needed. RHS Pyridine analogues generally showed lower efficicacy whereas Cl-substituted LHS analogues containing a tetrazole group exhibited good activity in $K_v2.1$ channels. Furthermore, the ideal purpose of research is to improve the efficacy, permeability and solubility of lead compounds but in the experiment, it was found that all selected compounds presented low permeability and solubility and high metabolic stability ($t_{1/2}$) but were poor in terms of CL_{int}. Therefore, the development of improved drug candidates for $K_v2.1$ channel is needed to improve for further studies.

4.7. Experimental

General Experimental

Solvents, reagents, and consumables were purchased from commercial suppliers and solvents and reagents were used without purification. ^1H, ^{13}C and ^{19}F NMR spectroscopy was performed on a Varian 400 or 600 MHz spectrometer and chemical shifts are reported in ppm. LCMS measurements were performed on a Shimadzu LCMS-2020 equipped with a Gemini® 5 µm C18 110 Å column and percentage purity measurements were run over 30 minutes in water/acetonitrile with 0.1% formic acid (5 min at 5%, 5–95% over 20 min, 5 min at 95%) with the UV detector set at 254 nm. High-Resolution Accurate Mass Spectrometry measurements were taken using a Waters Xevo G2 Q-ToF HRMS (Wilmslow, Cheshire, UK), equipped with an ESI source and MassLynx software. Experimental parameters were: (1)—ESI source: capillary voltage 3.0 kV, sampling cone 35 au, extraction cone 4 au, source temperature 120 °C and desolvation gas 450 °C with a desolvation gas flow of 650 L/h and no cone gas; (2)—MS conditions: MS in resolution mode between 100 and 1500 Da. Additionally, a Waters (Wilmslow, Cheshire, UK)

Acquity H-Class UHPLC chromatography pumping system with column oven was used, connected to a Waters Synapt G2 HDMS high-resolution mass spectrometer.

Monowave is a conventionally heated synthesis reactor that faster than traditionally stirrer hot-plate setups. Monowave was performed on a Monowave50 Anton Paar, maximum operation pressure 20 bar (290 psi), maximum temperature 250ºC, maximum power 315 W and maximum volume 6 mL.

4.7.1 Chiral purity analysis

This was carried out at Reach Separations, UK (https://reachseparations.com/). Method: sample was dissolved to ~1 mg/mL in EtOH and was then analysed by SFC. The conditions are described in the table below.

Column Details	Lux C2 (4.6mm x 250mm, 5um)
Column Temperature	40 °C
Flow Rate	3 mL/min
Detector Wavelength	210-400nm
Injection Volume	1.0 uL
BPR	125 BarG
Isocratic Conditions	40:60 EtOH:CO2 (0.2% v/v NH3)

4.7.2 Thallium Flux Assay

This, and the other bioassays, were carried out at the Sussex Drug Discovery Centre (SDDC), University of Sussex in the Biology Division by Claire Adcock, Hedaythul Choudhury, Jessica Booth and Luke Young.

HEK293 cells constitutively expressing $K_v2.1$ were maintained in 1X DMEM (Dulbeco's Modified Eagle Medium) F12 HAM (Invitrogen, 31331-028), 10% FBS - tetracycline free (Invitrogen, 10108-157), 0.1 mg/ml Hygromycin-B 0.1mg/ml (Invitrogen, 10687-010), 200 mM L-Glutamine (Invitrogen R210-01) and 1% Penicillin-Streptomycin (10,000 U/ml) [Invitrogen 15140122] in a 5% CO_2 incubator at 37ºC.

On reaching 70-80% confluence the HEK293 $K_v2.1$ cells were seeded at 40,000 cells per 100 µl into each well of a black 96 well clear-bottom poly-d-lysine coated (0.1 mg/ml) plate (Corning 3603) and incubated overnight at 37 ºC to form a complete monolayer over the well surface.

The thallium assay was performed according to the FluxOR™ II Green Potassium Ion Channel Assay protocol (ThermoFisher, F20017). Briefly, dye-loading buffer was prepared by diluting FluxOR™ II Green Reagent (1000X), Powerload (100X), Probenecid (100X) and FluxOR™ II Assay Buffer (10X) in distilled H_2O to 1X. The 96 well assay plate (containing HEK $K_v2.1$ cells) was removed from the incubator and cell culture media discarded. Dye-loading buffer (80 µl) was added to all wells and incubated (covered and in the dark) for 75 minutes. The neat stock compounds (10 mM) were then diluted in 100% DMSO to provide an 8-point, 1 in 3 serial dilution (10 mM to 1 µM). A stimulation plate was then prepared by diluting the following reagents in distilled water; the compounds above 1:66.6 to (5X, 150 µM to 15 nM), Chloride free stimulus buffer (5X), Potassium Sulfate 75mM (5X) and Thallium Sulfate 10 mM (5X). Next, background suppressor buffer was prepared by diluting FluxOR™ II Background Suppressor (10X), Probenecid (100X) and FluxOR™ II Assay Buffer (10X) in distilled H_2O to 1X. Control compound A769662 (10 mM) was diluted in the stimulation plate to 150 µM (5X) and DMSO (100%) to 1.5% (5X) for control wells.

After 75 minutes' incubation, the loading buffer was removed from the cell assay plate and background suppressor buffer (80 µl) was added to all wells. The cell assay plate and stimulation plate were added to the Flexstation. The Flexstation took 20 µl from the stimulation plate and added it to 80 µl of suppression buffer in the assay plate (1 in 5 dilution). This resulted in final assay concentrations of positive control compound A769662 (30 µM), negative control DMSO only (0.3%) and 8-point 1 in 3 compound dose-responses (from 30 µM to 3 nM).

Data Analysis

The Flexstation reads fluorescence every 3 seconds up to 60 seconds at excitation: 485 nm and emission: 525 nm. A Max-Min value was calculated by taking the difference between the fluorescence at 50 seconds (after addition of the compounds) and the baseline fluorescence at 15 seconds (before addition of the compounds).

Flexstation was used to measure fluorescence in DMSO only (negative control) and A7769662 (positive control) wells. The data were normalized to the response of reference compound A769662 @30µM. The following equation was used to normalise the raw data values:

% Activation = ((RD-negative control)/(positive control-negative control))*100

RD = Raw data value for test compounds

Prism software (GraphPad Software, USA) was used to calculate EC$_{50}$ by applying 4-parameter logistic fits to the dose-response data.

4.7.3 Permeability Method

This was carried out at Pharmidex, UK (https://www.pharmidex.com/) under an MTA and on "blinded samples" (no structures revealed).

All compounds were dissolved in DMSO to provide a 10 mM stock solution from which donor (dose) solutions were prepared in DMEM to give a final drug concentration of 10 µM. All dose solutions contained 10 µM propranolol as an internal standard. hMDR1-MDCK (multidrug resistance mutation 1-Madin-Darby canine kidney cells) seeded filters were exposed to a fixed volume of the donor solution containing the compound of interest and its ability to traverse the monolayer and appear in the receiver compartment measured over a 30 minutes period at 37 °C. Bidirectional permeability measurements were derived by examining the transfer of compound in both the apical to basolateral compartment, and vice versa. Sample analysis was conducted using UHPLC-T of MS or UPLC-MSMS. Labetolol was assayed as positive control for PGP activity. Results are reported as

low permeability (e.g. sucrose, mannitol, atenolol etc.)   Papp < 2×10^{-6} cm/s

medium permeability 2×10^{-6} cm/s < Papp < 20×10^{-6} cm/s

high permeability (e.g. propranolol, diazepam etc.)   Papp > 20×10^{-6} cm/s

4.7.4 Solubility Method

This was carried out at Pharmidex, UK.

All compounds were measured at 1 µM and equilibrated in phosphate buffer saline (PBS) pH 7.4. Solubility was measured at 25 °C. The test solutions are allowed to equilibrate for 24 h. Centrifugation at 15,000 rpm for 10 minutes. A 100 µL sample of the supernatant is carefully collected and the sample quantified using the analytical method. The standard curve for each compound was prepared in 100% acetonitrile. Soluble amount is determined by LC-MS/MS. Results are reported as low (less than 0.1 mg/ml), medium (0.1 – 0.5 mg/ml) and high (>0.5 mg/ml).

4.7.5 Synthesis of compounds

Compounds were synthesised and characterised on the basis of ^{1}H NMR, ^{13}C NMR and mass spectrometry. Intermediates were taken through crude, hence, only ^{1}H NMR spectra were recorded. The % efficacy and EC$_{50}$ measurements on synthesised compounds were performed by SDDC biologists, University of Sussex, as acknowledged above. In many cases, we were unable to observe a M$^+$ or M$^-$ so we have no LC-MS data/ purity for a number of tetrazole products e.g. **4.18** – **4.20**, **4.22**, **4.23**, **4.30** – **4.40**. Moreover, for NMR spectra, $^1J_{CF}$ or $^2J_{CF}$ couplings were not always visible, e.g. no $^1J_{CF}$ for **4.35** and no $^2J_{CF}$ for **4.10** and a proton peak due to the N**H** is missing in tetrazole derivatives, e.g. **4.15**, **4.17** – **4.41**.

4.7.5.1 Modification of LHS by using cyclohexane instead of phenyl ring
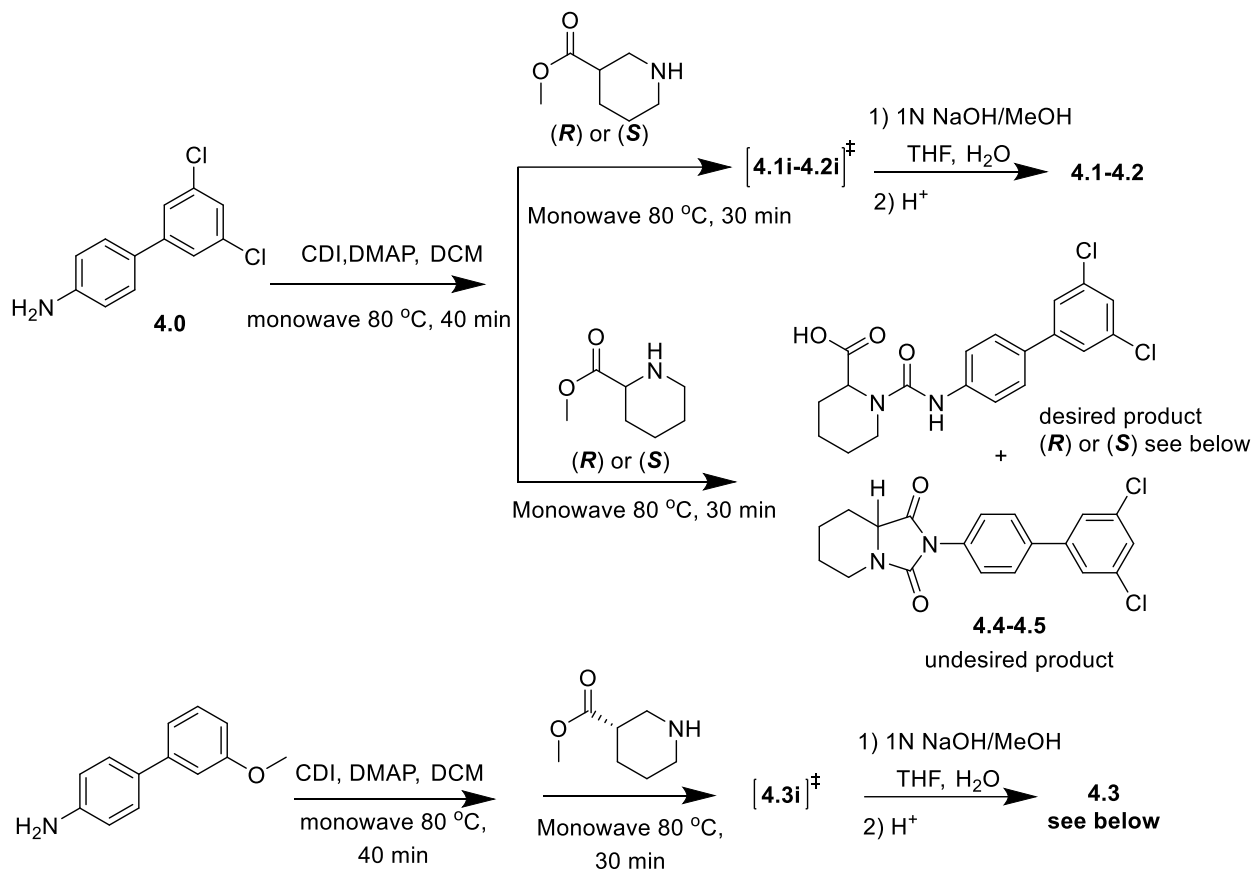
(S)-Methyl 1-((3',5'-dichloro-[1,1'-biphenyl]-4-yl)carbamoyl)piperidine-3-carboxylate (4.1i)
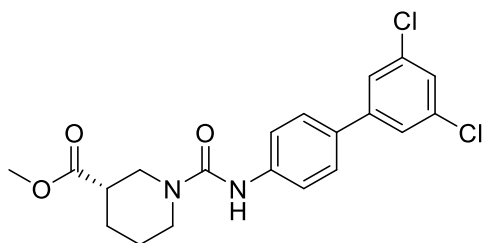
A solution of 3',5'-dichloro-[1,1'-biphenyl]-4-amine (200 mg, 0.84 mmol), 4-dimethylaminopyridine (DMAP) (410.5 mg, 3.36 mmol), carbonyldiimidazole (CDI) (149.8 mg, 0.92 mmol) in dichloromethane (DCM) 4.5 mL. The solution was stirred at 80 °C for 40 min under Monowave irradiation then (S)-methylpiperidine-3-carboxylate
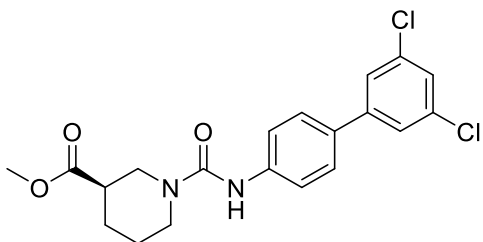
hydrochloride, CAS: 164323-84-6 (301.8 mg, 1.68 mmol) was also added to the reaction mixture. After that, the mixture was stirred at 80 °C for 30 min under Monowave irradiation. The mixture was allowed to cool to room temperature and saturated sodium bicarbonate solution (25 mL) was added to the reaction mixture. The aqueous phase was extracted with dichloromethane (25 mL×3), The organic phases were combined, washed with brine, dried over anhydrous Na_2SO_4 and concentrated. The residue was purified by chromatography on silica using a gradient of hexane: diethyl ether (0 - 70%), thus the final product was obtained as a colourless solid; yield: 80.9 mg (22%).

^{1}H NMR (600 MHz, CDCl$_3$) δ 7.48 – 7.44 (m, 3H), 7.42 (s, 2H), 7.39 (s, 1H), 7.27 (s, 1H), 3.81 (m, 2H), 3.76 (s, 3H), 3.59 (d, J = 14.2 Hz, 1H), 3.23 (t, J = 10.6 Hz, 1H), 2.68 (s, 1H), 2.13 – 2.07 (m, 1H), 1.97 – 1.90 (m, 1H), 1.62 – 1.53 (m, 2H). (NH invisible)

LCMS (MDAP): tR = 25.81 min, 93%; m/z (ESI+) 407.0 [M + H]$^+$, 428.9 [M + Na]$^+$.

Chemical formula: $C_{20}H_{20}Cl_2N_2O_3$

(*R*)-Methyl 1-((3',5'-dichloro-[1,1'-biphenyl]-4-yl)carbamoyl)piperidine-3-carboxylate (4.2i)
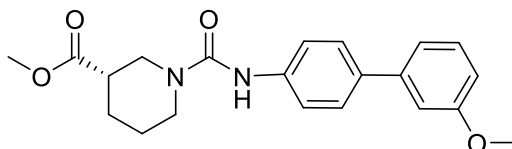

This was synthesised on a 0.84 mmol scale 3',5'-dichloro-[1,1'-biphenyl]-4-amine by the same procedure as **4.1i** although (*R*)-methylpiperidine-3-carboxylate hydrochloride, CAS: 1255651-12-7 (301.8 mg, 1.68 mmol) was used instead of (*S*)-methylpiperidine-3-carboxylate hydrochloride. The final product was obtained as a colourless solid; yield: 79 mg (20%).

¹H NMR (600 MHz, CDCl₃) δ 7.47 (aps, 1H), 7.43 (aps, 4H), 7.39 (aps, 2H), 3.74 (m, 4H), 3.68 (dd, J = 12.2, 5.7 Hz, 1H), 3.63 (d, J = 14.1 Hz, 1H), 3.27 (t, J = 9.0 Hz, 1H), 2.65 (s, 1H), 2.08 – 2.04 (m, 1H), 1.92 (t, 1H), 1.58 (s, 2H). (NH invisible)

LCMS (MDAP): tR = 25.85 min, 88%; m/z (ESI⁺) 407.0 [M + H]⁺, 429.0 [M + Na]⁺.

Chemical formula: $C_{20}H_{20}Cl_2N_2O_3$

(*S*)-methyl 1-((3'-methoxy-[1,1'-biphenyl]-4-yl)carbamoyl)piperidine-3-carboxylate (4.3i)

This was synthesised on a 0.50 mmol scale 3'-methoxy-[1,1'-biphenyl]-4-amine by the same procedure as **4.1i** that was used instead of 3',5'-dichloro-[1,1'-biphenyl]-4-amine. The final product was obtained as a colourless solid; yield: 55.3 mg (24%).

¹H NMR (600 MHz, CDCl₃) δ 7.52 (d, J = 8.8 Hz, 2H), 7.42 (d, J = 8.8 Hz, 2H), 7.31 (d, J = 7.6 Hz, 2H), 7.15 (d, J = 7.6 Hz, 1H), 7.09 (brs, 1H), 6.87 – 6.83 (m, 1H), 3.85 (m, 3H), 3.75 (m, 4H), 3.70 (m, 1H), 3.65 (m, 1H), 3.34 – 3.26 (m, 1H), 2.67 (p, J = 5.7 Hz, 1H), 2.06 (m, 1H), 1.94 (m, 1H), 1.60 (m, 2H).

LCMS (MDAP): tR = 21.52 min, 81%; m/z (ESI+) 368.8 [M + H]⁺, 390.9 [M + Na]⁺

Chemical formula: $C_{21}H_{24}N_2O_4$

(*S*)-1-((3',5'-Dichloro-[1,1'-biphenyl]-4-yl)carbamoyl)piperidine-3-carboxylic acid (4.1)
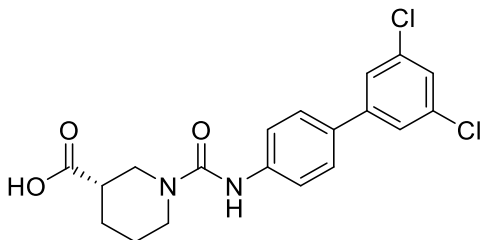
To a stirred solution of (*S*)-methyl-1-((3',5'-dichloro-[1,1'-biphenyl]-4-yl)carbamoyl) piperidine-3-carboxylate (79.2 mg, 0.19 mmol) in THF (2.0 mL) and water (3.0 mL) was added 1 N NaOH in methanol (MeOH) (0.29 mmol, 2.9 mL). This was vigorously stirred at room temperature overnight. The solution was diluted with water (20.0 mL) and 2 M hydrochloric acid (10.0 mL) was added. The aqueous phase was extracted with dichloromethane (25.0 mL×3), the organic phases were combined, washed with brine, dried over anhydrous Na_2SO_4 and concentrated. The residue was purified by chromatography on silica using a gradient of hexane: ethyl acetate (EtOAc) (30 - 100%), the final product was obtained as a colourless solid; yield: 20.3 mg (26%).

^{1}H NMR (600 MHz, DMSO-*d*6) δ 8.73 (brs, 1H), 7.63 (d, *J* = 8.7 Hz, 2H), 7.56 (d, *J* = 8.7 Hz, 2H), 7.50 (s, 1H), 4.14 – 4.08 (m, 1H), 3.93 – 3.87 (m, 1H), 3.00 (dd, *J* = 13.4, 10.1 Hz, 1H), 2.95 – 2.87 (m, 1H), 2.41 – 2.34 (m, 1H), 1.98 – 1.93 (m, 1H), 1.68 – 1.62 (m, 1H), 1.62 – 1.52 (m, 1H), 1.46 – 1.37 (m, 1H). (OH invisible)

^{13}C NMR (151 MHz, DMSO-*d*6) δ 175.2, 155.0, 143.9, 142.0, 135.0, 130.3, 127.4, 126.4, 125.0, 120.0, 46.3, 44.6, 41.3, 27.5, 24.6.

HR-MS-ESI (m/z) Calculated for $C_{19}H_{19}N_2O_3Cl_2$ [M + H]$^+$: 393.0773, found: 393.0768.

LCMS (MDAP): tR =23.59 min, 98%; m/z (ESI$^+$) 392.9 [M + H]$^+$, 414.9 [M + Na]$^+$.

(*R*)-1-((3',5'-Dichloro-[1,1'-biphenyl]-4-yl)carbamoyl)piperidine-3-carboxylic acid (4.2)
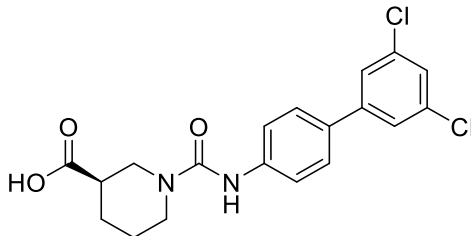
This was synthesised on a 0.19 mmol scale from (*R*)-methyl-1-((3',5'-dichloro-[1,1'-biphenyl]-4-yl)carbamoyl)piperidine-3-carboxylate by the same procedure as **4.1.** The final product was obtained as a colourless solid; yield: 40.0 mg (49%).

FT-IR (cm^{-1}): 3327 (N-H stretch), 2946 (N-H stretch), 2946 (N-H strech), 1733 (C=O), 1587 cm^{-1} (C=C, arom.), 1505 (C=C, arom.), 1398 (C=C, arom.), 815 (*m*-Disub), 794 (*m*-Disub) 680 (*m*-Disub)

m.p. 227.5-228 °C

^{1}H NMR (600 MHz, DMSO-*d*$_6$) δ 12.42 (brs, 1H), 8.70 (brs, 1H), 7.68 (s, 2H), 7.63 (d, *J* = 8.4 Hz, 2H), 7.55 (d, *J* = 8.4 Hz, 2H), 7.49 (s, 1H), 4.12 (d, *J* = 13.4 Hz, 1H), 3.91 (d, *J* = 13.4 Hz, 1H), 2.98 (t, *J* = 12.1 Hz, 1H), 2.89 (t, *J* = 12.1 Hz, 1H), 2.40 – 2.33 (m, 1H), 1.95 (d, *J* = 12.5 Hz, 1H), 1.65 (d, *J* = 14.9 Hz, 1H), 1.55 (q, *J* = 12.5 Hz, 1H), 1.40 (q, *J* = 12.5 Hz, 1H).

^{13}C NMR (151 MHz, DMSO-*d*$_6$) δ 175.1, 155.0, 143.9, 142.0, 135.0, 130.3, 127.4, 126.4, 125.0, 120.0, 46.3, 44.6, 41.4, 27.5, 24.7.

HR-MS-ESI (m/z) Calculated for C$_{19}$H$_{19}$N$_2$O$_3$Cl$_2$ [M + H]$^+$: 393.0773, found: 393.0765.

LCMS (MDAP): tR = 23.67 min, 94%; m/z (ESI⁺) 392.9 [M + H]⁺, 414.9 [M + Na]⁺.

(*S*)-1-((3'-Methoxy-[1,1'-biphenyl]-4-yl)carbamoyl)piperidine-3-carboxylic acid (4.3)
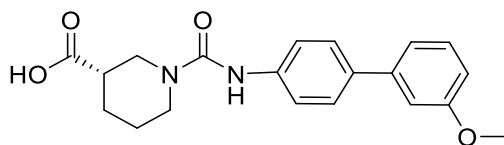
This was synthesised on a 0.15 mmol scale from (*S*)-methyl 1-((3'-methoxy-[1,1'-biphenyl]-4-yl)carbamoyl)piperidine-3-carboxylate by the same procedure as **4.1.** The final product was obtained as a colourless solid; yield: 14.0 mg (26%).

¹H NMR (600 MHz, DMSO-d_6) δ 12.46 (brs, 1H), 8.65 (brs, 1H), 7.53 (m, 4H), 7.31 (t, *J* = 7.9 Hz, 1H), 7.17 (d, *J* = 7.7 Hz, 1H), 7.13 (s, 1H), 6.85 (d, *J* = 10.4 Hz, 1H), 4.12 (d, *J* = 12.1 Hz, 1H), 3.91 (d, *J* = 13.4 Hz, 1H), 3.79 (s, 3H), 2.98 (t, 1H), 2.89 (t, 1H), 2.37 (t, *J* = 10.5 Hz, 1H), 1.96 (d, *J* = 13.2 Hz, 1H), 1.68 – 1.61 (m, 1H), 1.56 (q, *J* = 10.7 Hz, 1H), 1.42 (q, *J* = 12.3 Hz, 1H).

¹³C NMR (151 MHz, DMSO-d_6) δ 175.2, 160.2, 155.2, 141.9, 140.8, 133.5, 130.3, 127.0, 120.1, 118.9, 112.8, 111.9, 55.5, 46.4, 44.6, 41.3, 27.5, 24.6.

HR-MS-ESI (m/z) Calculated for $C_{20}H_{23}N_2O_4$ [M + H]⁺: 355.1658, found: 355.1661.

LCMS (MDAP): tR = 19.41 min, 98%; m/z (ESI+) 355.0 [M + H]⁺, 377.0 [M + Na]⁺.

(*R*)-2-(3',5'-Dichloro-[1,1'-biphenyl]-4-yl)tetrahydroimidazo[1,5-a]pyridine-1,3(*2H,5H*)-dione (**4.4**)
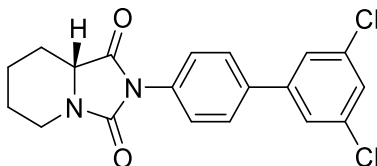
This was synthesised on a 0.84 mmol scale from 3',5'-dichloro-[1,1'-biphenyl]-4-amine by the same procedure as **4.1i** although (*R*)-methylpiperidine-2-carboxylate hydrochloride, CAS: 18650-38-9 (301.8 mg, 1.68 mmol) was used instead of (*S*)-methylpiperidine-3-carboxylate hydrochloride. The final product was obtained as a colourless solid; yield: 124.3 mg (39%).

^{1}H NMR (600 MHz, CDCl$_3$) δ 7.61 (d, *J* = 8.8 Hz, 2H), 7.53 (d, *J* = 8.8 Hz, 2H), 7.45 (d, *J* = 2.1 Hz, 2H), 7.35 (s, 1H), 4.28 (d, *J* = 13.0 Hz, 1H), 3.96 (d, *J* = 12.9 Hz, 1H), 2.94 (t, *J* = 13.0 Hz, 1H), 2.33 (d, *J* = 12.9 Hz, 1H), 2.10 – 2.04 (m, 1H), 1.82 (d, *J* = 13.0 Hz, 1H), 1.57 – 1.44 (m, 3H).

HRMS *m/z* (ESI$^+$) Calculated for C$_{19}$H$_{17}$N$_2$O$_2$Cl$_2$ [M + H]$^+$: 375.0667, found: 375.0649.

LCMS (MDAP): tR = 25.10 min, 92%; m/z (ESI$^+$) 396.9 [M + Na]$^+$.

(*S*)-2-(3',5'-Dichloro-[1,1'-biphenyl]-4-yl)tetrahydroimidazo[1,5-a]pyridine-1,3(*2H,5H*)-dione (**4.5**)
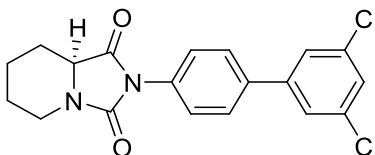

This was synthesised on a 0.84 mmol scale from 3',5'-dichloro-[1,1'-biphenyl]-4-amine by the same procedure as **4.1i** although (*S*)-methylpiperidine-2-carboxylate hydrochloride, CAS: 18650-39-0 (301.8 mg, 1.68 mmol) was used instead of (*S*)-methylpiperidine-3-carboxylate hydrochloride. The final product was obtained as a colourless solid; yield: 83.3 mg (23%).

^{1}H NMR (600 MHz, CDCl$_3$) δ 7.59 (d, *J* = 8.0 Hz, 2H), 7.52 (d, *J* = 8.0 Hz, 2H), 7.43 (s, 2H), 7.33 (s, 1H), 4.27 (d, *J* = 13.1 Hz, 1H), 3.94 (d, *J* = 12.0 Hz, 1H), 2.92 (t, *J* = 13.1 Hz, 1H), 2.31 (d, *J* = 13.3 Hz, 1H), 2.05 (d, *J* = 13.1 Hz, 1H), 1.80 (d, *J* = 13.3 Hz, 1H), 1.55 (d, *J* = 12.0 Hz, 1H), 1.53 – 1.45 (m, 2H).

HRMS *m/z* (ESI$^+$) Calculated for C$_{19}$H$_{17}$N$_2$O$_2{}^{35}$Cl$_2$ [M + H]$^+$: 375.0667, found: 375.0668.

LCMS (MDAP): tR = 25.14 min, 87%; m/z (ESI$^+$) [M + H]$^+$, 396.9 [M + Na]$^+$.
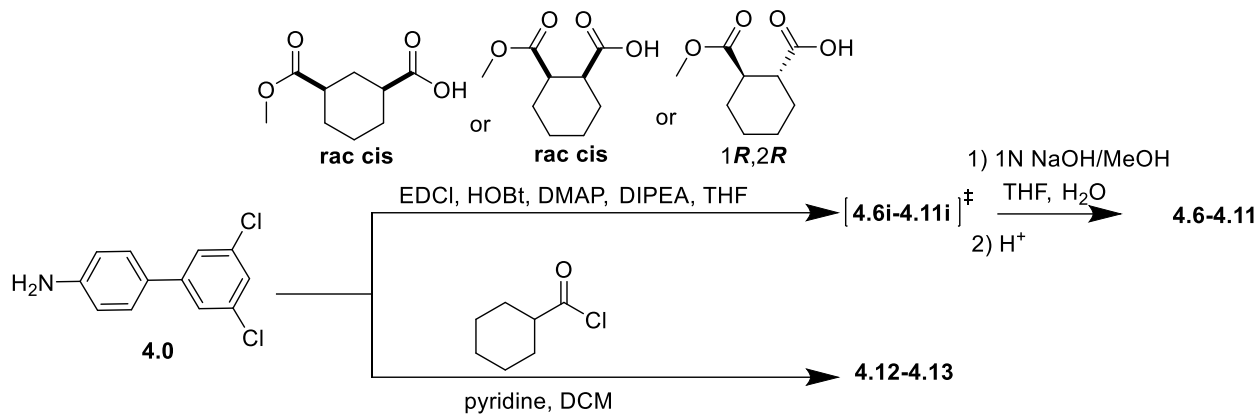
Methyl 3-((3',5'-dichloro-[1,1'-biphenyl]-4-yl)carbamoyl)cyclohexanecarboxylate (4.6i)
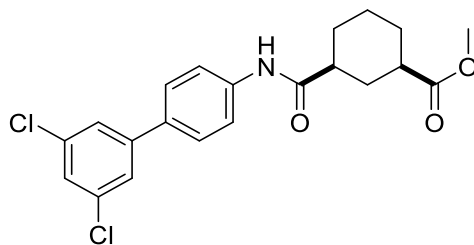
A solution of 3',5'-dichloro-[1,1'-biphenyl]-4-amine (100 mg, 0.42 mmol), (+-)-cis-cyclohexane-1,3-dicarboxylic acid monomethyl ester, CAS:25090-39-5 (93.2 mg, 0.25), 4-dimethylaminopyridine (DMAP) (51.32 mg, 2.1 mmol), *N*-(3-dimethylaminopropyl)-*N'*-ethylcarbodiimide hydrochloride (EDC) (80.52 mg, 0.42 mmol), 1-hydroxybenzotriazole hydrate (HOBT) (5.60 mg, 0.042 mmol), *N,N*-diisopropylethylamine (DIPEA) (0.37 mL, 2.1 mmol) in tetrahydrofuran (4.0 mL). The solution was stirred at 70° C overnight under nitrogen. The mixture was allowed to cool to room temperature. Water (20 mL) and EtOAc (20 mL) were added to the solution then the aqueous phase was extracted with EtOAc (20 mL × 2). The organic phases were combined, washed successively with 1 N HCl, saturated sodium bicarbonate solution, brine, dried over anhydrous Na_2SO_4 and concentrated. The residue was purified by chromatography on silica using a gradient of hexane: diethyl ether (0 - 60%), thus final product was obtained as a pale-yellow solid; yield: 71.1 mg (38%).

^{1}H NMR (600 MHz, CDCl$_3$) δ 7.95 (brs, 1H), 7.60 (d, J = 6.0 Hz, 2H), 7.43 (d, J = 6.0 Hz, 2H), 7.35 (d, J = 2.9 Hz, 2H), 7.26 (s, 1H), 3.65 (s, 3H), 2.33 (t, J = 12.5 Hz, 2H), 2.21 (d, J = 13.2 Hz, 1H), 2.00 – 1.94 (m, 3H), 1.72 (q, J = 12.6 Hz, 1H), 1.52 (q, J = 12.8 Hz, 1H), 1.42 – 1.30 (m, 2H).

LCMS (MDAP): tR = 26.92 min, 92%; m/z (ESI$^+$) 406.0 [M + H]$^+$, 428.0 [M + Na]$^+$.

Chemical Formula: C$_{21}$H$_{21}$Cl$_2$NO$_3$

(1R,2R)-Methyl 2-((3',5'-dichloro-[1,1'-biphenyl]-4-yl)carbamoyl)cyclohexanecarboxylate (4.7i)
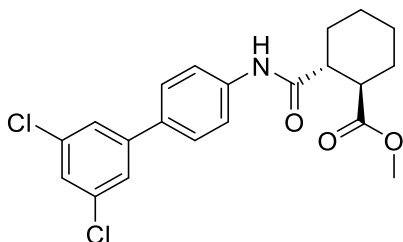
This was synthesised on a 0.34 mmol scale from 3',5'-dichloro-[1,1'-biphenyl]-4-amine by the same procedure as **4.6i** although (1R,2R)-2-(methoxycarbonyl) cyclohexanecarboxylic acid, CAS: 96894-64-3 (76.3 mg, 0.41) was used instead of (+-)-cis-cyclohexane-1,3-dicarboxylic acid monomethyl ester. The final product was obtained as a colourless solid; yield: 42.4 mg (29%).

^{1}H NMR (600 MHz, CDCl$_3$) δ 7.91 (brs, 1H), 7.52 (d, J = 8.4 Hz, 2H), 7.36 (d, J = 8.4 Hz, 2H), 7.31 (d, J = 2.1 Hz, 2H), 7.26 (s, 1H), 3.68 (s, 3H), 2.81 (t, J = 11.9 Hz, 1H), 2.62 (t, J = 11.9 Hz, 1H), 2.16 (d, J = 9.7 Hz, 1H), 2.02 (d, J = 13.1 Hz, 1H), 1.88 (s, 1H), 1.85 (d, J = 9.7 Hz, 1H), 1.62 (q, J = 13.1 Hz, 1H), 1.41 – 1.34 (m, 2H), 1.32 – 1.24 (m, 1H).

LCMS (MDAP): tR = 26.73 min, 94%; m/z (ESI$^+$) 405.9 [M + H]$^+$, 428.0 [M + Na]$^+$.

Chemical Formula: $C_{21}H_{21}Cl_2NO_3$

2-(3',5'-Dichloro-[1,1'-biphenyl]-4-yl)hexahydro-1H-isoindole-1,3(2H)-dione (**4.8i**)

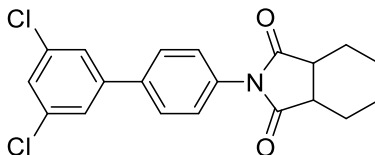

This was synthesised on a 0.34 mmol scale from 3',5'-dichloro-[1,1'-biphenyl]-4-amine by the same procedure as **4.6i** although (+-)-cis-cyclohexane-1,2-dicarboxylic acid monomethyl ester, CAS: 111955-05-6 (76.3 mg, 0.41) was used instead of (+-)-cis-cyclohexane-1,3-dicarboxylic acid monomethyl ester. The final product was obtained as a colourless solid; yield: 42.1 mg (28%).

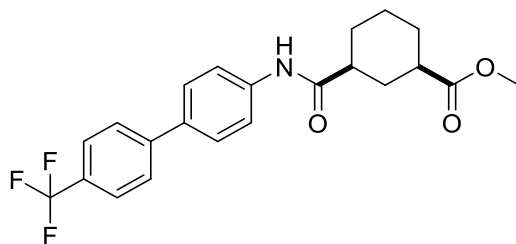^{1}H NMR (600 MHz, CDCl$_3$) δ 7.61 (d, J = 8.0 Hz, 2H), 7.43 (s, 2H), 7.40 (d, J = 8.0 Hz, 2H), 7.34 (s, 1H), 3.06 (t, J = 4.1 Hz, 2H), 1.97 (m, 4H), 1.89 (m, 4H).

^{13}C NMR (151 MHz, CDCl$_3$) δ 178.5, 143.2, 138.5, 135.4, 132.3, 127.8, 127.6, 126.8, 125.7, 40.2, 24.0, 21.9.

LCMS (MDAP): tR = 26.18 min, 84%; m/z (ESI$^+$) 426.0 [M + Na]$^+$.

Chemical Formula: $C_{20}H_{17}Cl_2NO_2$

Methyl 3-((4'-(trifluoromethyl)-[1,1'-biphenyl]-4-yl)carbamoyl)cyclohexanecarboxylate (4.9i)

This was synthesised on a 0.34 mmol scale from 4′-trifluoromethyl-biphenyl-4-ylamine that was used instead of 3',5'-dichloro-[1,1'-biphenyl]-4-amine by the same procedure as **4.6i.** The final product was obtained as a colourless solid; yield: 16.5 mg (10%).

^{1}H NMR (600 MHz, CDCl$_3$) δ 7.66 (s, 4H), 7.63 (d, J = 8.2 Hz, 2H), 7.56 (d, J = 8.2 Hz, 2H), 7.35 (brs, 1H), 3.69 (s, 3H), 2.39 (t, J = 12.5 Hz, 1H), 2.28 (m, 2H), 2.02 – 1.96 (m, 2H), 1.74 (q, J = 12.5 Hz, 1H), 1.54 (t, J = 12.5 Hz, 1H), 1.46 – 1.40 (m, 3H).

LCMS (MDAP): tR = 24.93 min, 82%; m/z (ESI$^+$) 406.0 [M + H]$^+$, 427.9 [M + Na]$^+$.

Chemical Formula: C$_{22}$H$_{22}$F$_3$NO$_3$

(1R,2R)-Methyl 2-((4'-(trifluoromethyl)-[1,1'-biphenyl]-4-yl)carbamoyl) cyclohexane carboxylate (4.10i)
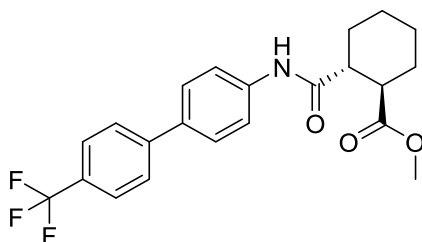
This was synthesised on a 0.27 mmol scale from 4′-trifluoromethyl-biphenyl-4-ylamine by the same procedure as **4.9i** although (1R,2R)-2-(methoxycarbonyl)
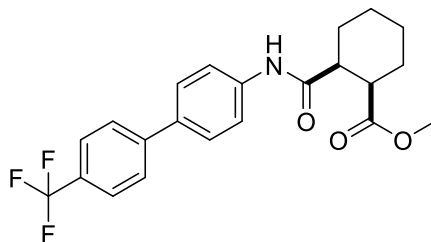
cyclohexanecarboxylic acid, CAS: 96894-64-3 (60.7 mg, 0.33) was used instead of 3-(methoxycarbonyl)cyclohexanecarboxylic acid monomethyl ester. The final product was obtained as a colourless solid; yield: 31.8 mg (26%).

^{1}H NMR (600 MHz, CDCl$_3$) δ 7.78 (brs, 1H), 7.61 (d, J = 8.2 Hz, 2H), 7.59 – 7.54 (m, 4H), 7.46 (d, J = 8.2 Hz, 2H), 3.68 (s, 3H), 2.81 (t, J = 10.7 Hz, 1H), 2.65 – 2.57 (m, 1H), 2.16 (d, J = 7.8 Hz, 1H), 2.02 (d, J = 13.0 Hz, 1H), 1.88 (s, 1H), 1.85 (d, J = 11.3 Hz, 1H), 1.65 (d, J = 7.8 Hz, 1H), 1.38 (t, J = 11.3 Hz, 2H), 1.30 (d, J = 13.0 Hz, 1H).

LCMS (MDAP): tR = 25.05 min, 90%; m/z (ESI$^+$) 406.0 [M + H]$^+$, 428.0 [M + Na]$^+$.

Chemical Formula: C$_{22}$H$_{22}$F$_3$NO$_3$

(1R,2S)-Methyl 2-((4'-(trifluoromethyl)-[1,1'-biphenyl]-4-yl)carbamoyl)cyclohexanecarboxylate (4.11i)

This was synthesised on a 0.38 mmol scale from 4′-Trifluoromethyl-biphenyl-4-ylamine by the same procedure as **4.9i** although (+-)-cis-cyclohexane-1,2-dicarboxylic acid monomethyl ester, CAS: 111955-05-6 (84.0 mg, 0.51) was used instead of 3-(methoxycarbonyl)cyclohexanecarboxylic acid monomethyl ester. The final product was obtained as a colourless solid; yield: 84.9 mg (45%).
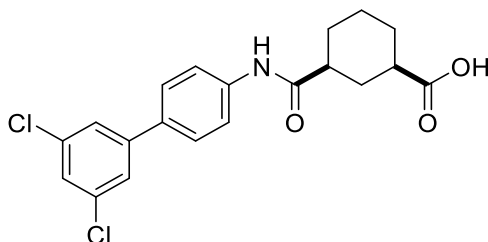
^{1}H NMR (600 MHz, CDCl$_3$) δ 7.67 (m, 6H), 7.40 (d, J = 8.0 Hz, 2H), 3.45 (s, 6H), 3.06 (s, 2H), 1.99 – 1.94 (m, 2H), 1.91 – 1.87 (m, 2H), 1.60 (s, 2H).

LCMS (MDAP): tR = 24.36 min, 81%; m/z (ESI⁺) 403.8 [M + H]⁺, 426.0 [M + Na]⁺.

and tR = 24.81 min, 18%; m/z (ESI⁺) 405.9 [M + H]⁺, 428.0 [M + Na]⁺.

Chemical Formula: $C_{22}H_{22}F_3NO_3$

3-((3',5'-Dichloro-[1,1'-biphenyl]-4-yl)carbamoyl)cyclohexane-1-carboxylic acid (**4.6**)

To a stirred solution of methyl 3-((3',5'-dichloro-[1,1'-biphenyl]-4-yl)carbamoyl)cyclohexane-1-carboxylate 76.3 mg, 0.19 mmol in THF 2.0 mL and H_2O 3.0 mL was added 1 N NaOH in MeOH (0.28 mmol, 2.9 mL). Vigorous stirred at room temperature overnight. The solution was diluted with water (20 mL) and 2 M hydrochloric acid (10 mL) was added. The aqueous phase is extracted with dichloromethane 25 mL×3, The organic phases were combined, washed with brine, dried over anhydrous Na_2SO_4 and concentrated. The residue was purified by chromatography on silica using a gradient of hexane: EtOAc (30 - 100%), thus the final product was obtained as a colourless solid; yield: 30.0 mg (37%).

¹H NMR (600 MHz, DMSO-d_6) δ 12.15 (brs, 1H), 10.03 (brs, 1H), 7.69 (m, 6H), 7.53 (m, 1H), 2.38 (t, J = 9.1 Hz, 1H), 2.26 (t, J = 11.9 Hz, 1H), 2.00 (d, J = 11.9 Hz, 1H), 1.88 (d, J = 12.8 Hz, 1H), 1.81 (d, J = 9.1 Hz, 2H), 1.45 (q, J = 12.8 Hz, 1H), 1.32 (t, J = 10.9 Hz, 2H), 1.21 (m, 1H).

¹³C NMR (151 MHz, DMSO-d_6) δ 176.8, 174.3, 143.7, 140.5, 135.1, 131.8, 127.8, 126.7, 125.2, 119.8, 44.4, 42.2, 31.8, 29.0, 28.6, 24.9.

HR-MS-ESI (m/z) Calculated for $C_{20}H_{20}NO_3Cl_2$ [M + H]$^+$: 392.0820, found: 392.0800.

LCMS (MDAP): tR = 24.87 min, 91%; m/z (ESI$^+$) 392.0 [M + H]$^+$, 413.8 [M + Na]$^+$.

(1*R*,2*R*)-2-((3',5'-Dichloro-[1,1'-biphenyl]-4-yl)carbamoyl)cyclohexanecarboxylic acid (4.7)
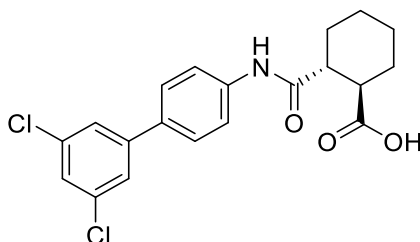
To a stirred solution of (1*R*,2*R*)-methyl 2-((3',5'-dichloro-[1,1'-biphenyl]-4-yl)carbamoyl) cyclohexanecarboxylate (42.4 mg, 0.10 mmol) in THF (1.2 mL) and H_2O (1.8 mL) was added 1 N NaOH in MeOH (0.34 mmol, 1.5 mL). Vigorous stirred at room temperature overnight. The work up and purification process used the same procedure as compound **4.6**. The final product was obtained as a colourless solid; yield: 21.5 mg (59%).

^{1}H NMR (600 MHz, DMSO-d_6) δ 12.07 (brs, 1H), 10.09 (brs, 1H), 7.68 (m, 6H), 7.52 (s, 1H), 3.15 (s, 1H), 2.53 (t, *J* = 9.2 Hz, 2H), 2.00 (d, *J* = 8.7 Hz, 1H), 1.93 (d, *J* = 9.2 Hz, 1H), 1.74 (t, *J* = 8.7 Hz, 2H), 1.34 − 1.31 (m, 1H), 1.28 − 1.26 (m, 2H).
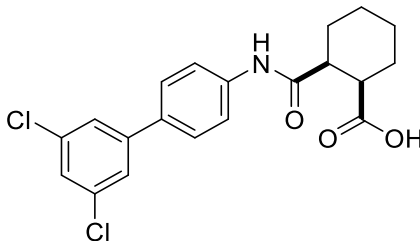
^{13}C NMR (151 MHz, DMSO-d_6) δ 176.6, 174.2, 143.7, 140.6, 135.1, 131.7, 127.8, 126.7, 125.2, 119.6, 46.9, 44.6, 30.0, 29.3, 25.6, 25.5.

HR-MS-ESI (m/z) Calculated for $C_{20}H_{20}NO_3Cl_2$ [M + H]$^+$: 392.0820, found: 392.0822.

LCMS (MDAP): tR t = 24.68 min, 69%; m/z (ESI⁺) 392.0 [M + H]⁺, 414.0 [M + Na]⁺.

and tR = 24.68 min, 28%; m/z (ESI⁺) 392.0 [M + H]⁺, 414.0 [M + Na]⁺.

(1*R*,2*S*)-2-((3',5'-Dichloro-[1,1'-biphenyl]-4-yl)carbamoyl)cyclohexanecarboxylic acid (4.8)

Stirred solution of (1*R*,2*S*)-methyl 2-((3',5'-dichloro-[1,1'-biphenyl]-4-yl)carbamoyl) cyclohexanecarboxylate 40.0 mg, 0.10 mmol in THF (1.4 mL) and H_2O (2.0 mL) was added 1 N NaOH in MeOH (0.34 mmol, 1.6 mL) with vigorous stirring at room temperature overnight. The work up and purification process used the same procedure as compound **4.6**. The final product was obtained as a colourless solid; yield: 29.4 mg (64%).

¹H NMR (600 MHz, DMSO-*d₆*) δ 11.99 (brs, 1H), 9.89 (brs, 1H), 7.68 (m, 6H), 7.51 (s, 1H), 2.95 (s, 1H), 2.59 (t, *J* = 9.3 Hz, 1H), 2.13 – 2.06 (m, 1H), 2.02 – 1.96 (m, 1H), 1.75 – 1.61 (m, 3H), 1.43 – 1.36 (m, 2H), 1.29 (m, 1H).

¹³C NMR (151 MHz, DMSO-*d₆*) δ 175.6, 173.4, 143.7, 140.7, 135.1, 131.6, 127.7, 126.6, 125.2, 119.7, 43.0, 42.4, 28.1, 25.6, 24.4, 22.8.

HR-MS-ESI (m/z) Calculated for $C_{20}H_{20}NO_3Cl_2$ [M + H]⁺: 392.0820, found: 392.0809.

LCMS (MDAP): tR = 24.68 min, 91%; m/z (ESI⁺) 391.9 [M + H]⁺, 413.9 [M + Na]⁺.

3-((4'-(Trifluoromethyl)-[1,1'-biphenyl]-4-yl)carbamoyl)cyclohexanecarboxylic acid (4.9)

To a stirred solution of methyl 3-((4'-(trifluoromethyl)-[1,1'-biphenyl]-4-yl)carbamoyl) cyclohexanecarboxylate (16.5 mg, 0.04 mmol) in THF (0.4 mL) and H_2O (0.6 mL) was added 1 N NaOH in MeOH (0.16 mmol, 0.6 mL). Vigorous stirred at room temperature overnight. The work up and purification process used the same procedure as compound **4.6**. The final product was obtained as a pale-yellow solid; yield: 14.2 mg (79%).
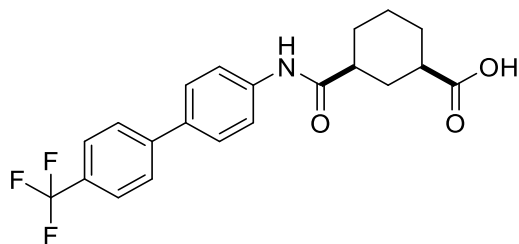
^{1}H NMR (600 MHz, DMSO-d_6) δ 12.15 (brs, 1H), 10.03 (brs, 1H), 7.85 (d, J = 8.1 Hz, 2H), 7.76 (d, J = 8.1 Hz, 2H), 7.73 (d, J = 8.7 Hz, 2H), 7.68 (d, J = 8.7 Hz, 2H), 2.39 (t, J = 11.2 Hz, 1H), 2.27 (t, J = 13.0 Hz, 1H), 2.01 (d, J = 13.0 Hz, 1H), 1.89 (d, J = 13.0 Hz, 1H), 1.81 (d, J = 10.3 Hz, 2H), 1.46 (q, J = 13.0 Hz, 1H), 1.32 (t, J = 10.3 Hz, 2H), 1.24 – 1.20 (m, 1H).

^{13}C NMR (151 MHz, DMSO-d_6) δ 176.8, 174.3, 144.1, 140.3, 133.3, 127.8, 127.6 (q, $^2J_{CF}$ = 32.0 Hz), 127.3, 126.2 (q, $^3J_{CF}$ = 4.0 Hz), 125.8 (q, $^1J_{CF}$ = 273.0 Hz), 124.0, 119.9, 44.4, 42.2, 31.8, 29.0, 28.6, 24.9.

^{19}F NMR (376 MHz, DMSO-d_6) δ -60.86 (brs).

HR-MS-ESI (m/z) Calculated for $C_{21}H_{21}NO_3F_3$ [M + H]$^+$: 392.1474, found: 392.1469.

LCMS (MDAP): tR = 22.85 min, 89%; m/z (ESI⁺) 391.8 [M + H]⁺, 413.9 [M + Na]⁺.

(1*R*,2*R*)-2-((4'-(Trifluoromethyl)-[1,1'-biphenyl]-4-yl)carbamoyl) cyclohexanecarboxylic acid (4.10)
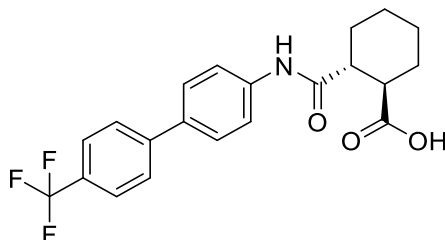
A stirred solution of (1*R*,2*R*)-methyl 2-((4'-(trifluoromethyl)-[1,1'-biphenyl]-4-yl)carbamoyl) cyclohexanecarboxylate (31.2 mg, 0.08 mmol) in THF (1.0 mL) and H_2O (1.5 mL) was added 1 N NaOH in MeOH (0.12 mmol, 1.3 mL) with vigorous stirring at room temperature overnight. The work up and purification process used the same procedure as compound **4.6**. The final product was obtained as a pale-yellow solid; yield: 13.1 mg (30%).

¹H NMR (600 MHz, DMSO-d_6) δ 12.15 (brs, 1H), 10.03 (brs, 1H), 7.85 (d, *J* = 8.1 Hz, 2H), 7.76 (d, *J* = 8.1 Hz, 2H), 7.73 (d, *J* = 8.6 Hz, 2H), 7.68 (d, *J* = 8.6 Hz, 2H), 2.40 (d, *J* = 13.1 Hz, 1H), 2.27 (t, *J* = 8.2 Hz, 1H), 2.01 (d, *J* = 13.1 Hz, 1H), 1.89 (d, *J* = 12.8 Hz, 1H), 1.81 (d, *J* = 8.2 Hz, 2H), 1.46 (q, *J* = 12.8 Hz, 1H), 1.33 (t, *J* = 10.3 Hz, 2H), 1.25 – 1.20 (m, 1H).

¹³C NMR (151 MHz, DMSO-d_6) δ 176.6, 174.2, 144.2, 140.4, 133.1, 127.8, 127.7, 127.3, 126.2 (q, $^3J_{CF}$ = 3.8 Hz), 125.8 (q, $^1J_{CF}$ = 271.5 Hz), 119.7, 46.9, 44.61, 30.0, 29.3, 25.6, 25.5. ($^2J_{CF}$ not seen).
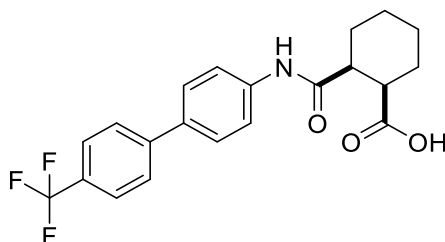
¹⁹F NMR (376 MHz, DMSO-d_6) δ -60.85 (brs).

HR-MS-ESI (m/z) Calculated for $C_{21}H_{21}NO_3F_3$ [M + H]$^+$: 392.1474, found: 392.1459.

LCMS (MDAP): tR = 22.86 min, 57%; m/z (ESI$^+$) 391.7 [M + H]$^+$, 413.7 [M + Na]$^+$.

and tR = 23.09 min, 41%; m/z (ESI$^+$) 391.7 [M + H]$^+$, 413.7 [M + Na]$^+$.

(1*R*,2*S*)-2-((4'-(Trifluoromethyl)-[1,1'-biphenyl]-4-yl)carbamoyl) cyclohexanecarboxylic acid (**4.11**)

A stirred solution of (1*R*,2*S*)-methyl 2-((4'-(trifluoromethyl)-[1,1'-biphenyl]-4-yl)carbamoyl) cyclohexanecarboxylate (84.90 mg, 0.23 mmol) in THF (3.0 mL) and H_2O (4.5 mL) was added 1 N NaOH in MeOH (0.34 mmol, 3.9 mL) with vigorous stirring at room temperature overnight. The work up and purification process used the same procedure as compound **4.6**. The final product was obtained as a pale-yellow solid; yield: 41.8 mg (48%).

^{1}H NMR (600 MHz, DMSO-d_6) δ 11.99 (brs, 1H), 9.92 (brs, 1H), 7.85 (d, *J* = 8.1 Hz, 2H), 7.76 (d, *J* = 8.1 Hz, 2H), 7.70 (d, *J* = 8.4 Hz, 2H), 7.67 (d, *J* = 8.4 Hz, 2H), 2.95 (s, 1H), 2.59 (s, 1H), 2.09 (q, *J* = 11.4 Hz, 1H), 2.03 – 1.97 (m, 1H), 1.76 – 1.67 (m, 2H), 1.63 (s, 1H), 1.43 – 1.36 (m, 2H), 1.32 – 1.27 (m, 1H).
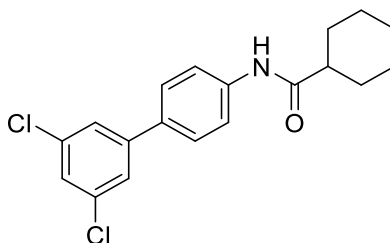
^{13}C NMR (151 MHz, DMSO-d_6) δ 175.6, 173.3, 144.2, 140.5, 133.0, 127.7, 127.6 ($^2J_{CF}$ = 31.4 Hz), 127.3, 126.2 (q, $^3J_{CF}$ = 3.7 Hz), 125.8 (q, $^1J_{CF}$ = 271.5 Hz), 119.9, 43.1, 42.5, 28.2, 25.7, 24.5, 22.8.

^{19}F NMR (376 MHz, DMSO-d_6) δ -60.85 (brs).

HR-MS-ESI (m/z) Calculated for $C_{21}H_{21}NO_3F_3$ [M + H]$^+$: 392.1474, found: 392.1460.

LCMS (MDAP): tR = 22.80 min, 95%; m/z (ESI$^+$) 391.8 [M + H]$^+$, 413.8 [M + Na]$^+$.

N-(3',5'-Dichloro-[1,1'-biphenyl]-4-yl)cyclohexanecarboxamide (4.12)

A solution of cyclohexanecarbonyl chloride (55.7 mg, 0.38 mmol) in pyridine (1.0 mL) then 3',5'-dichloro-[1,1'-biphenyl]-4-amine (50 mg, 0.21 mmol) in DCM was added dropwise. The solution was stirred at room temperature for 2 hrs. After completion of the reaction, DCM was added to the solution then washed with H_2O. The organic phases were dried over anhydrous Na_2SO_4 and concentrated. The residue was purified by chromatography on silica using a gradient of hexane: EtOAc (0 - 20%), thus the product was obtained as a colourless solid; yield: 21.1 mg (27%).

^{1}H NMR (600 MHz, DMSO-d_6) δ 9.96 (brs, 1H), 7.68 (m, 6H), 7.51 (s, 1H), 2.32 (t, J = 13.0 Hz, 1H), 1.79 (d, J = 13.0 Hz, 2H), 1.74 (d, J = 13.0 Hz, 2H), 1.63 (d, J = 13.0 Hz, 1H), 1.39 (q, J = 13.0 Hz, 2H), 1.25 (q, J = 13.0 Hz, 2H), 1.18 (m, 1H).

^{13}C NMR (151 MHz, DMSO-d_6) δ 175.0, 143.7, 140.6, 135.1, 131.7, 127.7, 126.7, 125.2, 119.7, 45.4, 29.6, 25.8, 25.7.

HR-MS-ESI (m/z) Calculated for $C_{19}H_{20}NOCl_2$ [M + H]$^+$: 348.0922, found: 348.0932.

LCMS (MDAP): tR = 28.08 min, 92%; m/z (ESI$^+$) 348.0 [M + H]$^+$, 413.0 [M + Na]$^+$.

N-(4'-(Trifluoromethyl)-[1,1'-biphenyl]-4-yl)cyclohexanecarboxamide (**4.13**)
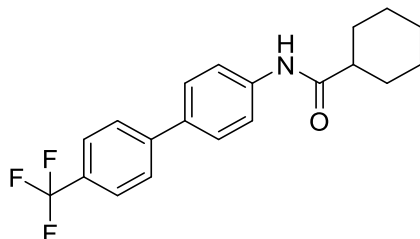
This was synthesised on a 0.38 mmol scale with cyclohexanecarbonyl chloride by the same procedure as **4.12** although 4'-(trifluoromethyl)-[1,1'-biphenyl]-4-amine (50 mg, 0.21 mmol) was used instead of 3',5'-dichloro-[1,1'-biphenyl]-4-amine. The final product was obtained as a colourless solid; yield: 28.7 mg (36%).

^{1}H NMR (600 MHz, DMSO-d_6) δ 9.98 (brs, 1H), 7.84 (d, J = 8.1 Hz, 2H), 7.76 (d, J = 8.1 Hz, 2H), 7.73 (d, J = 9.0 Hz, 2H), 7.67 (d, J = 9.0 Hz, 2H), 2.33 (t, J = 11.3 Hz, 1H), 1.79 (d, J = 12.9 Hz, 2H), 1.74 (d, J = 11.3 Hz, 2H), 1.64 (d, J = 12.9 Hz, 1H), 1.40 (q, J = 12.5 Hz, 2H), 1.26 (q, J = 12.5 Hz, 2H), 1.21 – 1.14 (m, 1H).
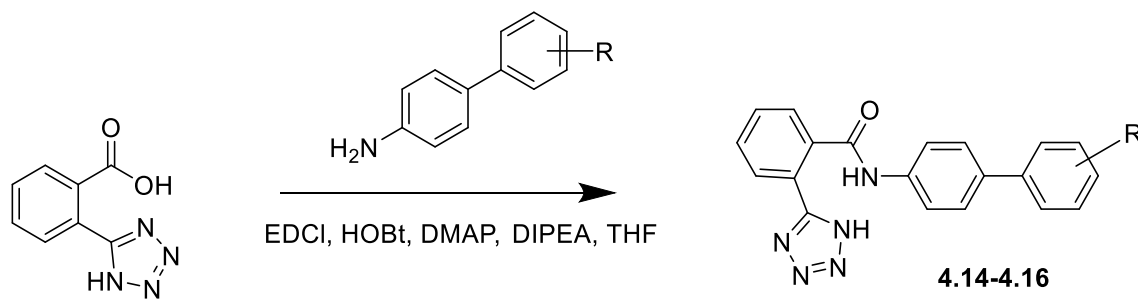
^{13}C NMR (151 MHz, DMSO-d_6) δ 175.0, 144.2, 140.4, 133.2, 128.0 (q, $^2J_{CF}$ = 31.5 Hz), 127.8, 127.3, 126.2 (q, $^3J_{CF}$ = 3.5 Hz), 125.8 (q, $^1J_{CF}$ = 271.1 Hz), 119.8, 45.4, 29.6, 25.8, 25.7.
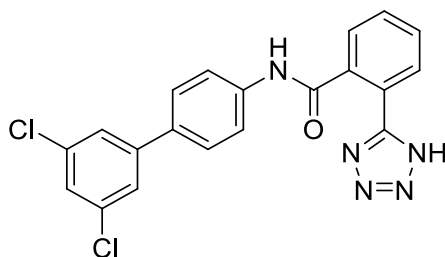
^{19}F NMR (376 MHz, DMSO-d_6) δ -60.86 (brs)

HR-MS-ESI (m/z) Calculated for $C_{20}H_{21}NOF_3$ [M + H]$^+$: 348.1575, found: 348.1570.

LCMS (MDAP): tR = 26.26 min, 91%; m/z (ESI$^+$) 347.9 [M + H]$^+$, 411.0 [M + Na]$^+$.

4.7.5.2 Modification of LHS by using tetrazole instead of carboxyl group in phenyl ring: Hybrid series

N-(3',5'-Dichloro-[1,1'-biphenyl]-4-yl)-2-(1H-tetrazol-5-yl)benzamide (4.14)

A stirred solution of 3',5'-dichloro-[1,1'-biphenyl]-4-amine (50 mg, 0.25 mmol), 2-(1H-tetrazol-5-yl)benzoic acid (47.54 mg, 0.25), DMAP (25.66 mg, 0.21 mmol), EDC (40.19 mg, 0.21 mmol), HOBT (2.84 mg, 0.021 mmol), DIPEA (0.18 mL, 1.05 mmol) in THF (3.0 mL) was stirred at 70 °C overnight under nitrogen. The mixture was allowed to cool to room temperature. Water (20 mL) and EtOAc (20 mL) were added to the solution then the separated aqueous phase was extracted with EtOAc (20 mL × 2). The organic phases were combined, washed successively with 1 N HCl, saturated sodium bicarbonate solution, brine, dried over anhydrous Na_2SO_4 and concentrated. The residue was purified

by chromatography on silica using a gradient of hexane: diethyl ether (0 - 60%), thus the final product was obtained as a colourless solid; yield: 9.1 mg (11%).
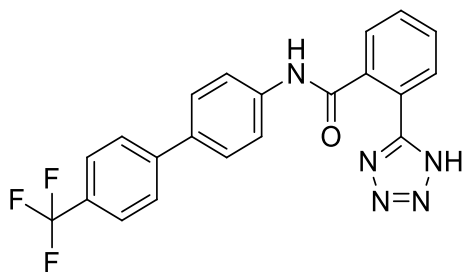
^{1}H NMR (600 MHz, DMSO-d_6) δ 10.69 (brs, 1H), 7.83 (d, J = 6.8 Hz, 1H), 7.73 (m, 8H), 7.67 (m, 2H), 7.54 (s, 1H).

^{13}C NMR (151 MHz, DMSO-d_6) δ 167.0, 156.3, 143.7, 140.4, 137.4, 135.1, 132.4, 130.7, 130.6, 130.0, 129.0, 127.8, 126.8, 125.3, 124.5, 120.4.

HR-MS-ESI (m/z) Calculated for $C_{20}H_{14}N_5OCl_2$ [M + H]$^+$: 410.0575, found: 410.0560.

LCMS (MDAP): tR = 24.35 min, 99%; m/z (ESI+) 409.6 [M + H]$^+$, 431.8 [M + Na]$^+$.

2-(1H-Tetrazol-5-yl)-N-(4'-(trifluoromethyl)-[1,1'-biphenyl]-4-yl)benzamide (4.15)

This was synthesised on a 0.41 mmol scale with 2-(1H-tetrazol-5-yl)benzoic acid by the same procedure as **4.14** although 4'-(trifluoromethyl)-[1,1'-biphenyl]-4-amine (80.00 mg, 0.34 mmol) was used instead of 3',5'-dichloro-[1,1'-biphenyl]-4-amine. The final product was obtained as a colourless solid; yield: 44.8 mg (31%).

FT-IR (cm^{-1}): 3280 (N-H stretch), 1649 (C=O), 1597 (C=C, arom.), 1510 (C=C, arom.), 1397 (C=C, arom.), 820 (*p*-Disub)

m.p. 259.7-260 ºC

^{1}H NMR (600 MHz, DMSO-d_6) δ 10.63 (s, 1H), 7.87 (d, J = 8.0 Hz, 2H), 7.82 (s, 1H), 7.80 – 7.75 (m, 5H), 7.72 (m, 4H).
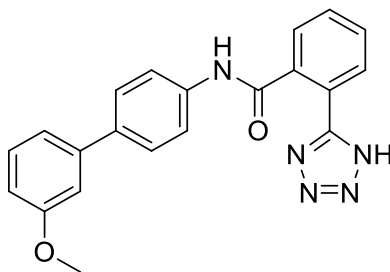
^{13}C NMR (151 MHz, DMSO-d_6) δ 168.8, 166.6, 144.2, 140.1, 137.6, 133.9, 131.2, 130.8, 130.1, 129.0, 127.9 (q, $^2J_{CF}$ = 34.4 Hz), 127.8, 127.4, 126.2 (q, $^3J_{CF}$ = 3.2 Hz), 125.8 ($^1J_{CF}$ = 271.7 Hz), 124.0, 120.6.

^{19}F NMR (376 MHz, DMSO-d_6) δ -60.86 (brs).

HR-MS-ESI (m/z) Calculated for $C_{21}H_{15}N_5OF_3$ [M + H]$^+$: 410.1229, found: 410.1215.

LCMS (MDAP): tR = 23.09 min, 97%; m/z (ESI+) 409.7 [M + H]$^+$, 431.7 [M + Na]$^+$.

N-(3'-Methoxy-[1,1'-biphenyl]-4-yl)-2-(1H-tetrazol-5-yl)benzamide (4.16)

This was synthesised on a 0.30 mmol scale from 2-(1H-tetrazol-5-yl)benzoic acid by the same procedure as **4.14** although 3'-methoxy-[1,1'-biphenyl]-4-amine (50 mg, 0.25 mmol) was used instead of 3',5'-dichloro-[1,1'-biphenyl]-4-amine. The final product was obtained as a colourless solid; yield: 13.1 mg (14%).

^{1}H NMR (600 MHz, DMSO-d_6) δ 10.64 (brs, 1H), 7.83 (d, J = 7.8 Hz, 1H), 7.73 (m, 3H), 7.69 – 7.64 (m, 2H), 7.63 (d, J = 8.3 Hz, 2H), 7.34 (t, J = 7.9 Hz, 1H), 7.21 (d, J = 7.7 Hz, 1H), 7.16 (s, 1H), 6.89 (d, J = 8.3 Hz, 1H), 3.80 (s, 3H).

^{13}C NMR (151 MHz, DMSO-d_6) δ 166.9, 160.2, 156.4, 141.7, 139.4, 137.5, 135.5, 130.6, 130.5, 130.4, 130.1, 129.0, 127.4, 124.6, 120.4, 119.1, 113.0, 112.3, 55.6.

HR-MS-ESI (m/z) Calculated for $C_{21}H_{18}N_5O_2$ [M + H]$^+$: 372.1460, found: 372.1440.

LCMS (MDAP): tR = 20.65 min, 99%; m/z (ESI+) 371.9 [M + H]$^+$, 394.0 [M + Na]$^+$.

4.7.5.3 Modification of RHS with containing tetrazole on LHS: Trans amide Series
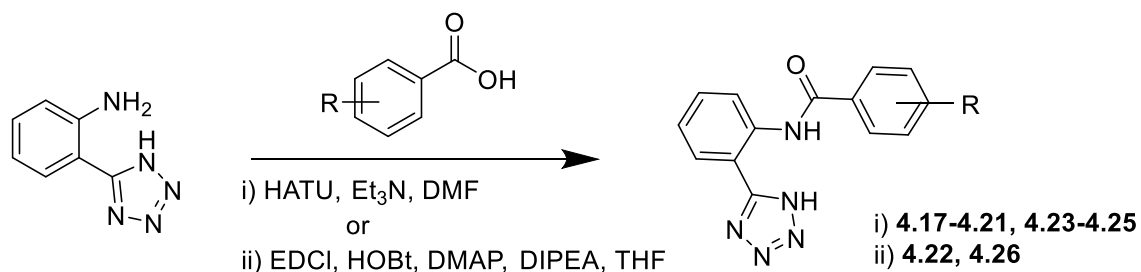
N-(2-(1H-Tetrazol-5-yl)phenyl)-4-fluorobenzamide (4.17)
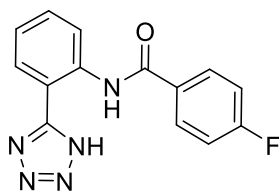
A stirred solution of 2-(1H-tetrazol-5-yl)-phenylamine (70.0 mg, 0.43 mmol), 4-fluorobenzoic acid (72.86 mg, 0.52 mmol), DMAP (52.53 mg, 0.43 mmol), EDC (82.43

mg, 0.43 mmol), HOBT (5.81 mg, 0.043 mmol), DIPEA (0.37 mL, 2.15 mmol) in THF (4.1 mL). The solution was stirred at 70 °C overnight under nitrogen. The mixture was allowed to cool to room temperature. Water (20 mL) and EtOAc (20 mL) were added to the solution then the aqueous phase was extracted with EtOAc (20 mL × 2). The organic phases were combined, washed successively with 1 N HCl, saturated sodium bicarbonate solution, brine, dried over anhydrous Na_2SO_4 and concentrated. The residue was purified by chromatography on silica using a gradient of EtOAc: MeOH (0 - 30%), thus the final product was obtained as a colourless solid; yield: 46.9 mg (42%).

^{1}H NMR (600 MHz, DMSO-d_6) δ 12.72 (brs, 1H), 8.65 (d, J = 8.3 Hz, 1H), 8.20 (m, 2H), 8.16 (d, J = 7.8 Hz, 1H), 7.43 (m, 3H), 7.23 (t, J = 7.8 Hz, 1H).

^{13}C NMR (151 MHz, DMSO-d_6) δ 164.3, 163.9 (d, $^1J_{CF}$ = 249.6 Hz), 158.6, 137.0, 131.8, 130.5 (d, $^3J_{CF}$ = 9.4 Hz), 129.7, 128.3, 124.0, 120.8, 117.9, 116.2 (d, $^2J_{CF}$ = 21.8 Hz).

^{19}F NMR (376 MHz, DMSO-d_6) δ -108.40 (tt, J = 8.8, 5.4 Hz).
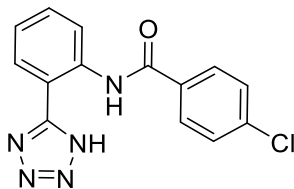
HR-MS-ESI (m/z) Calculated for $C_{14}H_{11}N_5OF$ [M + H]$^+$: 284.0948, found: 284.0952.

LCMS (MDAP): tR = 23.54 min, 99%; m/z (ESI+) 282.80 [-H]$^-$.

N-(2-(1H-Tetrazol-5-yl)phenyl)-4-chlorobenzamide (4.18)

This was synthesised on a 0.63 mmol scale from 2-(1H-tetrazol-5-yl)-phenylamine by the same procedure as **4.17** although 4-chlorobenzoic acid (100 mg, 0.64 mmol) was used instead of 4-fluorobenzoic acid. The final product was obtained as a colourless solid; yield: 15.5 mg (10%).

^{1}H NMR (600 MHz, DMSO-d_6) δ 12.43 (brs, 1H), 8.59 (d, J = 8.3 Hz, 1H), 8.12 (t, J = 8.6 Hz, 3H), 7.68 (d, J = 8.1 Hz, 2H), 7.47 (t, J = 7.8 Hz, 1H), 7.27 (t, J = 7.5 Hz, 1H).

^{13}C NMR (151 MHz, DMSO-d_6) δ 164.4, 157.6, 137.3, 137.0, 134.0, 130.3, 129.7, 129.4, 128.5, 124.4, 121.4, 117.2.

HR-MS-ESI (m/z) Calculated for $C_{14}H_{11}N_5OCl$ [M + H]$^+$: 300.0652, found: 300.0657.

N-(2-(1H-Tetrazol-5-yl)phenyl)-4-(trifluoromethyl)benzamide (4.19)
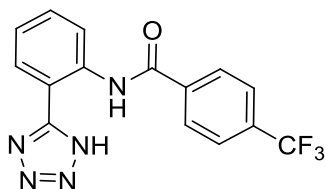
This was synthesised on a 0.58 mmol scale 2-(1H-Tetrazol-5-yl)-phenylamine by the same procedure as **4.17** although 4-(trifluoromethyl)benzoic acid (100 mg, 0.53 mmol) was used instead of 4-fluorobenzoic acid. The final product was obtained as a colourless solid; yield: 62.7 mg (48%).

^{1}H NMR (600 MHz, DMSO-d_6) δ 13.50 (brs, 1H), 8.75 (d, J = 8.4 Hz, 1H), 8.35 (d, J = 7.9 Hz, 2H), 8.27 (d, J = 7.8 Hz, 1H), 8.00 (d, J = 7.9 Hz, 2H), 7.36 (t, J = 8.0 Hz, 1H), 7.20 (t, J = 7.6 Hz, 1H).

^{13}C NMR (151 MHz, DMSO-d_6) δ 164.1, 160.0, 139.4, 136.5, 132.1 (q, $^2J_{CF}$ = 32.0 Hz), 128.7, 128.6, 127.8, 126.4 (q, $^3J_{CF}$ = 3.8 Hz), 125.3 (q, $^1J_{CF}$ = 272.0 Hz), 124.0, 120.0, 119.5.

^{19}F NMR (376 MHz, DMSO-d_6) δ -61.38 (brs).

HR-MS-ESI (m/z) Calculated for $C_{15}H_{11}N_5OF_3$ [M + H]$^+$: 334.0916, found: 334.0900.

N-(2-(1H-Tetrazol-5-yl)phenyl)-4-(benzyloxy)benzamide (4.20)
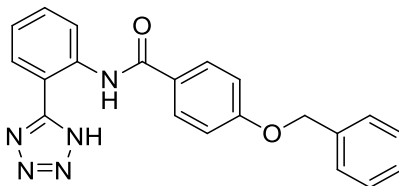
This was synthesised on a 0.48 mmol scale 2-(1H-tetrazol-5-yl)-phenylamine by the same procedure as **4.17** although 4-(benzyloxy)benzoic acid (100 mg, 0.44 mmol) was used instead of 4-fluorobenzoic acid. The final product was obtained as a colourless solid; yield: 45.6 mg (31%).

^{1}H NMR (600 MHz, DMSO-d_6) δ 12.77 (brs, 1H), 8.73 (d, J = 8.3 Hz, 1H), 8.20 (d, J = 7.8 Hz, 1H), 8.14 (d, J = 8.4 Hz, 2H), 7.48 (d, J = 7.5 Hz, 2H), 7.43 – 7.36 (m, 3H), 7.34 (d, J = 7.4 Hz, 1H), 7.23 – 7.17 (m, 3H), 5.22 (s, 2H).

^{13}C NMR (151 MHz, DMSO-d_6) δ 164.9, 161.6, 158.9, 137.3, 137.1, 129.8, 129.5, 129.0, 128.5, 128.3, 128.2, 127.7, 123.6, 120.4, 117.7, 115.3, 69.9.

HR-MS-ESI (m/z) Calculated for $C_{21}H_{16}N_5O_2$ [M - H]$^-$: 370.1304, found: 370.1308.
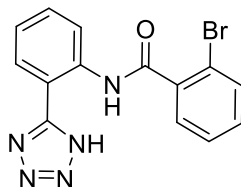
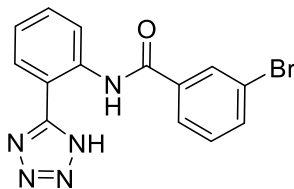**N-(2-(1H-Tetrazol-5-yl)phenyl)-2-bromobenzamide (4.21)**

This was synthesised on a 0.43 mmol scale from 2-(1H-tetrazol-5-yl)-phenylamine by the same procedure as **4.17** although 2-bromobenzoic acid (104.5 mg, 0.52 mmol) was used instead of 4-fluorobenzoic acid. The final product was obtained as a colourless solid; yield: 44.6 mg (33%).

^{1}H NMR (600 MHz, DMSO-d_6) δ 12.75 (brs, 1H), 8.66 (d, J = 8.3 Hz, 1H), 8.20 (d, J = 7.7 Hz, 1H), 7.75 (d, J = 8.0 Hz, 1H), 7.65 (d, J = 7.4 Hz, 1H), 7.53 (t, J = 7.5 Hz, 1H), 7.46 (t, J = 7.7 Hz, 1H), 7.35 (t, J = 8.0 Hz, 1H), 7.19 (t, J = 7.5 Hz, 1H).

^{13}C NMR (151 MHz, DMSO-d_6) δ 166.1, 159.4, 139.5, 136.5, 133.7, 132.0, 129.3, 128.7, 128.5, 127.9, 124.0, 120.1, 119.5, 119.1.

HR-MS-ESI (m/z) Calculated for $C_{14}H_{11}N_5OBr$ [M + H]$^+$: 344.0147, found: 344.0147.

LCMS (MDAP): tR = 20.98 min, 99%; m/z (ESI+) 342.7 [-H]$^-$.

N-(2-(1H-Tetrazol-5-yl)phenyl)-3-bromobenzamide (4.22)

A stirred solution of *m*-bromobenzoic acid (104.5 mg, 0.52 mmol), HATU (103.2 mg, 0.27 mmol), triethylamine (0.18 mL, 1.29 mmol) in DMF (2.0 mL) for 10 minutes then 2-(1*H*-tetrazol-5-yl)-phenylamine (70.0 mg, 0.43 mmol) was added. The solution was stirred at room temperature for 16 hrs. After completion of the reaction, water (20 mL) and EtOAc 20 mL were added to the solution then the aqueous phase was extracted with EtOAc (20 mL × 2). The organic phases were combined, washed successively with 1 N HCl, saturated sodium bicarbonate solution, brine, dried over anhydrous Na_2SO_4 and concentrated. The residue was purified by chromatography on silica using a gradient of dichloromethane: methanol (0 - 20%), thus providing the product as a pink solid; yield: 15.5 mg (10%).

^{1}H NMR (600 MHz, DMSO-d_6) δ 11.47 (brs, 1H), 8.39 (d, *J* = 8.4 Hz, 1H), 8.17 (s, 1H), 7.99 (dd, *J* = 14.1, 7.8 Hz, 2H), 7.83 (d, *J* = 8.0 Hz, 1H), 7.60 (t, *J* = 8.4 Hz, 1H), 7.55 (t, *J* = 8.4 Hz, 1H), 7.37 (t, *J* = 7.7 Hz, 1H).

^{13}C NMR (151 MHz, DMSO-d_6) δ 164.1, 157.8, 155.3, 137.1, 135.2, 132.0, 131.5, 130.7, 129.3, 126.8, 125.2, 123.1, 122.5, 115.6.

HR-MS-ESI (m/z) Calculated for $C_{14}H_{11}N_5OBr$ [M + H]$^+$: 344.0147, found: 344.0144.

N-(2-(1H-Tetrazol-5-yl)phenyl)-4-bromobenzamide (4.23)
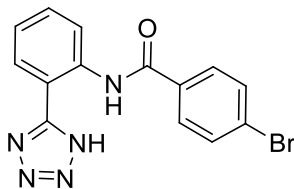
This was synthesised on a 0.43 mmol scale 2-(1H-tetrazol-5-yl)-phenylamine by the same procedure as **4.17** although 4-bromobenzoic acid (104.5 mg, 0.52 mmol) was used instead of 4-fluorobenzoic acid. The final product was obtained as a colourless solid; yield: 70.3 mg (57%).

^{1}H NMR (600 MHz, DMSO-d_6) δ 13.40 (brs, 1H), 8.74 (d, J = 8.3 Hz, 1H), 8.26 (d, J = 7.7 Hz, 1H), 8.11 (d, J = 8.1 Hz, 2H), 7.83 (d, J = 8.1 Hz, 2H), 7.33 (t, J = 7.7 Hz, 1H), 7.17 (t, J = 7.7 Hz, 1H).

^{13}C NMR (151 MHz, DMSO-d_6) δ 164.4, 159.2, 136.8, 134.6, 132.3, 129.9, 129.2, 128.1, 126.2, 124.0, 120.5, 118.6.

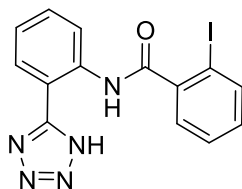HR-MS-ESI (m/z) Calculated for $C_{14}H_{11}N_5O^{79}Br$ [M + H]$^+$: 344.0147, found: 344.0163.

N-(2-(1H-Tetrazol-5-yl)phenyl)-2-iodobenzamide (4.24)

This was synthesised on a 0.36 mmol scale from 2-(1H-tetrazol-5-yl)-phenylamine by the same procedure as **4.17** although o-iodobenzoic acid (128.97.0 mg, 0.52 mmol) was used

instead of 4-fluorobenzoic acid. The final product was obtained as a colourless solid; yield: 19 mg (13%).

^{1}H NMR (600 MHz, DMSO-d_6) δ 11.01 (s, 1H), 8.36 (d, J = 8.3 Hz, 1H), 7.96 (d, J = 7.9 Hz, 1H), 7.93 (d, J = 7.8 Hz, 1H), 7.67 – 7.61 (m, 2H), 7.55 (t, J = 7.5 Hz, 1H), 7.40 (t, J = 7.6 Hz, 1H), 7.26 (t, J = 7.6 Hz, 1H).

^{13}C NMR (151 MHz, DMSO-d_6) δ 167.8, 154.8, 142.6, 140.0, 137.1, 132.3, 132.1, 129.5, 128.8, 128.6, 125.4, 123.1, 115.3, 93.9.

HR-MS-ESI (m/z) Calculated for $C_{14}H_{11}N_5OI$ [M + H]$^+$: 392.0008, found: 391.9991.

LCMS (MDAP): tR = 24.88 min, 98%; m/z (ESI+) 389.55 [M + H]$^+$.

N-(2-(1H-tetrazol-5-yl)phenyl)-3-iodobenzamide (4.25)

This was synthesised on a 0.43 mmol scale 2-(1H-tetrazol-5-yl)-phenylamine by the same procedure as **4.17** although 3-iodobenzoic acid (128.97 mg, 0.52 mmol) was used instead of 4-fluorobenzoic acid. The final product was obtained as a colourless solid; yield: 47.3 mg (31%).
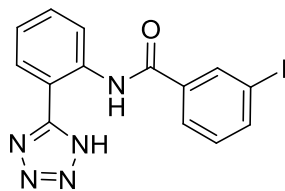
^{1}H NMR (600 MHz, DMSO-d_6) δ 13.48 (brs, 1H), 8.74 (d, J = 8.3 Hz, 1H), 8.47 (s, 1H), 8.26 (d, J = 7.7 Hz, 1H), 8.22 (d, J = 7.8 Hz, 1H), 7.99 (d, J = 7.8 Hz, 1H), 7.42 (t, J = 7.8 Hz, 1H), 7.31 (t, J = 7.8 Hz, 1H), 7.16 (t, J = 7.5 Hz, 1H).

^{13}C NMR (151 MHz, DMSO-d_6) δ 163.7, 160.2, 140.8, 137.6, 136.7, 136.5, 131.4, 128.3, 127.7, 127.0, 123.7, 119.8, 119.7, 95.8.

HR-MS-ESI (m/z) Calculated for $C_{14}H_{11}N_5OI$ [M + H]$^+$: 392.0008, found: 392.0002.

LCMS (MDAP): tR = 16.82 min, 98.3%; m/z (ESI+) 395.10 [M + H]$^+$.

N-(2-(1H-Tetrazol-5-yl)phenyl)-4-iodobenzamide (**4.26**)
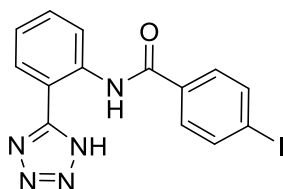
This was synthesised on a 0.43 mmol scale 2-(1H-Tetrazol-5-yl)-phenylamine by the same procedure as **4.22** although *p*-iodobenzoic acid (129.0 mg, 0.52 mmol) was used instead of *m*-bromobenzoic acid. The final product was obtained as a yellow solid; yield: 4.1 mg (2%).

^{1}H NMR (600 MHz, DMSO-d_6) δ 13.21 (brs, 1H), 8.72 (d, J = 8.4 Hz, 1H), 8.24 (aps, 1H), 8.01 (d, J = 8.1 Hz, 2H), 7.94 (d, J = 8.1 Hz, 2H), 7.36 (aps, 1H), 7.20 (aps, 1H).

^{13}C NMR (151 MHz, DMSO-d_6) δ 164.7, 152.1, 138.2, 136.7, 135.0, 129.7, 128.8, 127.9, 123.8, 120.2, 119.0, 100.2.

HR-MS-ESI (m/z) Calculated for $C_{14}H_{11}N_5OI$ [M + H]$^+$: 392.0008, found: 391.9999.

i) **4.27, 4.29,4.31-4.38**

ii) **4.28, 4.30**
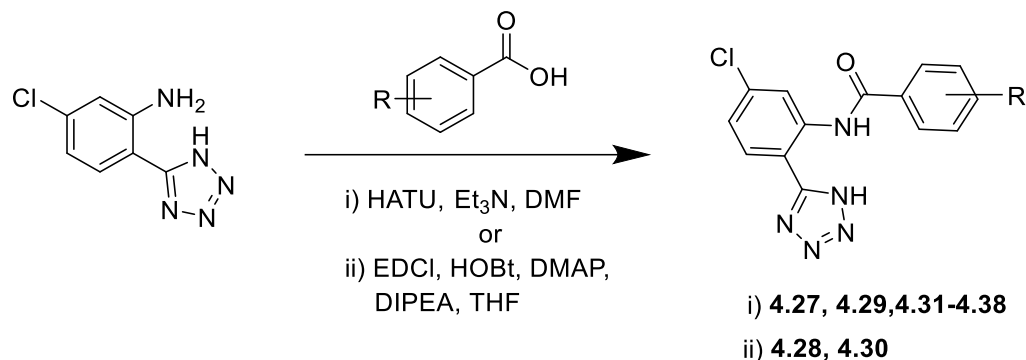
Compounds **4.27** and **4.35** were made by Dr. Andrew McGown in SDDC and are here as they are important as part of the overall SAR in the series.
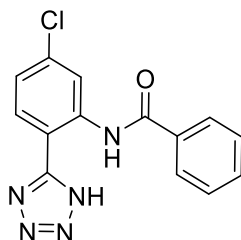
N-(5-Chloro-2-(1*H*-tetrazol-5-yl)phenyl)benzamide (**4.27**)

A solution of benzoic acid (225.0 mg, 1.84 mmol), HATU (875.0 mg, 2.3 mmol), triethylamine (0.64 mL, 4.6 mmol) in DMF (5.0 mL) was stirred for 10 minutes then 5-chloro-2-(1*H*-tetrazol-5-yl)aniline (300.0 mg, 1.53 mmol) was added. The solution was stirred at room temperature overnight. After completion of the reaction, water (15 mL) and DCM (15 mL) were added to the solution then the aqueous phase was extracted with EtOAc (15 mL × 2). The organic phases were combined, washed successively with 1N HCl, saturated sodium bicarbonate solution, brine, dried over anhydrous Na_2SO_4 and concentrated. The resulting residue was suspended in DCM and stirred leading to the formation of a precipitate which was collected by filtration as a colourless solid; yield: 77.4 mg (16%).
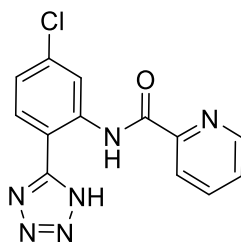
^{1}H NMR (600 MHz, Acetone-d_6) δ 12.10 (brs, 1H), 9.13 (d, J = 2.1 Hz, 1H), 8.23 – 8.15 (m, 3H), 7.67 (m, 3H), 7.39 (dd, J = 8.5, 2.1 Hz, 1H).

^{13}C NMR (151 MHz, Acetone-d_6) δ 165.5, 155.5, 139.3, 137.4, 134.5, 132.4, 129.6, 129.0, 127.5, 123.5, 120.4, 110.7.

HR-MS-ESI (m/z) Calculated for $C_{14}H_{11}N_5OCl$ [M + H]$^+$: 300.0647, found: 300.0653.

LCMS (MDAP): tR = 6.95 min, 95.7%; m/z (ESI+) 298.75 [M - H]$^-$.

N-(4-Chloro-2-(1H-tetrazol-5-yl)phenyl)picolinamide (**4.28**)

A solution of 5-chloro-2-(1H-tetrazol-5-yl)aniline (100.0 mg, 0.51 mmol), piconilic acid (75.3 mg, 0.61 mmol), DMAP (62.3 mg, 0.51 mmol), EDC (97.8 mg, 0.51 mmol), HOBT (13.8 mg, 0.10 mmol), DIPEA (0.46 mL, 2.55 mmol) in THF (3.0 mL). The solution was stirred at 70 °C overnight under nitrogen. The mixture was allowed to cool to room temperature. Water (20 mL) and EtOAc (20 mL) were added to the solution then the aqueous phase was extracted with EtOAc (20 mL× 2). The organic phases were combined, washed successively with 1 N HCl, saturated sodium bicarbonate solution, brine, dried over anhydrous Na_2SO_4 and concentrated. The resulting residue was suspended in DCM and stirred leading to the formation of a precipitate which was collected by filtration and identified as pure product as a yellow solid; yield: 12.5 mg (8%)

^{1}H NMR (600 MHz, DMSO-d_6) δ 13.70 (brs, 1H), 8.91 (m, 1H), 8.80 (m, 1H), 8.20 (d, J = 7.8 Hz, 1H), 8.17 (d, J = 7.9 Hz, 1H), 8.06 (t, J = 7.8 Hz, 1H), 7.67 (t, J = 6.1 Hz, 1H), 7.25 (d, J = 8.3 Hz, 1H).

^{13}C NMR (151 MHz, DMSO-d_6) δ 164.2, 159.0, 150.6, 149.3, 138.4, 137.3, 132.4, 129.6, 127.4, 123.7, 123.0, 120.0, 119.1.

HR-MS-ESI (m/z) Calculated for $C_{13}H_{10}N_6OCl$ [M + H]$^+$: 301.0605, found: 301.0611.

LCMS (MDAP): tR = 19.9 min, 56%; m/z (ESI+) 299.8 [M - H]$^-$, and Rt = 28.6 min, 42%; m/z (ESI+) 299.9 [M - H]$^-$.

N-(4-Chloro-2-(1H-tetrazol-5-yl)phenyl)nicotinamide (4.29)
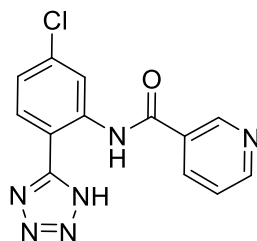
This was synthesised on a 0.51 mmol scale from 5-chloro-2-(1H-tetrazol-5-yl)aniline by the same procedure as **4.27** although nicotinic acid (75.1 mg, 0.61 mmol) was used instead of benzoic acid. After completion of the reaction, water (15 mL) and EtOAc (20 mL) were added to the solution then the aqueous phase was extracted with EtOAc (20 mL × 2). The organic phases were combined, washed successively with 1 N HCl (10 mL), saturated sodium bicarbonate solution, brine, dried over anhydrous Na_2SO_4 and concentrated. The residue was purified by chromatography on silica using a gradient of dichloromethane: methanol (0 - 20%). The final product was obtained as a colourless solid; yield: 10.0 mg (7%).

^{1}H NMR (600 MHz, DMSO-d_6) δ 13.66 (brs, 1H), 9.35 (s, 1H), 8.85 (d, J = 2.2 Hz, 1H), 8.83 (d, J = 4.6 Hz, 1H), 8.50 (d, J = 8.0 Hz, 1H), 8.27 (d, J = 8.5 Hz, 1H), 7.67 (dd, J = 8.0, 4.6 Hz, 1H), 7.25 (dd, J = 8.5, 2.2 Hz, 1H).

^{13}C NMR (151 MHz, DMSO-d_6) δ 164.1, 157.3, 153.1, 149.0, 137.5, 135.6, 132.5, 130.6, 129.1, 124.5, 123.8, 119.3, 118.4.

HR-MS-ESI (m/z) Calculated for $C_{13}H_{10}N_6OCl$ [M + H]$^+$: 301.0605, found: 301.0612.

LCMS (MDAP): tR = 16.55 min, 97.3%; m/z (ESI+) 392.80 [M + H]$^+$.

N-(5-Chloro-2-(1H-tetrazol-5-yl)phenyl)isonicotinamide (4.30)
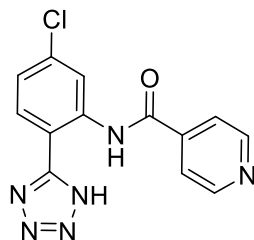
This was synthesised on a 0.51 mmol scale from 5-chloro-2-(1H-tetrazol-5-yl)aniline by the same procedure as **4.28** although isonicotinic acid (75.1 mg, 0.61 mmol) was used instead of piconilic acid. The final product was obtained as a colourless solid; yield: 8.1 mg (5%).

^{1}H NMR (600 MHz, DMSO-d_6) δ 12.00 (brs, 1H), 8.88 (s, 2H), 8.59 (s, 1H), 8.08 (d, J = 8.5 Hz, 1H), 7.94 (s, 2H), 7.48 (d, J = 8.5 Hz, 1H).

^{13}C NMR (151 MHz, DMSO-d_6) δ 164.2, 155.5, 151.1, 141.7, 137.9, 135.9, 130.6, 125.2, 122.0, 121.7, 114.8.

HR-MS-ESI (m/z) Calculated for $C_{13}H_{10}N_6OCl$ [M + H]$^+$: 301.0605, found: 301.0612.

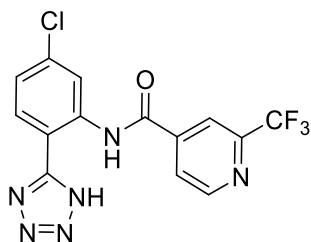**N-(5-Chloro-2-(1H-tetrazol-5-yl)phenyl)-2-(trifluoromethyl)isonicotinamide** (**4.31**)

This was synthesised on a 1.02 mmol scale from 5-chloro-2-(1H-tetrazol-5-yl)aniline by the same procedure as **4.27** although 2-(trifluoromethyl)isonicotinic acid (200 mg, mmol) was used instead of benzoic acid. After completion of the reaction, water (15 mL) and EtOAc (20 mL) were added to the solution then the aqueous phase was extracted with EtOAc (20 mL × 2). The organic phases were combined, washed successively with 1 N HCl (10 mL), saturated sodium bicarbonate solution, brine, dried over anhydrous Na_2SO_4 and concentrated. The residue was purified by chromatography on silica using a gradient of EtOAc: methanol (0 - 20%). The combined final product was obtained as a colourless solid; yield: 28.4 mg (8%).

^{1}H NMR (600 MHz, DMSO-d_6) δ 13.78 (brs, 1H), 9.09 (d, J = 4.9 Hz, 1H), 8.78 (s, 1H), 8.49 (s, 1H), 8.37 (d, J = 4.9 Hz, 1H), 8.26 (d, J = 8.4 Hz, 1H), 7.31 (d, J = 8.4 Hz, 1H).

^{13}C NMR (151 MHz, DMSO-d_6) δ 162.5, 159.0, 152.2, 148.0 (q, $^2J_{CF}$ = 34.4 Hz), 144.2, 137.1, 132.9, 129.3, 125.3, 124.5, 121.0 (q, $^1J_{CF}$ = 274.3 Hz), 119.7, 118.7 (q, $^3J_{CF}$ = 3.2 Hz), 118.4.

^{19}F NMR (376 MHz, DMSO-d_6) δ -66.67 (brs).

HR-MS-ESI (m/z) Calculated for $C_{14}H_9N_6OF_3Cl$ [M + H]$^+$: 369.0478, found: 369.0479.

N-(5-Chloro-2-(1H-tetrazol-5-yl)phenyl)-6-(trifluoromethyl)nicotinamide (4.32)
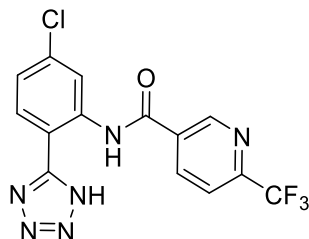
This was synthesised on a 0.77 mmol scale from 5-chloro-2-(1H-tetrazol-5-yl)aniline by the same procedure as **4.27** although 6-(trifluoromethyl)nicotinic acid (174.9 mg, 0.92 mmol) was used instead of benzoic acid. After completion of the reaction, water (15 mL) and EtOAc (20 mL) were added to the solution then the aqueous phase was extracted with EtOAc (20 mL × 2). The organic phases were combined, washed successively with 1 N HCl (10 mL), saturated sodium bicarbonate solution, brine, dried over anhydrous Na_2SO_4 and concentrated. The resulting residue was suspended in EtOAc and stirred leading to the formation of a precipitate which was collected by filtration. The filtrate was also collected and purified by chromatography on silica using a gradient of EtOAc: methanol (0 - 20%). The combined final product was obtained as a pale-pink solid; yield: 81.5 mg (29%).

^{1}H NMR (600 MHz, DMSO-d_6) δ 13.12 (brs, 1H), 9.41 (s, 1H), 8.70 (d, J = 2.2 Hz, 1H), 8.69 (dd, J = 8.3, 2.2 Hz, 1H), 8.20 (dd, J = 8.3, 5.4 Hz, 2H), 7.37 (dd, J = 8.3, 2.2 Hz, 1H).

^{13}C NMR (151 MHz, DMSO-d_6) δ 163.0, 157.9, 149.5, 148.9 (q, $^2J_{CF}$ = 34.3 Hz), 138.2, 137.4, 133.8, 133.7, 129.7, 124.7, 122.7 (q, $^1J_{CF}$ = 274.3 Hz), 121.6 (q, $^3J_{CF}$ = 2.8 Hz), 120.6, 117.4.

^{19}F NMR (376 MHz, DMSO-d_6) δ -66.70 (brs).

HR-MS-ESI (m/z) Calculated for $C_{14}H_9N_6OF_3Cl$ [M + H]$^+$: 369.0478, found: 369.0478.

N-(5-Chloro-2-(1H-tetrazol-5-yl)phenyl)-2-(trifluoromethyl)benzamide (4.33)
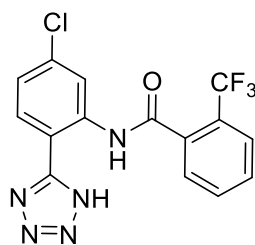
This was synthesised on a 0.36 mmol scale from 5-chloro-2-(1H-tetrazol-5-yl)aniline by the same procedure as **4.31** although 2-(trifluoromethyl)benzoic acid (115.4 mg, 0.43 mmol) was used instead of benzoic acid. The final product was obtained as a yellow solid; yield: 39.2 mg (14%).

^{1}H NMR (600 MHz, DMSO-d_6) δ 13.05 (brs, 1H), 8.72 (s, 1H), 8.22 (d, J = 8.5 Hz, 1H), 7.90 (d, J = 7.8 Hz, 1H), 7.85 (s, 2H), 7.78 (d, J = 7.8 Hz, 1H), 7.28 (d, J = 8.5 Hz, 1H).

^{13}C NMR (151 MHz, DMSO-d_6) δ 166.3, 158.9, 137.4, 136.4, 133.5, 132.8, 131.2, 129.3, 128.8, 127.3 (q, $^3J_{CF}$ = 4.8 Hz), 126.5 (q, $^2J_{CF}$ = 31.6 Hz), 125.1 (q, $^1J_{CF}$ = 273.7 Hz), 124.0, 119.4, 118.0.

^{19}F NMR (376 MHz, DMSO-d_6) δ -57.79 (brs).

HR-MS-ESI (m/z) Calculated for $C_{15}H_{10}N_5OF_3Cl$ [M + H]$^+$: 368.0526, found: 368.0523.

N-(5-Chloro-2-(1H-tetrazol-5-yl)phenyl)-3-(trifluoromethyl)benzamide (**4.34**)

This was synthesised on a 0.77 mmol scale from 5-chloro-2-(1H-tetrazol-5-yl)aniline by the same procedure as **4.32** although 3-(trifluoromethyl)benzoic acid (174.0 mg, 0.92 mmol) was used instead of benzoic acid. The final product was obtained as a pale-pink solid; yield: 60.0 mg (21%).
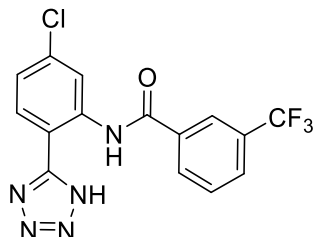
^{1}H NMR (600 MHz, DMSO-d_6) δ 12.98 (brs, 1H), 8.73 (d, J = 2.2 Hz, 1H), 8.43 – 8.41 (m, 2H), 8.18 (d, J = 8.5 Hz, 1H), 8.04 (d, J = 7.8 Hz, 1H), 7.88 (t, J = 8.0 Hz, 1H), 7.35 (dd, J = 8.5, 2.2 Hz, 1H).

^{13}C NMR (151 MHz, DMSO-d_6) δ 164.2, 157.6, 137.8, 135.8, 134.1, 131.7, 130.7, 130.3 (q, $^2J_{CF}$ = 34.4 Hz), 129.7, 129.2, 125.2 (q, $^1J_{CF}$ = 272.6 Hz), 124.6 (q, $^2J_{CF}$ = 4.0 Hz), 124.3, 120.5, 116.6.

^{19}F NMR (376 MHz, DMSO-d_6) δ -61.32 (brs).

HR-MS-ESI (m/z) Calculated for $C_{15}H_{10}N_5OF_3Cl$ [M + H]$^+$: 368.0526, found: 368.0522.

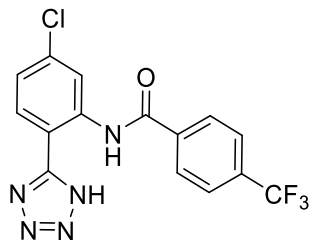**N-(5-Chloro-2-(1H-tetrazol-5-yl)phenyl)-4-(trifluoromethyl)benzamide** (**4.35**)

This was synthesised on a 1.53 mmol scale from 5-chloro-2-(1H-tetrazol-5-yl)aniline by the same procedure as **4.31** although 4-(trifluoromethyl)benzoic acid (350 mg, 1.84 mmol) was used instead of benzoic acid and the residue was purified by reverse phase column chromatography on C-18 using a gradient of acetonitrile: water (+0.1 % Formic acid). The final product was obtained as a colourless solid; yield: 114.2 mg (19%).

^{1}H NMR (600 MHz, DMSO-d_6) δ 11.68 (brs, 1H), 8.58 (d, J = 2.2 Hz, 1H), 8.20 (d, J = 8.1 Hz, 2H), 8.01 (dd, J = 13.4, 8.3 Hz, 3H), 7.50 (dd, J = 8.5, 2.2 Hz, 1H).

^{13}C NMR (151 MHz, DMSO-d_6) δ 164.7, 138.3, 138.3, 136.5, 132.6 (q, $^2J_{CF}$ = 31.9 Hz), 130.7, 128.8, 126.5 (q, $^3J_{CF}$ = 3.3 HZ), 125.2, 125.1, 123.4, 122.3, 113.9.

^{19}F NMR (376 MHz, DMSO-d_6) δ -61.49 (brs).

HR-MS-ESI (m/z) Calculated for $C_{15}H_{10}N_5OClF_3$ [M + H]$^+$: 368.0526, found: 368.0517.
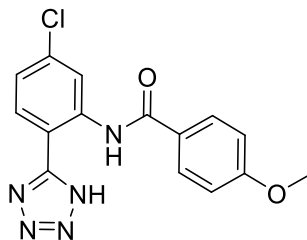
N-(4-Chloro-2-(1H-tetrazol-5-yl)phenyl)-4-methoxybenzamide (**4.36**)

This was synthesised on a 0.51 mmol scale 5-chloro-2-(1H-tetrazol-5-yl)aniline by the same procedure as **4.31** although *p*-anisic acid (92.8 mg, 0.61 mmol) was used instead of benzoic acid. The final product was obtained as a colourless solid; yield: 29.8 mg (18%).

^{1}H NMR (600 MHz, DMSO-d_6) δ 12.64 (brs, 1H), 8.82 (d, *J* = 2.2 Hz, 1H), 8.15 (d, *J* = 8.5 Hz, 1H), 8.10 (d, *J* = 8.4 Hz, 2H), 7.30 (dd, *J* = 8.5, 2.2 Hz, 1H), 7.15 (d, *J* = 8.4 Hz, 2H), 3.85 (s, 3H).

^{13}C NMR (151 MHz, DMSO-d_6) δ 165.2, 162.8, 157.6, 138.5, 134.3, 129.8, 129.7, 126.9, 123.5, 120.0, 115.6, 114.7, 56.0.

HR-MS-ESI (m/z) Calculated for $C_{15}H_{11}N_5O_2Cl$ [M - H]$^{-}$: 328.0601, found: 328.0607.
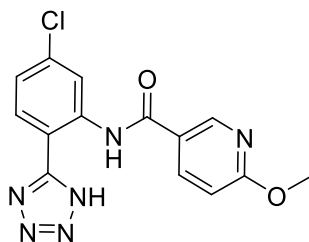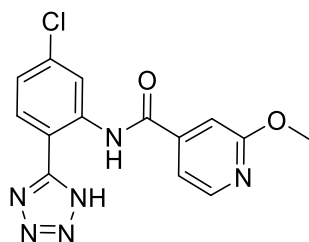
N-(5-Chloro-2-(1H-tetrazol-5-yl)phenyl)-6-methoxynicotinamide (**4.37**)

This was synthesised on a 0.51 mmol scale from 5-chloro-2-(1H-tetrazol-5-yl)aniline by the same procedure as **4.31** although 6-methoxynicotinic acid (93.42 mg, 0.61 mmol) was used instead of benzoic acid. The final product was obtained as a yellow solid; yield: 27.2 mg (16%).

^{1}H NMR (600 MHz, DMSO-d_6) δ 11.66 (brs, 1H), 8.56 (d, J = 2.4 Hz, 1H), 8.42 (d, J = 5.2 Hz, 1H), 8.02 (m, 1H), 7.52 – 7.48 (m, 2H), 7.34 (d, J = 4.2 Hz, 1H), 3.93 (s, 3H).

^{13}C NMR (151 MHz, DMSO-d_6) δ 164.7, 164.0, 154.9, 148.7, 144.8, 138.0, 136.4, 130.8, 125.3, 122.3, 115.0, 114.1, 109.0, 54.2.

HR-MS-ESI (m/z) Calculated for $C_{14}H_{12}N_6O_2Cl$ [M + H]$^+$: 331.0710, found: 331.0713.

N-(5-Chloro-2-(1H-tetrazol-5-yl)phenyl)-2-methoxyisonicotinamide (**4.38**)

This was synthesised on a 3.06 mmol scale from 5-chloro-2-(1H-tetrazol-5-yl)aniline by the same procedure as **4.31** although 2-methoxyisonicotinic acid (200 mg, 1.22 mmol)
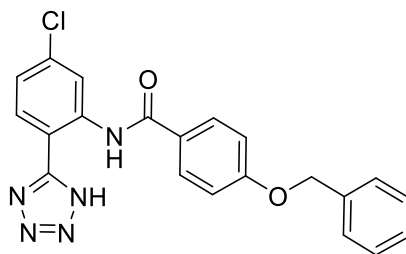
was used instead of benzoic acid. The final product was obtained as a colourless solid; yield: 14.5 mg (4%).

^{1}H NMR (600 MHz, DMSO-d_6) δ 13.08 (brs, 1H), 9.01 (s, 1H), 8.79 (s, 1H), 8.36 (d, J = 8.6 Hz, 1H), 8.21 (d, J = 8.6 Hz, 1H), 7.27 (d, J = 8.7 Hz, 1H), 7.04 (d, J = 8.7 Hz, 1H), 3.96 (s, 3H).

^{13}C NMR (151 MHz, DMSO-d_6) δ 166.2, 163.9, 158.5, 147.8, 138.8, 137.9, 133.4, 129.5, 124.3, 123.7, 119.7, 117.1, 111.3, 54.4.

HR-MS-ESI (m/z) Calculated for $C_{14}H_{12}N_6O_2Cl$ [M + H]$^+$: 331.0710, found: 331.0713.

4-(Benzyloxy)-*N*-(4-chloro-2-(1*H*-tetrazol-5-yl)phenyl)benzamide (**4.39**)

This was synthesised on a 1.02 mmol scale from 5-chloro-2-(1*H*-tetrazol-5-yl)aniline by the same procedure as **4.31** although 4-(benzyloxy)benzoic acid (278.5 mg, 1.02 mmol) was used instead of benzoic acid. The final product was obtained as a colourless solid; yield: 20.0 mg (5%).

^{1}H NMR (600 MHz, DMSO-d_6) δ 11.68 (brs, 1H), 8.74 (s, 1H), 8.02 (d, J = 9.0 Hz, 3H), 7.47 (d, J = 7.5 Hz, 2H), 7.43 (m, 1H), 7.40 (t, J = 7.5 Hz, 2H), 7.34 (t, J = 7.5 Hz, 1H), 7.22 (m, 2H), 5.22 (s, 2H).

^{13}C NMR (151 MHz, DMSO-d_6) δ 165.2, 162.1, 155.1, 139.0, 137.0, 136.5, 130.5, 129.8, 128.9, 128.5, 128.3, 126.7, 124.2, 121.1, 115.5, 112.5, 70.0.

HR-MS-ESI (m/z) Calculated for $C_{21}H_{15}N_5O_2Cl$ [M - H]$^-$: 404.0914, found: 404.0917.

3',5'-Dichloro-*N*-(5-chloro-2-(1*H*-tetrazol-5-yl)phenyl)-[1,1'-biphenyl]-4-carboxamide (4.40)
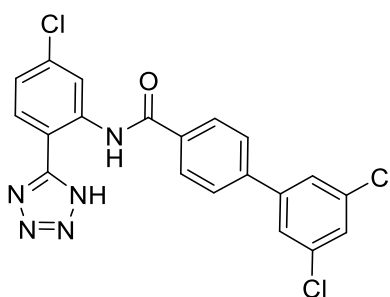

This was synthesised on a 0.36 mmol scale from 5-chloro-2-(1*H*-tetrazol-5-yl)aniline by the same procedure as **4.27** although 3',5'-dichlorobiphenyl-4-carboxylic acid (115.4 mg, 0.43 mmol), was used instead of benzoic acid. After completion of the reaction, water (15 mL) and EtOAc (20 mL) were added to the solution then the aqueous phase was extracted with EtOAc (20 mL × 2). The organic phases were combined, washed successively with 1 N HCl (10 mL), saturated sodium bicarbonate solution, brine, dried over anhydrous Na_2SO_4 and concentrated. The resulting residue was suspended in MeOH and stirred leading to the formation of a precipitate which was collected by filtration and identified as pure product. The final product was obtained as an orange solid; yield: 64.3 mg (40%).

^{1}H NMR (600 MHz, DMSO-d_6) δ 12.19 (brs, 1H), 8.74 (d, *J*= 2.4 Hz, 1H), 8.16 (d, *J*= 7.9 Hz, 2H), 8.08 (d, *J*= 8.4 Hz, 1H), 8.01 (d, *J*= 7.9 Hz, 2H), 7.88 (s, 2H), 7.66 (s, 1H), 7.42 (d, *J*= 8.4 Hz, 1H).

^{13}C NMR (151 MHz, DMSO-d_6) δ 165.1, 156.0, 142.8, 141.2, 138.4, 135.6, 135.3, 134.4, 130.3, 128.6, 128.2, 128.1, 126.2, 124.4, 121.1, 114.3.

HR-MS-ESI (m/z) Calculated for $C_{20}H_{11}N_5OCl_3$ [M - H]⁻: 442.0029, found: 442.0033.

N-(5-Chloro-2-(1H-tetrazol-5-yl)phenyl)-4'-(trifluoromethyl)-[1,1'-biphenyl]-4-carboxamide (4.41)
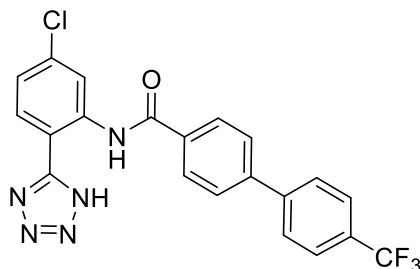

This was synthesised on a 0.77 mmol scale from 5-chloro-2-(1H-tetrazol-5-yl)aniline by the same procedure as **4.32** although 4'-(trifluoromethyl)-[1,1'-biphenyl]-4-carboxylic acid (244.9 mg, 0.92 mmol), was used instead of benzoic acid and EtOAc was also used instead of DCM. The final product was obtained as an orange solid; yield: 95.8 mg (28%).

¹H NMR (600 MHz, DMSO-d_6) δ 12.22 (brs, 1H), 8.75 (s, 1H), 8.17 (d, J= 7.9 Hz, 2H), 8.07 (d, J= 8.4 Hz, 1H), 7.98 (d, J = 8.2 Hz, 2H), 7.96 (d, J = 8.2 Hz, 2H)), 7.83 (d, J= 7.9 Hz, 2H), 7.39 (d, J= 8.4 Hz, 1H).

¹³C NMR (151 MHz, DMSO-d_6) δ 165.2, 156.0, 143.3, 142.6, 138.5, 135.6, 134.2, 130.2, 129.1 (q, $^2J_{CF}$ = 31.7 Hz), 128.6, 128.3, 128.0, 126.3 (q, $^3J_{CF}$ = 4.1 Hz), 125.6 (q, $^1J_{CF}$ = 272.0 Hz), 124.3, 120.9, 114.0.

¹⁹F NMR (376 MHz, DMSO-d_6) δ -61.04 (brs).

HR-MS-ESI (m/z) Calculated for $C_{21}H_{12}N_5OF_3Cl$ [M - H]⁻: 442.0682, found: 442.0680.

LCMS (MDAP): tR = 15.94 min, 99%; m/z (ESI+) 328.80 [-H]⁻.

4.8 References

1   M. A. Ashburn and P. S. Staats, *Lancet*, 1999, **353**, 1865–1869.

2   C. Tsantoulas and S. B. McMahon, *Trends Neurosci.*, 2014, **37**, 146–158.

3   R. Labianca, P. Sarzi-Puttini, S. M. Zuccaro, P. Cherubino, R. Vellucci and D. Fornasari, *Clin. Drug Investig.*, 2012, **32**, 53–63.

4   C. Knox, V. Law, T. Jewison, P. Liu, S. Ly, A. Frolkis, A. Pon, K. Banco, C. Mak, V. Neveu, Y. Djoumbou, R. Eisner, A. C. Guo and D. S. Wishart, *Nucleic Acids Res.*, 2011, **39**, D1035–D1041.

5   D. S. Wishart, Y. D. Feunang, A. C. Guo, E. J. Lo, A. Marcu, J. R. Grant, T. Sajed, D. Johnson, C. Li, Z. Sayeeda, N. Assempour, I. Iynkkaran, Y. Liu, A. Maclejewski, N. Gale, A. Wilson, L. Chin, R. Cummings, Di. Le, A. Pon, C. Knox and M. Wilson, *Nucleic Acids Res.*, 2018, **46**, D1074–D1082.

6   D. S. Wishart, C. Knox, A. C. Guo, D. Cheng, S. Shrivastava, D. Tzur, B. Gautam and M. Hassanali, *Nucleic Acids Res.*, 2008, **36**, D901–D906.

7   V. Law, C. Knox, Y. Djoumbou, T. Jewison, A. C. Guo, Y. Liu, A. Maclejewski, D. Arndt, M. Wilson, V. Neveu, A. Tang, G. Gabriel, C. Ly, S. Adamjee, Z. T. Dame, B. Han, Y. Zhou and D. S. Wishart, *Nucleic Acids Res.*, 2014, **42**, D1091–D1097.

8   D. S. Wishart, C. Knox, A. C. Guo, S. Shrivastava, M. Hassanali, P. Stothard, Z. Chang and J. Woolsey, *Nucleic Acids Res.*, 2006, **34**, D668–D672.

9   M. Takeda, Y. Tsuboi, J. Kitagawa, K. Nakagawa, K. Iwata and S. Matsumoto, *Mol. Pain*, 2011, **7**, 24–26.

10   A. Mathie, *J. Pharm. Pharmacol.*, 2010, **62**, 1089–1095.

11   M. W. Barnett and P. M. Larkman, *Pract. Neurol.*, 2007, **7**, 192–197.

12   X. Du and N. Gamper, *Curr. Neuropharmacol.*, 2013, **11**, 621–640.

13   J. E. Linley, K. Rose, L. Ooi and N. Gamper, *Pflugers Arch. Eur. J. Physiol.*, 2010, **459**, 657–669.

14   G. Edwards and A. H. Weston, *Cardiovasc. Drugs Ther.*, 1995, **9**, 185–193.

15   Q. Kuang, P. Purhonen and H. Hebert, *Cell. Mol. Life Sci.*, 2015, **72**, 3677–3693.

16   D. M. Kim and C. M. Nimigean, *Cold Spring Harb. Perspect. Biol.*, 2016, **8**, 1–19.

17   M. Ocaña, C. M. Cendán, E. J. Cobos, J. M. Entrena and J. M. Baeyens, *Eur. J. Pharmacol.*, 2004, **500**, 203–219.

18   H. Wulff, N. A. Castle and L. A. Pardo, *Nat. Rev. Drug Discov.*, 2009, **8**, 982–1001.

19   S. L. Worley, *P T*, 2016, **41**, 107–114.

20   R. C. Dart, H. L. Surratt, T. J. Cicero, M. W. Parrino, S. G. Severtson, B. Bucher-Bartelson and J. L. Green, *N. Engl. J. Med.*, 2015, **372**, 241–248.

21   A. Abd-Elsayed, M. Jackson, S. L. Gu, K. Fiala and J. Gu, *Mol. Pain*, 2019, **15**, 1–8.

22   X. Xu, X. Xu, Y. Hao, X. Zhu, J. Lu, X. Ouyang, Y. Lu, X. Huang, Y. Li, J. Wang and X. Shen, *iScience*, 2020, **23**, 1–32.

23   R. V. Frolov and S. Singh, *Eur. J. Pharmacol.*, 2014, **730**, 61–71.

24   C. Tsantoulas, L. Zhu, Y. Shaifta, J. Grist, J. P. T. Ward, R. Raouf, G. J. Michael and S. B. McMahon, *J. Neurosci.*, 2012, **32**, 17502–17513.

25   Invitrogen, *FluxOR™ II Green Potassium Ion Channel Assay*, 2017.

26   K. J. Black, J. M. Koller and B. D. Miller, *PeerJ*, 2013, **2013**, 1–26.

27   F. Lovering, J. Bikker and C. Humblet, *J. Med. Chem.*, 2009, **52**, 6752–6756.

28   M. A. Malik, M. Y. Wani, S. A. Al-Thabaiti and R. A. Shiekh, *J. Incl. Phenom. Macrocycl. Chem.*, 2014, **78**, 15–37.

29   C. Liljebris, S. D. Larsen, D. Ogg, B. J. Palazuk and J. E. Bleasdale, *J. Med. Chem*, 2002, **45**, 1785–1798.

30   A. Daina, O. Michielin and V. Zoete, *Sci. Rep.*, 2017, **7**, 1–13.

31   C. A. Lipinski, *Drug Discov. Today Technol.*, 2004, **1**, 337–341.

32   L. Di and E. H. Kerns, in *Drug-Like Properties Concepts, Structure Design and Methods from ADME to Toxicity Optimization*, Elsevier Inc., Second edi., 2016, pp. 29–38.

33   A. Daina and V. Zoete, *ChemMedChem*, 2016, **11**, 1117–1121.

34   A. Daina, M. C. Blatter, V. Baillie Gerritsen, P. M. Palagi, D. Marek, I. Xenarios, T. Schwede, O. Michielin and V. Zoete, *J. Chem. Educ.*, 2017, **94**, 335–344.

35   A. Daina, O. Michielin and V. Zoete, *Chem. Inf. Model.*, 2014, **54**, 3284–3301.

36   P. Panyatip, N. Nunthaboot and P. Puthongking, *Int. J. Tryptophan Res.*, 2020, **13**, 1–7

Chapter 5

Conclusions and Future Directions

5.1 Conclusions

Amide compounds continue to attract much consideration in medicinal chemistry (Chapter 1). Effective small molecule amides and related compounds (sulphonamides, hydrazides) have been synthesised using the 'rule of five' considerations, acid bioisosteres and tested against various targets (Scheme 5.1).
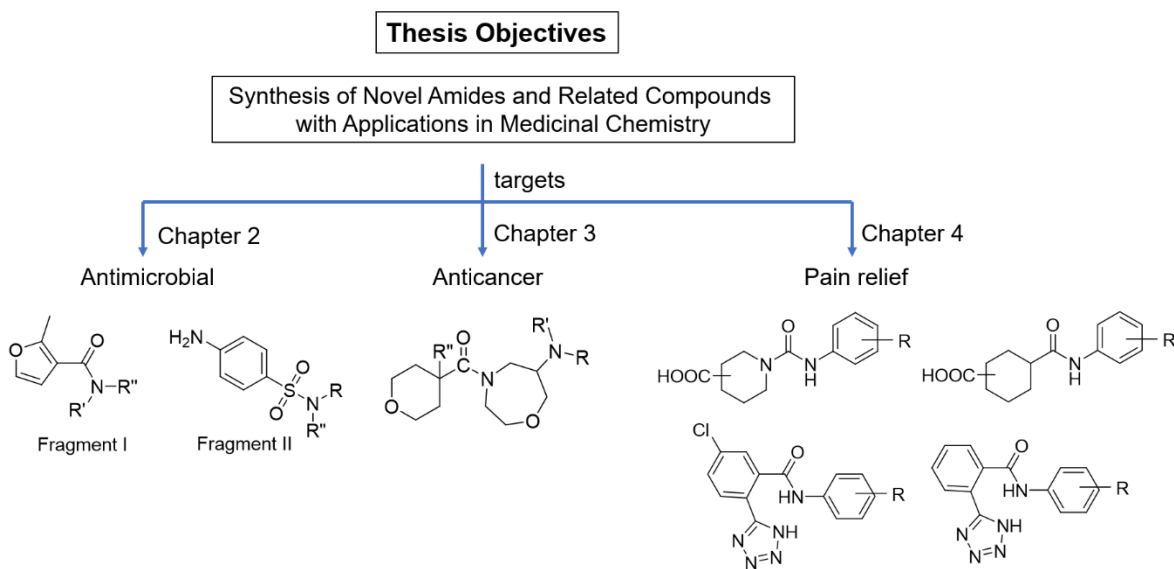
Scheme 5.1. *Thesis Objectives.*

In Chapter 1, we review the importance of amide and sulfonamide compounds in medicinal chemistry, coupling agents for the synthesis of amides, the synthesis of sulfonamides and acid bioisosteres.

In Chapter 2, libraries of furan containing amides, sulphonamides and hydrazides have been produced for targeting peptidyl-tRNA hydrolase (Pth). It was found that the furan ring in fragment I can bind in active site from a fragment screen (Hare group, Sussex) was undertaken using X-ray crystallography, the chemical structure as shown in Figure 5.1.
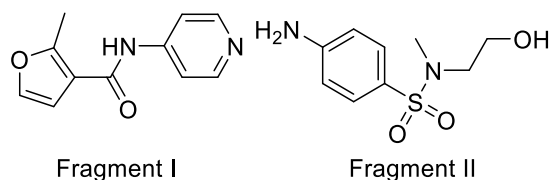

Fragment I   Fragment II

Figure 5.1. *Initial fragment hits from X-ray crystallography.*

In Chapter 3, LMO2-SCL inhibitors were made by using tert-butyl 6-oxo-1,4-oxazepane-4-carboxylate as a building block. (6-((Pyridin-2-ylmethyl)amino)-1,4-oxazepan-4-yl)(tetrahydro-2*H*-pyran-4-yl)methanone (**3.8**) showed the lowest in K_d (6 nM) that needs more development to a drug in the future, the chemical structure as shown in Figure 5.2.
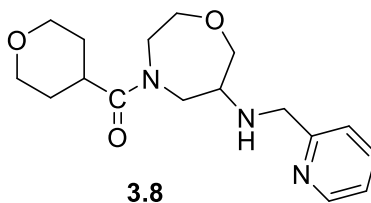

3.8

Figure 5.2. *This compound had the lowest K_d.*

In Chapter 4, a series of low molecular compounds have been synthesised by using a simple amide coupling methods with parallel attempts to improve the solubility and permeability of our lead compounds. Biological assays showed the compounds to display good potency as activators of K$_v$2.1 channels and promising compounds were chosen to further study solubility, permeability and metabolic stability in an *in vitro* study (Figure 5.3).
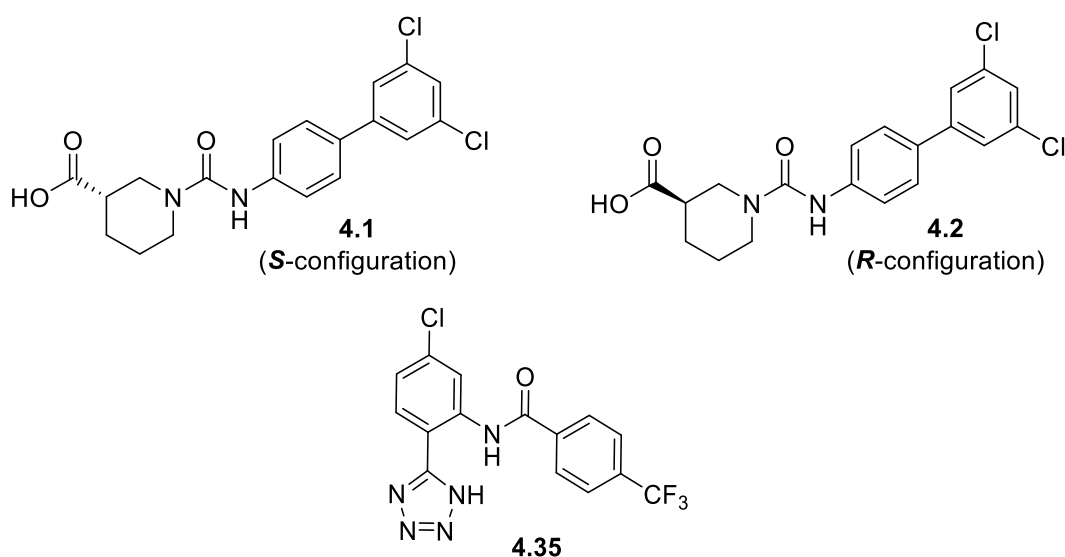

Figure 5.3. Compounds *4.1*, *4.2* and *4.3* that were chosen to in vitro test.

5.2 Future Directions

Fragments I and II libraries in Chapter 2 have been sent for antimicrobial testing to colleagues at the INEOS Centre, University of Oxford (https://www.ineosoxford.ox.ac.uk/). These will be investigated, if active, against clinically relevant gram + and – bacteria.

In addition to testing with other antimicrobials, the synthesised compounds can be tested for binding to novel protein targets using the MST technique.

Compounds in Chapter 3 will be sent for further study *vs* a related LMO4 target for anticancer since we have no structural data on LMO2 (xray), the use of a surrogate protein (LMO4) with better crystallisation properties (unpublished) may help us better understand binding and SAR properties.

Compounds in Chapter 4 still can be developed in terms of SAR to produce a lead compound in order to improve their efficacy, permeability and solubility. We anticipate several publications arising from this work.

5.3 Thesis Outcomes

Publications;

Publications for Chapter 3 and 4 will be published soon.

The following paper has been published on work related to this thesis:

Synthesis of a Thiazole Library via an Iridium Catalyzed Sulfur Ylide Insertion Reaction. Storm Hassell-Hart,* Elisa Speranzini, Sirihathai Srikwanjai, Euan Hossack, S. Mark Roe, Daren Fearon, Daniel Akinbosede, Stephen Hare and John Spencer*. *Org. Lett.* **2022**, 24(43),7924-7927.

Oral presentation:

Sirihathai Srikwanjai and John Spencer, "*Synthesis of potential compounds for potassium ion channel targets in pain relief*", Chemistry PhD Colloquium 2022, 9th September 2022, University of Sussex, Brighton, UK.

Sirihathai Srikwanjai, Hazel Cox and John Spencer, "*Synthesis of amide compounds for Biological Applications*", Chemistry PhD Colloquium 2022 (online), 18th September 2020, University of Sussex, Brighton, UK.

Attending Events:

Life Sciences Research Symposium, 7th January 2023, University of Sussex, Brighton, UK.

Life Sciences Research Symposium, 30th June 2021, University of Sussex, Brighton, UK.

First symposium on Organic Synthesis and Drug Discovery, 1st November 2019, Kingston University, London.